THE YESO AQUIFER OF THE MIDDLE PECOS BASIN, ANALYSIS AND INTERPRETATION

Final report submitted to
New Mexico Interstate Stream Commission

Report H-16 December, 1985

Hydrogeological Analysis of Geophysical Well Logs from the Pecos Slope *)

by

Amy Childers
Graduate Research Assistant

and

Gerardo Wolfgang Gross
Professor of Geophysics, Principal Investigator

New Mexico Institute of Mining and Technology
Socorro, New Mexico 87801

*) This report is based on research performed by A. Childers in partial fulfillment of the requirements for the M.S. degree in Geoscience with specialization in Hydrology.

ACKNOWLEDGEMENTS

The authors wish to thank the Interstate Stream Commission for funding the project. Robert Bieberman and Tom Chaves of the New Mexico Bureau of Mines and Mineral Resources were extremely helpful in the search for well logs and well cuttings. Also, Larry Brooks of the Oil Conservation Division in Artesia and Art Bowser at Yates Petroleum Company were very generous with their time and information. Exxon Company in Midland, Texas contributed well logs which were unavailable at the New Mexico Bureau Log Library. Special thanks to Dr. Allan Gutjahr for his assistance in the time series analysis, and to Dr. John Schlue for use of the digitizer.

ABSTRACT

The people of Southeastern New Mexico depend largely on groundwater for their supply of water for irrigation and domestic use. The threat of saline encroachment and depletion of the principal aquifer in the Roswell basin has created a need to model the basin in order to determine maximum pumping rates and water level decline. Although the basin has been studied since the early 1900's, there are still many unanswered questions.

In order to model the groundwater, information about the recharge to the aquifer is needed. It is believed that a substantial part of the recharge comes from below the principal aquifer. The Yeso formation, which underlies the principal aquifer, was investigated with geophysical well logs used in the petroleum exploration of the basin. Wells sample an area approximately 2,600 square miles east of the Sacramento Mountains and west of Roswell and Artesia, which is part of the Pecos Slope. Lithology, porosity, and water volume, were estimated for 15 wells. Permeability was estimated qualitatively for all wells with resistivity logs and quantitatively for one well with a drill stem test. Three permeable groundwater zones, continuous throughout the Pecos Slope, were recognized. There are, in addition numerous discontinuous or perched zones. Estimation of water quality of permeable zones was attempted for all wells with porosity and resistivity logs, but few gave reliable results. Water quality appears to be variable and generally poor, ranging from 1,000 ppm to 430,000ppm (NaCl). The great vertical and lateral variability of lithology in the Yeso, do not allow a more detailed assessment without further research.

A major obstacle to this investigation has been the lack of deep water quality data and subsurface mineralogic information, especially relating to clay minerals. In order to accurately interpret well logs and determine the hydrologic characteristics of a zone, the clay type must be known.

TABLE OF CONTENTS

LIST OF FIGURES

LIST OF TABLES

LIST OF SYMBOLS

LOGS

GR	Gamma Ray Log (API units)
CNL	Compensated Neutron Log
FDC	Formation Density Log
DLL	Dual Laterolog
MSFL	Micro Spherically Focused Log
EL	Electric Log
SP	Spontaneous Potential
LTD	Lithodensity Log
IE	Induction Electric Log
ML	Micro Log
DI-FL	Dual Induction Focused Log
DILL	Dual Induction Laterolog

PARAMETERS

Rt	Undisturbed Formation Resistivity
Ro	Undisturbed Formation Resistivity at 100% Saturation
Rxo	Resistivity of Invaded Zone
Rm	Resistivity of Drilling Mud
Rmf	Resistivity of Mud Filtrate
Rw	Resistivity of Formation Water
RLLD	Resistivity from Deep Laterolog
RLLS	Resistivity from shallow Laterolog
Pe	Photoelectric Effect (parameter from LTD)
VSH	Volume of Shale
DG	Density of Mineral (in limestone porosity units)
DSH	Density of Shale (in limestone porosity units)
DF	Density of Fluid (in limestone porosity units)
DEN	Density from FDC (in limestone porosity units)
CNL	Porosity from the Neutron log
CNLsh	Neutron Porosity Response of Shale
t	Sonic Travel Time (usec/ft)
tm	Sonic Travel Time of Clean Matrix of Zero Porosity
tsh	Sonic Travel Time of Shale
tf	Sonic Travel Time of Fluid
F	Formation Factor
m	Cementation Factor
ppm	parts per million

II. INTRODUCTION

A. Previous Work

The geology and hydrology of the Roswell Basin has been studied since the early 1900's. Oil was discovered in Dayton around 1920, and since then the geology has been studied with great interest. The oil and gas exploration wells in the study area are the sole source on information of the subsurface used in this report. Works by Lloyd (1949), Kelley (1971), Havenor (1968), and Fiedler and Nye (1933) have greatly contributed to an understanding of the geology and structure of the basin.

The first extensive report on the ground-water resources of the Roswell basin was done by Fiedler and Nye (1933). They outlined the principal aquifers and recharge areas of the basin. Hantush (1957) did a quantitative investigation of the principal aquifer to determine hydraulic conductivity and storativity. Further investigation by Gross and others (1976), Duffy and others (1978), and Rehfeldt and Gross (1982) have added to the understanding of the recharge and water budget of the principal aquifer. Welder (1983) prepared water table contour maps which show the long-term hydrostatic head changes in the aquifers of the basin.

B. Purpose of Study

The attempts to model the aquifer have been unsuccessful for lack of understanding of the mechanisms of recharge to the principal aquifer, the San Andres. A recent study by Rehfeldt and Gross (1982) of the principal aquifer indicates that a significant amount of recharge must come from deeper formations, in particular, the Yeso Fm. and Glorieta Ss. The Yeso has been poorly understood because the formation only crops out in a few locations in the area and is below most water wells. The purpose of this study is to use geophysical well logs to determine lithology, porosity, water quality and permeability of the Yeso in hopes of using these parameters in future numerical models.

C. Location and Physiography

The area studied is part of the Pecos Slope and is 2,592 square miles, ranging from 14E to 22E, and 11S to 19S, just west of Roswell and Artesia. Figure 1 shows the location of the area and the wells used in the analysis. West of this area are the north-south trending Sacramento Mountains which reach an elevation of 12,003 ft above sea level. The study area is part of the eastern slope of these mountains. The broad slope is sparsely vegetated with desert flora, such as xerophytic grasses and cactus, and grades into pinon and then aspens and pines in the mountains. Average annual precipitation ranges from 18 inches in Mayhill to 12 inches in Roswell. The average annual temperature is 52 F in Mayhill and 59 F in Roswell.

D. Geology and Hydrology

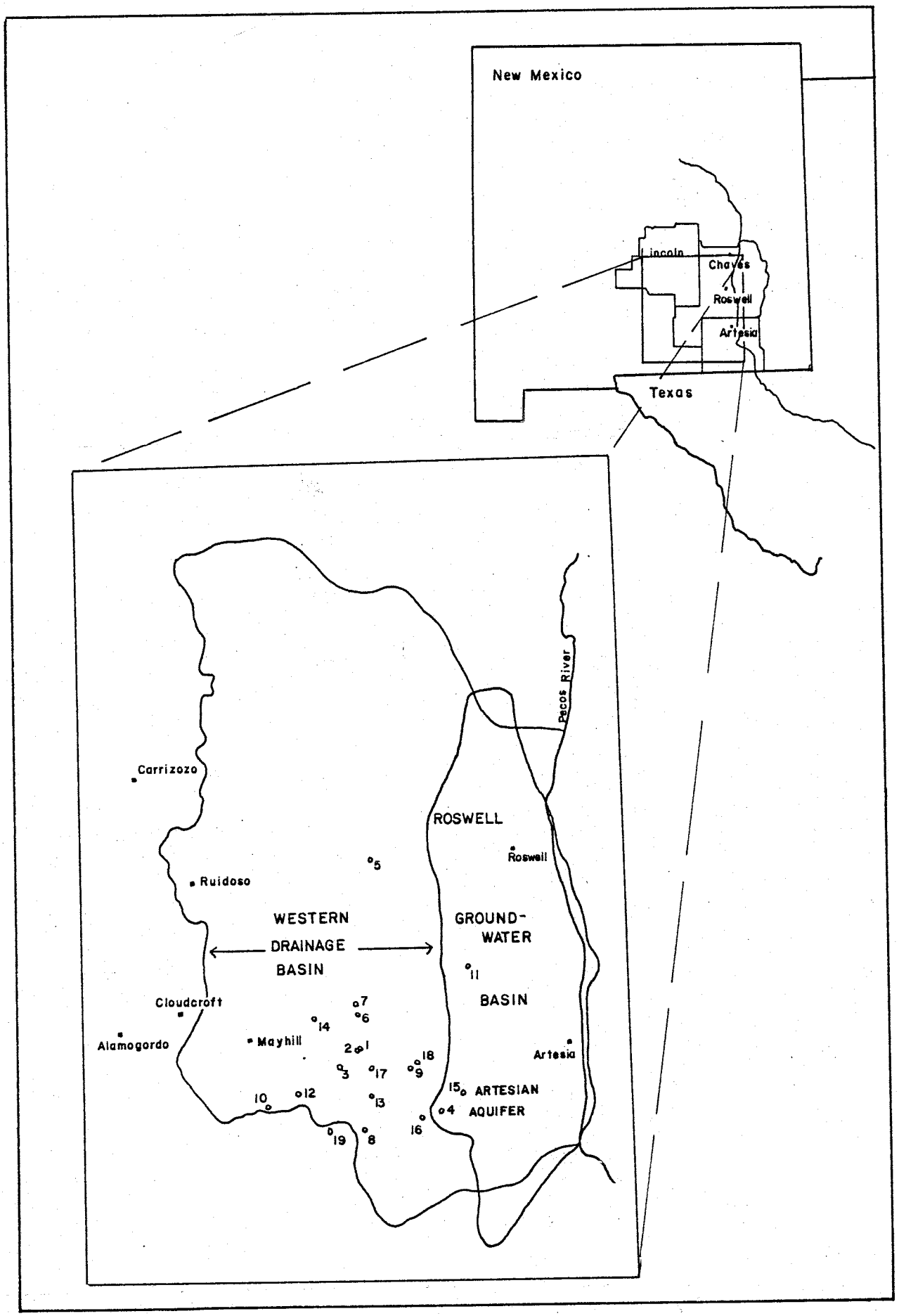

Figure 1. Location of Study Area

The major emphasis of this report is on the Yeso Formation, which overlies the Abo and underlies the Glorieta Sandstone of the San Andres Formation. Fig 2 shows a generalized cross section of the regional geology. Most petroleum exploration wells were cased to below the top of the Yeso, before they were logged, and therefore not much information was gained about the Glorieta and upper Yeso, which is a significant hydrologic unit. The following is a simplified explanation of the geologic units in the area starting with the Abo Formation and ending with the San Andres Formation. For a complete detailed explanation see Lloyd (1949), Pray (1961), Fiedler and Nye (1933), and Kelley (1971).

1. Stratigraphy and Hydrogeologic Characteristics

Permian Abo Formation (middle to late Wolfcampian)

The Abo consists of dark red shales, sandstones, arkose, limestone and dolomite. Near the Pedernal uplift, the Abo is continental in origin, with the Pedernal Mountains as provenance. Further east the Abo has dolomites and anhydrites, representing a transition to a marine environment. In the study area, the Abo was defined on well logs by a sharp increase in the natural gamma radiation, indicating a shale. This shale was also observed in well cuttings as a very dark red fine-grained siltstone. The upper shale unit seems to thin toward the south of the area. The Abo ranges from 200 feet in the northern Sacramento mountains, to 550 feet in the southern part (Pray, 1961) and to 1300 feet in the eastern part of the study area. Little is known about the hydrologic significance of the Abo. It is more than 3000 feet deep in most of the basin and therefore has not been investigated as an aquifer. It appears to be relatively impermeable except toward the south of the study area, where the shale thins and the limestone thickens, there appear to be some beds which are permeable. This is discussed later in this report.

Permian Yeso Formation (Leonard Series)

Yeso is the spanish word for gypsum and is appropriately named because it contains numerous gypsum beds, the provenance for White Sands National Monument (Weber and Kottlowski 1959). The Yeso is a very heterogeneous formation with many thin beds, of limestone, sandstone, dolomite, shale, anhydrite (gypsum at surface), and salt, which were deposited in a saline epicontinental sea. The thickness is approximately 2000 feet and is fairly uniform throughout the study area. Figure 3 is a generalized stratigraphic column for the Yeso.

The lower 400 feet of the Yeso consists of anhydrite and dolomite interbedded, and some lenses of sandstone and salt beds. Above this zone is the Drinkard Sandstone (also known as the Tubb or Fullerton) which ranges from 150 to 400 feet in thickness. The Drinkard consists of sandstone, shaly sandstone, shaly limestone and sandy dolomite. Above this is a 300 to 1100 ft

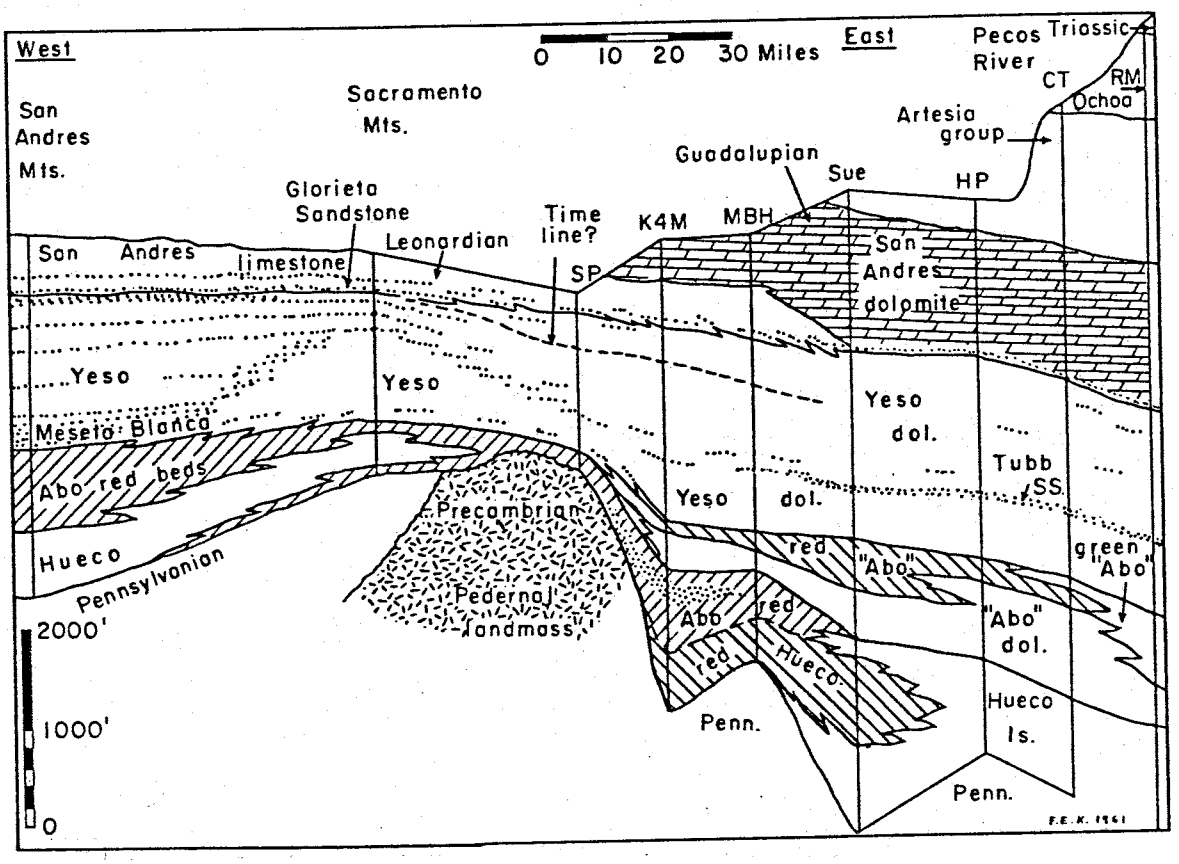

Figure 2. Generalized Cross Section of the Regional Geology (Kottlowski, 1961)

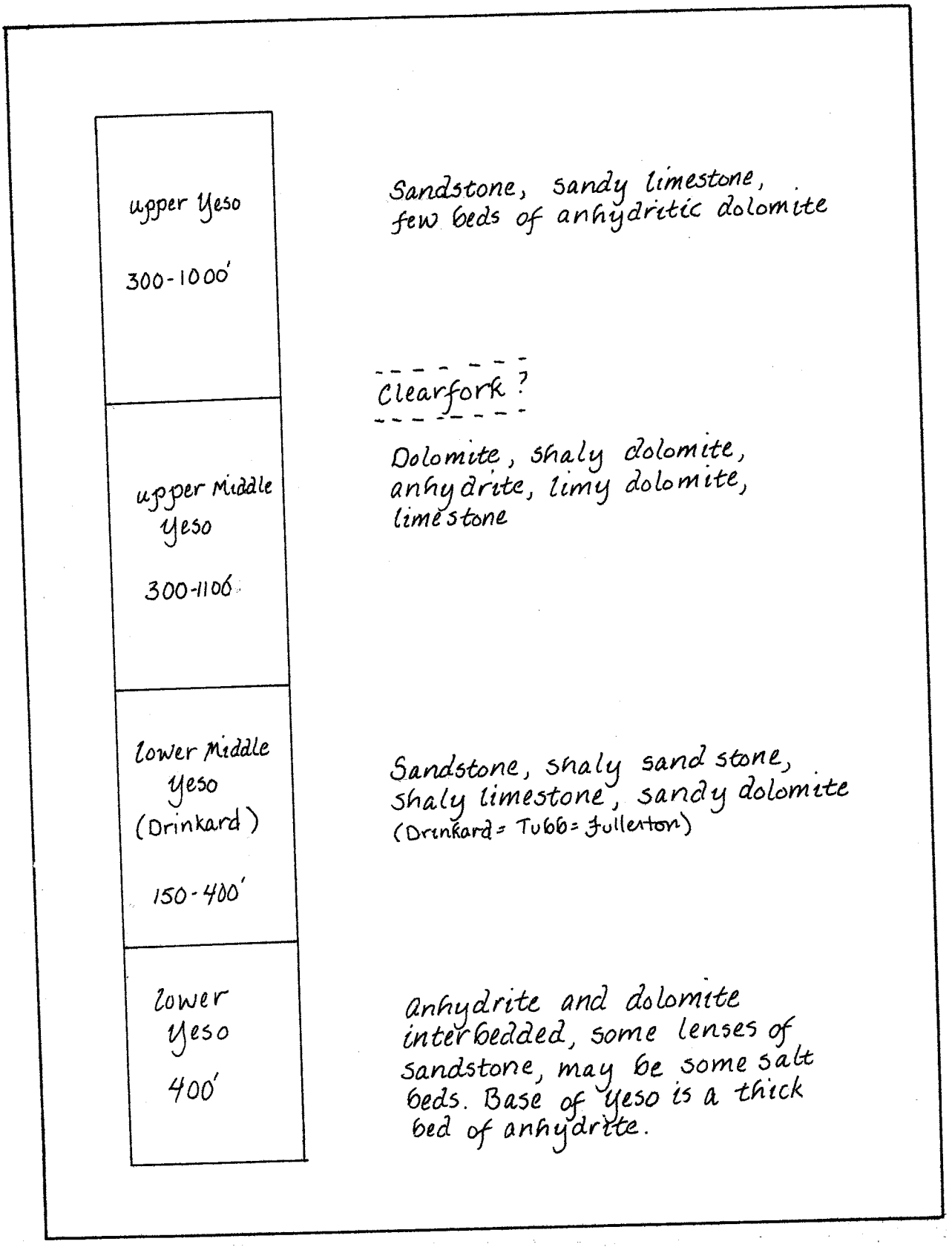

Figure 3. Generalized Stratigraphic Column of the Yeso Formation

zone of dolomite, shaly dolomite, anhydrite, limy dolomite and limestone. The upper unit of the Yeso is 300 to 1000 ft thick and comprises sandstone, sandy limestone, and a few beds of anhydritic dolomite.

A marker bed, designated by a low gamma-ray deflection and bound above and below by a shaly zone, may be the Clearfork (or Blinebry pay) described by Lloyd (1949). This zone is sandstone and sandy limestone or dolomite in some wells and appears to be dolomite and limestone in other wells.

The Yeso contains many water-bearing units, some of which are perched aquifers. Because of the numerous beds of gypsum and salt beds, the water is generally unsuitable for domestic use, however, in some wells the water is adequate for irrigation and stock.

Permian San Andres Formation (Guadalupe Series)

The San Andres is a rather homogeneous formation of limestone, dolomite, and anhydrite approximately 1000 feet thick. At the base of the San Andres is the Glorieta Sandstone which forms a distinctive lithologic unit between the Yeso and San Andres Formation. In the Sacramento Mountains this sand is not a well defined layer, but occurs as thin layers interfingering with the San Andres Carbonates. It is difficult to determine the exact nature of the Glorieta from well logs in the study area because it is unsaturated in the wells of which there are logs. The San Andres has a high secondary porosity due to the solution enlargement of fractures, and has a high permeability. It is considered the principal aquifer in the basin and has good water except in some areas where water at the base of the San Andres is saline, and is believed to be contaminated by upward leakage from the Yeso.

2. General Structure

The Roswell basin is the eastern limit of the Basin and Range type structure. The Sacramento Mountains were formed by the uplift of a pre-Cambrian Pedernal landmass. The eastern dipslope of the mountains is gentle (dipping approximately one degree to the east), but structurally it is complex. Three prominent structural zones of folding and faulting, "Buckles", transect the slope from NE to SW (see Fig 4). The Yeso has numerous incompetent folds caused by solution collapse, hydration of anhydrite, and surficial slump (Kelley, 1971).

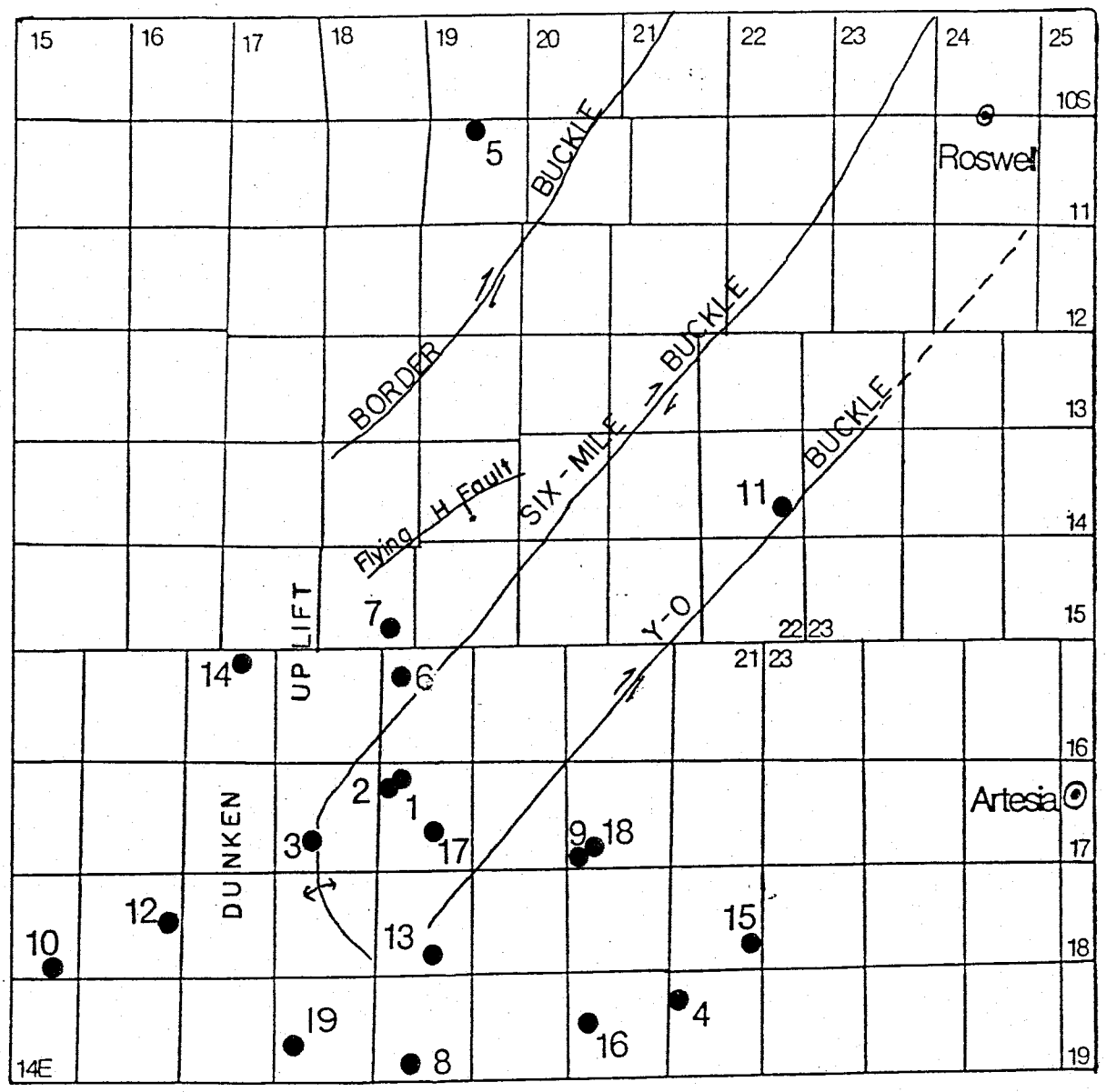

Figure 4. Map Showing Prominent Structural Zones

II. WELL LOGS

A. Location of Wells and Types of Logs Available

The Roswell Basin has been extensively explored by the petroleum industry since 1943. These exploration wells are the key to understanding the Yeso Formation in the study area. Most water wells are only drilled down to the Glorieta and upper Yeso, and the only outcrops of Yeso are in the Sacramento Mountains. Therefore, the information obtained from petroleum exploration wells are the main source to understanding the complex hydrology of the Yeso.

As the petroleum technology developed, more information was obtained from each well, so that the early wells drilled in the 40's and 50's only had "drillers logs" ,or "lithologic logs", which are descriptions of cuttings, and perhaps a resistivity and/or gamma log. These logs provided a means of correlation between wells to determine the subsurface structure. Today, it is common, with each well drilled by the petroleum companies, to collect the cuttings and describe them, to run a series of geophysical logs, which help determine lithology, porosity, and permeability, and to run drill stem tests on specific stratigraphic horizons. Table I is a list of wells and the different logs available for each well. The older wells proved useful, along with the newer, more informative wells, in determining the structure of the study area.

B. General Theory of Well Logs

Geophysical well logs are run immediately after a well has been drilled and before it is cased. The logs are run by lowering, into the hole, a tool which measures a rock parameter, such as resistivity or hydrogen content. When drilling through the Yeso Formation, salt or gypsum based muds were used in most of the wells in order to reduce the amount of caving-in from dissolution of the formation. The following is a brief explanation of the different types of logs, how they work, the problems or errors involved, and how they were applied in this study.

1. Resistivity

There are a variety of resistivity tools, all of which measure either the conductivity or resistivity of the formation. There are many different configurations, however they all generally consist of a transmitter and a receiver in the probe. The spacing of these determines the depth of investigation, that is, the distance into the sidewall. The most useful resistivity logs in this study are ones that measure the resistivity of the formation at varying depths. Figure 5 is a diagram of the borehole environment and the symbols of parameters measured by different resistivity logs. These tools, when used together, give an idea on how much invasion of drilling fluid into the formation has occurred, and therefore, the relative permeability

Table I. List of wells, date drilled and type of logs available.

Well	Location	date drilled	logs available
1	7-17S-18E	4-18-76	Caliper,GR, Sonic, CNL/FDC,DLL
2	7-17S-18E	1-8-77	Caliper,GR,CNL/FDC,DLL
3	21-17S-17E	2-25-81	Caliper,GR,SP,CNL/FDC,DI-FL
4	7-19S-21E	8-4-80	Caliper,GR,Sonic,CNL/FDC,DLL
5	4-11S-19E	11-9-82	Caliper,GR,CNL/FDC,DLL/MSFL
6	8-16S-18E	10-24-66	GR,Sonic,IE/ML
7	26-15S-18E	4-21-67	Caliper,GR,Sonic,IE
8	28-19S-18E	4-3-64	GR,Sonic,ILL
9	31-17S-20E	4-3-51	GR,SP,EL
10	35-18S-14E	1-10-82	Caliper,GR,Sonic,CNL/FDC,DLL/MSFL
11	24-14S-22E	4-9-83	Caliper,GR,CNL/LTD,DLL
12	15-18S-15E	1-11-84	Caliper,GR,CNL/FDC,DLL/MSFL
13	27-18S-18E	6-18-55	GR,SP,EL
14	3-16S-16E	1-8-52	GR-Neutron
15	25-18S-21E	9-22-79	Computer processed log
16	17-19S-20E	3-14-66	GR,Sonic,FDL,DILL
17	20-17S-18E	10-29-82	Caliper,GR,CNL/FDC,DLL/MSFL
18	28-17S-20E	5-27-53	GR,SP,EL
19	19-19S-17E	10-28-51	GR-Neutron

Symbols Used in Log Interpretation

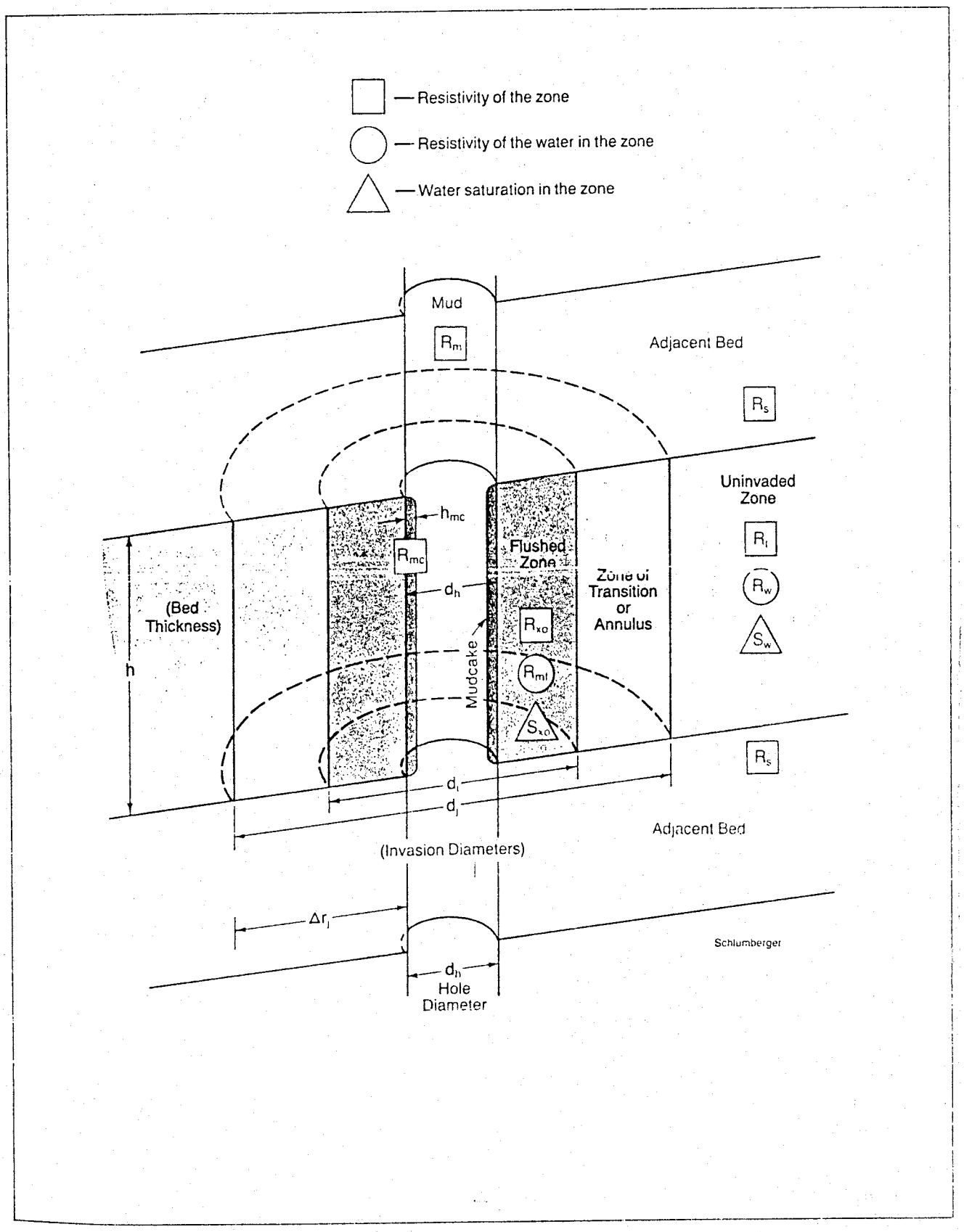

Figure 5. Symbols Used in Resistivity Log Interpretation (Schlumberger, 1985)

of the formation (this is explained in the methods section). Induction logs (IL) are usually "deep" resistivity logs and are good tools for determining the bulk resistivity of the formation because the "borehole and the invaded zone are eliminated from materials being measured" (Hilchie, 1798). However, problems occur when the drilling mud is saline. Kwader (1982) states that the resistivity of the mud must be 2.5 times greater than the resistivity of the formation water in order for the induction tool to work. The Deep Laterolog (LLD) can be used in salt based muds and should be corrected for invasion. Because the Yeso Formation was drilled with salt muds, most of the resistivity logs in the study area are Laterologs (DLL- Dual Laterolog). It is necessary to have an Rxo tool, such as the MSFL (Micro-Spherically Focused log) to correct for invasion. If the porosity and rock type are known, it is possible to determine the resistivity of the formation water. The resistivity logs are affected by bed thickness, some tool configurations more than others. For any quantitative work using a deep resistivity tool, the stratigraphic zone being investigated should be at least eight to ten feet thick. The logs should also be corrected for invasion and for the borehole environment.

Resistivity logs were used in this study to qualitatively determine permeable zones and attempt to estimate water quality. The Micro-Focused logs are excellent tools for determining permeable zones, however, the Yeso was not logged with a Micro-Focused log in any of the wells. This is because Micro-Focused logs do not work well in salt or gypsum based muds.

2. Gamma Ray Log

The Gamma Ray log is a measure of the natural gamma activity emitted from the formation. This parameter is most useful in stratigraphic correlations but may also be used to help infer lithology. The gamma radiation is primarily due to the decay of three naturally occurring elements; potassium-40 (K^{40}), and daughter isotopes in the uranium (U) and thorium (Th) decay series. The Gamma Ray log is often considered a "shale indicator" because shales usually have higher gamma radiation than other sediments. This is not always the case, however. Any formation with minerals which incorporate potassium, uranium, or thorium in their lattice structure will have high gamma activity. Potassium feldspars, micas, volcanic ashes and illite clays are a few potassium-rich minerals and rock types with high gamma activity. Phosphorites, apatites, organic materials, uraniferous sands and dolomites have relatively high concentrations of uranium and thorium. Therefore, if any of these minerals are present in the formation in high concentrations, they may appear to be "shaly". The Gamma Ray log must be used cautiously and is more useful when used in conjunction with other lithologic indicators. For instance, if the neutron-density log indicates that the formation is a dolomite and the gamma count is high, it could either be a shaly limestone or a 'hot' dolomite. If the resistivity logs indicate the formation is permeable, then it is probably a 'hot' dolomite. A permeable formation is generally

Table II. Range of Gamma Activities for Selected Minerals. (Keys and MacCary)

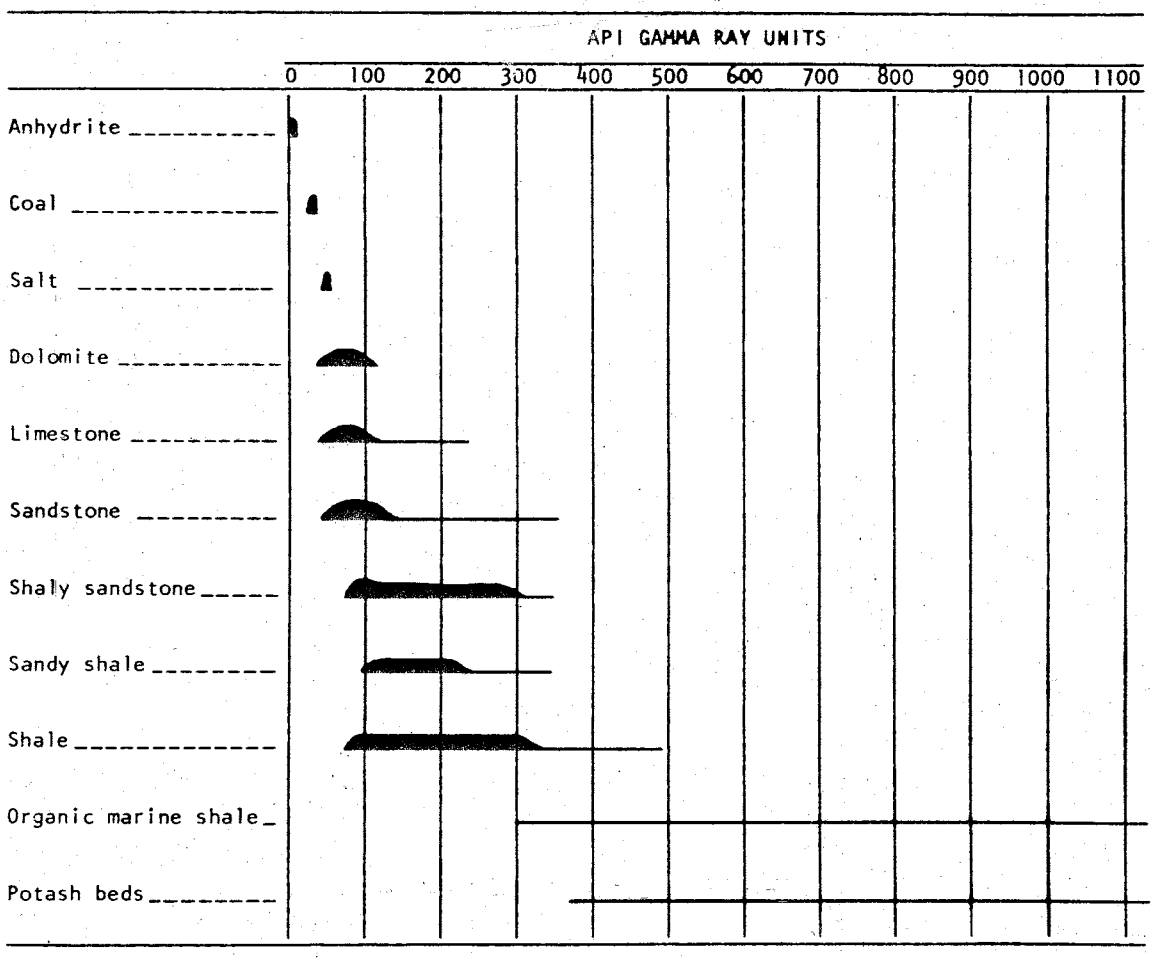

not "shaly", because shale resists the movement of water, and dolomites are usually not shaly because it is necessary for water to migrate through a formation for dolomitization to occur.

Another geophysical log is the Gamma Spectrometer probe which distinguishes potassium from thorium and uranium,and therefore could be used to distingiush gamma-active dolomites from clays. However, a study, by Kwader(1982), of clays and dolomites showed no fractionation of the gamma source, both the clays and the dolomites had equal proportions of potassium, thorium, and uranium. This may mean that the Gamma Spectrometer is not useful in carbonate environments because the clays are derived from weathered carbonates. No Gamma Spectrometer logs were available for any wells in the study area.

The Gamma Ray log was also helpful in another case where the neutron, density, and sonic logs indicated that there was possibly carnalite in the formation. Carnalite is potassium-rich and should therefore have a high gamma activity, however, the gamma count was low, and carnalite was ruled out.

The emission of gamma rays is a random statistical process and is therefore affected by the rate of logging. Some of the older logs were run at a faster rate, which has the effect of smoothing and makes it difficult to pick thin beds. The Gamma Ray log is an excellent tool for correlation over a large region because the gamma activity is greatly affected by slight changes in depositional environments and sediment source areas. However, it can be difficult to correlate the older gamma logs with the newer ones which were run much slower. The problem was overcome by smoothing the gamma ray for the newer log and then correlating it with the older logs.

The Gamma Ray log was used in this study to pick formation tops, determine lithology, and calculate percent clay. Table II shows the range of gamma activity for selected minerals.

3. Neutron-Density and Lithodensity logs

The Neutron and Density (Gamma-Gamma) logs are usually run together. These two logs are very useful in determining lithology and porosity. A more recent log is the Lithodensity log which provides an additional parameter that helps clarify lithology.

The Neutron log measures a formation's ability to attenuate the movement of neutrons through the formation from the neutron source, usually americium-beryllium, to the detector. The neutrons are attenuated by hydrogen atoms, so this log basically measures the hydrogen content in the formation. The source of hydrogen is oil or water, which both have the same amount of hydrogen. Water is present in the pore space, or it is bound to clay minerals or incorporated in the mineral structure as OH groups, as in gypsum or clay minerals. If the only source of hydrogen is water or oil, than the amount of hydrogen can be an

indicator of porosity if the lithology is known. A higher porosity, if saturated, will have more water, and thus a greater neutron attenuation, than a lower porosity formation. There are two types of neutron logs, the Sidewall Neutron (SNP) and the Compensated Neutron (CNL) log. The Sidewall Neutron log is less reliable because it is easily affected by the borehole environment. Only the CNL Neutron log was used, along with the Density log, to determine porosity and lithology.

The Density (Gamma-Gamma) log measures the electron density of the formation using Compton scattering of gamma rays. A source of medium high energy (0.6-1.3 Mev) usually Cs^{137} or Co^{60} in the probe emits gamma photons into the formation. When these photons collide with an electron they lose energy and are "scattered". The greater the density of electrons (i.e. the greater the atomic number), the greater the attenuation of the gamma photons. Therefore, the attenuation of gamma rays can be related to formation density and porosity if the lithology is known.

The Lithodensity log also determines electron density using Compton scattering, but in addition it measures the results of low energy gamma ray interactions with the formation (photoelectric effects). The lower energy gamma rays have collided with the nucleus of the atom and have lost more energy than in the Compton scattering. Therefore, the size of the atom can be related to the probability for collision, and thus, larger atoms cause greater attenuation. This is expressed as a "photoelectric cross section" (Pe). This can then be related to the lithology. Only two wells in the study area had a Lithodensity log, which greatly aided the determination of lithology.

The Neutron and Density logs are generally used together to determine lithology and porosity with the aid of empirical graphs provided by the logging companies.

4. Sonic Log

The Sonic log, or Acoustic Velocity log, is a measure of the travel time of a pulse between the transmitter and receiver in a probe. The travel time is influenced by lithology and density of the formation. If the lithology is known, porosity can be determined from the log. Along with the neutron log, the Sonic log can help determine lithology.

The Sonic log can also be used to determine secondary porosity if used in conjunction with other porosity logs. In a formation, the acoustic pulse will travel the fastest path between two points, which is through the densest portion of the rock, and by-pass the large vugs and fractures. The log will then record a faster travel time, thus indicating a lower porosity than the actual value. Comparison of this value with the porosity determined from the Neutron and Density logs gives an estimate of secondary porosity.

The Sonic log was used in this study to determine lithology, secondary porosity, and to estimate porosity when no other porosity log was available.

5. Spontaneous Potential

The Spontaneous Potential (SP) log can be useful in identifying permeable beds, estimating water quality, and qualitatively indicating shaliness. The SP works by measuring the potential drop of a current flowing around a triple junction between fresh water, salt water and shale. The triple junction occurs where the contact between shale and a permeable formation is cut by a borehole. If the drilling mud is "fresh" and the formation water saline, the current will flow from the borehole into the permeable formation. It is necessary that a considerable contrast exist between the formation water and the drilling mud in order to obtain a measurable SP deflection. It is also necessary that the permeable zone be granular and bounded by a shale in order for a potential to develop. For quantitative interpretation, beds must be of sufficient thickness. These requirements are violated throughout the Yeso Formation, and therefore the SP was not used in this study. In many cases, wells in the Yeso were drilled with salty mud (Rm < Rw), and this invalidates the assumptions on which quantitative interpretation of the SP log is based.

6. Caliper Log

The Caliper Log measures the diameter of the uncased well. This must be known to correct many of the logs, especially the Resistivity log. Many of the logs are borehole compensated already, such as the Sonic log and the Compensated Neutron Density log. The Caliper log will indicate zones which have "washed out" or "caved in". This can help in determining lithology. Shales usually cave in, anhydrites do not. At the base of the Yeso, there is much caving in, and this increases more to the west. This may indicate salt beds which dissolve easily during drilling (anhydrite also has a high solubility, but is very "tight", thus water does not flow through to rapidly dissolve it). It is reasonable that there would be more salt westward toward the mountains (which was the coastline at the time of deposition) because salt is one of the last minerals to form as water evaporates, and therefore it will precipitate in enclosed lagoons near the shore.

C. METHODS OF INTERPRETATION

There are two methods of dealing with the data from well logs. One way is to roll the logs from a well out on a table and pick beds to be analyzed. The other way is to digitize the logs and then run the values through computer programs to determine various parameters. Both of these methods were used in this study. The lithology and permeability needed to be determined by hand, but the digitized data proved to be a very useful and efficient method for determining porosity and for developing statistical relationships between porosity and resistivity. The different methods for determining the various parameters are explained in the following discussion.

1.ESTIMATION OF POROSITY

a.Neutron-Density Crossplot

An estimate of the porosity (POR) at a depth can be made by plotting the Neutron porosity (CNL) versus the Density (DEN) on the interpretation chart reproduced in Figure 6. This chart is for logs which are calibrated for limestone matrix (density of 2.71 g/cc). The Density log is expressed in terms of porosity of limestone, or any designated matrix. If the matrix is dolomite with zero porosity, the Density porosity will read approximately -9% and the Neutron porosity, +2.5%. If the matrix is sandstone with zero porosity, the Density porosity will be approximately +3% and the Neutron porosity will be approximately -3%. If a point does not plot on a matrix line (e.g. the dolomite line), then porosity can be interpolated between isoporosity contours (Hilchie, 1978,p.10-2). An approximation to the curves of this chart is given by the equation (Hilchie, 1978, p.10-12):

$$POR = \sqrt{\frac{CNL^2 + DEN^2}{2}} \qquad (1)$$

When the density or neutron porosity is negative, then the following approximation can be used (Hilchie, 1982, p.V-11):

$$POR = 2/3(CNL-DEN) + DEN \qquad (2)$$

These equations were used in a computer program (called VOID.FOR, App 6g) to estimate porosity from the digitized data.

If shale is present in the formation it will usually increase the apparent porosity on the CNL log and lower the apparent porosity on the Density log. To correct for clay in the formation, if the clay type is known (which is not easily determined), and the clay is dispersed, the following equations can be used (Frost and Fertle,1980, p.17):

Figure 6. Neutron-Density Crossplot

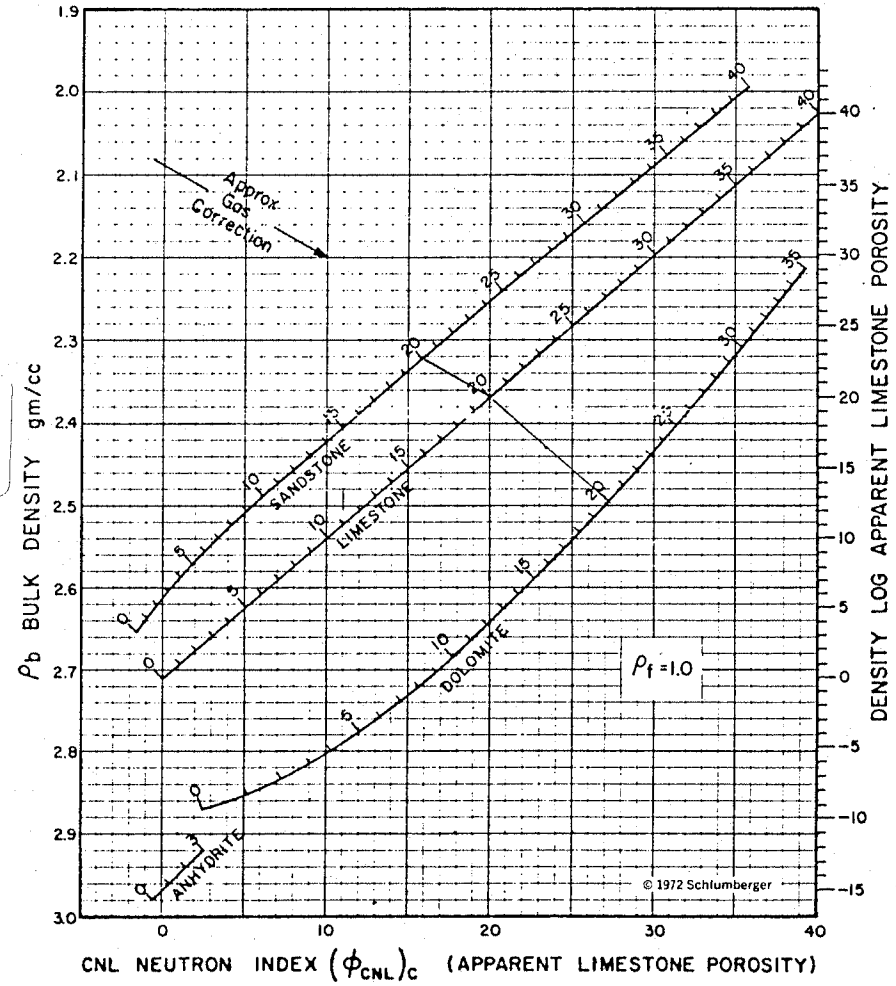

Figure 7. Neutron-Sonic Crossplot (Schlumberger, 1985)

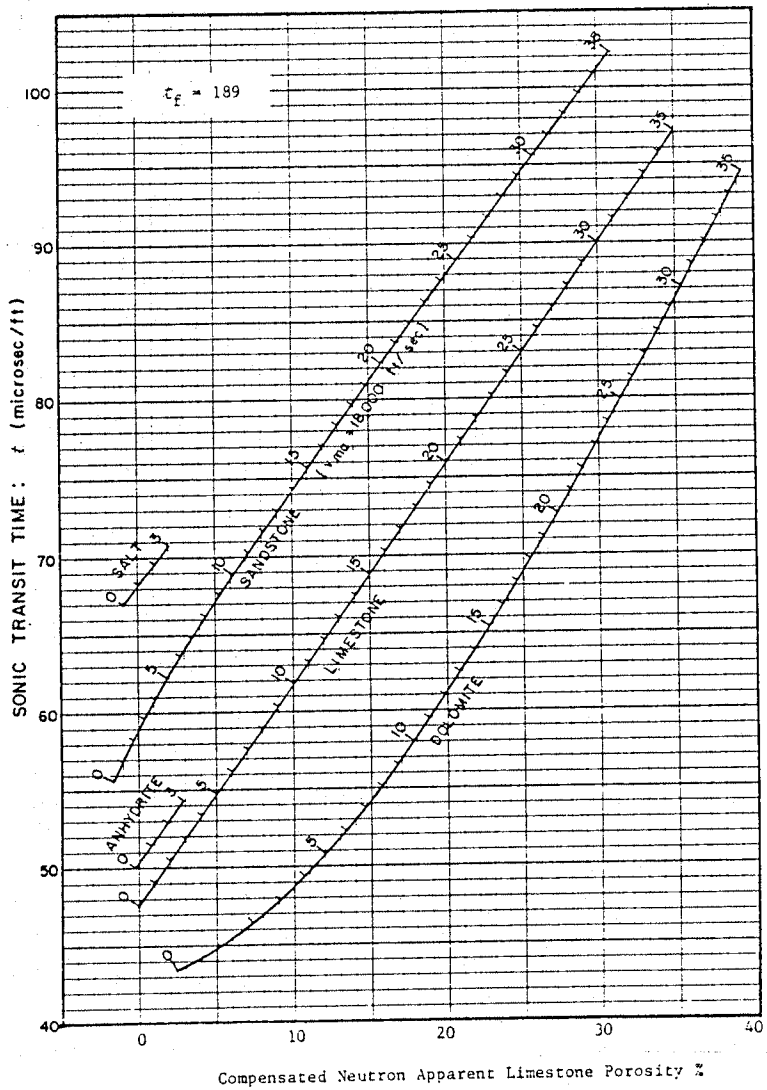

Correction for the Density log

$$POR = \frac{(DEN-DG)-VSH(DSH-DG)}{DF-DG} \quad (3)$$

where:
DEN = porosity from the Density log
DG = density of mineral (in limestone porosity) = -.05
DSH = density of shale (in limestone porosity) = .02
DF = density of fluid (in limestone porosity) = 1.0
VSH = percent volume of shale

Correction for the Neutron log

$$POR = CNL - VSH(CNLsh), \quad (4)$$

where:
CNL = porosity read from Neutron log
CNLsh = Neutron porosity response of shale

Determining the type of shale is discussed in the lithology section in detail. Briefly, the value of .02 for the Density porosity and .3 for the Neutron porosity response of shale was determined from the log where the Gamma Ray had the highest activity. A value of 2.80 g/cc (-0.05 in terms of limestone porosity) was chosen for the grain density because it is intermediate between dolomite and limestone.

b.Neutron-Sonic Crossplot

Porosity can be determined by plotting the Neutron porosity versus Sonic travel time on Figure 7. This will also give an idea of the lithology. The travel time can also be corrected for clay content from the following equation (Frost and Fertle, 1980, p.17):

$$POR = \frac{(t-tm) - VSH(tsh-tm)}{(tf-tm)}, \quad tsh < 100 \text{ usec} \quad (5)$$

where:
t = interval transit time read from log
tm = travel time of clean matrix of zero porosity
tsh = travel time in shale
tf = travel time in fluid

This corrected value can then be cross-plotted with the corrected CNL to obtain a corrected porosity.

c.Density-Sonic Crossplot

The Density-Sonic crossplot will estimate porosity (see Fig 8), but it is not particularly useful in distinguishing lithologies. An effective porosity can be estimated by the following equation (Frost and Fertle, 1980, p.17):

$$POR = \frac{(DEN-DG)(tsh-tm)-(t-tm)(DSH-DG)}{(DF-DG)(tsh-tm)-(tf-tm)(DSH-DG)} \quad (6)$$

d.Sonic Log

The sonic log alone does not determine porosity unless the lithology is known. If that is the case, then Figure 9 can be used or Wiley's time weighted equation (Hilchie, 1978, pg 6-1):

$$POR = \frac{t-tm}{tf-tm} \quad (7)$$

This equation was used in three well where there were no other porosity logs available. Values of 189 microseconds for tf and 45 microseconds for tm were used. This proved to approximate the porosity fairly well if secondary porosity was not significant (see Table III of Comparisons of Porosity and Lithology Estimates).

Because of the complex lithology in the Yeso, the equations for correcting for volume of shale were not necessarily accurate because there are too many unknowns. When corrected, the porosity did not change significantly (see Table III), and consequently the uncorrected value for porosity was used in the final analysis.

Table III uses three examples to compare lithology and porosity as estimated from various methods. The number in each column is the porosity (except for t, which is the travel time in usec) and lithology is written in abbreviated form, LS for limestone, 'sand' for sandstone, 'dolo' for dolomite, and 'anhy' for anhydrite.

2. ESTIMATION OF LITHOLOGY

Information about lithology is essential for quantitative well log interpretation. Furthermore, it is important in hydrologic studies to know what lithology is present in order to understand the type of porosity, the nature of the permeability, and to determine the quality of the water.

a. Estimating Clay Content

LITHOLOGY IDENTIFICATION FROM FORMATION DENSITY LOG AND SONIC LOG

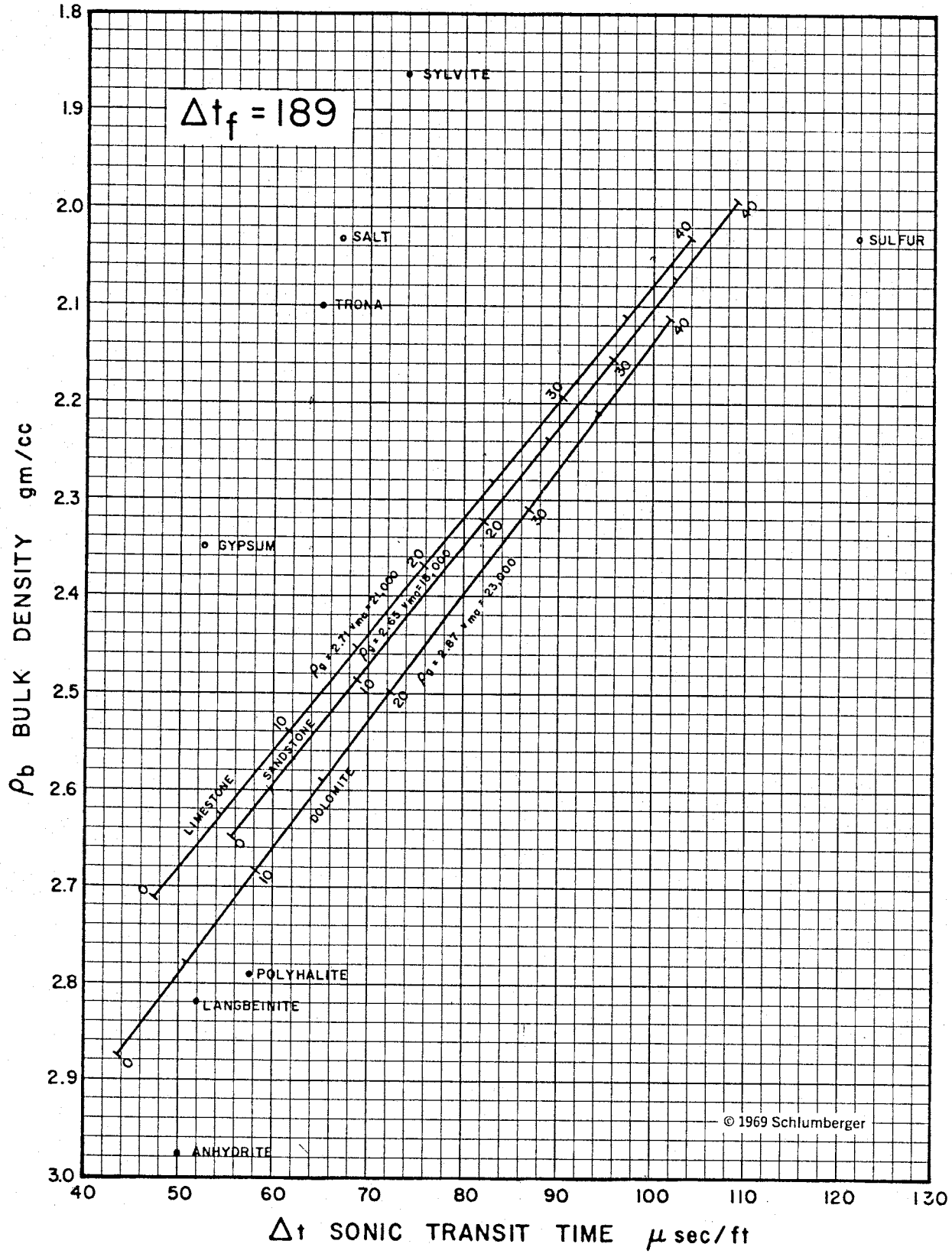

Figure 8. Density-Sonic Crossplot

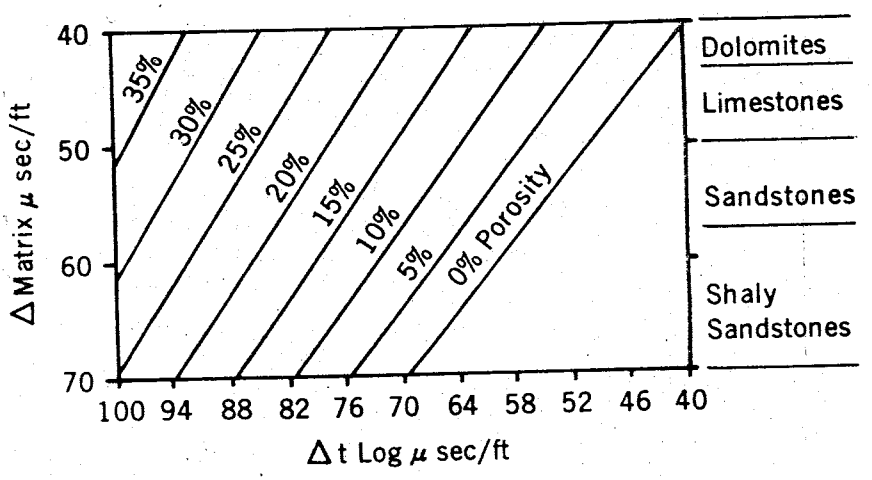

Figure 9. Porosity Determined from the Sonic Log (Keys and MacCary, 1971)

Table III. Comparisons of Porosity and Lithology Estimates

		Example 1	2	3
measured from log	Travel time t (usec)	90	53	58
	Density porosity (DEN)	28	2	11
	Neutron porosity (CNL)	30	2	24
	% clay (VSH)	22	11	11
POROSITY =	DEN vs CNL crossplot	30 LS	2 LS	17.5 dolo
	CNL vs t crossplot	30 LS	3.5 anhy	16.5 dolo
	$\left[\frac{CNL^2 + DEN^2}{2}\right]^{-2}$	29	2	18.7
	2/3(CNL-DEN)+DEN	29.3	2	19.7
	t-tma tma = 45 tf-tma tma = 47	31.3 30.3	5.6 4.2	9 7.8
	$\frac{(DEN+.05)26-(t-45).07}{17.22}$	31.5	7.3	18.0
	$\frac{(t-45)-VHS(26)}{144}$	27.3	3.6	7.0
DENcor	$\frac{(DEN+.05)-VSH(.07)}{1.05}$	29.96	5.9	14.5
CNLcor	CNL - .3(VSH)	23.4	-1.3	21.0
	DENcor vs CNLcor crossplot	27 sand	2 sand	18 LS
	CNLcor vs tcor crossplot	25 LS/sand	0 anhy	13 dolo
Lith	MID	calcite	calcite	dolo (sec. por)
	M-N	dolo-ss-ls	dolo-ss-ls	lime (sec. por)

Determining the amount and type of clay has been one of the most difficult problems in analyzing the well logs. It is also one of the most important parameters because it will affect porosity, water quality, and lithology determinations. Table IV lists the types of clays and their response on logs. All clays respond as high porosity (more than 40%) on the Neutron log. There are many equations for correcting for clay content, but the type of clay must be known, the volume of clay, and whether the clay is laminated or dispersed.

A common method of determining clay content is by using the Gamma Ray log as a shale indicator. There is much room for error when using the Gamma Ray log for quantitative work, when very little is known about the rock type. These problems were presented in the discussion of the theory of the Gamma Ray log.

If the gamma activity throughout a formation is all due to a particular type of clay, then the percent clay can be determined by solving for the Gamma Ray Index (GRI), (Eq 8), and then determining the percent clay from Figure 10.

$$GRI = \frac{GRlog - GRclean}{GRshale - GRclean} \qquad \text{(Hilchie, 1982)} \qquad (8)$$

This method was used to determine percent clay, which is probably a maximum value since some "clean" or non clay rocks may have a relatively high natural radioactivity.

In order to determine the type of clay, the zones with the highest gamma readings were analyzed. The values for CNLsh, DENsh, and tsh were determined from these zones and used to solve the mixing equations for lithology and to correct for shale volume. Typically, the zone of highest gamma response, in the studied wells, showed a Neutron porosity of 30 %, Density of 2%, and a gamma count of 180 API. This indicates a kaolinite. It seems odd that there would be kaolinite in a carbonate environment, since kaolinite forms in acid swamp environments, however the clay may be derived from weathering of another formation. Another potential difficulty is that the zone analyzed for clay type was in the Abo Formation, which is below the Yeso. The Yeso has low gamma activity, and perhaps no pure shale beds, as compared to the Abo which is mostly shale. This may not present a problem since the source area probably did not change much for the two formations in the vicinity of the study area. Lloyd (1949) states that during the Permian, in the area of the Pedernal Mountains, erosion was mostly of Precambrian rocks. Kelley (1971) states that "Arkosic sandstone and conglomerate are common in the basal parts of the Abo, Yeso and locally in the San Andres where these beds lap onto or are in proximity to Precambrian exposures." However, weathering of the Precambrian rocks may not have been the only source of clay in the Yeso, and therefore, there may be many types of clays.

Table IV. Response of Clay on Logs

Mineral	Kaolinite	Montmorillonite	Illite
Formula	$Al_4Si_4O_{10}(OH)_8$	$Al_2Si_4O_{10}(OH)_8 \times H_2O$	$K_{1.5}Al_4(Si,Al)_8O_{20}(OH)_4$
Gamma	Mod	Low	High
Neutron	High H (40+)	High H (40+)	High H (40+)
Density	2.69g/cc	2.33	2.76
Acoustic	Increases t	Increases t	Increases t
EL	Mod Res	Low Res	Low Res

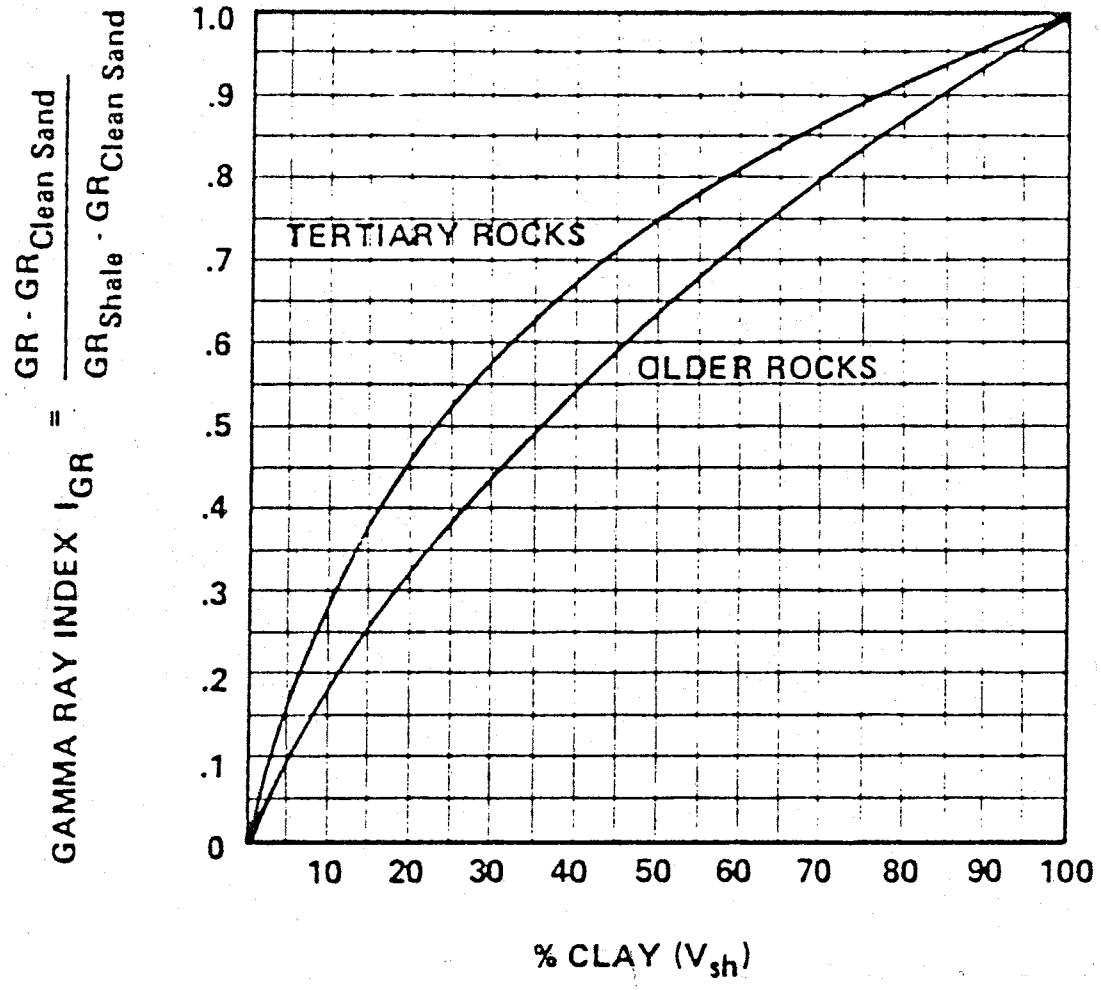

Figure 10. Shale Volume Determined From Gamma Ray log (Hilchie, 1982)

Hilchie (1982) suggests the possibility of using the Lithodensity log, in conjunction with the Gamma Ray log, to distinguish clay types. Figure 11 is a crossplot of Gamma versus Pe for well no 12. The points for mineral identification (on Fig 11) are from Hilchie (1982). The Gamma Ray value (API units) is highly variable, and therefore, this method will not distinguish clay types unless the approximate radioactivity of each clay (and dolomite) is known. If this were known, and a crossplot of Gamma Ray versus Pe showed a definite grouping near a specific clay type, then this method might be useful in distinguishing clay types.

Figure 12 is called a Z-plot and is a crossplot of CNL versus DEN porosity. The different symbols represent ranges of % clay calculated from the Gamma Ray log with Equation 8. Supposedly, the high Gamma Ray values (high percent clay) should converge on one point, the clay point on the Z-plot. The clay point is supposed to be the point where a "pure clay" would plot on the Neutron-Density crossplot. As shown in Figure 12, the higher percent clay values do not converge on a point. Z-plots for wells 1,2,3,4,10, and 11 are in Appendix 1. The high percent clay values for wells no 1,2, and 3 do appear to cluster in an area near the montmorillonite point which is the high porosity portion of the limestone and dolomite lines. This, therefore, does not help determine whether the high Gamma-Ray count is from radioactive dolomite or from clay. In wells no 4 and 11, there is no differentiation between percent clay values, all points plot on the low porosity portion of the dolomite and limestone lines. In well no 10, there is a great deal of scatter for all percent clay values, indicating much lithologic heterogeneity.

The problem with these techniques for determining shale type and volume is that the clean matrix is supposed to be granular (i.e. a sandstone), which is not always the case in the Yeso Formation. Another problem may be that there are no "pure" shale beds in the Yeso.

b. Crossplots

Figures 6, 7, and 8, used to estimate porosity, are also used to determine lithology. Figures 13 and 14 are the same as 6 and 7, but expanded to include more mineral types. If gas or shale are present, the lithology must be corrected by shifting the point plotted to the upper left if shale is present, or to the lower right is gas is present (see Fig 6). The Yeso was assumed to be 100 % saturated, and therefore, no gas correction was applied. The Shale correction can be done quantitatively by correcting the porosities for shale volume (Eq 3,4,5) and then plotting on the cross plots. These crossplots assume a clean, one or two-mineral matrix. From the upper left to the lower right of the crossplot, shows an increase in density; sandstone at 2.65g/cc, limestone at 2.71g/cc, and dolomite at 2.87g/cc. If a sand is iron-rich it will be more dense than pure quartz and might plot closer to the limestone line. If dolomite or anhydrite were present in the sandstone it would also tend toward

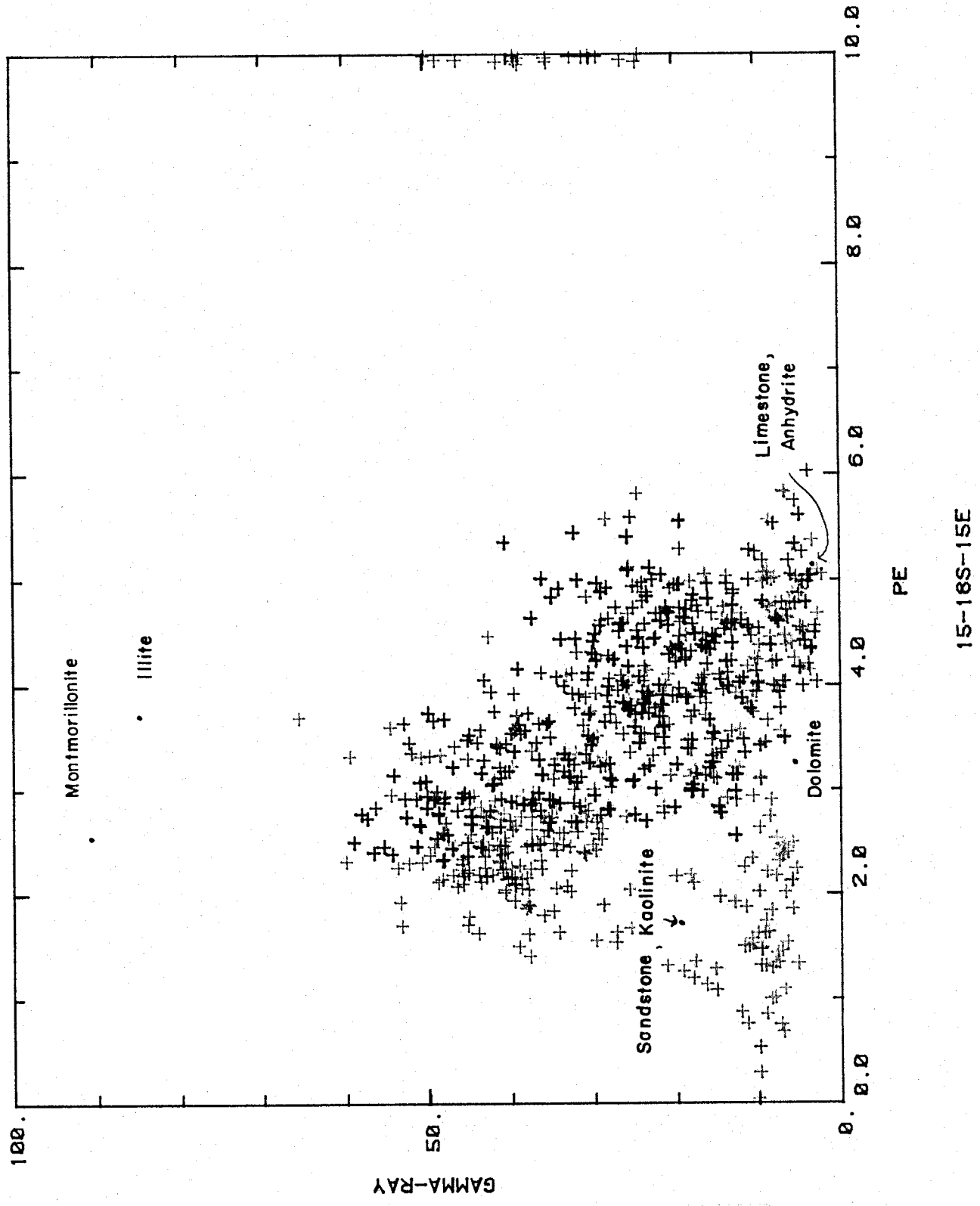

Figure 11. Plot of Gamma vs Pe for Determining Clay Type

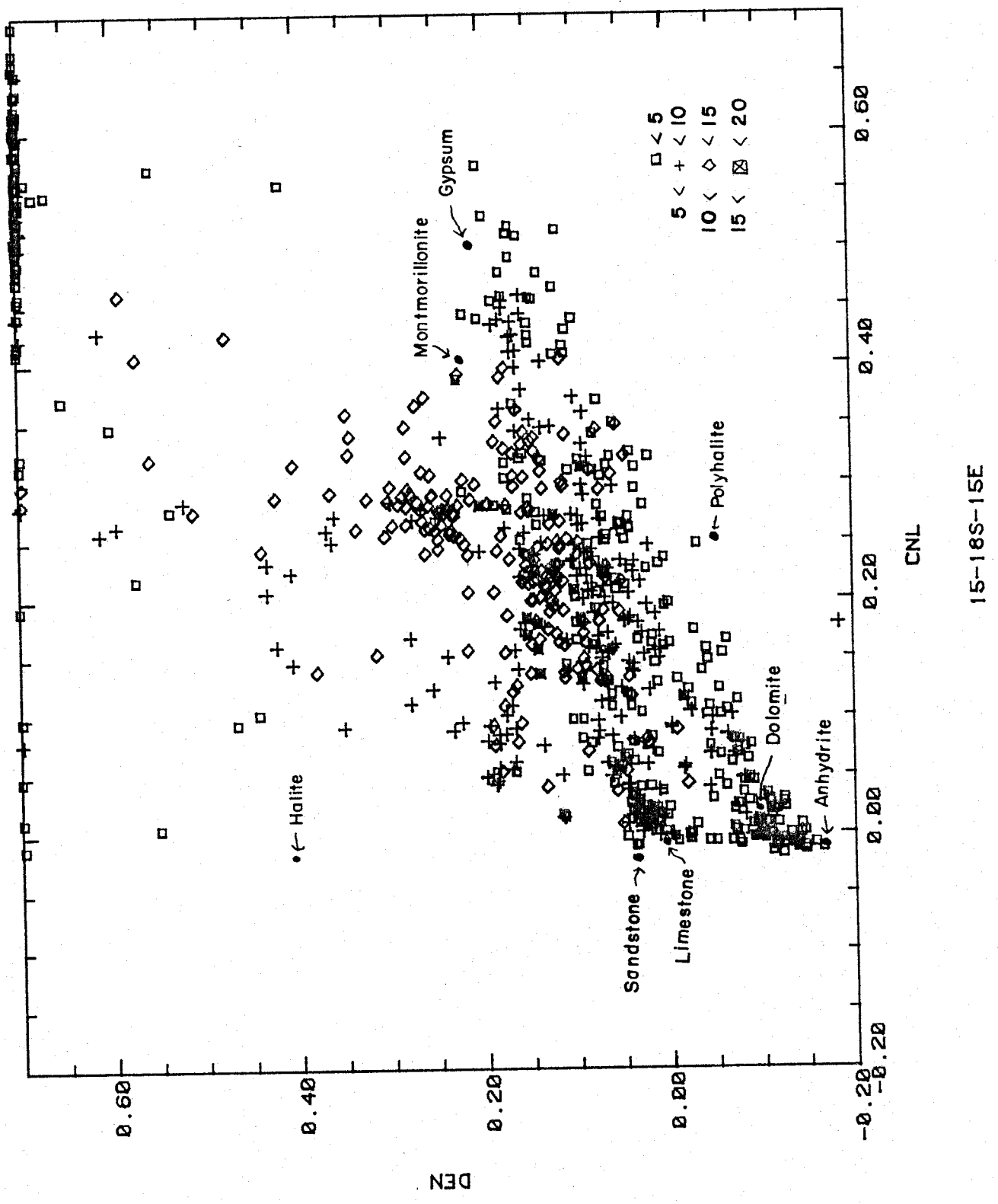

Figure 12. Z-plot for Well no 12

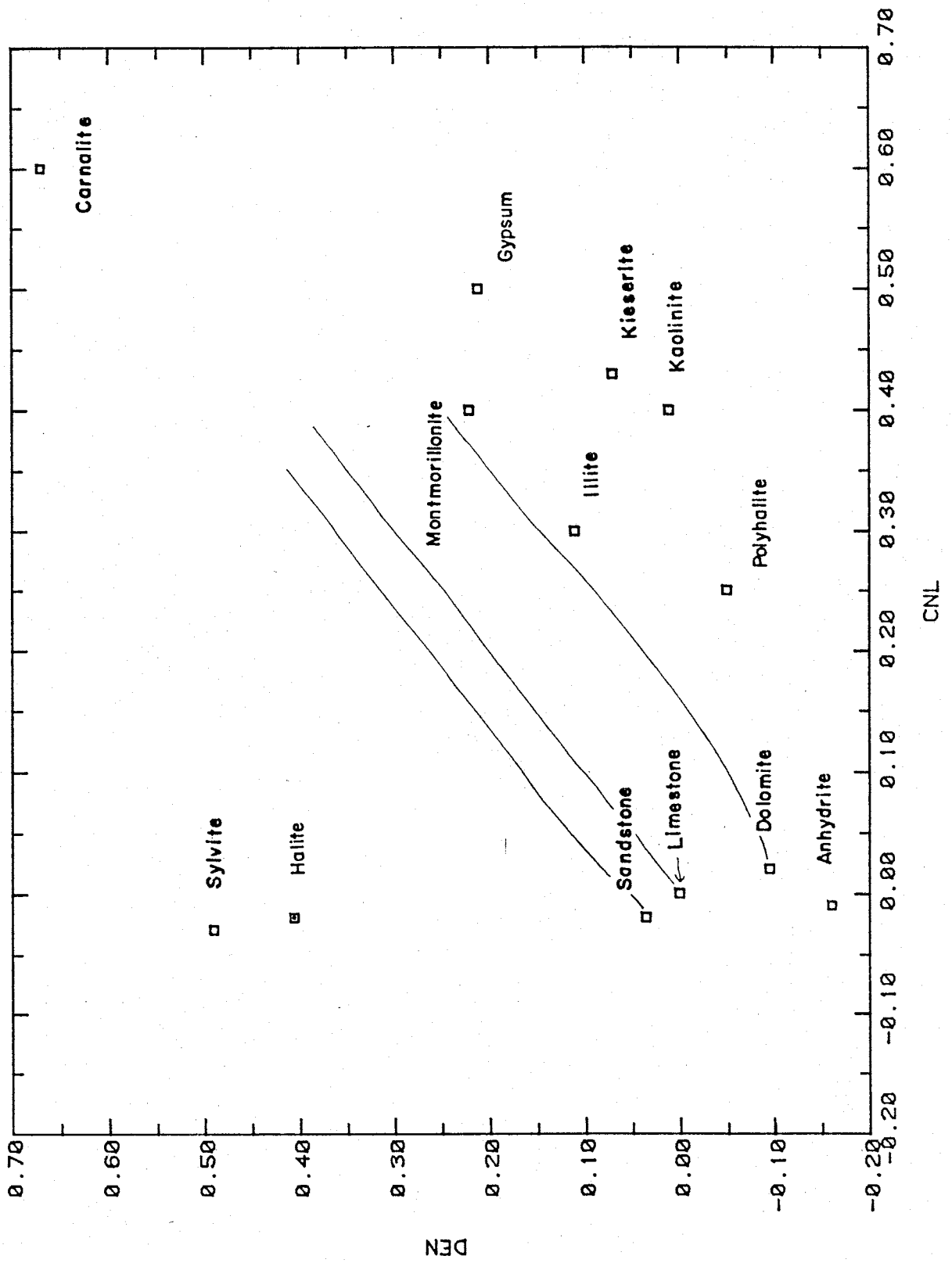

Figure 13. Neutron-Density Crossplot for Mineral Identification

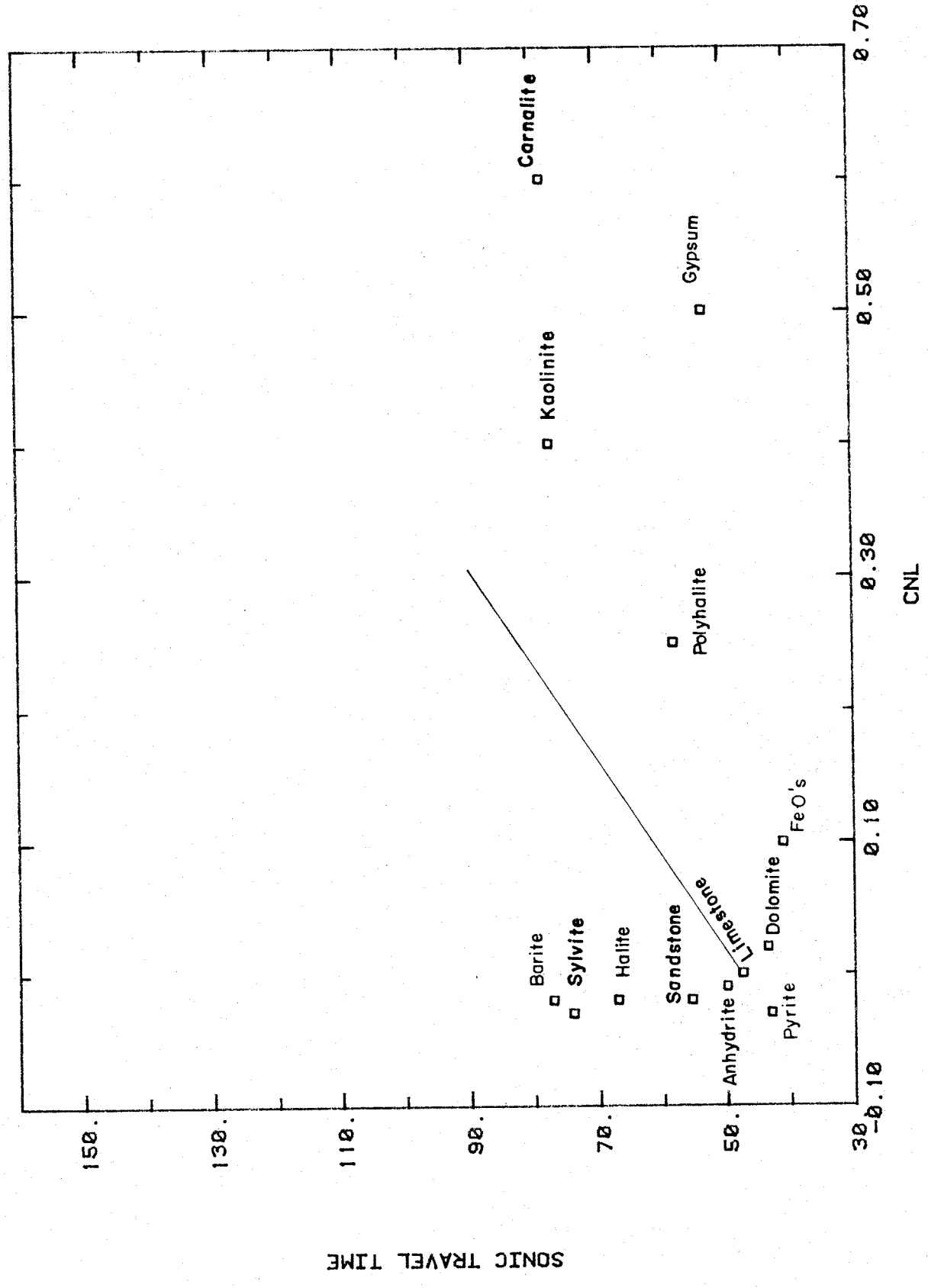

Figure 14. Neutron-Sonic Crossplot for Mineral Identification

the limestone line.

c. Use of Three Porosity Logs

An attempt to solve for lithology (of three minerals) with a computer program (see App 6b), solving four equations with four unknowns was unsuccessful for a variety of possible reasons. One possibility is that the equations do not have a unique solution, because the mineral response on the logs is not unique. Another possibility is that there are more than three different minerals, or the "known" parameters were incorrect. The mixing equations (Hilchie, 1978, pg 14-6):

$$t = tss(Vss) + tls(Vls) + tdolo(Vdolo) + tf(POR) \quad (9)$$

$$CNL = CNLss(Vss) + CNLls(Vls) + CNLdolo(Vdolo) + CNLf(POR) \quad (10)$$

$$DEN = DENss(Vss) + DENls(Vls) + DENdolo(Vdolo) + DENf(POR) \quad (11)$$

$$1 = Vss + Vls + Vdolo + POR \quad (12)$$

the unknowns:
POR = porosity
Vss = volume of sandstone
Vls = volume of limestone
Vdolo = volume of dolomite

Any combination of rock types can be substituted and additional equations were added using the Pe curve from the Lithodensity log and the Gamma Ray log, in order to solve for more rock types. The program solved a synthetic example, which means there should be a unique solution and that the response of the different minerals on the logs (i.e. CNLss, DENss, etc. used in the program) is not correct.

Another method of using the three porosity logs to determine lithology is the MID (Matrix Identification) Plot. (tma) a, apparent matrix travel time, and (ρma) a, apparent matrix density, must be determined and plotted on Figure 16 to determine the tri-matrix combinations. Determine (ρ ma) a by plotting CNL vs Density on Fig 15. (tma) a is determined by plotting CNL versus transit time on Figure 17. If specific percentages of various rock combinations need to be known, solutions can be determined graphically as shown in Figure 18.

Fig 15. Determination of ma a from Density and CNL logs (Schlumberger, 1985)

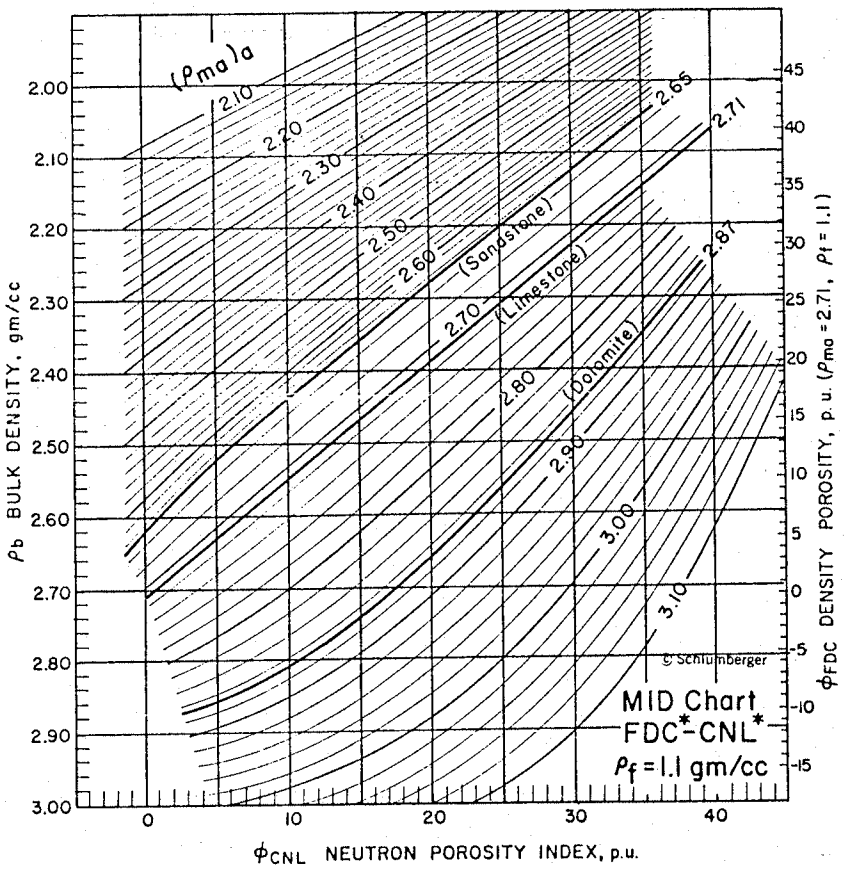

Figure 16. MID Plot of tma a vs ma a

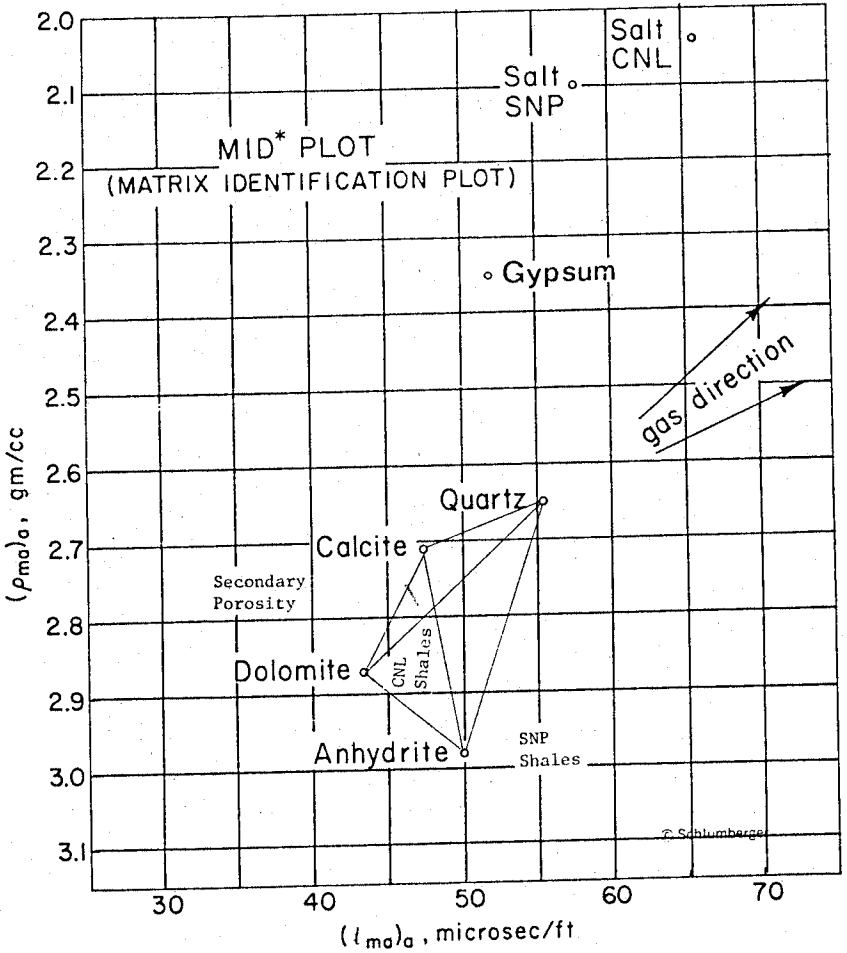

Figure 17.

DETERMINATION OF $(t_{ma})_a$ FROM SONIC AND CNL* LOGS

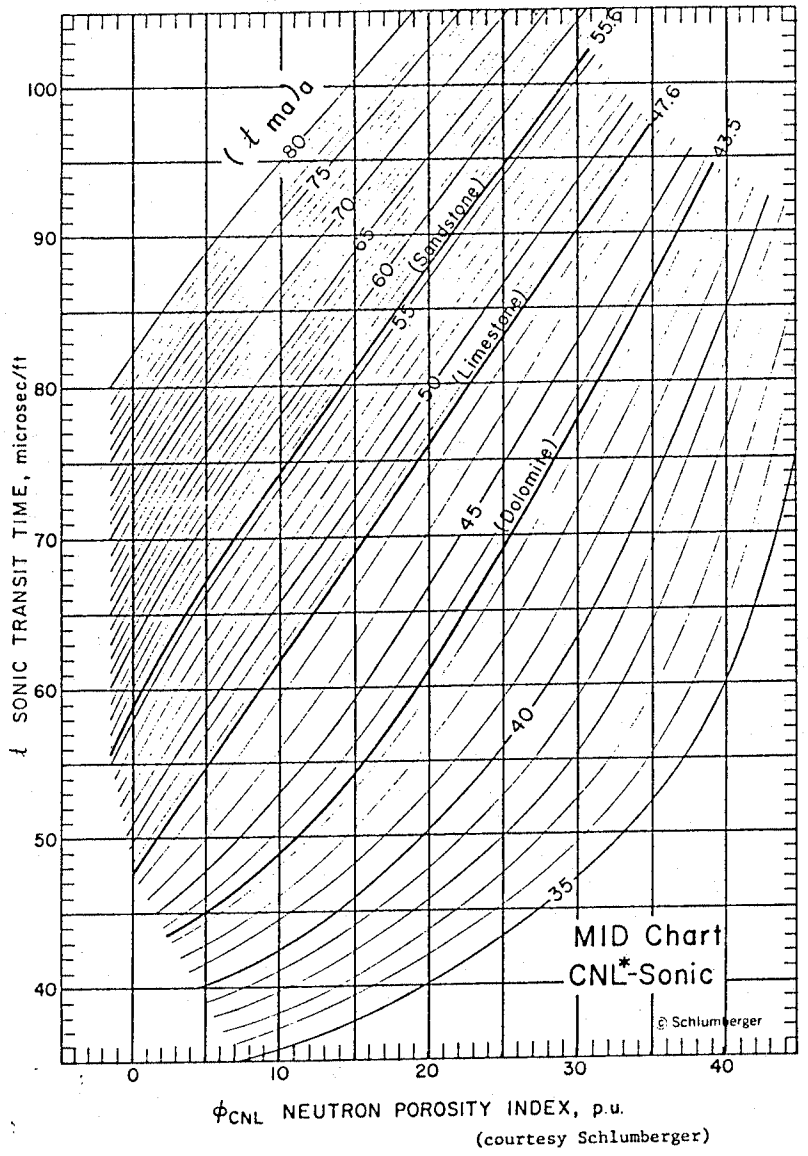

(courtesy Schlumberger)

Figure 18. MID Solutions for Various Rock Combinations (Hilchie, 1982)

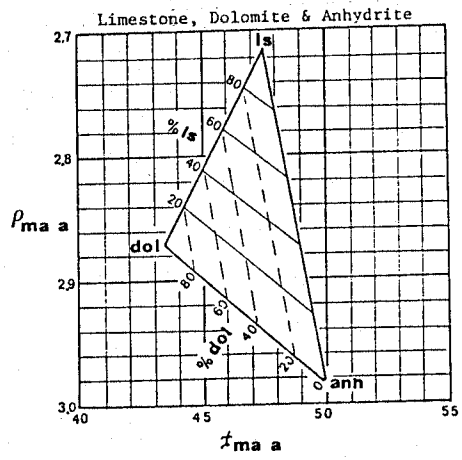

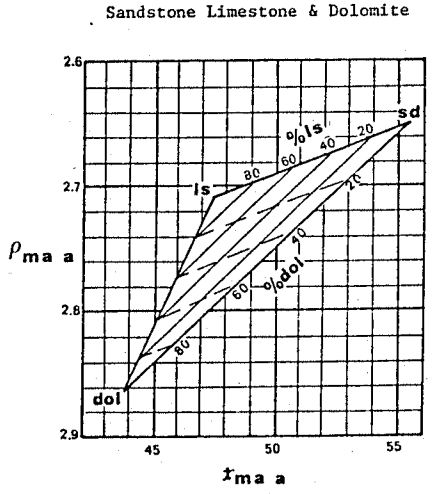

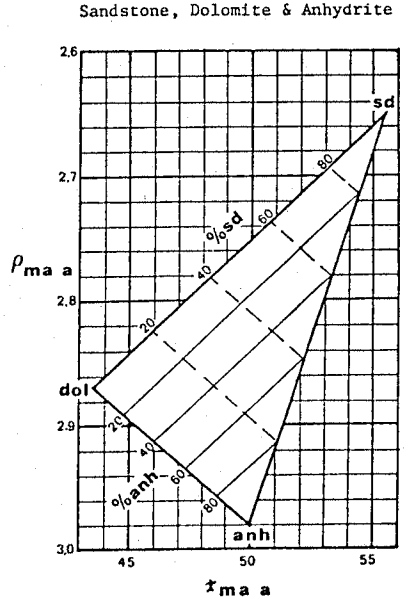

Another method to determine tri-matrix rock combinations is the MN system. M and N are calculated using (Hilchie, 1982, p.VI-16):

$$M = \frac{tf - t}{\rho b - \rho f} \times 0.01 \qquad (13)$$

$$N = \frac{CNLf - CNL}{\rho b - \rho f} \qquad (14)$$

where:
ρf = density of the fluid
ρb = bulk density determined from the density log by:

$$\rho b = \rho ma - DEN(\rho ma - \rho f) \qquad (15)$$

ρma = that matrix density for which the log is calibrated (usually limestone, 2.71g/cc)

M and N are then plotted on Fig 19 to identify lithologies. Precise percentages of the three rock types can be determined graphically as in the MID method (see Fig 20).

d. Lithodensity Log

The Lithodensity log is very useful in determining a variety of different tri-matrix combinations. First of all, Pe is read from the log, then ρma a is determined, as before, by plotting CNL and DEN on Figure 15. Then Uma must be determined from (Hilchie, 1982, p.VIII-1):

$$Uma = Pe\ \rho e \qquad (16)$$

where:

$$\rho e = (\rho b + .188)/1.07 \quad (g/cc) \qquad (17)$$

and

$$\rho b = 2.71 - DEN(1.71) \qquad (18)$$

(for logs calibrated to limestone).

Uma and ρma are plotted on Figure 21 to identify lithology (or Figure 22 can be used for Pe vs ρb). The tri-matrix percentages can be determined graphically as shown in Figure 21.

Figure 19. M-N Plot for Tri-Matrix Problems

(Schlumberger, 1985)

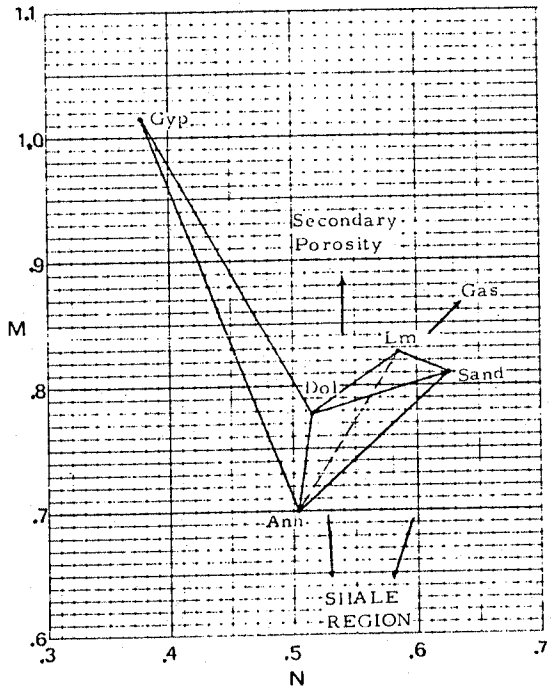

Figure 20. M-N Triangles for Various Rock Combinations (Hilchie, 1982)

Dolomite Anhydrite & Sand

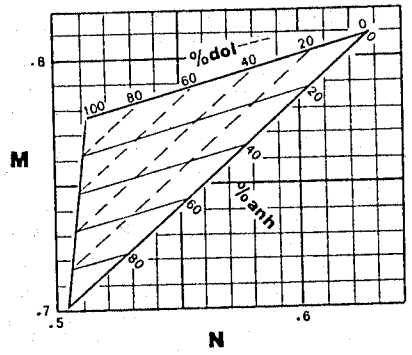

$V_{dol} + V_{anh} + V_{sd} = 100\%$

Dolomite, Limestone & Sand

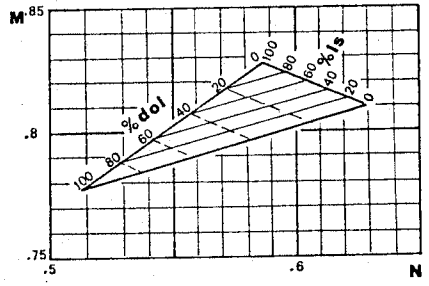

$V_{dol} + V_{ls} + V_{sd} = 100\%$

Dolomite, Anhydrite & Limestone

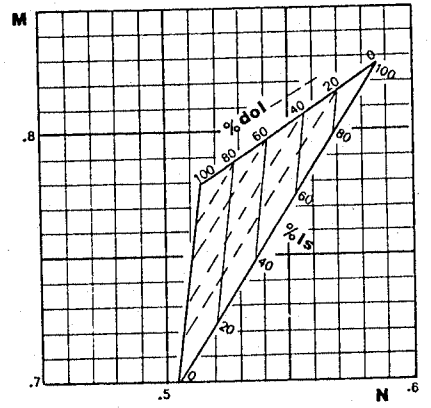

$V_{dol} + V_{ls} + V_{anh} = 100\%$

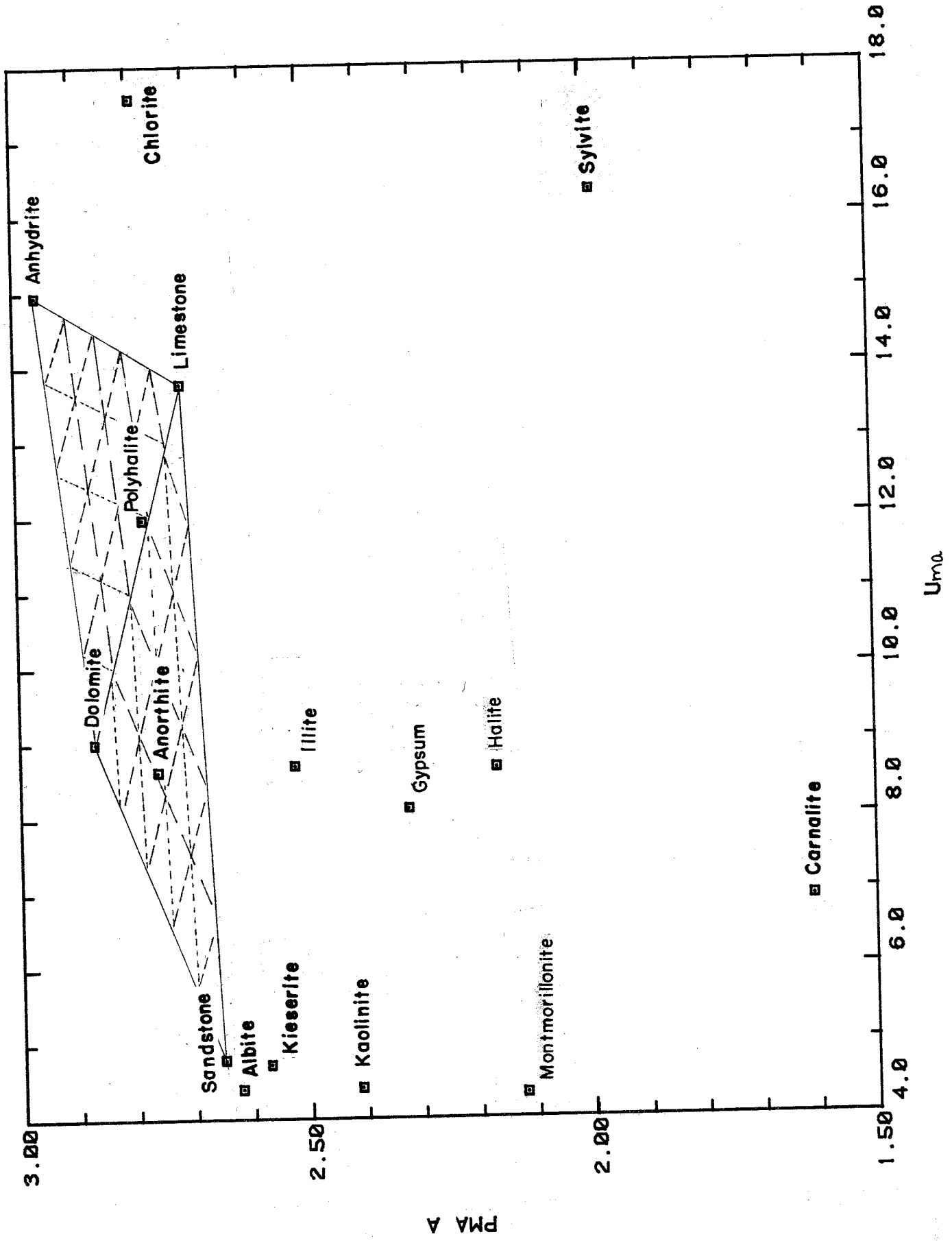

Figure 21. ρma a vs Uma for Mineral Identification

Figure 22. Porosity and Lithology Determination from Litho-Density* Log

Salt Water, Liquid-Filled Holes, $\rho_f = 1.1$

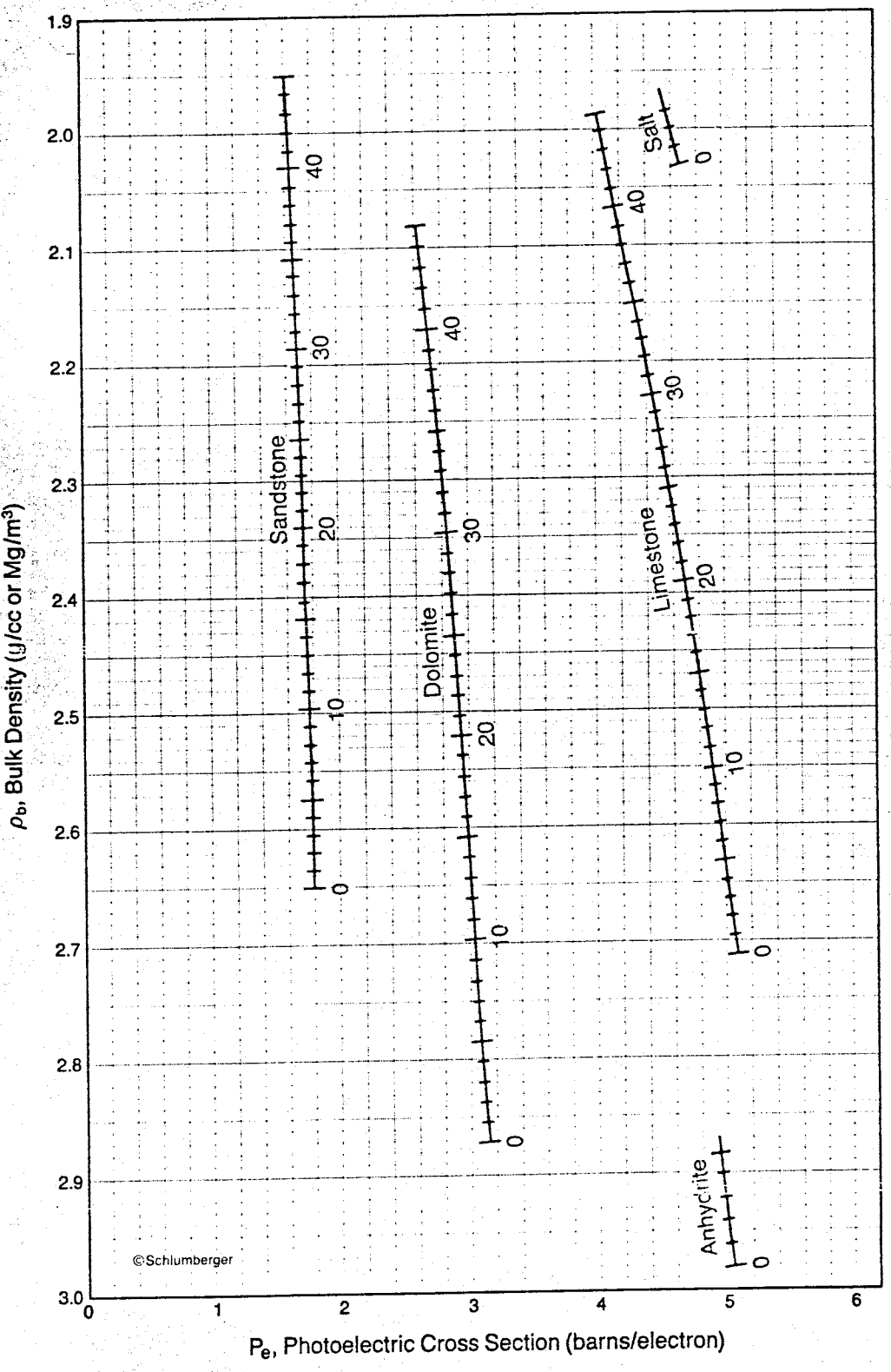

*Mark of Schlumberger

3.ESTIMATING WATER QUALITY

The Yeso is generally considered to have unsuitable water for most uses. However, in some areas west of R21, wells tap good water from the Yeso. It was hoped that water quality could be determined from well logs in order to define zones of different water quality. In almost all of the wells used in this study, the upper Yeso was cased before logging, and therefore, water quality could not be determined. This is unfortunate because the upper Yeso and lower San Andres is the main zone tapped by water wells in this area, and it would be interesting to determine the variability of water quality, of this zone, throughout the study area.

There are a variety of methods to determine water salinity. These are discussed below. All involve obtaining a value of water resistivity (Rw) first and from that, calculating TDS.

a. Calculating Water Resistivity

The resistivity of a rock is affected by the grain size, structure and composition, porosity, and water quality. If porosity and matrix structure are known, then water quality can be determined. In all of the following methods, water saturation is incorporated into the equations. There are too many unknowns to solve for water saturation and therefore it was assumed to be 100 %. It was also assumed that no shale was present in the zones analyzed. The presence of shale has the effect of overestimating solute content. Only the permeable zones were used to determine water quality.

Resistivity must be corrected for borehole conditions and temperature. Resistivity was corrected to 75 F by the following equation (Hilchie, 1978, p. 2-2):

$$R(75\ F) = Res(temp + 7.0)/(75.0 + 7.0) \qquad (19)$$

Borehole correction is done by determining the diameter of the well, at the analyzed depth, from the Caliper log and then dividing Rt by Rm (resistivity of mud given at log heading) and plotting on the correction charts (Fig 23). There are many correction charts for all the different types of logs. The Laterologs must also be corrected for invasion to get a true undisturbed formation resistivity. Corrections for invasion are only possible if three resistivity logs are available, where Rdeep, Rmedium, and Rshallow (Rxo), have been measured.

1.Spontaneous Potential

The SP is frequently a reliable method for determining Rw, but as stated earlier, the requirements for using the SP are not met in the Yeso formation, and therefore, unfortunately, it could not be used in the analysis of water quality.

Deep Laterolog Borehole Correction

DLS-B Tool Centered, Thick Beds

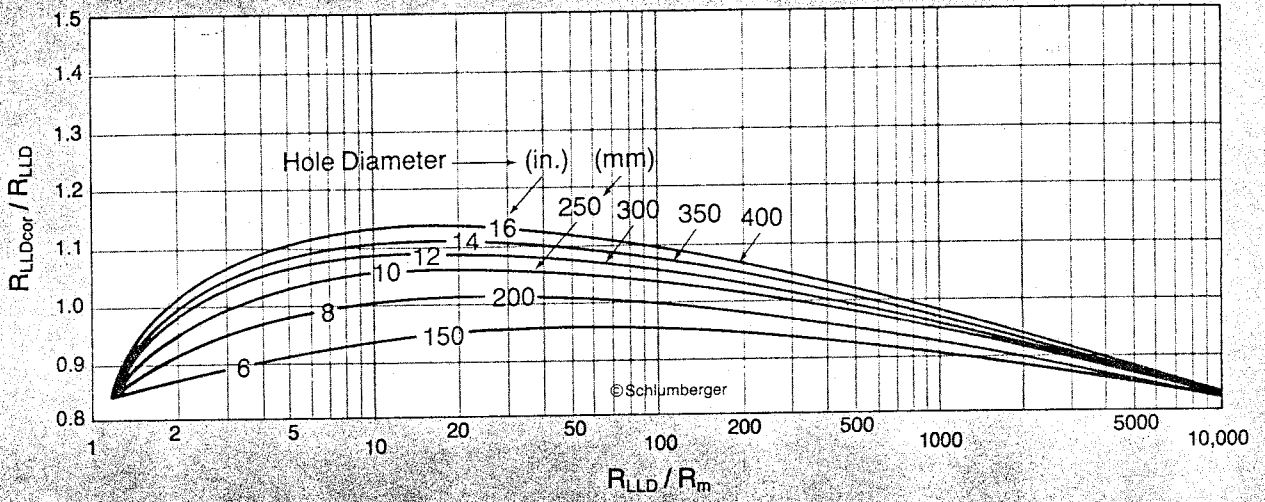

Shallow Laterolog Borehole Correction

DLS-B Tool Centered, Thick Beds

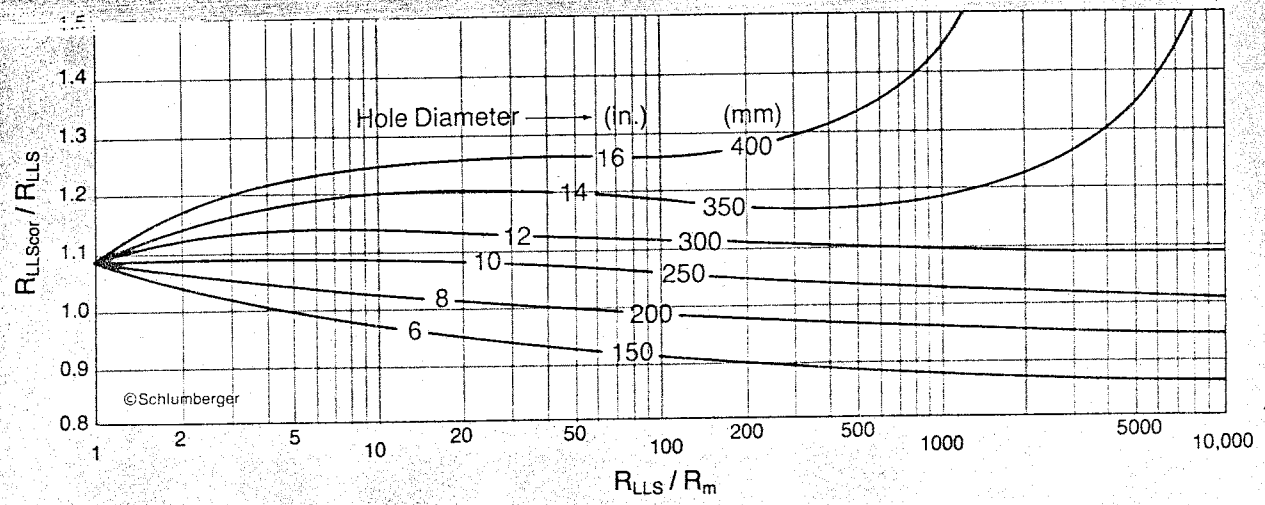

EXAMPLE: $R_{LLD} = 15\ \Omega\cdot m$, $R_{LLS} = 9.5\ \Omega\cdot m$, $R_m = 0.05\ \Omega\cdot m$, and $d_h = 9¾$ in.

Giving, $\frac{R_{LLD}}{R_m} = \frac{15}{0.05} = 300$ and $\frac{R_{LLS}}{R_m} = \frac{9.5}{0.05} = 190$

Therefore, $\frac{R_{LLDcor}}{R_{LLD}} = 0.98$, $\frac{R_{LLScor}}{R_{LLS}} = 1.03$ and $R_{LLDcor} = 14.7\ \Omega\cdot m$, $R_{LLScor} = 9.8\ \Omega\cdot m$

Note that the LL8 chart contains two sets of curves. One set for $R_m \geq 1.0\ \Omega\cdot m$ and one set for $R_m = 0.1\ \Omega\cdot m$. Similarly, the SFL chart contains curves for a centered tool and for a tool with 1½-in. standoff.

(Schlumberger, 1985)

Figure 23. Borehole Correction Charts for Laterolog

2.Holmes Method

Another technique to determine Rw was suggested by Holmes (Hilchie, 1982). It involves knowing the resistivity of the invaded zone (Rxo), the resistivity of the saturated rock (Ro) and the resistivity of the mud filtrate (Rmf). Rxo is determined from a shallow resistivity tool, Ro is determined from a deep resistivity tool, and Rmf is given at the log heading. The following equation, with substitutions and rearrangement, can be used to calculate Rw:

$$Rxo = F(Rmf)Sxo^{-2} \quad (20)$$

$$\text{and} \quad F = Rt/Rw\ Sw^{-2} \quad (21)$$

substitute for F:

$$Rw = (Rt\ Rmf\ Sxo^{-2})/(Rxo\ Sw^{-2}) \quad (22)$$

saturation = 100%; Sxo = Sw = 1.0,

$$Rw = Ro\ Rmf/Rxo \quad (23)$$

As an example, a zone from well no 11, depth of 1876 to 1898 feet, is analyzed for water quality.

At depth of 1884 feet, Ro = 12 ohm-m (corrected = 13.77)
Rxo = 9 ohm-m (corrected = 10.38)
Rmf = 0.098 ohm-m

Rw = 0.098 (13.77/10.38) = 0.13 ohm-m

The major uncertainty in this approach, is the value for Rxo. In the example above, the resistivity from the short normal was used as the resistivity of the invaded zone (Rxo).

3. Formation Factor

The resistivity of a rock, Ro, as stated earlier, is dependent on the formation water resistivity, Rw, and pore geometry. It is also dependent on the composition of the rock, but this does not change significantly for different minerals all of which, except for shales, have a nearly infinite resistivity. The formation factor, F, is used to relate Ro to Rw (Hilchie,1978,p. 2-6),

$$Ro = F\ Rw \quad (24)$$

where F is a function of the porosity and pore geometry expressed as:

$$F = a\ Por^{-m} \quad (25)$$

and, a = pore geometry coefficient
m = cementation factor

As a result of numerous calculations, the oil companies have come up with the following generalizations;

The Humble relationship for granular formations, such as sandstone:

$$F = .62\ por^{-2.15} \quad (26)$$

and for non granular rocks;

$$F = por^{-2} \quad (27)$$

It is necessary to know whether the zone is granular or not in order to use these equations, which tends to prohibit their use for formations, like the Yeso, which alternate between granular and nongranular. Table V gives typical m values for various sediments.

Using the same example as before, from well no 11, depth of 1884,

$$por = .147$$

$$Ro = 13.77 \text{ ohm-m}$$

$$F = por^{-2} = .147^{-2} = 46.3$$

$$Rw = 13.77/46.3 = .298 \text{ ohm-m}$$

or, $$F = .62\ por^{-2.15} = .62(.147)^{-2.15} = 38.25$$

$$Rw = 13.77/38.25 = .36 \text{ ohm-m.}$$

4. Porosity-Resistivity Crossplot

Another method of determining Rw is by plotting resistivity versus porosity for the zone under investigation. If a relationship exists between porosity and resistivity, then it is very easy to calculate Rw.

Plot porosity versus resistivity on log-log paper, then fit a line through these points. It is best to use a linear regression to get the best fit and to accurately determine m (Equation 25, with a = 1.0), which is the slope of the line. Rw can be read directly off the graph where the line intersects 100 % porosity (see Figure 24).

For the same example, Rw = 0.854, which is higher than the other estimates. Hilchie suggests using the lowest value of all methods, because most problems or errors with the resistivity cause it to be higher than it actually is. However, if, as in this example, there is such a strong correlation, $r^2 = 0.96$, I would tend to believe the Rw calculated from this method, rather than a general equation. Figure 24 shows four lines, three of which have been corrected for various effects, one corrected only for temperature, one only for borehole diameter, one for both, and one left uncorrected. From the original data to correcting for both effects, the Rw value varied from 0.65 to 0.85 ohm-m. Because we only wanted a close estimate of water resistivity, and

Table V. Measured Values of "m", the cementation factor, for Granular Systems (Hilchie, 1982)

Material	m
Na Montmorillinite	3.28
Ca Montmorillinite	2.70
Muscovite	2.46
Attapulgite	2.46
Illite	2.11
Kaolinite	1.87
Spheres	1.3
Natural Sands	1.6

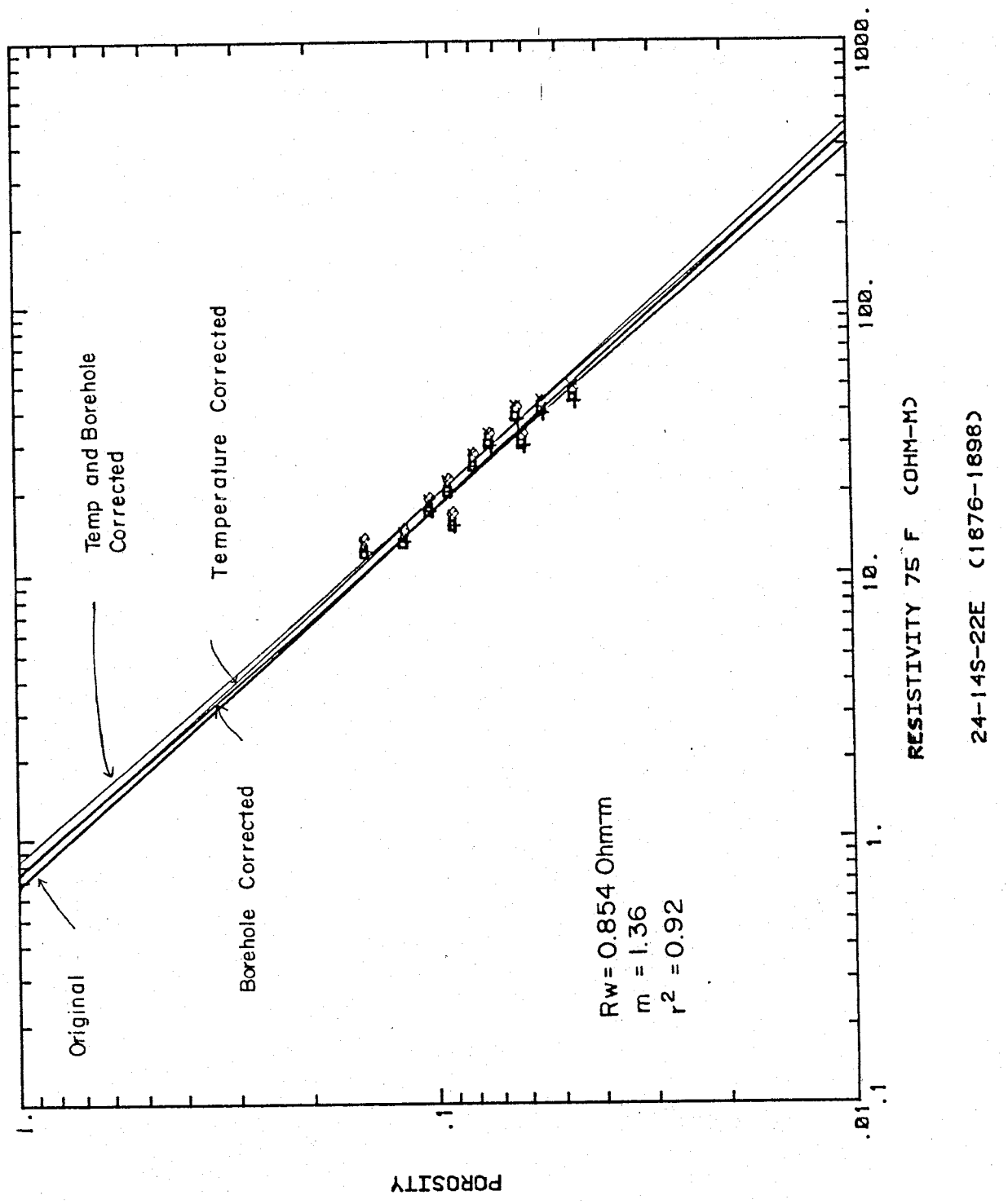

Figure 24. Porosity vs. Resistivity Plot for Well no. 11

since it is very tedious to correct for the borehole diameter, the data were corrected only for temperature in this study. We are confident that this will not affect the results because borehole corrections were made on many zones to see if it made a difference in the correlation, and in no case did it improve the results. In this example, the water resistivity estimate, when temperature corrected only, is 0.75 ohm-m. This gives a concentration of 7,382 ppm NaCl, whereas 0.854 ohm-m gives a concentration of 6,430 ppm NaCl.

In the wells which had three resistivity logs, corrections for invasion did change the Ro value, but did not change the correlation coefficient between Ro and porosity. Fig 25 is an example of a zone in well no 10 with a large amount of separation between resistivity curves. The data were corrected for borehole conditions and then corrected for invasion. The r^2 is approximately 0.17 for both the corrected and uncorrected data. The invasion correction only shifts the data to the right on Figure 26. Therefore, invasion corrections were only made on zones with a high r^2. The correction increased the Rw value by about 30% in well no 12. For instance, the Rw value, for a zone at a depth of 1202-1210, is 1.62 ohm-m, and when corrected for invasion, Rw = 2.08 ohm-m.

b. Water Quality Determined from Rw

Water resistivity can be related to water quality if the major dissolved solids are known. Fig 27 is a graph for determining NaCl concentrations from Rw at a specific temperature. For an approximation to this graph, for Rw at 75 F, concentration can be solved using the following equation:

$$\text{Conc} = 10^{\frac{3.562 - \log(Rw-0.0123)}{.955}} \qquad (28)$$

Where: Rw = ohm-m
Conc = ppm

This can also be done analytically by using the following relationship:

$$\text{Conc} = \frac{\sigma\ 1000}{\lambda} \qquad (29)$$

Where:
Conc = concentration (eq/L)
σ = conductivity (Ohm-cm)
λ = equivalent ionic conductance (cm^2/volt-sec)

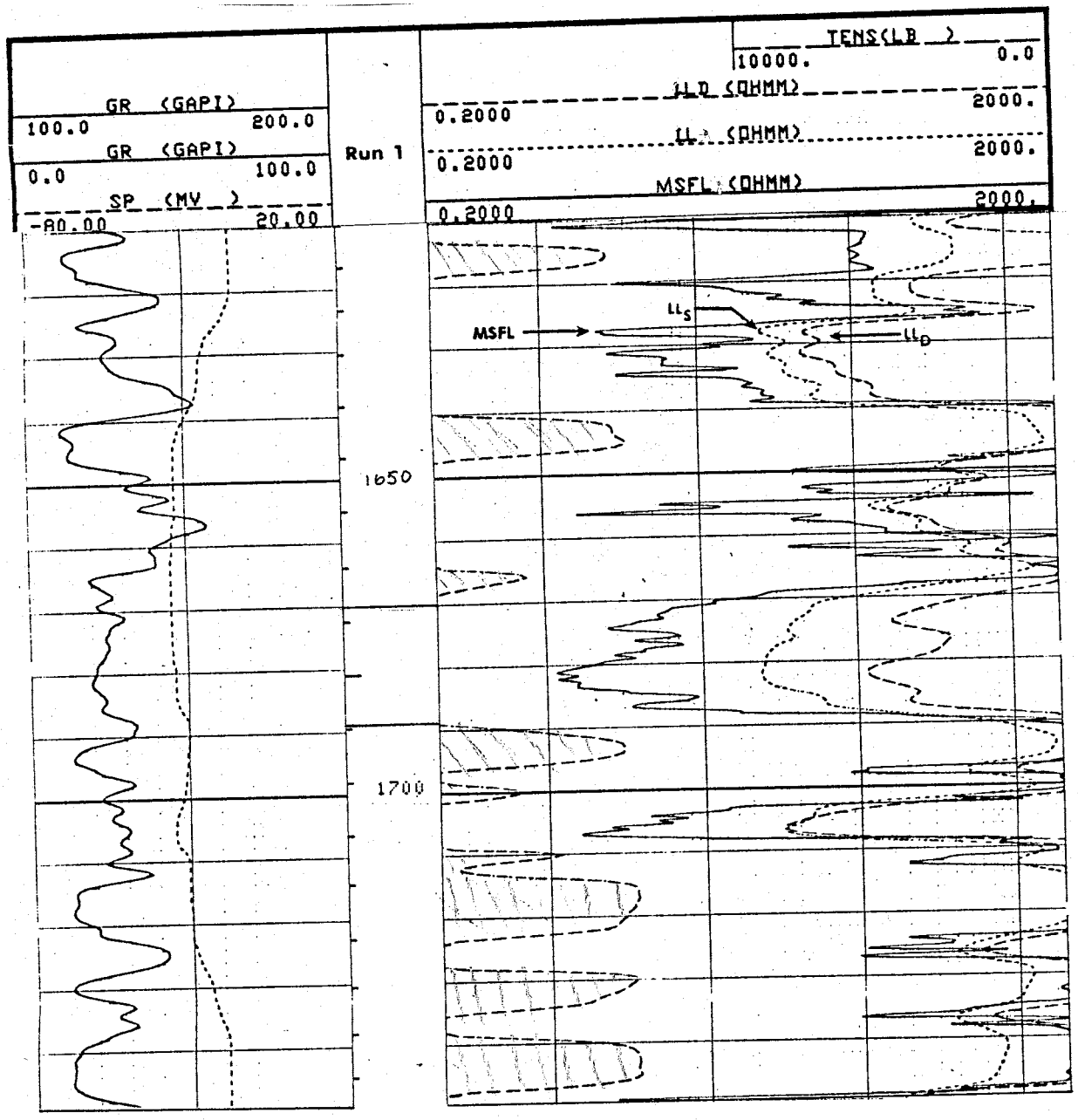

Figure 25. Laterolog-Micro-Spherically Focused Log For Well nq 10, showing permeable zone

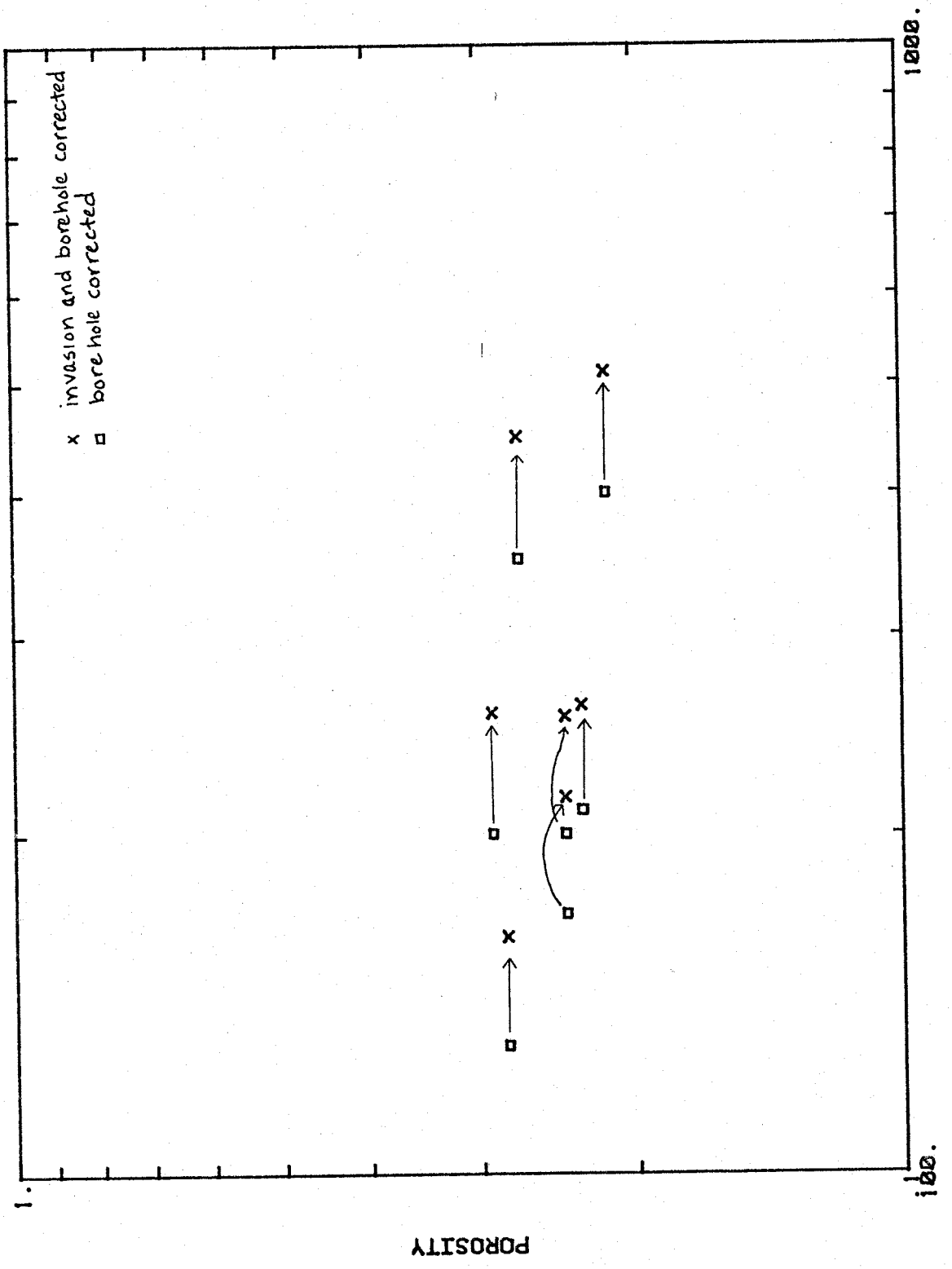

Figure 26. Porosity Versus Resistivity for Well no.10, Showing Shift in Data Corrected for Invasion

Resistivity of NaCl Solutions

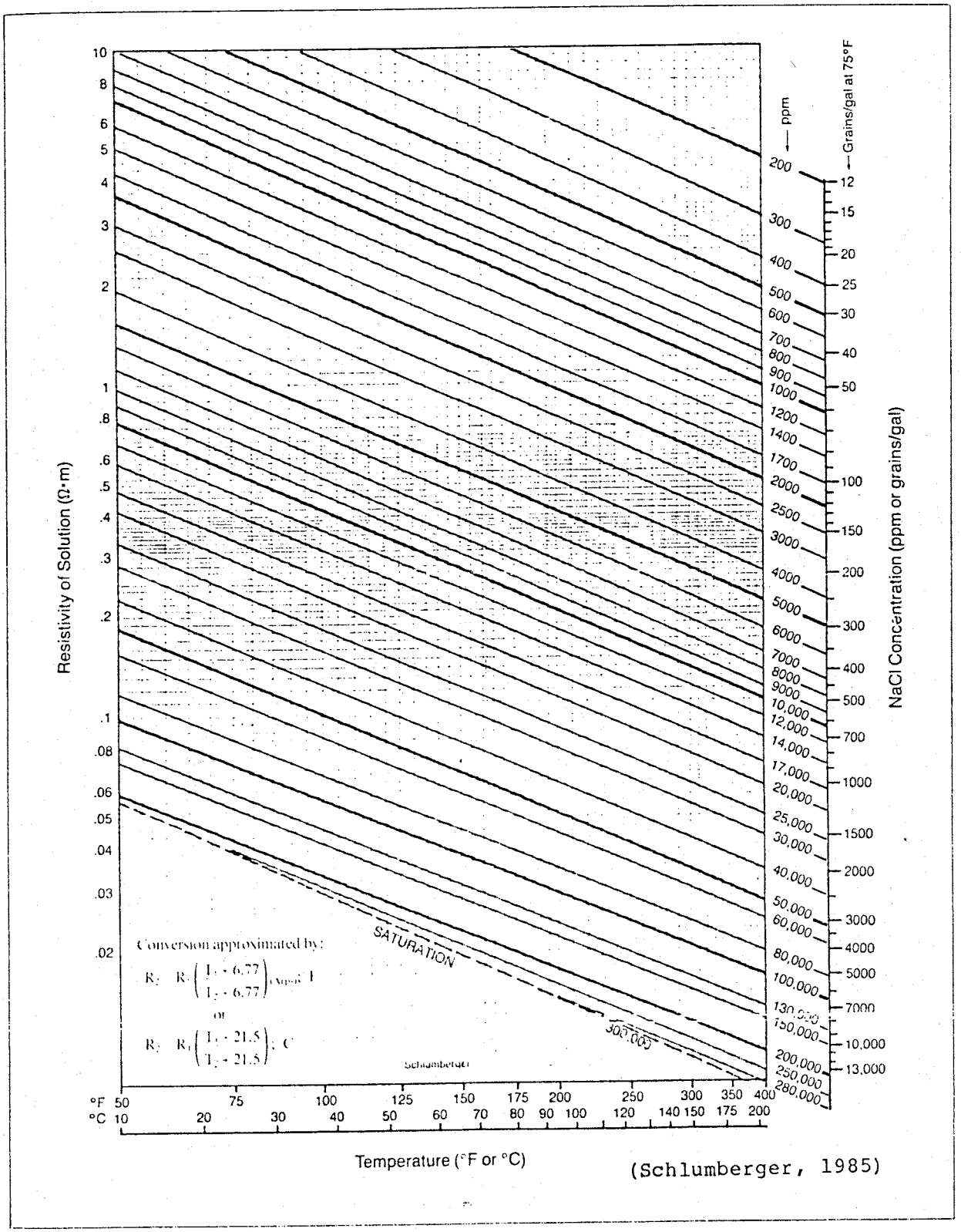

Figure 27. Graph of Resistivity of NaCl Solutions at Various Temperatures

To determine σ from Rw the relationship may be used:

$$\sigma = \frac{1}{100\ Rw}\ (\Omega\text{-cm})^{-1} \qquad (30)$$

Where:
Rw = Ohm-m
σ = $(\text{Ohm-cm})^{-1}$

λ is determined by adding the equivalent ionic conductances of Na and Cl (see Table VI for values of λ)

$$\lambda = \lambda_{Na} + \lambda_{Cl} = 52 + 79 = 131 \text{ cm /volt-sec} \qquad (31)$$

Substitution of λ into Eq 29 yields the following equation:

$$\frac{1000\ (\text{Ohm-cm})^{-1} \times 58 \text{ g/eq} \times 1000 \text{ mg}}{131 \text{ cm}^2\text{/volt-sec} \qquad \text{g}} = 442{,}748\ \text{ppm}\sigma \qquad (32)$$

or,

$$\frac{1000 \times 58 \text{ g/eq} \times 1000 \text{ mg}}{100(\text{Ohm-cm/Ohm-m})\ Rw\ (131 \text{ cm}^2\text{/volt-sec})\ \text{g}} = \frac{4{,}427.5 \text{ ppm}}{Rw} \qquad (33)$$

Suppose the dissolved ions in a sample are Ca^{2+} and SO_4^{2-}, and the concentration is given as 10,000 ppm NaCl. To convert the concentration in ppm NaCl to another ion, the same analytical method that was used to calculate concentration in ppm NaCl can be used.

$$\lambda = \lambda_{Ca} + \lambda_{SO} = 59.5 + 80.0 = 139.5 \text{ cm}^2\text{/volt-sec}$$

Substitute λ into Eq 29,

$$\text{Conc} = \sigma\ 1000/139.5 = 7.1685\ \sigma \quad \text{(eq/L)}$$

The conductivity of a sample with an equivalent concentration of 10,000 ppm is calculated by rearranging Eq 29:

$$10{,}000 \text{ ppm} \times 10^{-3} \text{g/l/ } 58\text{g/eq} = 0.1724 \text{ eq/L}$$

$$= (.1724\text{eq/L})\ (131 \text{ cm}^2\text{/volt-sec})/1000 = 0.0226\ (\text{ohm-cm})^{-1}$$

This gives a concentration of $CaSO_4$ of:

Conc = 7.1685 (.0226) = .162 eq/L

to convert this to ppm, multiply by the equivalent weight of CaSO ;

equivalent weight = 20 + 48 = 68g/eq

$$\text{Conc} = .162 \text{ eq/L} \times 68 \text{ g/eq} \times 10^3 \text{mg/g} = 11{,}016 \text{ ppm CaSO}$$

It is necessary to know the major ions present in the water in order to get an accurate estimate of TDS. If there were chemical analyses of water throughout the Yeso Formation, then

Table VI . Equivalent Conductivities of Ions at 25°C (From Robinson and Stokes,1955)

Ion	λ	Ion	λ
H^+	349.8	OH^-	198.6
Li^+	38.6	F^-	55.4
Na^+	50.1	Cl^-	76.35
K^+	73.5	Br^-	78.14
Rb^+	77.8	I^-	76.8
Cs^+	77.2	N_3^-	69
Ag^+	61.9	NO_3^-	71.46
NH_4^+	73.5	ClO_3^-	64.6
Be^{++}	45	BrO_3^-	55.7
Mg^{++}	53.0	ClO_4^-	67.3
Ca^{++}	59.5	HCO_3^-	44.4
Sr^{++}	59.4	SO_4^{--}	80.0
Ba^{++}	63.6	CO_3^{--}	69.3
Cu^{++}	56.6	$Fe(CN)_6^{---}$	100.9
Zn^{++}	52.8	$P_3O_9^{---}$	83.6
Co^{++}	55		
Ce^{+++}	69.8		

perhaps a constant ratio of the major constituents could be determined, and thus a correct value of TDS. However, there are few analyses of Yeso water (except from the very top) and therefore, TDS presented in Table VI is expressed in equivalent NaCl.

4. DETERMINATION OF PERMEABILITY

Permeability is the most difficult parameter to estimate. It requires more information than was available for the logs in the study area. The following is a discussion of the attempts to determine permeability and the problems associated.

a. Qualitative Estimation

Permeability was determined qualitatively by the separation of the deep and shallow resistivity logs. If a zone is permeable the drilling mud will invade the formation (see Fig 5). The depth of invasion depends on the porosity (with lower porosity, a deeper invasion). If the drilling mud has a resistivity different from the formation water, then the bulk resistivity of the formation will change. That is, if invasion has occured, the shallow resistivity log will read lower (if Rm < Rw) than the deep resistivity log (if invasion is not as deep as the depth that the deep resistivity tool reads). Therefore, zones where the curves are separate are permeable. All zones with a definite separation were considered permeable. Some zones showed a larger separation than others, which probably indicates a greater permeability, however, this was not designated. This does not always mean that, when the curves are together, the zone is impermeable. It is possible for a zone to have a very high porosity, such that invasion does not penetrate as deep as the depth that the shallow tool reads, thus both tools would read the same resistivity. Also, invasion may be deeper than the depth that the deep tool reads, and thus, both tools would read the same value. If the resistivity of the mud is the same as the formation water, then the resistivity tool will not be affected by invasion, and the shallow and deep tools will read the same value.

b. Quantitative Estimations

1. Formation Factor

It is difficult to determine an actual value of permeability from the resistivity logs. There have been many studies relating formation factor to permeability. However, these studies contradict each other, some showing an inverse relationship between F and K, and others a direct relationship between F and K, for different study areas (Kwader 1982, Urish 1981, Carothers 1968). This involves determining hydraulic conductivity from pump tests and comparing it to the formation factor determined from logs (Equation 25).

$$F = Ro/Rw \qquad (34)$$

$$F = a\ por^{-m}$$

where, Ro = Rt at 100% saturation

This method requires that the water resistivity be constant throughout the vertical section. F will increase as Ro increases, this implies that porosity decreases (Rw is always << Ro). If there is a direct correlation with F and K, then K is increasing as porosity decreases. This could be the case in silty or clayey soils. An inverse relationship might be expected in a coarser sediment.

2. Spontaneous Potential

The SP log can be used to determine permeability quantitatively, however the requirements for the SP to be valid are not met in the Yeso Formation, and therefore it was not used.

3. Drill Stem Tests

The only direct information that has helped to quantify permeability are drill stem tests on two wells. One test on well no 2 (7-17S-18E Unit 2) indicated borehole damage and was not useful (see Fig 28). However the test on well no 1 (7-17S-18E Unit 1), which was done on the upper part of the Drinkard, proved to be useful. The test indicated a moderate permeability (10^{-4} m/s), see following discussion on analysis.

Drill stem tests are commonly done by the petroleum industry. The equipment is expensive, but the test is fairly simple. It involves isolating a stratigraphic interval in the open hole with packers assembled on the drill stem test string.

Fig 29 is a pressure graph from well no 1. From point A to B in Fig 29 is a record of the packer being lowered into the well and packed off. The "noisy" appearance of this part is due to the addition of joints to the drill stem. At B, the valve is opened to atmospheric pressure, allowing the formation to produce. The increase in pressure from atmospheric to point C, is due to the weight of fluid building up in the drill stem. At point C, the valve is shut allowing pressure to recover to D, which approached the "undisturbed formation pressure" (Po). The valve is then opened and allowed to produce. The amount of water, drilling mud, oil or gas is recorded to determine a production rate. At F the valve is shut and allowed to recover to G. H to J is a record of the packers being deflated and the assembly pulled up.

The basic equation used to analyze the DST:

$$Pw = Po + \frac{2.3\ q\ \mu}{4kh\pi} \log \frac{to + \Delta t}{\Delta t} \qquad (35)$$

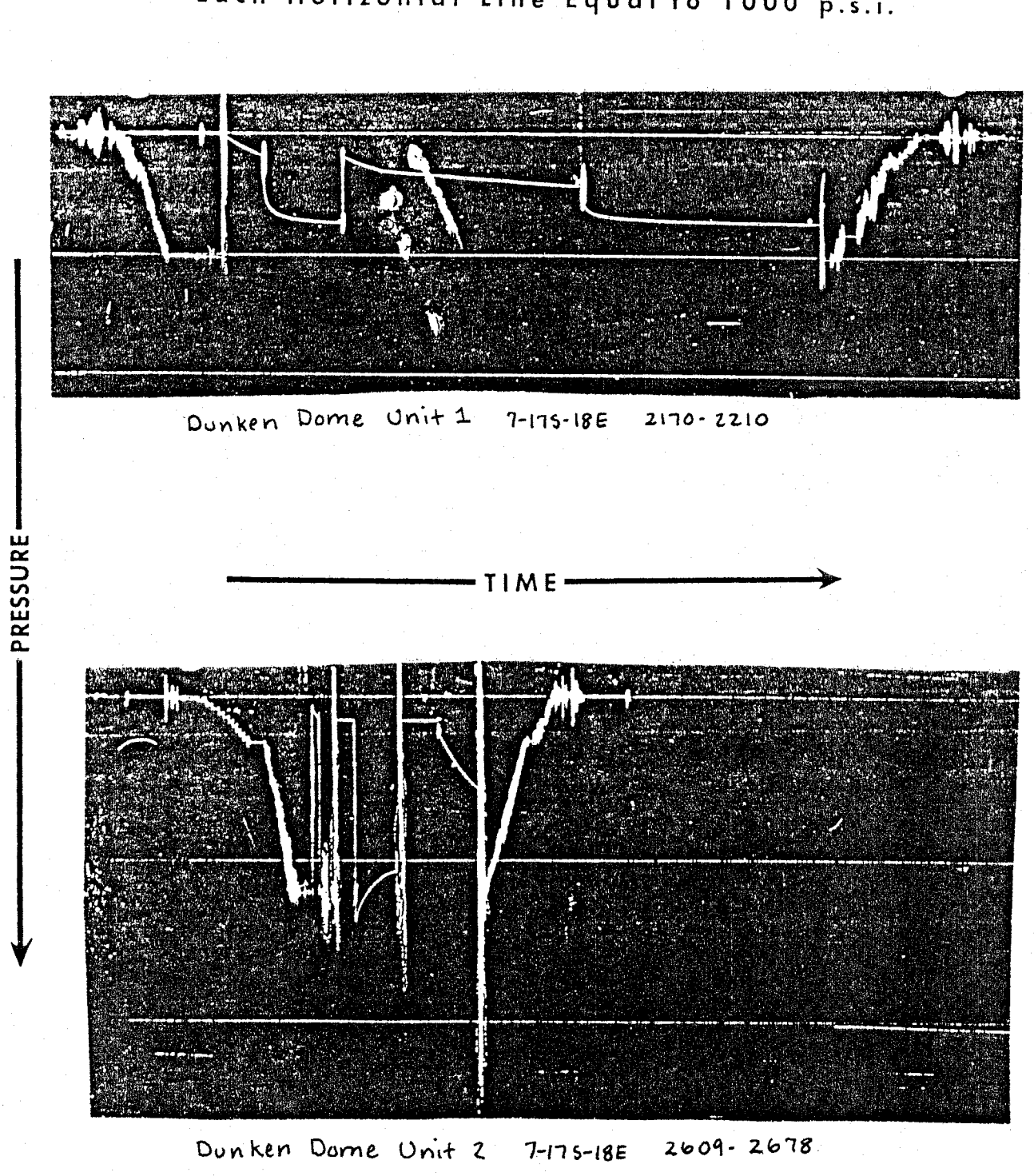

Figure 28. Drill Stem Test for Wells 1 and 2

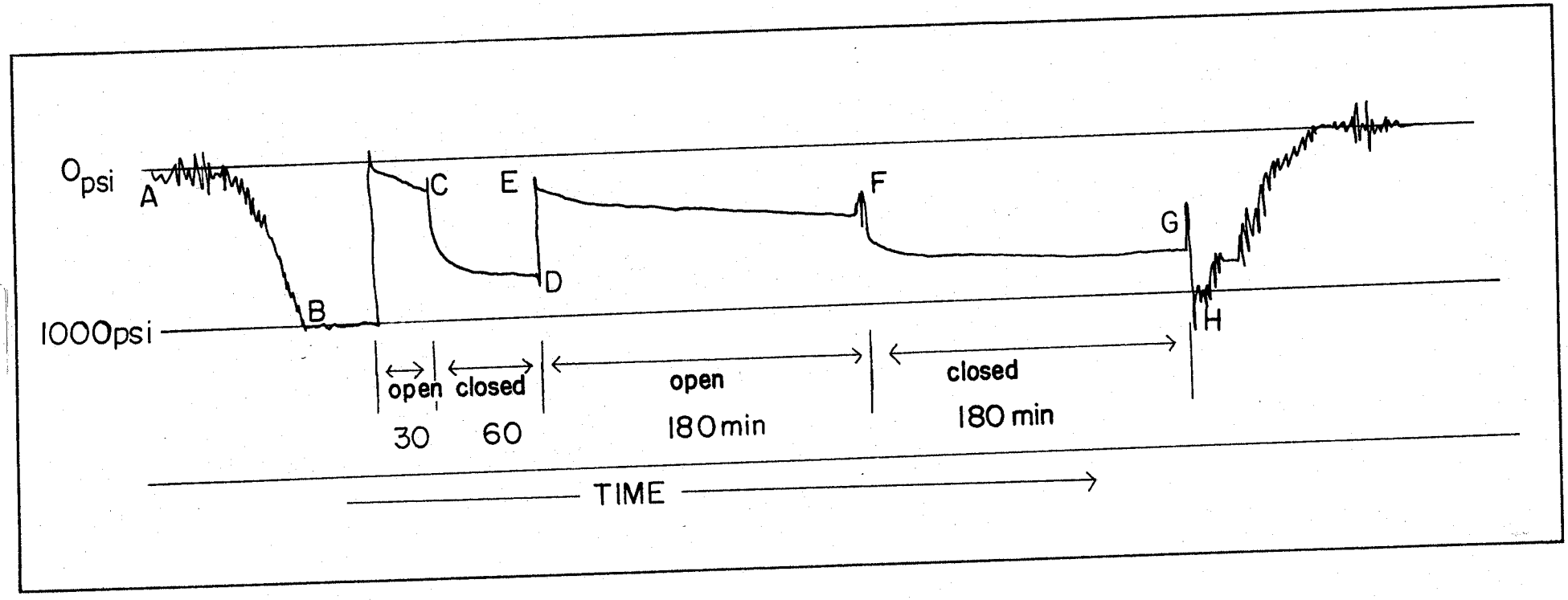

Figure 29. Drill Stem Test for Well no. 1

Pw = pressure at the well bore (F/L^2)
Po = undisturbed formation pressure (F/L^2)
q = rate of production (L^3/T)
u = viscosity of the fluid (FT/L^2)
k = permeability of the producing formation (L^2)
h = thickness of formation being tested (L)
t = interval of time of production (T)
Δt = time elapsed since closing in well after period of production (T)

It is necessary to have the graph of the pressure record to determine permeability. The oil companies only have to report the pressures before closing and opening the valves and what type and how much fluid is recovered. The following is the information recorded on the completion card for well 1;

2170-2210 (Yeso) TO 30, SI 60, TO 180, SI 180. Open w/weak blow, inc. to 2'' in water. Reop w/very weak, steady blow, 1-2'' in water, no gas. Recovered 465' DM, 620' water. Sampler: psi, 2200cc water no oil or gas. Pressures: HP = 1031-1031, IFP 70-175, ISIP 735, FFP 175-421, FSIP 735. BHT 70 F.

Symbols are as follows:

SI = shut in
TO = time open
HP = hydro pressure (point B on Fig 29)
IFP = initial flowwing pressure (point C)
ISIP = initial shut in pressure (point D)
FFP = final flowing pressure (point E-F)
FSIP = final shut in pressure (point G)

In order to solve the equation, pressure versus log $(t + \Delta t/\Delta t)$ is plotted, see Fig 30. These points should fall on a straight line. The pressure change, ΔP, over one log cycle is determined, and k, intrinsic permeability, can be solved by,

$$k = \frac{2.3\, q\, \mu}{4h\pi\, \Delta p} \qquad (36)$$

The production rate, q, is calculated by determining the volume of fluid produced, divided by the production period.

465' drilling mud + 670' water = 1135'; fluid diameter of well = 5.5'' = .458'

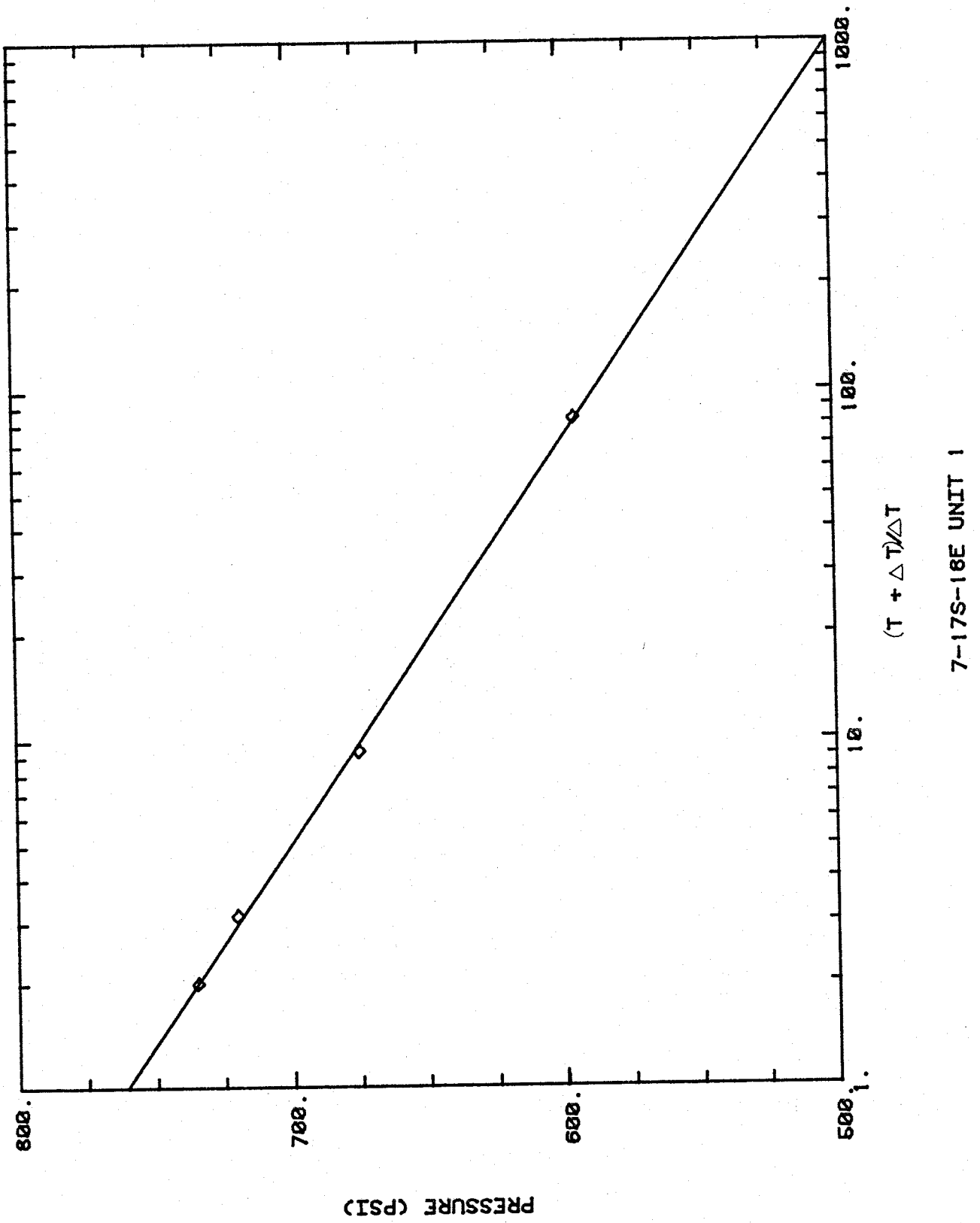

Figure 30. Pressure Versus log(t + Δt/Δt)

production period = 180 minutes = 10800 seconds

$$q = \frac{1135 \text{ ft } (2\pi)(0.0458)}{10{,}800 \text{ sec}} = 0.1358$$

viscosity of water at 70 F = 2.050 lb s/ft
h = 40 ft
P = 85.4 lbs/in = 12,298 lbs/ft
ρ = 62 lb/ft
g = 32.17 ft/s

The viscosity term can be eliminated by solving directly for hydraulic conductivity, K.

$$k = \frac{K \mu}{\rho g} \qquad (37)$$

$$\frac{K \cancel{\mu} h}{\rho \cancel{\mu} g} = \frac{2.3 q}{4\pi \Delta p}$$

$$K = \frac{2.3 q g \rho}{h 4\pi \Delta p} \qquad (38)$$

The density of water, ρ, is used, however, the density is probably much higher since there is drilling mud and the water is saline. This will underestimate the value of K.

$$K = \frac{2.3 \ (0.1385 \text{ft}^3/\text{sec})(62 \text{ lb/ft}^3)(32.17 \text{ ft/sec}^2)}{40 \text{ ft } (4\pi) \ 12{,}298 \text{ lbs/ft}^2}$$

$$= 1.03 \times 10^{-4} \text{ft/sec}$$

Not much emphasis should be placed on this one value. Drill stem tests have a large random error in K, and it is necessary to do numerous tests in other wells of the same stratigraphic zones.

4. Permeability From Grain Size Distribution

The cuttings for this zone were sieved to determine grain size distribution for use in the Kozeny-Carmen equation. This equation uses porosity and mean grain diameter to estimate permeability. It was hoped that there would be a similarity in values so that the cuttings could be used to quantify permeability. Only the sandy zones were sieved, the size of dolomite cuttings is only indicative of how sharp the drill bit was at the time of drilling. Most of the sand cuttings were not cemented, except for a few samples which were dissaggregated. A magnet was used to remove pieces of iron casing. Hydraulic conductivity varied by three orders of magnetude between the drill stem test value and the grain size method.

The Kozeny-Carmen equation:

$$K = \frac{\rho g}{\mu} \left[\frac{n^3}{(1-n)^2}\right] \frac{dm^2}{180} \qquad (39)$$

The grain size distributions in the Drinkard stratigraphic zone from two wells, no 6 and one at 22-17S-18E, which are near well no 1, were analyzed. The grain size distributions of the samples are in App 3 . A porosity of 20% was used in all calculations, and dm, mean grain diameter is calculated from:

$$dm = \frac{d_{16} + d_{50} + d_{84}}{3} \qquad (40)$$

where,

d_{16} = 16 % passing
d_{50} = 50 % passing
d_{84} = 84 % passing
ρ = 62 lb/ft
g = 32.17 ft/s
μ = 2.05 lb s/ft

$$K = \frac{(62\ lb/ft^3)(32.17\ ft/s^2)}{2.05\ lb\ s/ft^2} \left[\frac{.2^3}{(1-.2)^2}\right] \frac{dm^2}{180}$$

$$K = .0676\ dm^2\ (ft/s)$$

Another method to determine permeability from grain size distribution was developed by Bates and Wayment (1967). This method uses the uniformity coefficient (Cu), void ratio (VR), d_{10}, and d_{50}. The following restrictions must be met for this method to work:

$$.52 < VR < 1.08$$

$$.003 < d_{10} < 1.05$$
$$.060 < d_{50} < .240$$
$$2.0 < Cu < 22.0$$

where VR = por/(1-por), $Cu = d_{60}/d_{10}$, and d_{10} and d_{50} are measured in millimeters

If the restrictions are met, then K can be calculated from the following equation:

$$\ln K \text{ (in/hr)} = 11.02065 + 2.911802 \times \ln(VR \times d_{10}) - 0.085304 \times \ln VR \times \ln Cu + 0.1942394 \times VR \times Cu - 0.5648568 \times d_{10} \times d_{50}. \quad (41)$$

Unfortunately, the void ratio and d_{50} did not come within the above restrictions. For example, a sample from a well located at 22-17S-18E at a depth of 2220 feet, in the Drinkard Sandstone had the following distribution:

d_{10} = .18
d_{50} = .37
d_{60} = .40
Cu = 2.22
VR = .25

Even though the restrictions were not met, the K value from this method closely approximated the value obtained from the drill stem test.

5. ESTIMATING VOLUME OF WATER

The average volume of water per unit area and a thousand foot thickness was determined by multiplying the porosity by the interval thickness (for the digitized data, volume = 2 ft x porosity) and adding these, dividing by the total thickness and then multiplying by a thousand feet. For example, the total volume of water in well no. 1, for a thickness of 1600 ft (and a 1 ft area) was 200.3 ft^3. Dividing this by 1600 ft, gives 0.125 ft^3 per ft depth per 1 ft area. In other words, the average porosity for the 1600 ft thickness is 12.5 %. To standardize the value to 1000 ft thickness, multiply by 1000, which gives 125 ft^3 water per 1000 ft^3 rock.

The volume was figured from the digitized data for both Sonic and Neutron-Density porosity and from the crossplot data for Sonic-Neutron and Neutron-Density logs.

6. DETERMINING FORMATION TOPS

There is a discrepancy among drillers and geologists as to the top of the Glorieta and Yeso. In order to be consistent, the top of the Glorieta was "picked" below the first increase in the gamma ray deflection. See Figure 31. The Yeso was picked at the next increase. The Abo is easily determined by a major increase in the Gamma Ray count, indicating the Abo shale.

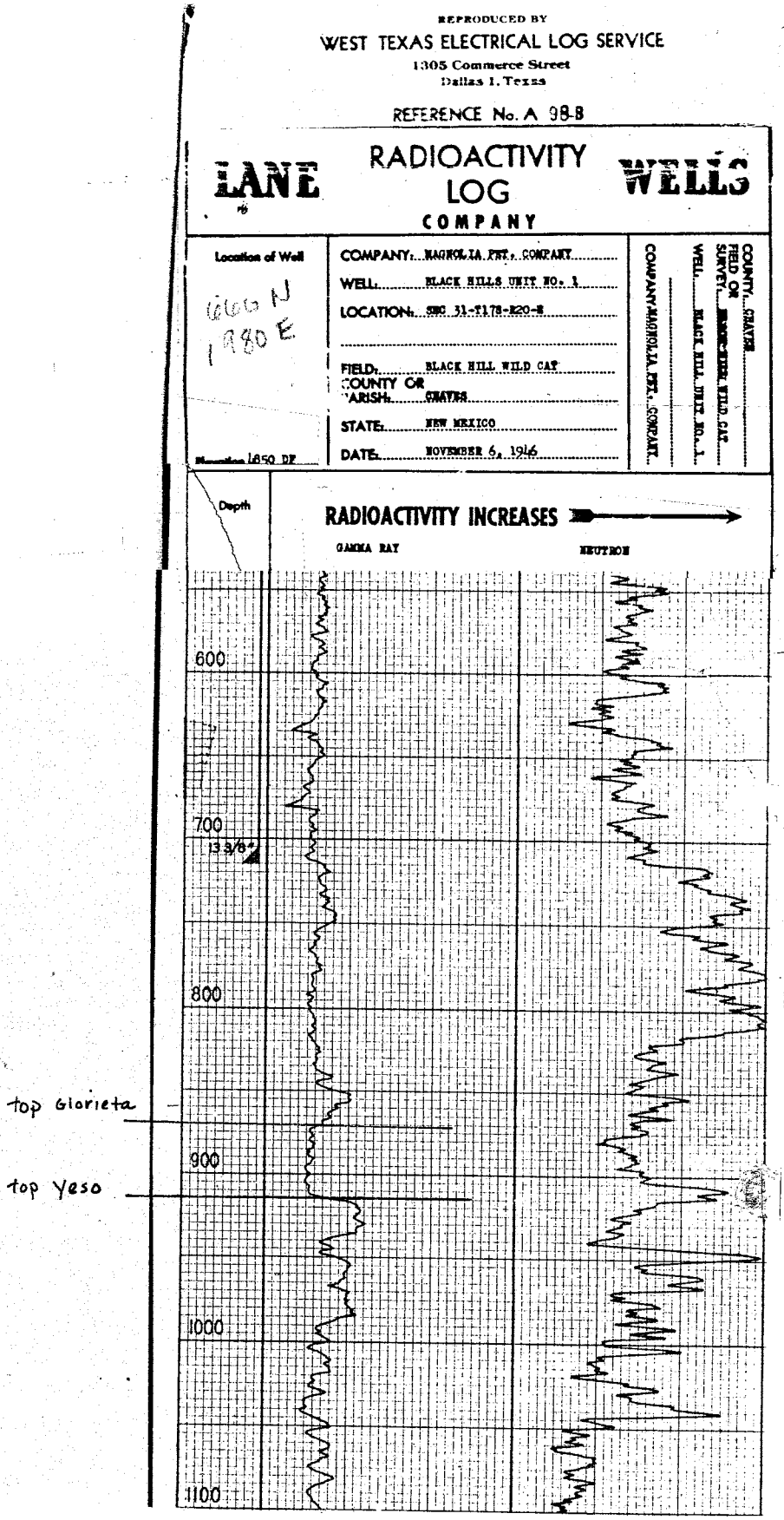

Figure 31. Gamma Log showing top of Glorieta and Yeso

V. RESULTS

A. Lithology

The results of the well log analysis are presented in the form of cross sections, Figures 33-37. The permeable Zones are colored in blue and correlated from well to well. Geologic horizons, that is , the tops of formation and marker beds are correlated with heavy black lines. In some of the wells there are no resistivity logs to delineate permeable zones, but the Gamma Ray log was available to determine formation tops. In these wells, the permeable zones from wells on either side were assumed to follow the geologic structure. The location of the wells in the cross section is shown on a map inset on each figure. The elevation above sea level is located on the left and there is no horizontal scale.

Each stratigraphic column, along with the well log data, is presented in Figures 38 - 52. A description of the porosity, secondary porosity, lithology and water quality is included next to the column. This description is from a manual analysis, whereas porosity, percent clay, and formation resistivity are from computer programs which analyzed the digitized data. The RES 75 F column is the deep resistivity log corrected to 75 F.

Figure 53 of well no. 2, shows the lithology from the driller's log compared to that determined by geophysical well log analysis. The over-generalized cross section from the drillers log is not very useful for hydrologic purposes in such a complex formation.

B. Water Quality

For every well that had a porosity and resistivity log, water quality was estimated for each permeable zone. App 2. gives the resistivity-porosity crossplots used to determine water resistivity. Some show a very good correlation, others are very scattered and had r^2 of .001. Table VII is a list of the results of all the crossplots. Actual salinity values were only calculated for zones with r^2 values greater than 0.5 , ($r > 0.7$).

C. Permeability

Table VIII shows the results of permeability estimates from grain size analysis and the value determined from the drill stem test.

D. Volume Estimates

Table IX and Figure 54 show the volume of water estimated for 1000ft of rock below each well. Volume for wells 1 and 4 was estimated from the sonic and neutron density logs for both the digitized and manual data.

Explanation of Lithology

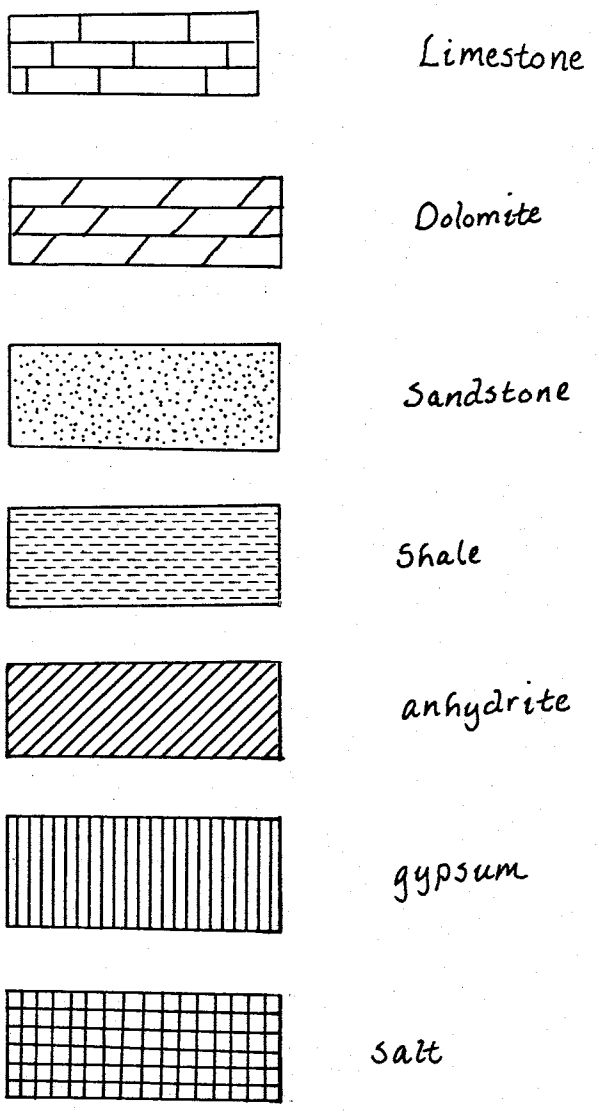

Figure 32. Explanation of Lithology

7-17S-18E UNIT 1 Dunken Dome

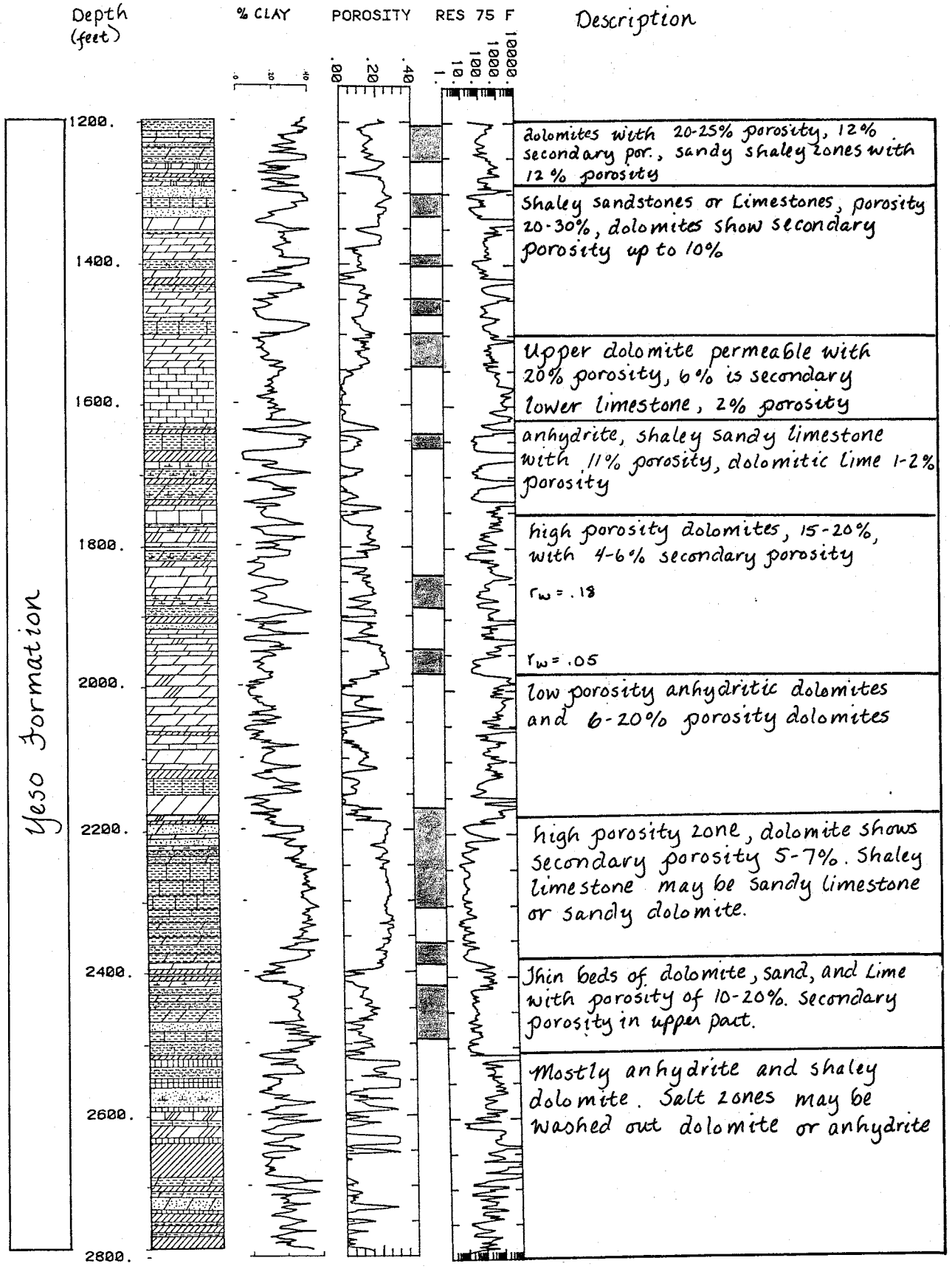

Fig 38. Well no 1

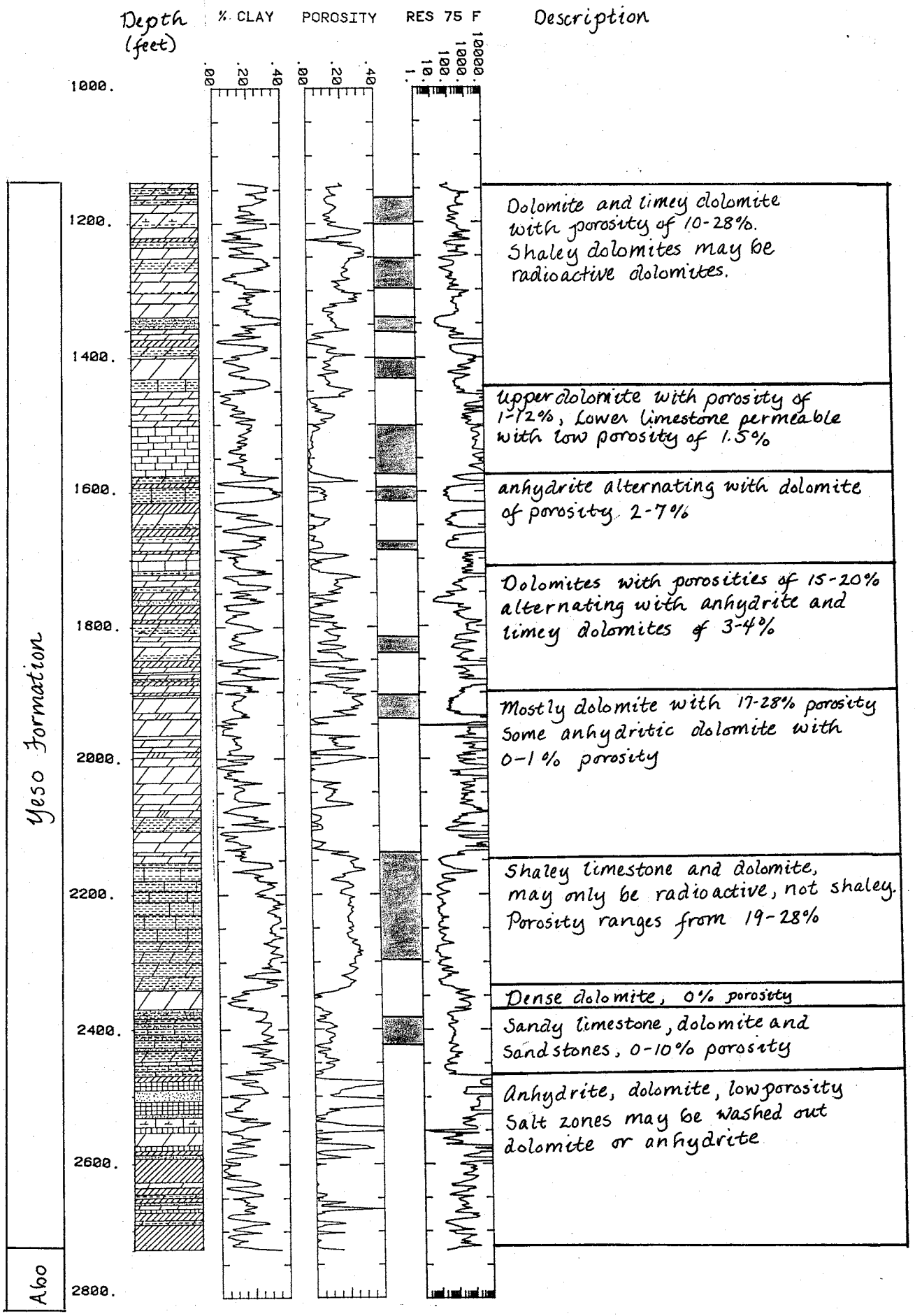

Fig 39. Well no 2

21-17S-17E T-L Watts No. 1

3

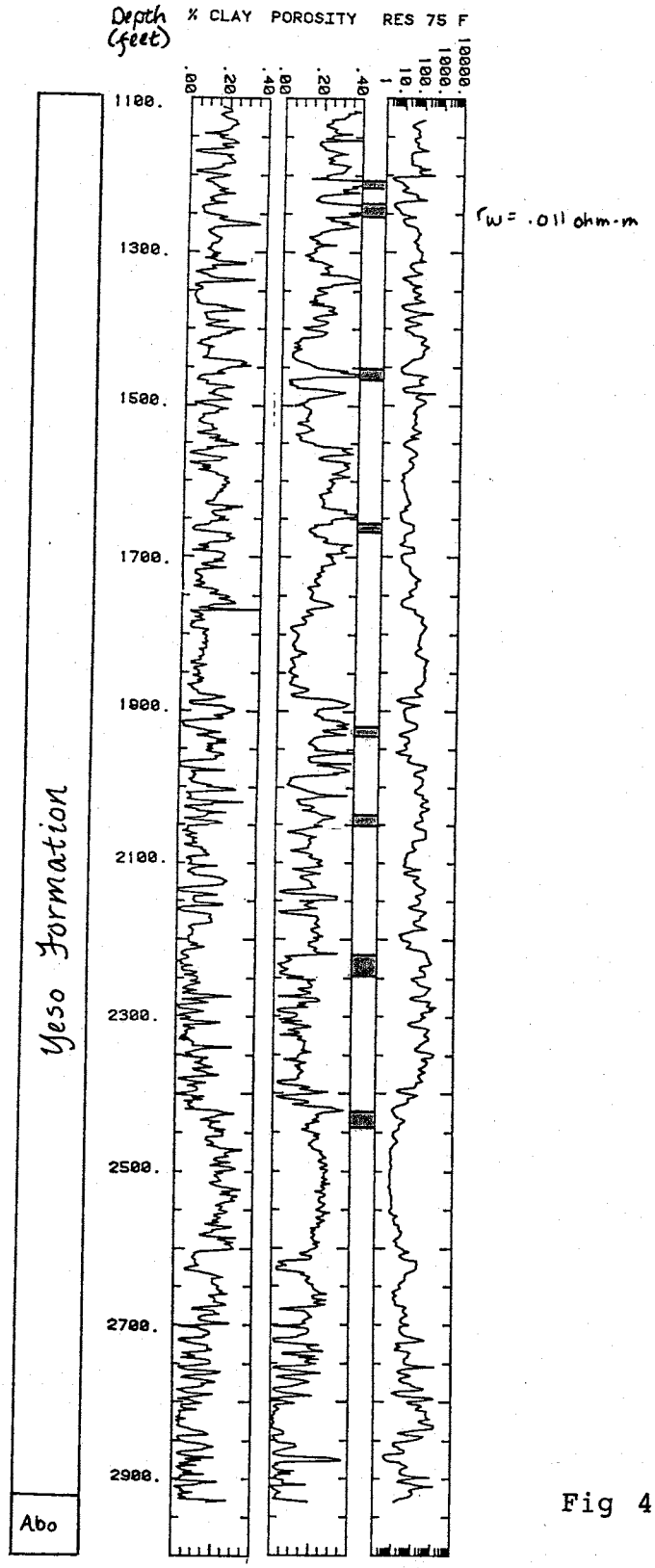

Fig 40. Well no 3

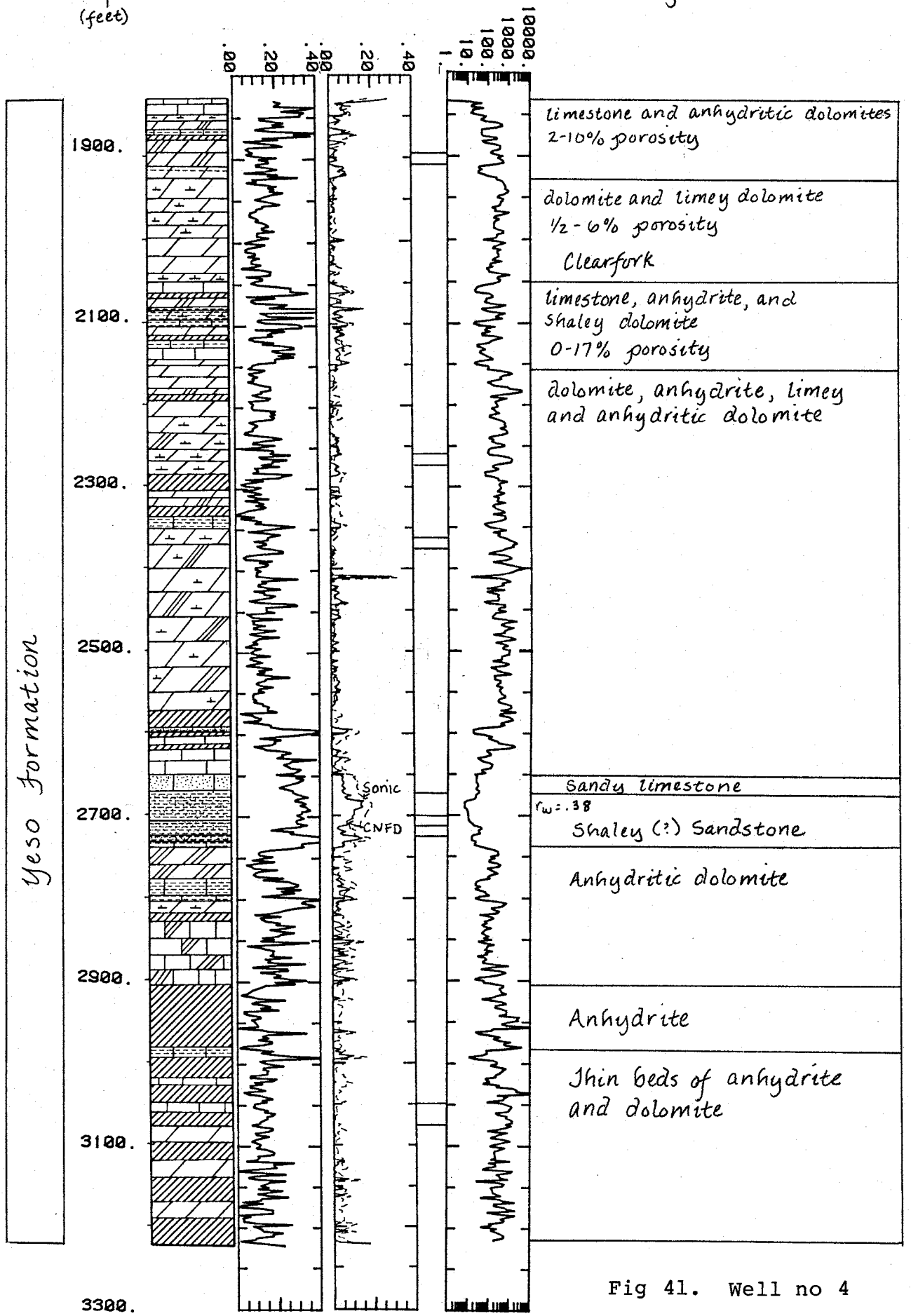

Fig 41. Well no 4

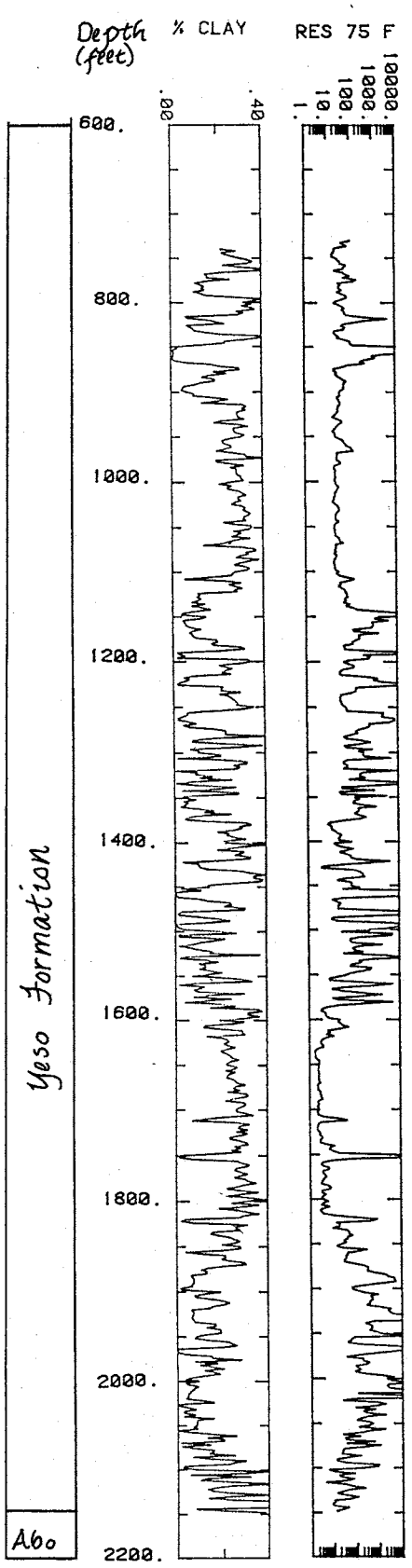

Fig 42. Well no 5

8-16S-18E New Mexico State #1

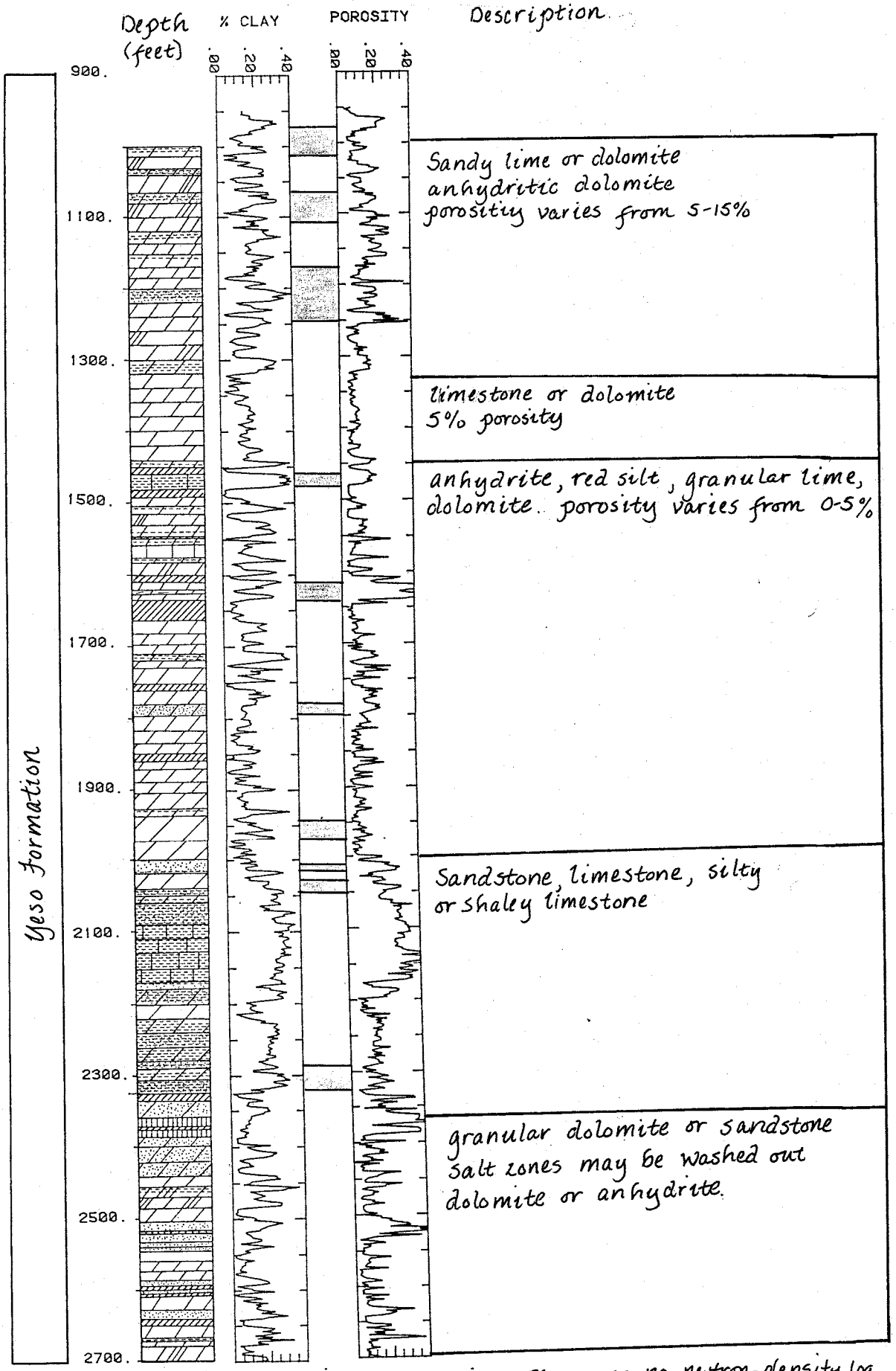

note: lithology is highly subjective. There was no neutron-density log

Fig 43. Well no 6

26-15S-18E Yates Federal No. 1

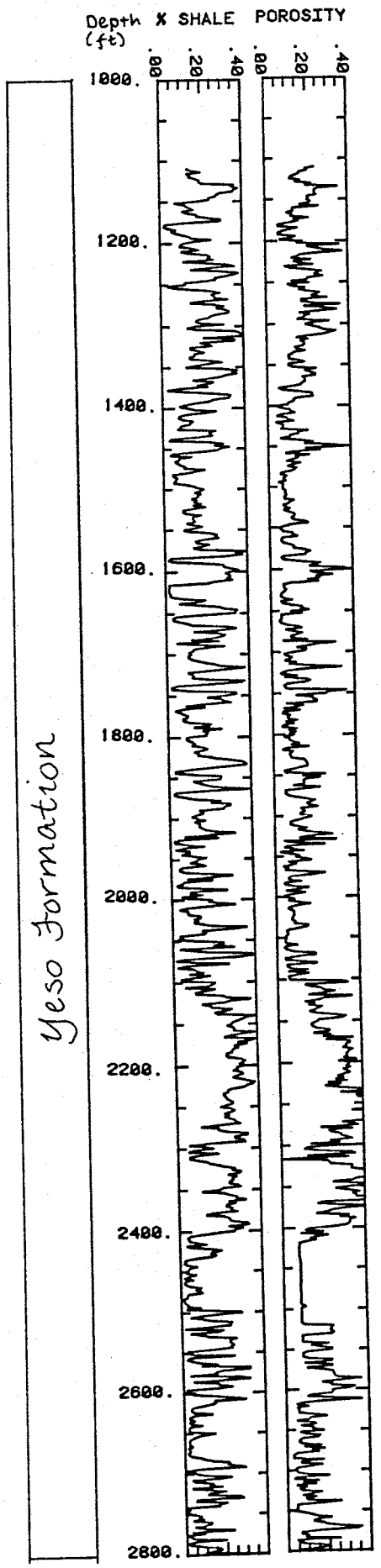

Fig 44. Well no 7

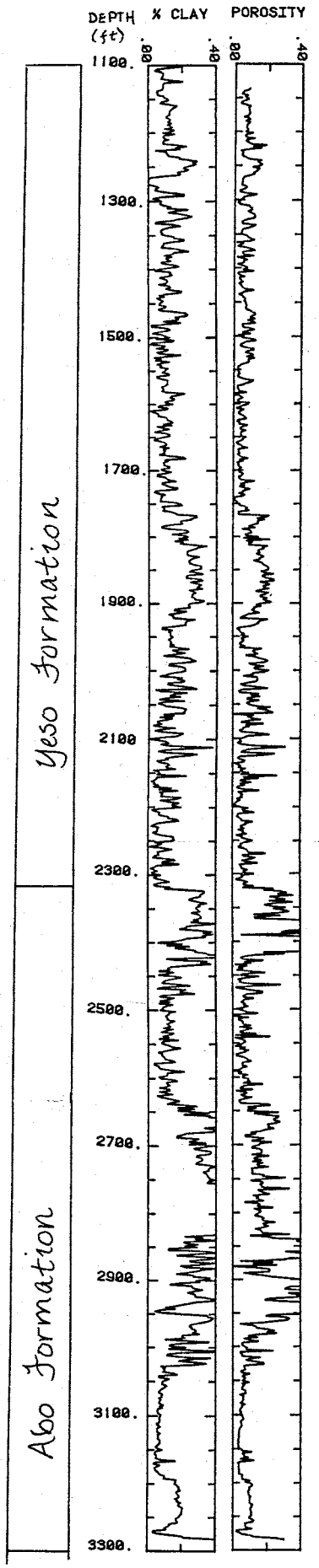

Fig 45. Well no 8

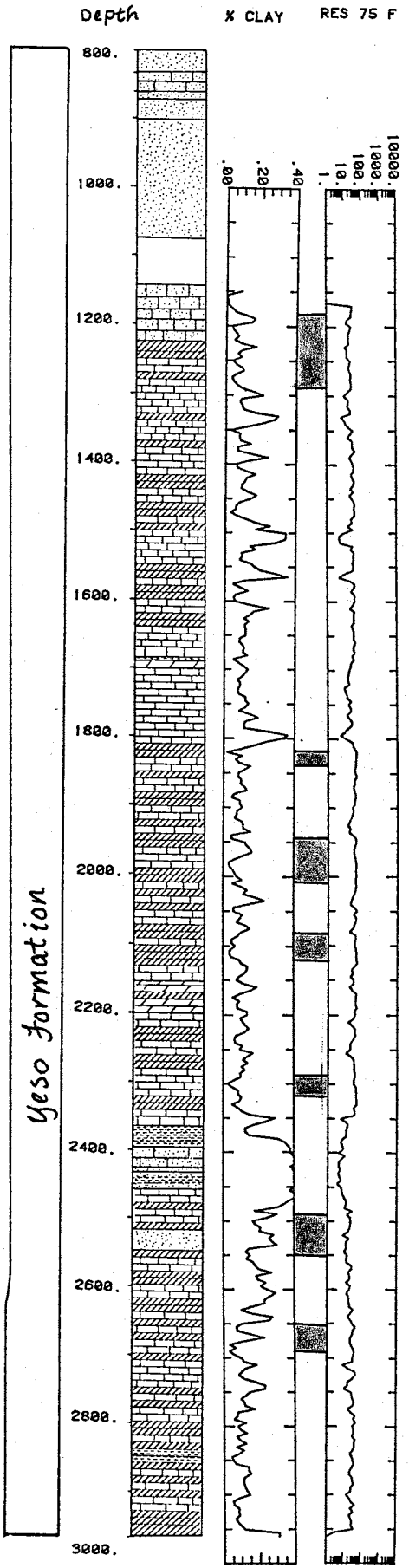

Lithology was determined from drillers log

Fig 46. Well no 9

35-18S-14E Mesa Verde Ranch No 1

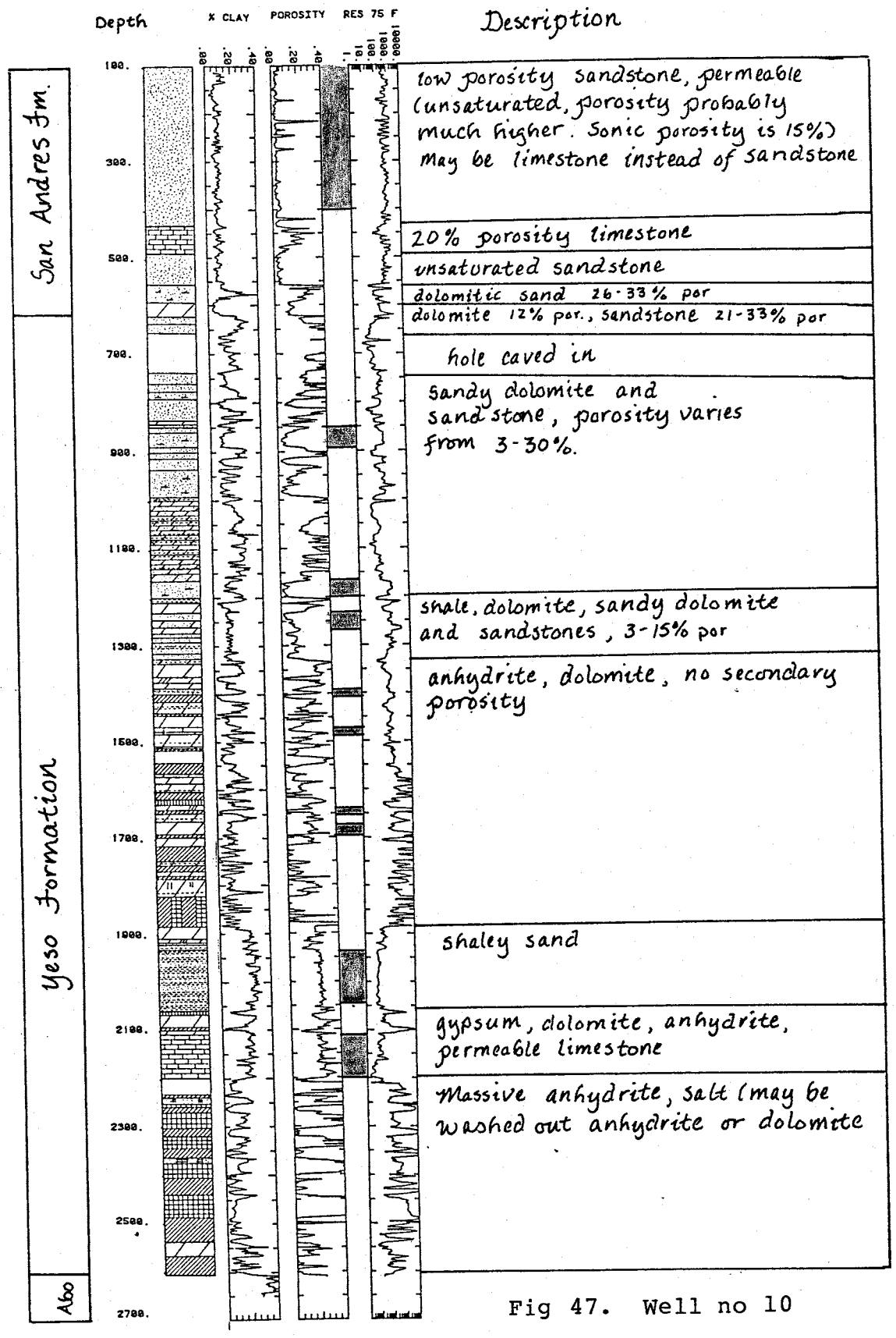

Fig 47. Well no 10

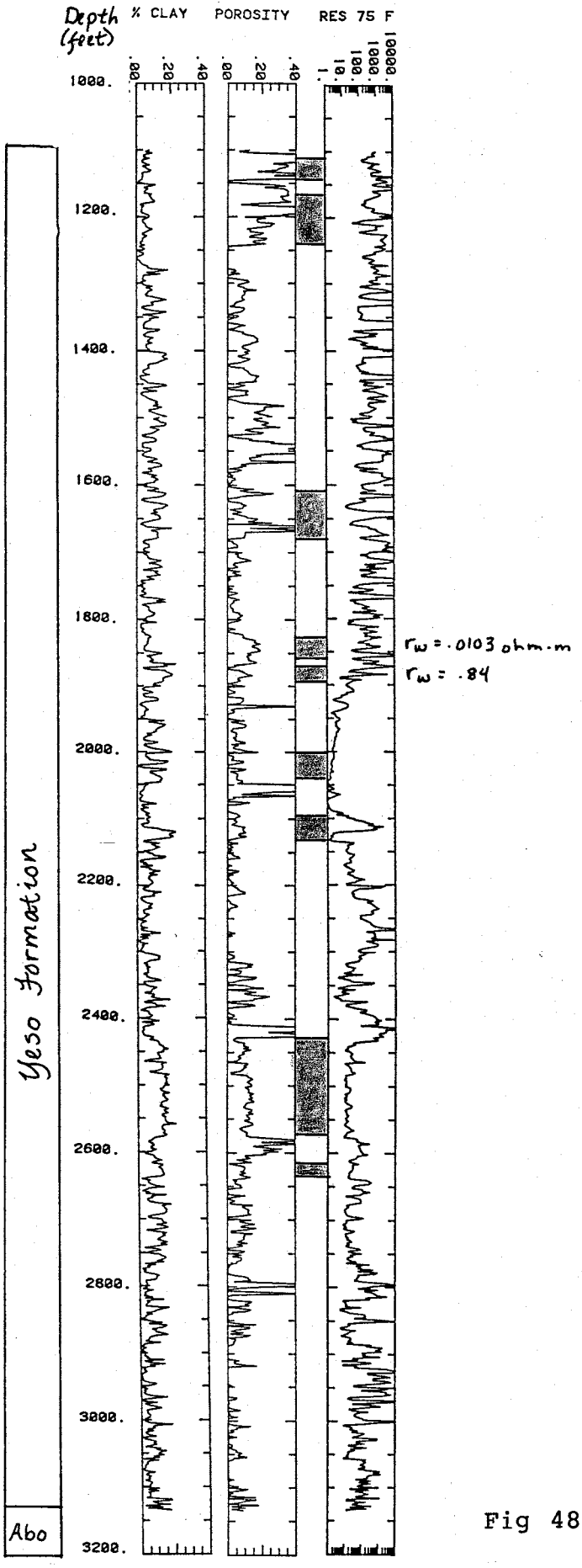

Fig 48. Well no 11

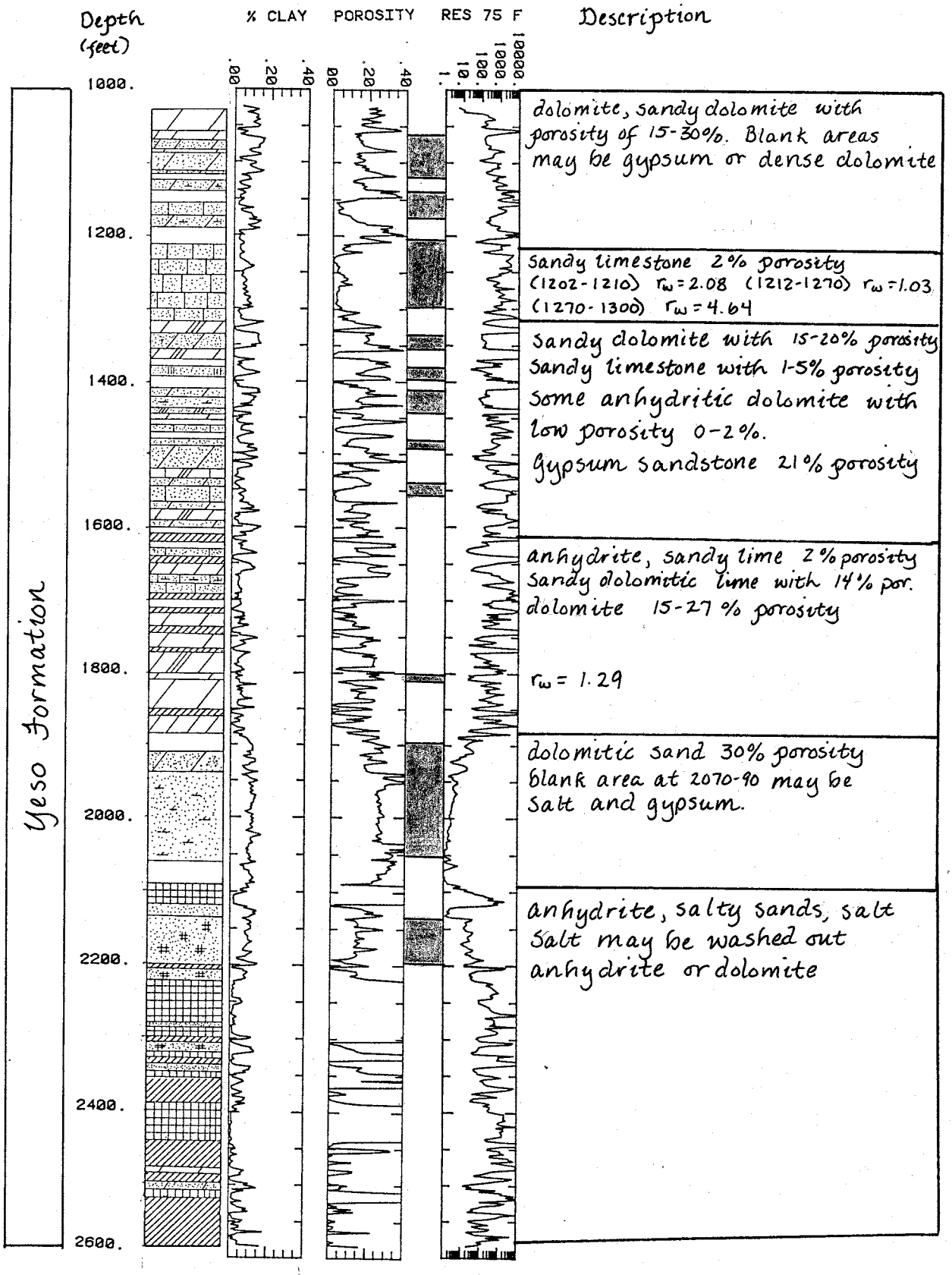

Fig 49. Well no 12

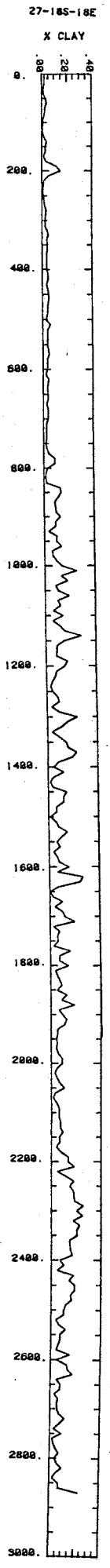

13

Fig 50. Well no 13

3-16S-16E

Anderson Randell No 1

14

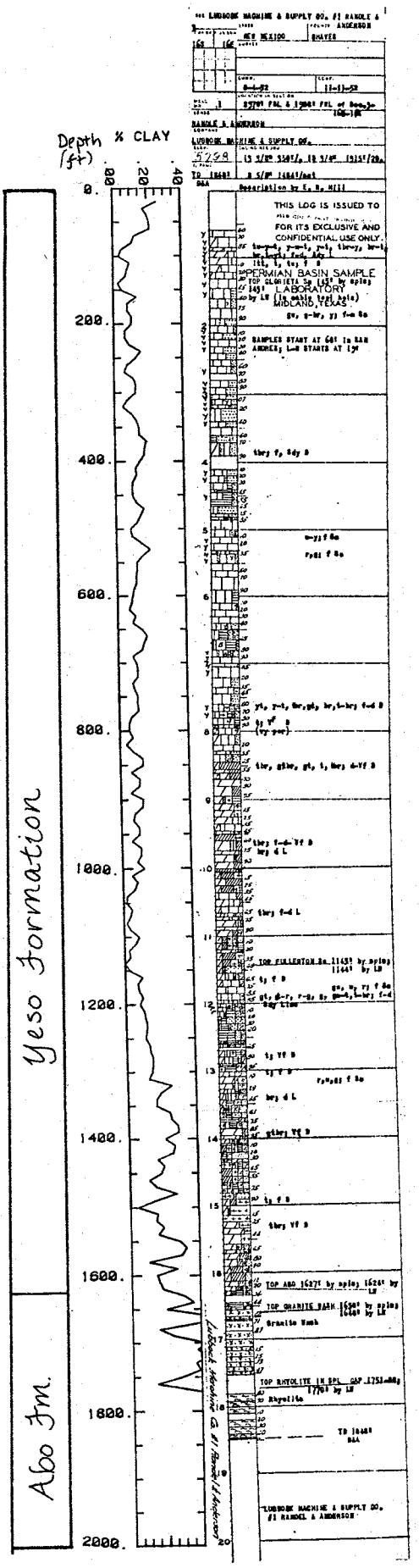

Fig 51. Well no 14

25-18S-21E Amoco McKay State #1

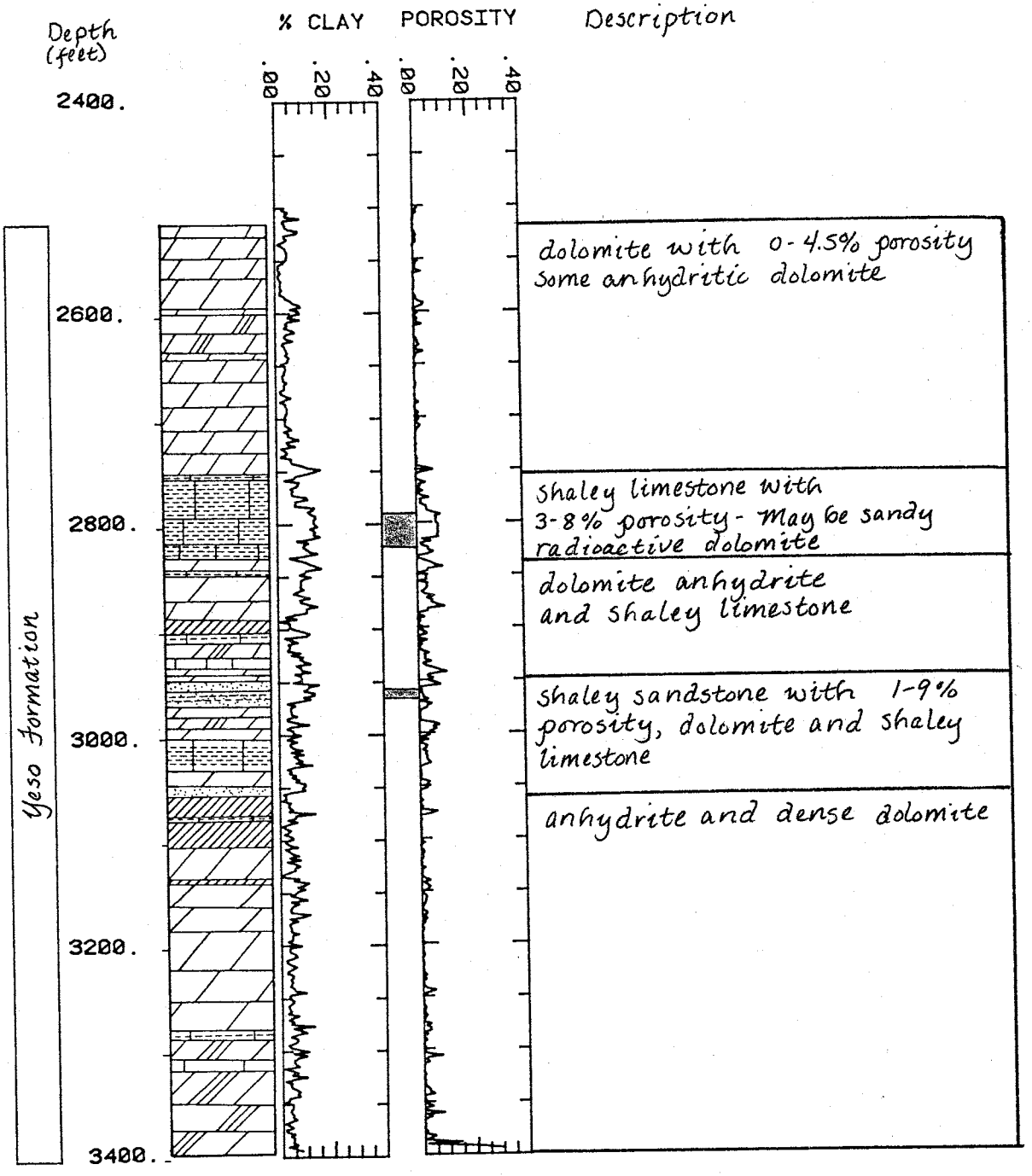

Fig 52. Well no 15

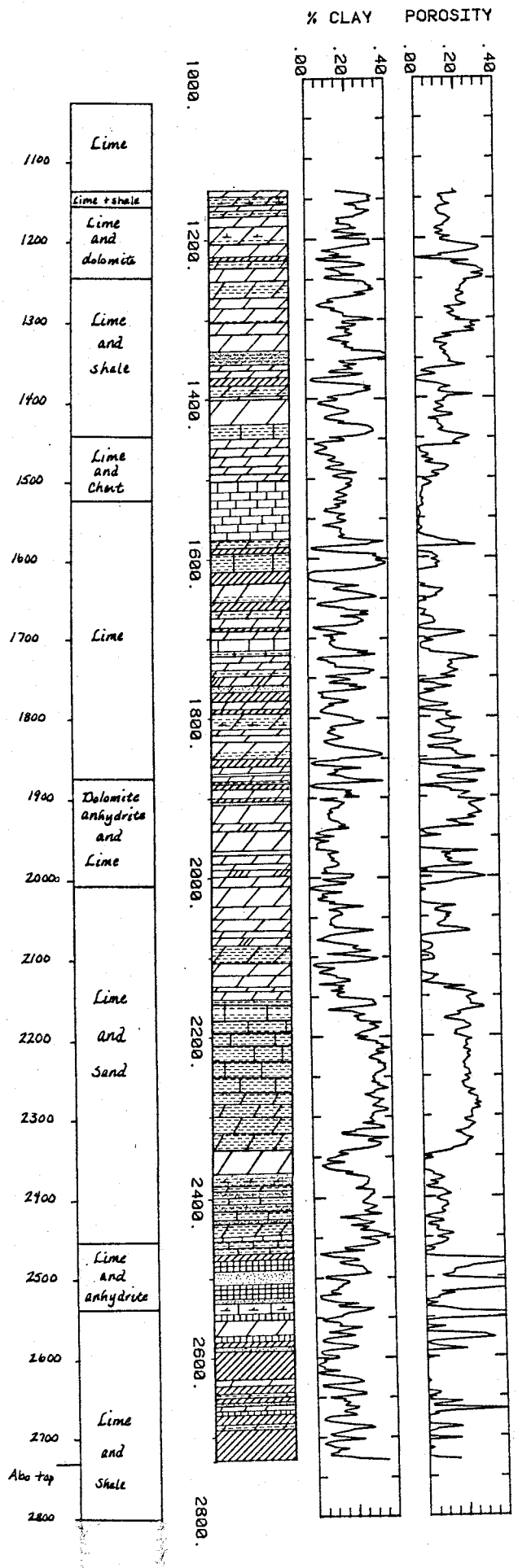

7-17S-18E
Dunken Dome
Unit No 2

Figure 53. Comparison of Lithology Determined from Geophysical Logs with Drillers Log

Table VII. Results of water quality estimation.

Well	depth	r^2	m	Rw	TDS (ppm)
1	1210-1260	.04			
	1300-1334	.16			
	1394-1406	.02			
	1456-1474	.29			
	1512-1550	.07			
	1642-1664	.00			
	1844-1884	.48	3.5	.18	24,597
	1956-1980	.58	4.9	.05	88,550
	2212-2312	.24			
	2362-2380	.05			
	2420-2464	.1			
	2474-2494	.12			
2	1176-1206	.01			
	1268-1300	.01			
	1338-1354	.00			
	1398-1430	.02			
	1502-1572	.34			
	1592-1614	.00			
	1674-1684	.02			
	1814-1836	.01			
	1908-1930	.01			
	2184-2294	.29			
3	1234-1250	.63	6.2	.011	402,500
4	2262-2272	.41	1.62	.478	
	2680-2704	.93	1.47	.376	11,775
10	110-410	.08			
	1944-2000	.32	4.44	.02	
	2000-2050	.07			
	2112-2146	.31	5.2	.0095	
11	1114-1146	.19	2.9		
	1168-1236	.18	4.74		
	1604-1618	.33	1.44	3.64	
	1830-1864	.62	3.64	.0103	429,854
	1876-1898	.92	1.36	.854	5,184
	2434-2578	.36	2.16	.15	
	2618-2638	.14	2.66	.024	

Table VII. (Continued)

Well	Depth	r^2	m	Rw	TDS (ppm)
12	1060-1118	.01			
	1130-1168	.03			
	1202-1210	.88	2.89	2.08	2,129
	1212-1270	.54	2.67	1.03	4,299
	1270-1300	.65	1.44	4.64	954
	1332-1354	0			
	1378-1392	.15			
	1408-1430	.75	-1.76	.454	
	1476-1486	.04			
	1534-1548	.16			
	1800-1810	.94	2.28	1.29	3,432
	1894-2050	.33	1.91	5.5	
	2136-2190	.08			

Table VIII. Hydraulic Conductivity for various depths as determined from grain size distributions.

Depth	dm (ft)	Kozeny-Carmen K (ft/s)	Bates and Wayment K (ft/s)
22-17S-18E			
2220	1.3×10^{-3}	1.14×10^{-7}	1.5×10^{-4}
2230	2.8×10^{-3}	5.3×10^{-7}	1.3×10^{-4}
2240	2.4×10^{-3}	3.38×10^{-7}	1.2×10^{-5}
8-16S-18E			
2050	1.1×10^{-3}	7.45×10^{-8}	2.7×10^{-5}
2080	9.1×10^{-4}	5.6×10^{-8}	2.6×10^{-5}
2100	5.5×10^{-4}	2.03×10^{-8}	9.0×10^{-6}
2140	7.9×10^{-4}	4.2×10^{-8}	1.4×10^{-5}
2160	1.7×10^{-3}	2.0×10^{-7}	6.3×10^{-6}

7-17S-18E From Drill Stem Test (depth of 2170-2210 ft)

$K = 1.03 \times 10^{-4}$ ft/s

Table IX. Volume of water estimates for a 1000ft^3 volume of rock below each well.

Well	$\frac{\text{Volume of water ft}^3}{\text{Volume of rock ft}^3} \times 1000$			
	Computer Estimate		Manual	
	Cnl-Den	Sonic	Cnl-Den	Cnl-Sonic
1	125.0	104.1	108.6	98.3
2	110.4			
3	181.7			
4	25.1	8.9	29.9	35.8
5	----			
6		130.7		
7		154.6		
8		124.1		
9	----			
10	180.4			
11	97.0			
12	213.0			
13	----			
14	----			
15	17.6			

VII. Discussion of Results and Interpretation

A. Definition of Aquifer Horizons in the Yeso Fm.

1.Continuity and Correlation Along Dip

As indicated by the cross sections, Figures 33-37, there is a great deal of heterogeneity in the Yeso. The blue colored zones are permeable zones and represent aquifers or rock units through which water might easily flow. We were reluctant to designate "tight" or non-permeable zones because a permeable zone may appear "tight" on the resistivity log for reasons explained previously. Therefore, the permeable zones represent a minimum.

Very few broad generalizations can be made. One is that the lithology becomes less heterogeneous to the east. There appears to be less shale and sandstone and more limestone and dolomite to the east. This increase in homogeneity of lithology is reflected in the Z-plots (see Fig 12 and Appendix 1). The Z-plots are crossplots of Neutron porosity versus Density porosity with values of percent clay designated with different symbols. Regardless of the percent clay value, the distribution of points changes from west to east, with more scatter in the western wells, indicating more variable rock types. The Z-plots of wells in the eastern part of the study area (no 4 and 11) show very little scatter, with most points plotting on the low porosity dolomite line. The points plotting near the carnalite point (near the NE corner of the crossplot, of Fig. 13), which have low percent clay and high porosity values, are probably from zones where the hole has caved in.

The porosity and the number and thickness of permeable zones in a well also decrease eastward. This is expected for the typical basin aquifer. As waters move basin-ward deposits build up, reducing the permeability of the aquifer. There are additional factors, however, that complicate the picture. the Y-O, 6-mile, and Border buckles have complicated the area. For instance, on Fig 34, well no.17 and no.3 are separated by the 6-mile buckle, an anticline. Well no.17 shows many more permeable zones than well no.3, which is west of 17. These permeable zones may be perched aquifers within the anticline. The decrease in permeability and porosity may also be a result of the change in lithology from west to east. The sandy units in the west are probably more permeable and porous than the limestone in the east.

Another generalization is that the permeable zones follow geologic layers, therefore having the same dip as the geologic beds. This, however, is the case because that is the way the zones were correlated. It is just as conceivable to have these zones cross geologic layers. However, the zones probably do follow the geologic beds because there are many impermeable units, such as anhydrite, which appear to cap permeable zones. Also, the large shale zone at the top of the Abo would preclude appreciable movement of water between the Yeso and the Abo.

Overall, there is one thick permeable zone in the lower part of the Yeso, which is generally part of the Drinkard Sandstone. The permeable zone of the Drinkard appears to thin in some areas, but it is the most prominent zone. There is a continuous permeable zone about 25-50 feet thick below the Drinkard. The upper marker bed is not consistently permeable throughout the area. Below this marker bed, however, there is a zone about 25 feet thick which is continuous throughout. There are numerous permeable zones which are only continuous in one direction. That is, some zones are continuous from North to South and not from East to West.

The discontinuity of permeable zones may be an indication that there are different groundwater systems within the Pecos Slope and that it cannot be treated as one system. The numerous fault blocks and folds may divide the slope into various systems. Many more wells are needed to clarify the nature of the heterogeneity of the Yeso.

2. Volume Estimates

The volume of water in the Yeso seems to be uniform until about 20 E where it decreases drastically (see Fig 54). This would indicate that the water must be forced upward (or downward) before it reaches about 20 E which is approximately where the San Andres changes from water table to artesian conditions.

The difference in volume estimated from the digitized and the crossplot data is probably due to the salt beds, or caved in zones, which appear as high porosity, but were assumed zero in the manual estimation. The difference in values between the Sonic and Neutron-Density values in well no.1 (see Table IX), is a result of secondary porosity. From the cross-plot estimation, it appears that one tenth of the porosity, overall, is secondary. In well no.4 the volume estimated from the Sonic-Neutron is higher than the volume from the Neutron-Density, as estimated from the crossplot data. This may indicate that gas is present, which is not unlikely, because this well is further east, closer to known petroleum resources. The volume estimated from the digitized Sonic data is much lower in well no.4 than the Neutron-Sonic value estimated from the crossplots. It may be that the porosity determined from the Sonic crossplot is not affected by secondary porosity as much as Wiley's time-weighted equation (Eq. 7).

3. Water Quality Estimates

Few of the permeable zones showed a good correlation between porosity and Rw. This leaves very little data for interpretation. This analysis does show the great variability in water quality even within one well. For example, well no. 11 shows a variation in TDS from 5,184 ppm to 429,854 ppm, and TDS does not increase systematically with depth. Some of the zones are very thin, only 8 feet thick, which means only 4 points were used to determine Rw. Therefore, the value determined from a

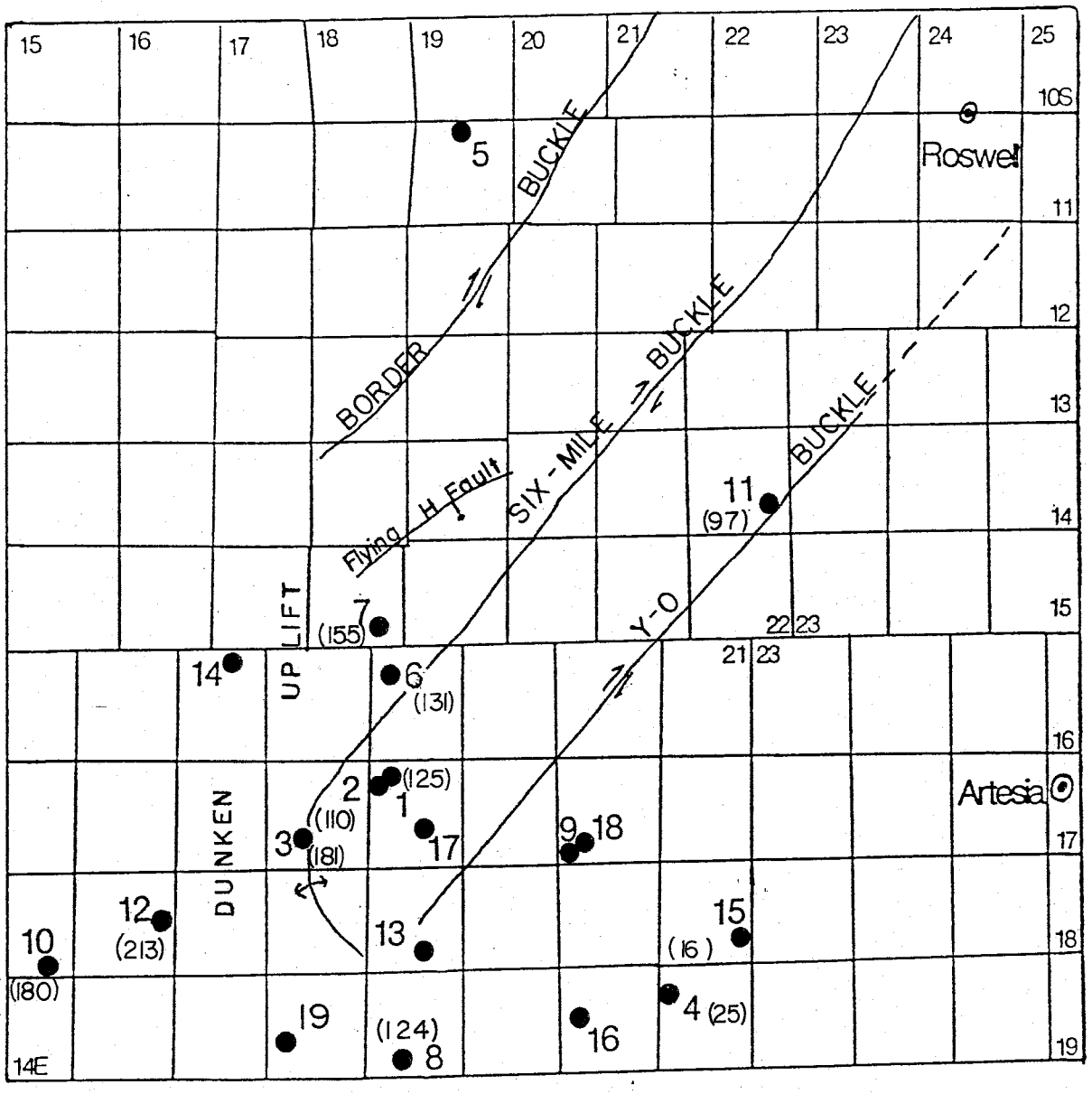

Figure 54. Map of Wells with Volume of Water Estimates (water volume in ft per 1000 ft of rock)

thin zone may not be reliable. The 'm' value (cementation factor) is reasonable for most zones with high r^2 values, except for one zone (1408-1430) from well no. 12. The r^2 value is .75, but the m value is negative. This can only be the case if the water is very pure and more resistive than the rock, which is highly unlikely in the Yeso Fm.

If these estimates of salinity are representative of the water quality of the Yeso in general, then it is unlikely that the Yeso contributes much recharge to the San Andres aquifer, since the San Andres generally has good quality water. It is possible, however, that ion filtration by shale and shaly zones in the upper Yeso could reduce the salinity of the water during recharge to the San Andres.

B. Indications of Groundwater Potential of the Abo

The top of the Abo is marked by a very thick section of shale, below this are limestones and anhydrites. As indicated by the resistivity logs, the Abo appears to be very "tight" throughout the formation. However, in one well (20-19S-20E) the Abo appeared more permeable than the Yeso. In well no. 8, there are permeable zones in the Abo which might be hydrologically connected with zones in the Yeso. There may be hydrologic connection between the Yeso and the Abo , but more information (more wells) is needed to determine the subsurface structure and hydrologic connection.

V. STATISTICAL ANALYSIS

The data were digitized in two foot intervals, which allows for time series analysis. The auto correlation function was used to determine any cyclic changes which might occur as a result of successive transgression -regression sequences. The correlation length was also determined to define the continuity of zones within the Yeso.

Autocorrelation is a process of comparing a sequence of data with itself. This is done by shifting the data in successive positions, or lags, and measuring the "goodness of fit" at each lag position. Davis, (1973), explains this by using the analogy of a chain. Each link represents a data point. Put two identical chains side by side and compare them, then shift one chain one link (one lag) and compare. At zero lag, there is perfect correlation. The auto correlation function, r_L, measures the correlation at each lag. At lag zero, r_L is equal to one. As the lag increases, r_L goes to zero, or becomes negative if there is an inverse correlation. If r_L decreases to a small number, then increases again (with increasing lag), this would indicate some type of cyclic change within the sequence. The auto correlation function, r_L, of a time series at lag L is given by:

$$r_L = \frac{\left[(n-L)(\Sigma Y_i Y_{i+L}) - \Sigma Y_i \Sigma Y_{i+L}\right] /(n-L)(n-L-1)}{\left[n \Sigma_{i=1}^{n} Y_i^2 - (\Sigma_{i=1}^{n} Y_i)^2\right] /n(n-1)} \qquad (41)$$

$$r_L = \frac{\mathrm{Cov}\ (Y_i, Y_{i+L})}{\sigma^2} \qquad (42)$$

where: n = number of observations (lenth of series)
Y = parameter in time series (i.e. porosity)
σ^2 = variance
and $-1 < r_L < 1$

The correlation length is an estimate of the distance over which a variable has a significant correlation. That is, if a zone is highly variable, the correlation length will be short compared to a zone which is more uniform. r_L generally has an exponential decay with increasing lag, and therefore, the correlation length is equal to the lag when $r_L = e^{-1} = 0.37$.

When the porosity and percent shale for the entire Yeso section was detrended and analyzed, the auto correlation function remained above zero, which would tend to indicate a very long correlation length, (see Figs 55 and 56). r_L did not equal zero even with a lag of 160 ft. It may be that the sequence analyzed is too long. A very long sequence may not be stationary, that is, its statistical properties may change with distance (or time). It is necessary for a sequence to be stationary in order

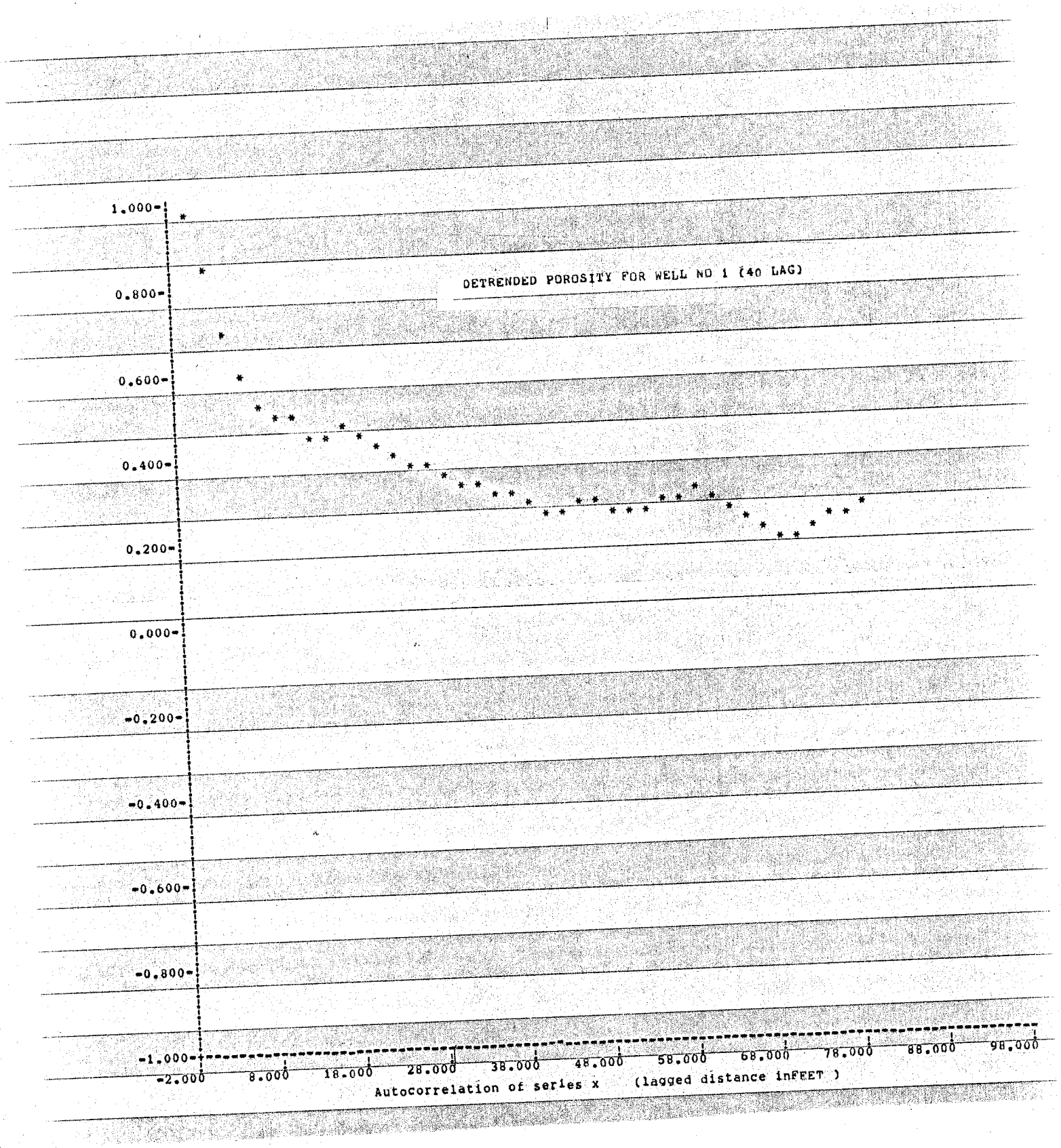

Figure 55. Correlogram for Porosity of Well no. 1

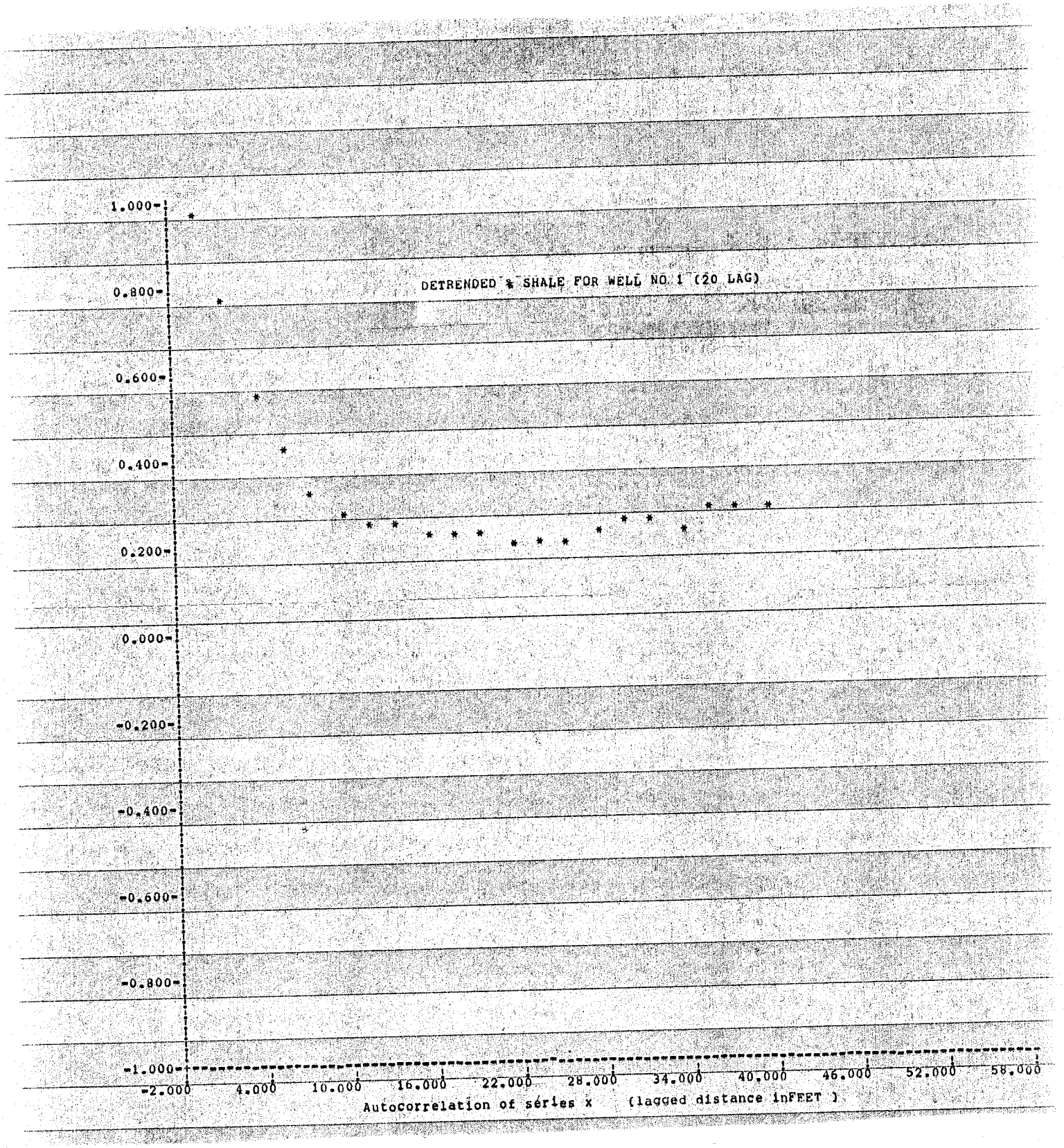

Figure 56. Correlogram for Percent Shale of Well no. 1

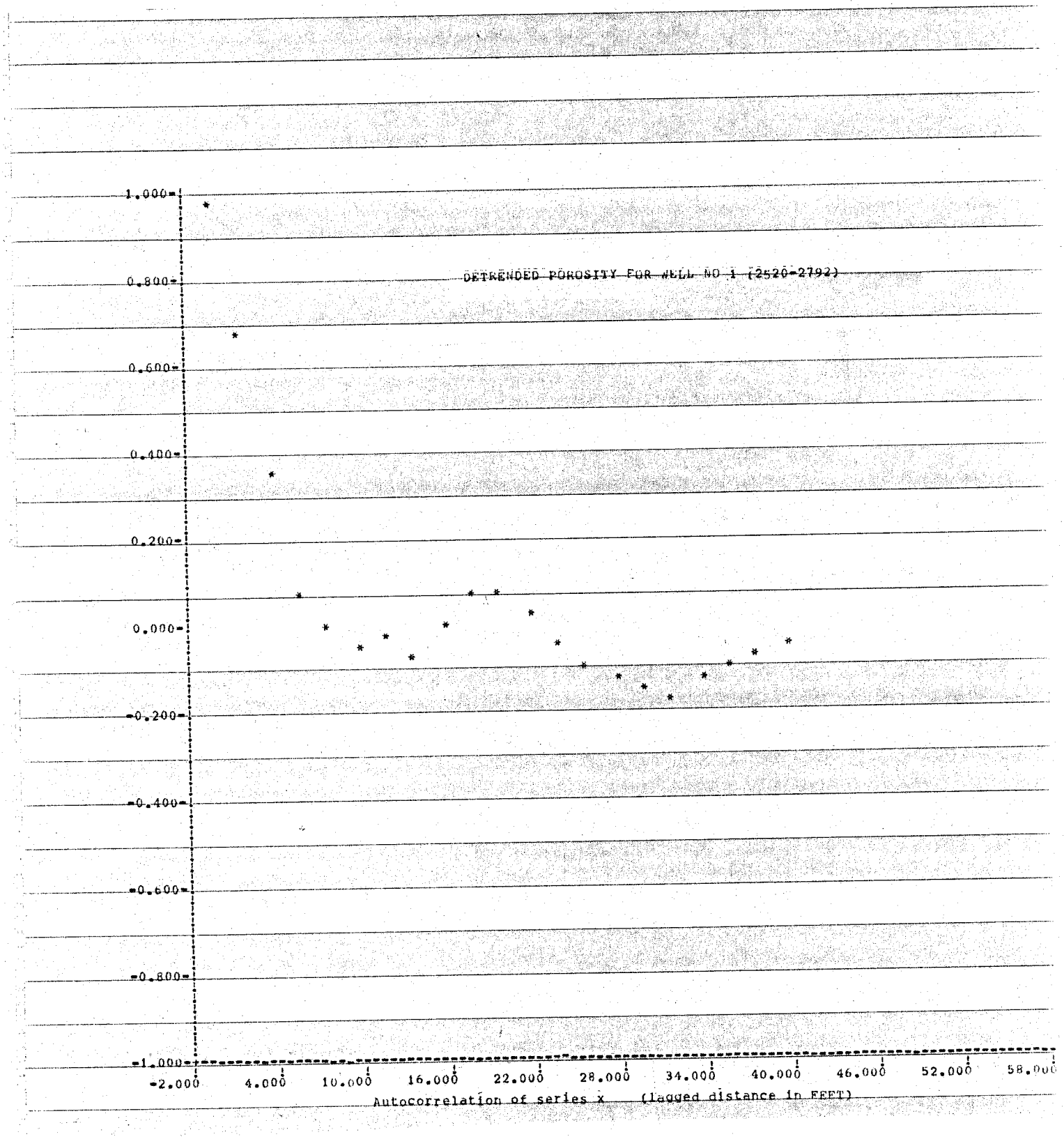

Figure 57. Correlogram for Porosity of Lower Section of Yeso Fm. of Well no. 1

to use this type of statistical analysis.

Therefore, the Yeso was analyzed in segments of approximately 400 feet, the upper Yeso, upper middle Yeso, lower middle Yeso (Drinkard), and the lower Yeso. See App 4 and 5 for the correlograms of wells 1 and 2.

The only zone which shows any slight cyclic change is in the lower Yeso. Fig 57 is the correlogram of porosity of the lower zone in well no 1. r_L drops to zero within 4 feet of lag, and then increases to 0.08 by 18 feet. Only 4 wells clearly showed this increase in r_L, which is at an average distance of 20 ft. This cyclic change is not significant, however, because the autocorrelation coefficient is low. The cyclic change is probably a result of the caved in sections in the lower Yeso, which are approximately 20 ft apart. The correlograms for percent shale of this zone show the same type of cycle with an average separation of 15 ft between peaks.

Table X lists the correlation lengths of each zone from each well, for porosity and percent shale. The average correlation length for porosity of the lower Yeso and the upper middle Yeso is 5 feet, whereas the average for the lower middle Yeso is 10 feet and the upper Yeso is 7 ft. These values are consistent with what is observed on the well logs. The lower and upper middle Yeso appear more variable than the lower middle and upper Yeso. The correlation lengths of percent shale show similar results, but are slightly shorter than the correlation lengths of porosity, which would indicate that the percent shale is more variable than porosity.

Table X . Correlation lengths (in feet) of porosity and percent shale for four zones in the Yeso.

POROSITY

well no.	1	2	3	4	6	7	10	11	12	15	Ave
Lower	4	5	3	1	6	4	9	3	13	3	5
Lower Middle	14	22	3	14	30	10	3	5	3	7	10
Upper Middle	8	7	4	2	14	3	3	6	3		5
Upper	13	4	10	3	6	6	8	9	7		7

PERCENT SHALE

well no	1	2	3	4	5	6	7	10	11	12	15	Ave
Lower	3	3	2	2	3	4	3	3	3	4	1	3
Lower Middle	9	8	4	5	3	14	6	4	8	3	9	7
Upper Middle	4	4	3	3	3	4	3	3	4	3		3
Upper	5	5	4	2	10	5	5	8	4	3		5

VI. SUMMARY OF CONCLUSIONS

1. Lithology becomes more homogeneous to the east. Porosity and permeability decrease to the east.
2. The volume of water decreases sharply at 20E, approximately where the principal aquifer comes under artesian pressure. This supports the notion that the Yeso Formation recharges the San Andres aquifer. The small number of water quality determinations we were able to derive from the logs does not allow conclusions as to the magnitude of this source. The salinities calculated may be overestimated due to the presence of clay.
3. Permeable zones follow geologic layers.
4. Many permeable zones are discontinuous, or "perched", but three zones appear to be continuous throughout the area;
    1. 25 ft zone below the upper marker bed
    2. 25-200 ft zone in the Drinkard Ss.
    3. 25-50 ft zone below the Drinkard Ss.
5. Water quality varies greatly within a well and does not decrease systematically with depth, perhaps reflecting the greatly varying lithologies of this formation.
6. Permeability could only be defined in a qualitative manner.
7. The average porosity for the Yeso in each well varies from 10 to 25 %, with an overall average of 13.5%.
8. The Yeso Formation is very anisotropic with respect to aquifer properties, such as porosity and permeability.
9. The upper Yeso and the lower middle Yeso are more homogeneous, with respect to porosity, than the upper middle and the lower zones.
10. Percent shale is more variable than porosity within a zone.

VII. RECOMMENDATIONS FOR FUTURE WORK

Many of the unanswered questions of this study could be solved by coring and logging a well, sampling the water, and testing for hydraulic conductivity in the Yeso Formation. A core would be useful to determine the exact lithology, type of clay and validity of the results determined from the geophysical logs. Determining whether the dolomites are shaly or radioactive would greatly aid the interpretation of logs in other wells. Sampling the water would pinpoint the changes in water quality with depth and would help determine hydraulic conductivity from the Resistivity log. It would also be interesting to compare the water resistivity value determined from the well log methods done in this paper with the actual value. An investigation of oxygen-18 and deuterium in water samples would be of great interest. Oxygen and deuterium are fractionated during ion filtration. Therefore, an analysis of oxygen-18 and deuterium

might indicate whether ion filtration is occurring and, if this is the case, then an estimate of recharge could also be determined. Water samples would need to be taken at various intervals, above and below shale layers.

Pump tests of the permeable zones determined from the Resistivity log would give values of hydraulic conductivity of the Yeso, of which there is virtually no information. If there is a correlation between hydraulic conductivity and formation factor, this might help predict conductivity in other wells.

Drilling this well is probably not financially feasible because it would need to be about 3000 ft deep. Perhaps some of the oil companies would be willing to take water samples or possibly do a pump test on the Yeso before they drill deeper.

It might be possible to determine clay type (or types) from the available cuttings using x-ray diffraction. If clay type was known, a better interpretation of lithology and porosity could be made.

If, in the future, more wells are drilled into the Yeso and water quality is determined, an iso-chloride contour map could be constructed. It might then be possible to relate, for example, high chloride concentrations with a perched aquifer, and thus define various systems, both laterally and vertically, within the Pecos Slope.

REFERENCES

Bates, R.C. and Wayment, W.R., 1967. "Laboratory Study of Factors Influencing Water Flow in Mine Backfill: Classified Mill Tailings", US Bureau of Mines , Report of Investigations 7034

Carothers, J.E., 1968, A Statistical Study of the Formation Factor Relation, The Log Analyst, Sept-Oct 1968

Coates, G.R., and Dumanoir, J.L., 1973. A New Approach to Improved Log Derived Permeability, SPWLA 14th Annual Logging Symposium, 1973

Davis, J.C.,1973, "Statistics and Data Analysis in Geology", John Wiley and Sons, Inc.

Duffy, C.J., Gelhar, L.W., and Gross, G.W., 1978. Recharge and Ground-water Conditions in the Western Region of the Roswell Basin: N.M. WRRI Report 100, 111p

Fiedler, A.G., and Nye, S.S., 1933. Geology and Ground-Water Resources of the Roswell Artesian Basin, New Mexico: U.S. Geological Survey WSP 639, 372p

Frost, E. JR., and Fertl, W.H.,1980. Prolog Wellsite Analysis, Part II, The Log Analyst. Jan-Feb 1980.

Gross, G.W., Hoy,R.N, and Duffy, C.J., 1976. Application of Environmental Tritium in the Measurement of Recharge and Aquifer Parameters in a Semi-arid Limestone Terrain, N.M. WRRI Report 80. 212p

Hantush, M.S. 1957. Preliminary Quantitative Study of the Roswell Groundwater Reservoir, New Mexico. NMIMT Research and Development Division, Socorro, N.M.

Havenor, K.C., 1968, Structure, Stratigraphy, and Hydrology of the Northern Roswell Artesian Basin, Chaves County, New Mexico: New Mexico State Bureau of Mines and Mineral Resources Circular 93, 30 p

Hilchie, D.W., 1978. Applied Open Hole Log Interpretation for Geologists and Engineers, Douglas W. Hilchie Inc., Golden Colorado.

Hilchie, D.W., 1979. Old (pre 1958) Electrical Log Interpretation, Douglas W. Hilchie Inc., Golden Colorado.

Hilchie, D.W., 1982. Advanced Well Log Interpretations, Douglas W. Hilchie Inc., Golden Colorado

Keys, W.S. and MacCary, L.M., 1971, Application of Borehole Geophysics to Water-Resource Investigations, Techniques of Water-Resource Investigations of the United States Geological Survey, Book 2 Chapter E1

Kottlowski, F.E., 1963. Paleozoic and Mesozoic Strata of Southwestern and South-Central New Mexico. New Mexico State Bureau of Mines and Mineral Resources Bulletin 79, 100pp

Kwader, T., 1982, Interpretation of Borehole Geophysical Logs in Shallow Carbonate Environments and Their Application to Ground Water Resources Investigation. Ph.D. Dissertation, Florida State University

Lloyd, E.R., 1949. Pre-San Andres Stratigraphy and Oil Producing Zones in Southeastern New Mexico: N.M. Bureau of Mines and Mineral Resources Bulletin 29. 87pp

Lynch, E.J., 1962. Formation Evaluation, Harper and Row, Publishers.

Morgan, A.M., 1938. Geology and Shallow-Water Resources of the Roswell Artesian Basin, New Mexico. New Mexico State Eng., 12th-13th Biann Rpts.

Morris, R.L., and Biggs, W.P., 1967, Using Log-Derived Values of Water Saturation and Porosity, SPWLA 8th Annual Log Symposium

Pirson, S.J., 1983. Geologic Well Log Analysis, 3rd Edition, Gulf Publishing Co.

Pray, L.C., 1961. Geology of the Sacramento Mountains Escarpment, Otero County, New Mexico. N.M. State Bureau of Mines and Mineral Resources Bulletin 35, ppl33.

Rehfeldt, K.R., and Gross, G.R., 1982. The Carbonate Aquifer of the Central Roswell Basin: Recharge Estimation By Numerical Modeling. WRRI Report No 142, 136 p

Robinson, R.A., and Stokes, R.H., 1955. Electrolyte Solutions. New York, Academic Press.

Ruhovets, N. and Fertl, W.H., 1982. Digital Shaley Sand Analysis Based of Waxman-Smits Model and Log-Derived Clay Typing, The Log Analyst, May-June 1982.

Schlumberger Log Interpretation Charts, 1985, Schlumberger Well Services

Simcox, A.C., 1983. Hydrology and Evolution of the Upper Rio Penasco Drainage Basin, New Mexico. Masters' Thesis, Dept. of Geoscience, New Mexico Institute of Mining and Technology, Socorro, N.M.

SPWLA Reprint Volume; Shaley Sand, 1982. Society of Proffesional Well Log Analysts.

Theis, C.V. and others, 1942. Groundwater Hydrology of Areas in the Pecos Valley, New Mexico. National Resource Planning Board, Pecos River Joint Investigation Reports, Washington, D.C.

Urish, D.W., 1981. Electrical Resistivity-Hydraulic Conductivity Relationships in Glacial Outwash Aquifers, Water Resources Research, Vol 17, No 5, Pages 1401-1408, Oct 1981

Weber, R.H., and Kottlowski, F.E., 1959. Gypsum Resources of New Mexico, Bulletin 68, 57pp, New Mexico State Bureau of Mines and Mineral Resources, Socorro, N.M.

Welder, G.E., 1983. Geohydrologic Framework of the Roswell Ground-Water Basin, Chaves and Eddy Counties, New Mexico. USGS Technical Report 42.

App 1a. Z-plot for well no 1

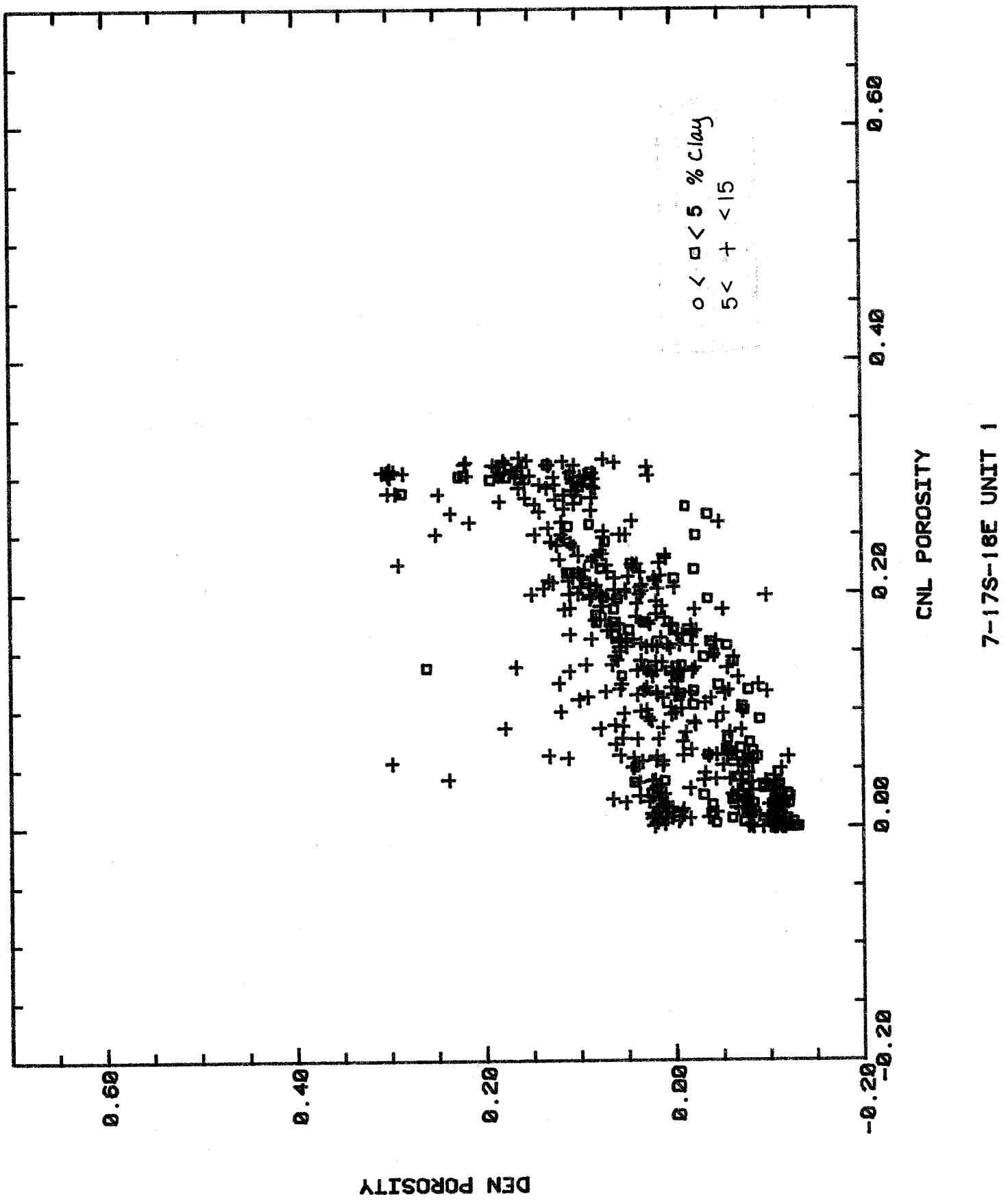

App 1b. Z-plot for well no 1

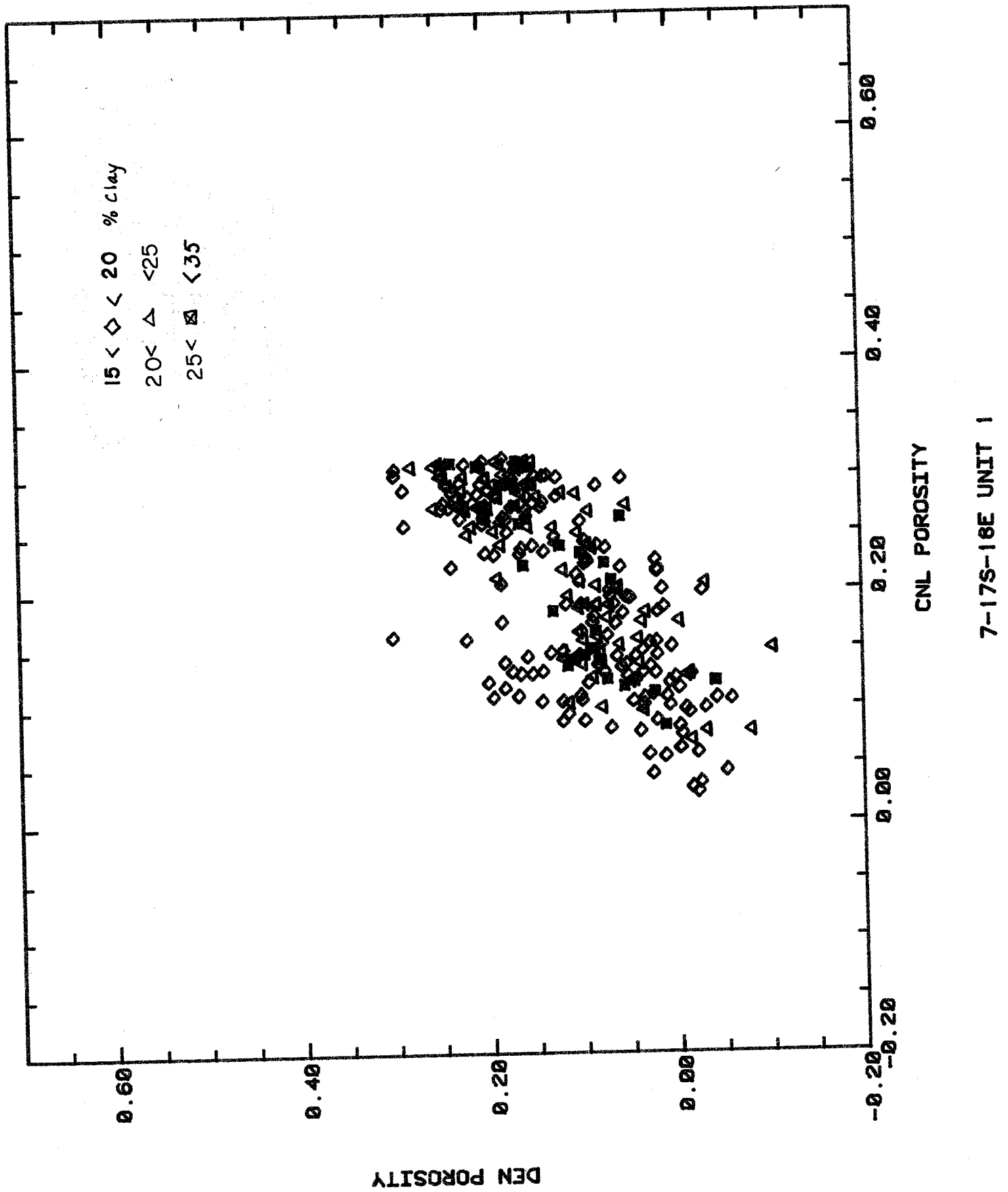

App 1c. Z-plot for well no 2

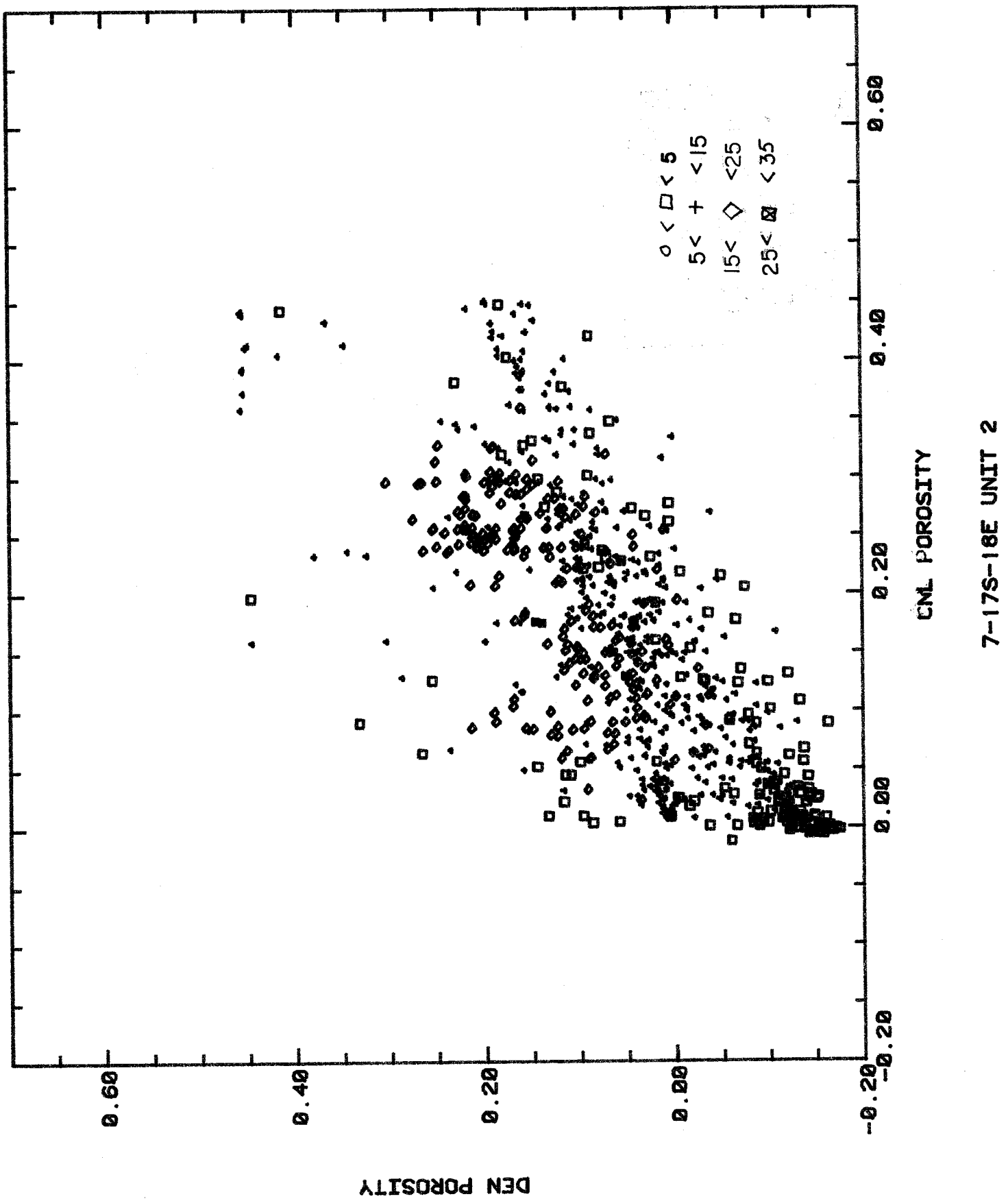

App 1d. Z-plot for well no 3

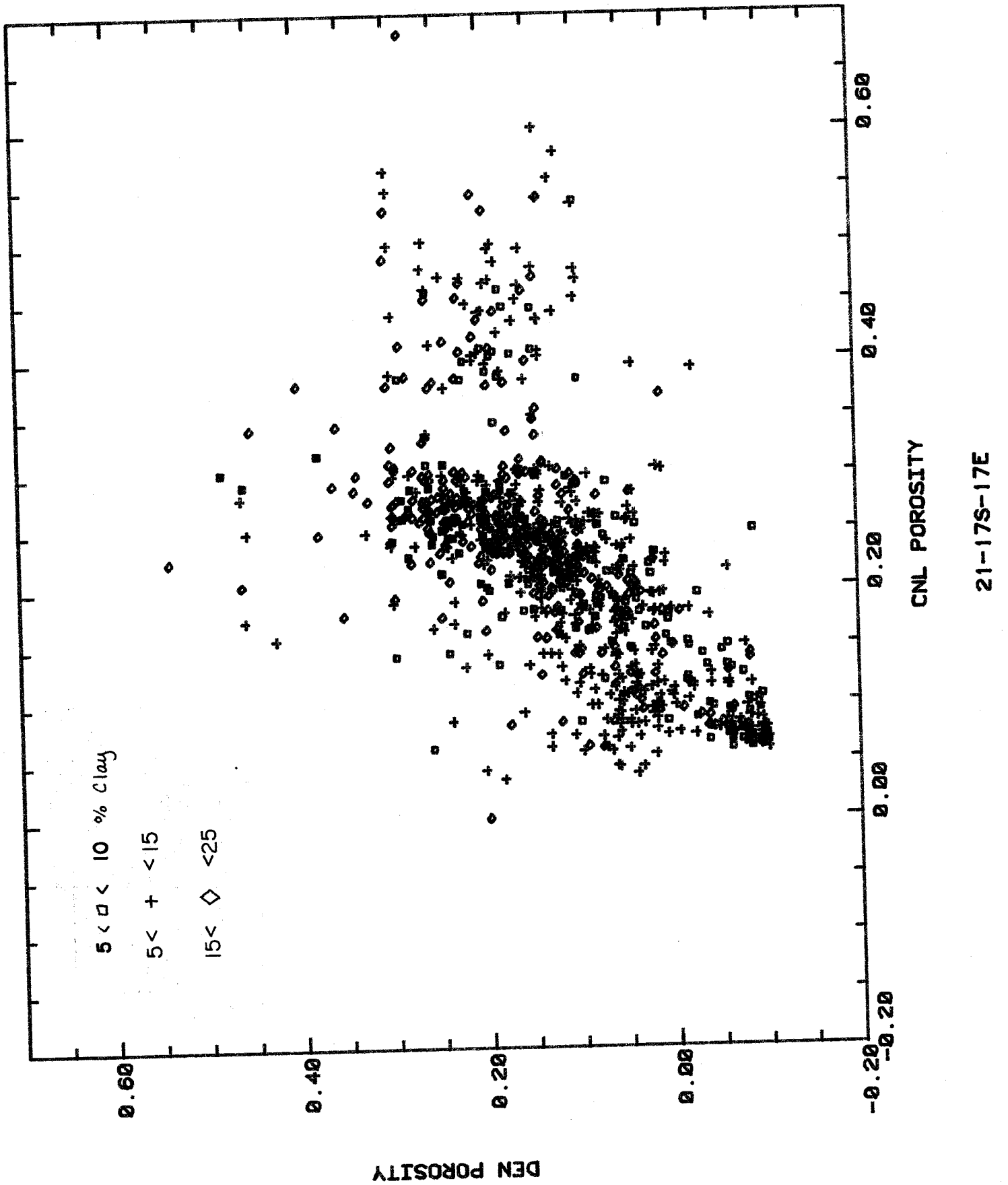

App 1e. Z-plot for well no 3

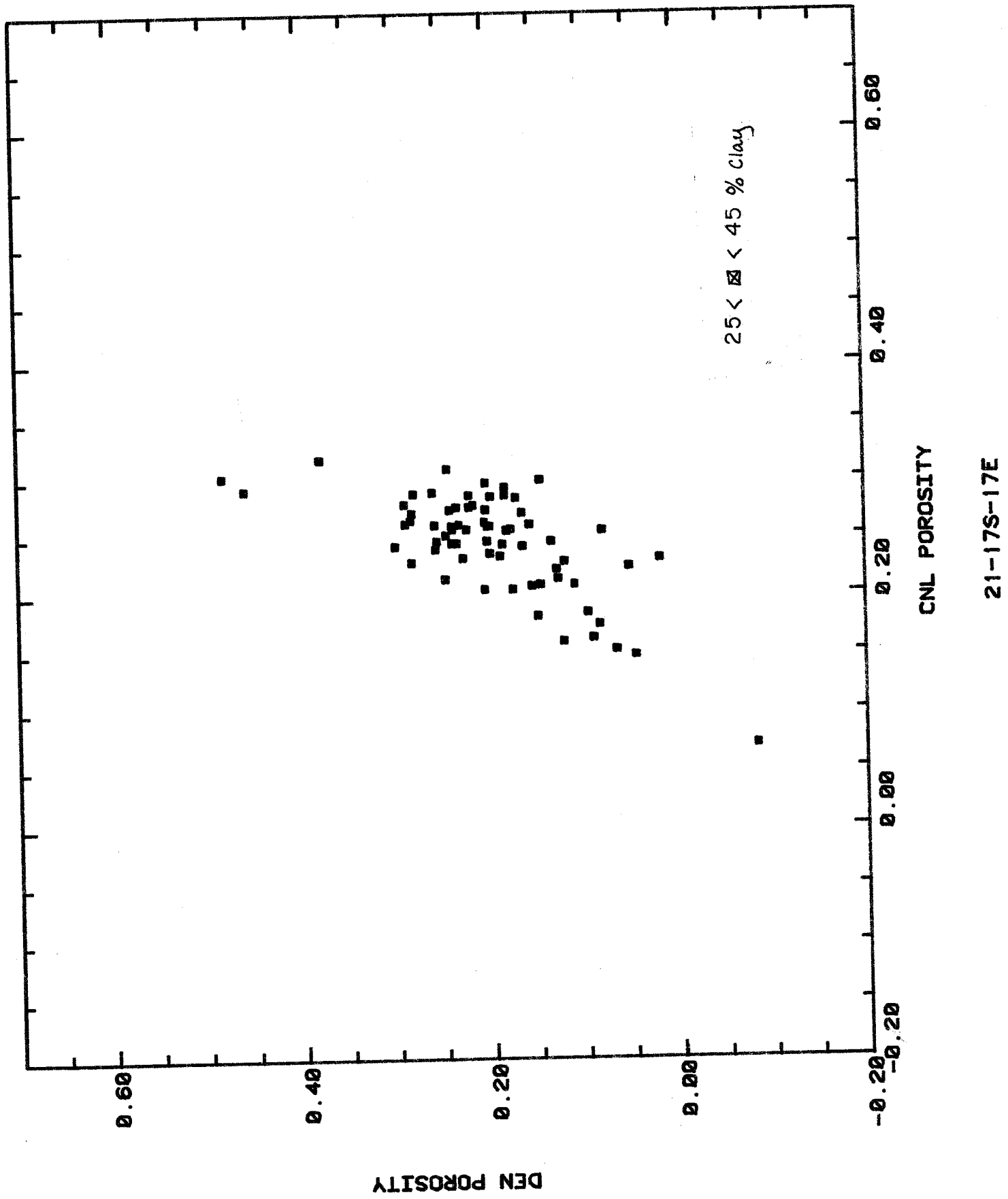

App 1f. Z-plot for well no 4

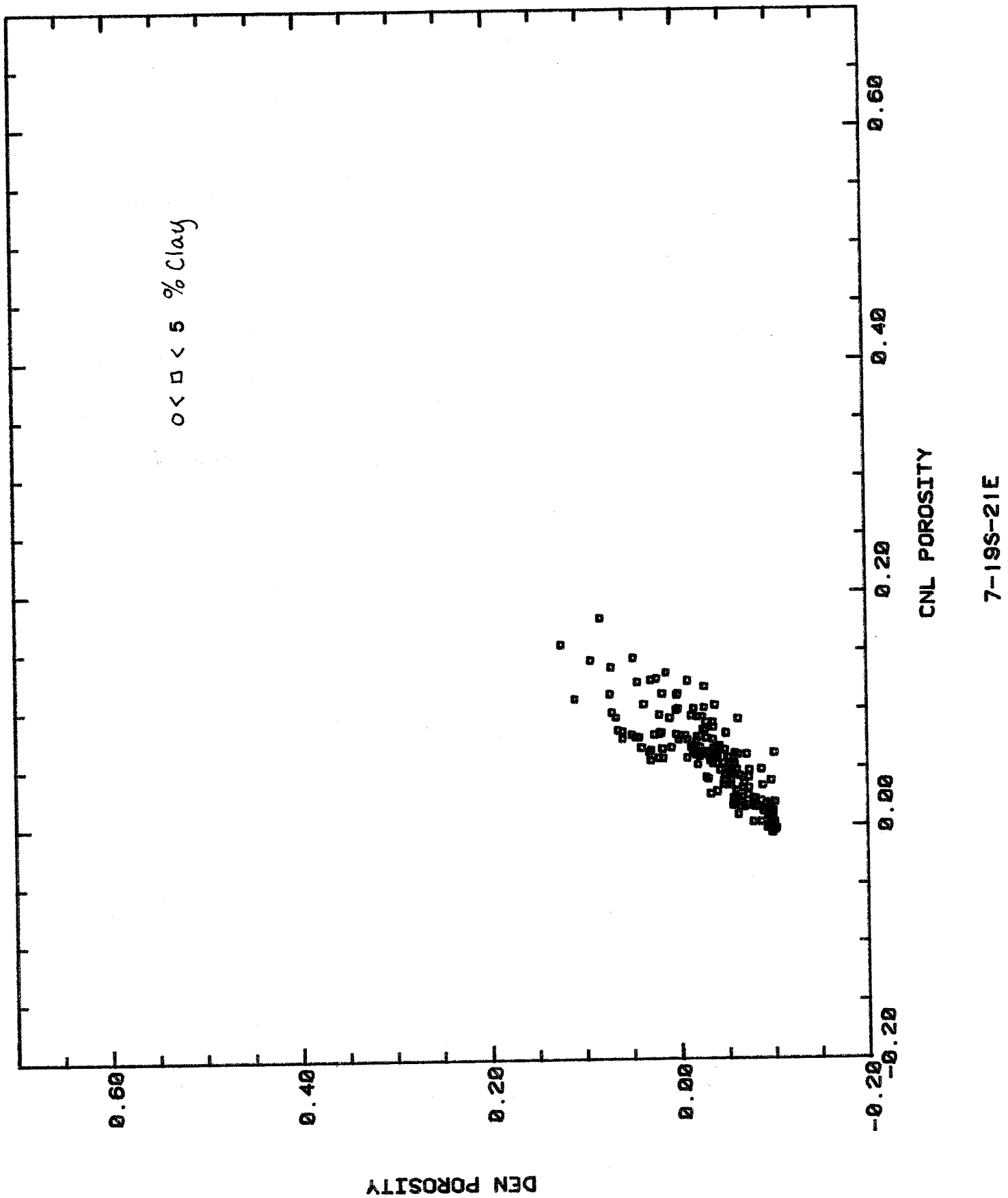

App lg. Z-plot for well no 4

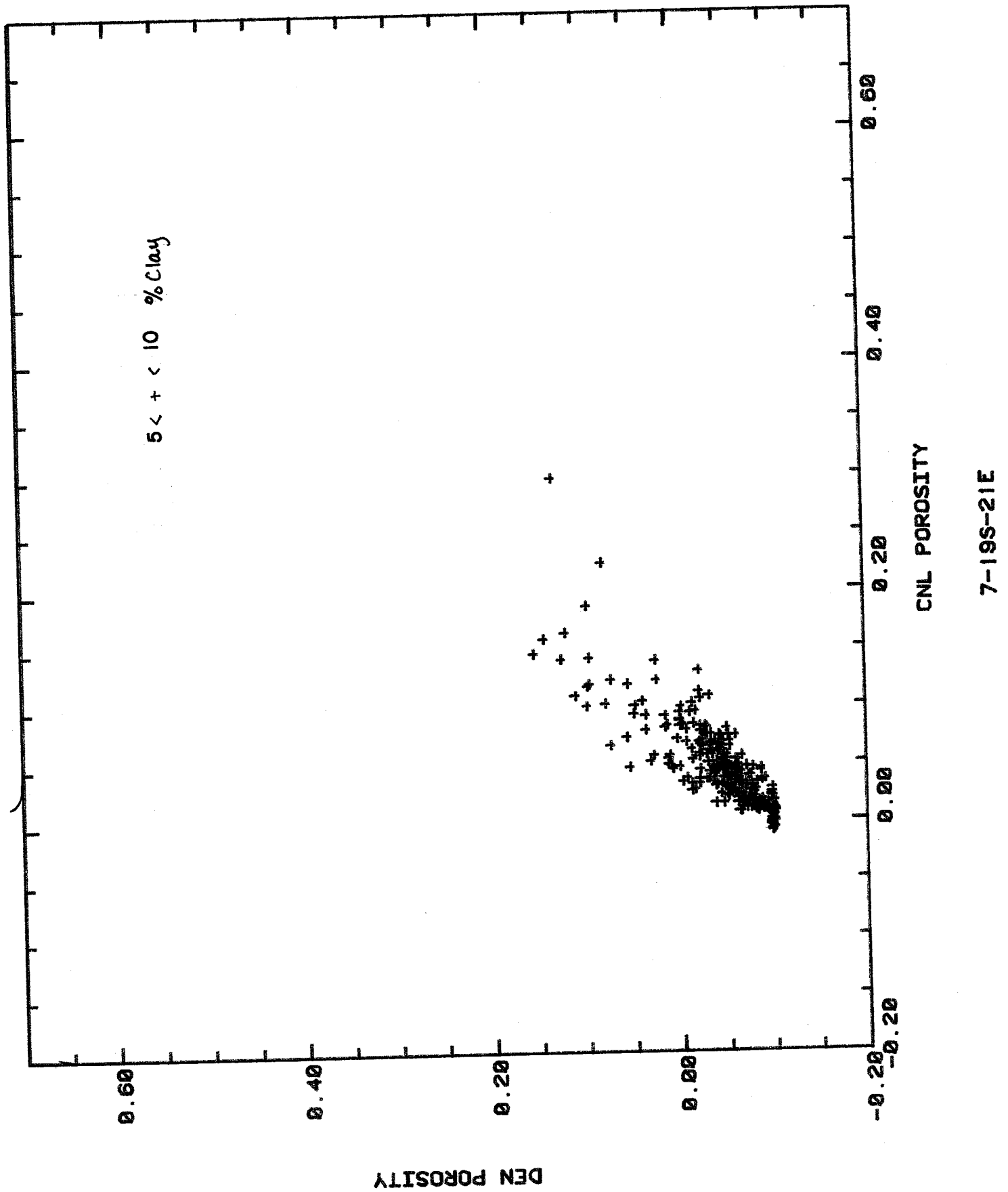

App 1h. Z-plot for well no 4

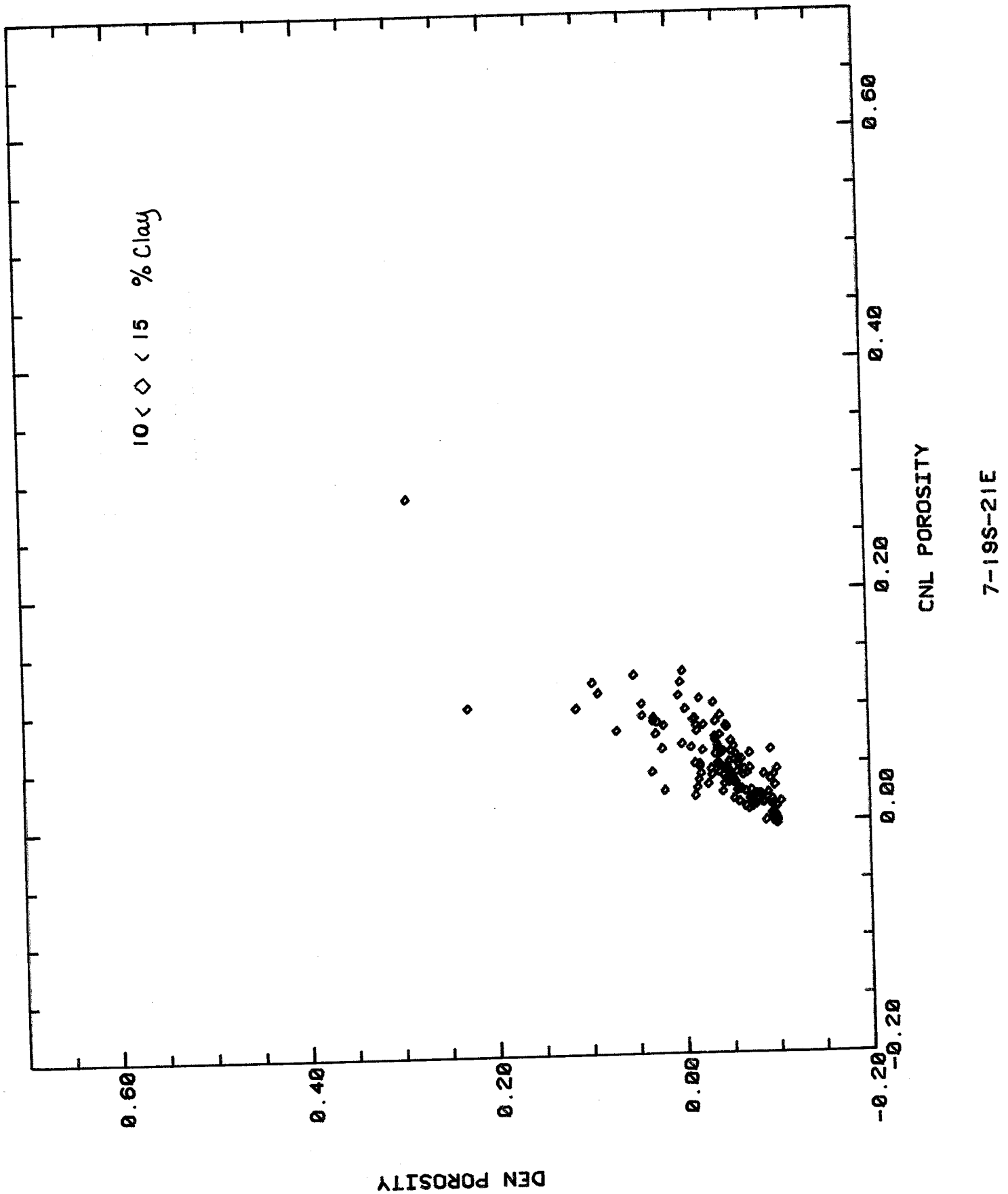

App li. Z-plot for well no 4

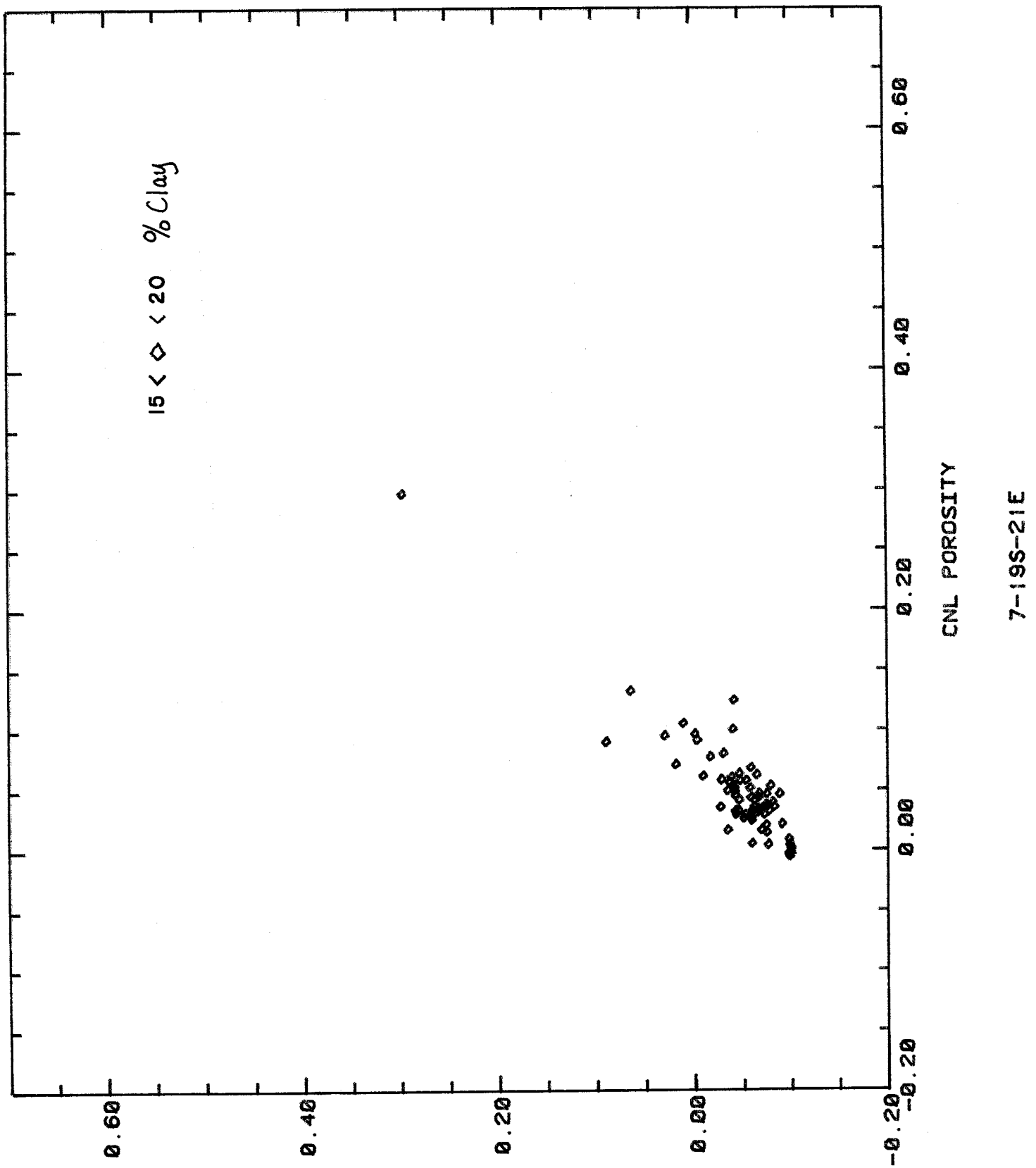

App lj. Z-plot for well no 4

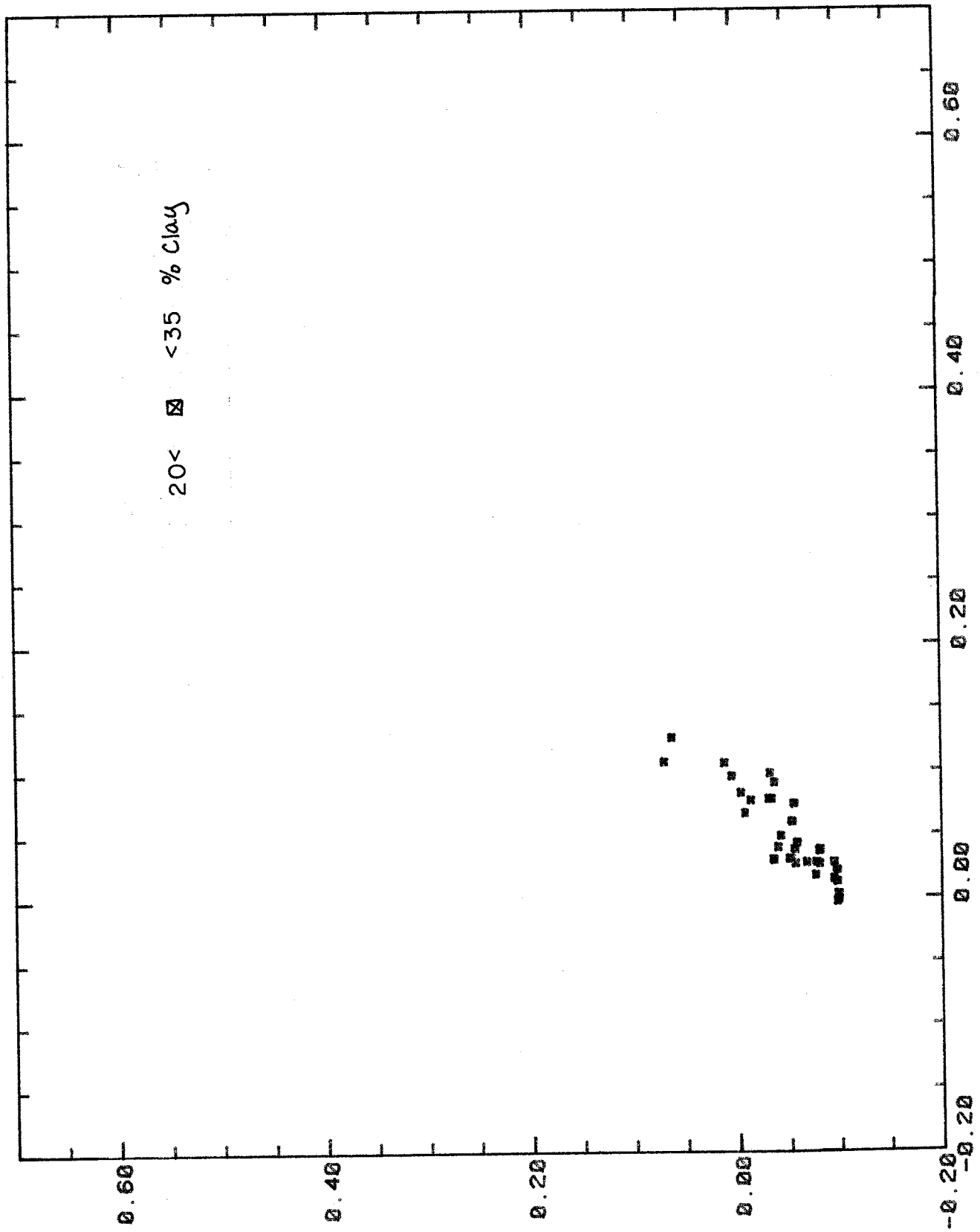

App 1k. Z-plot for well no 10

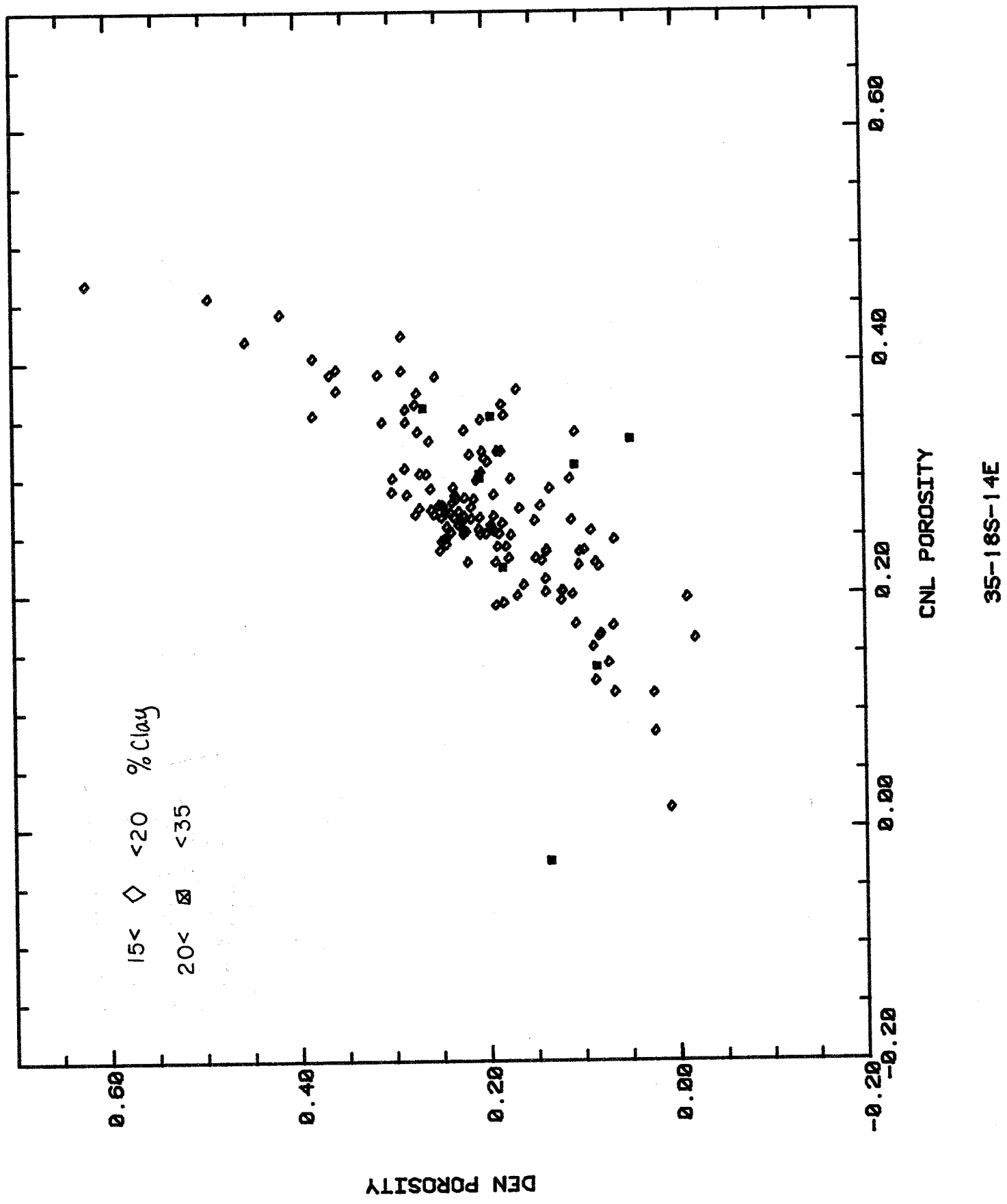

App 11. Z-plot for well no 10

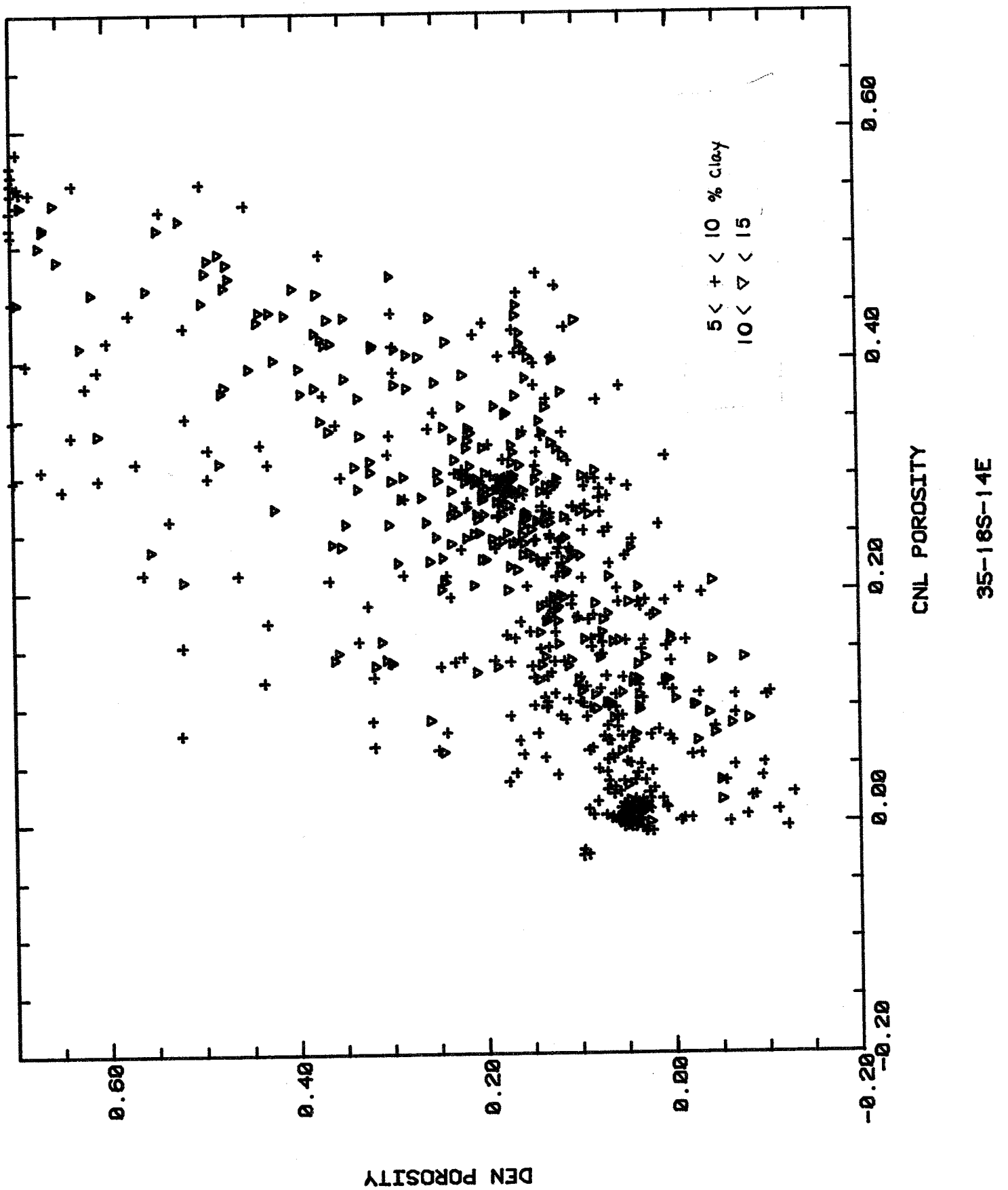

App 1m. Z-plot for well no 10

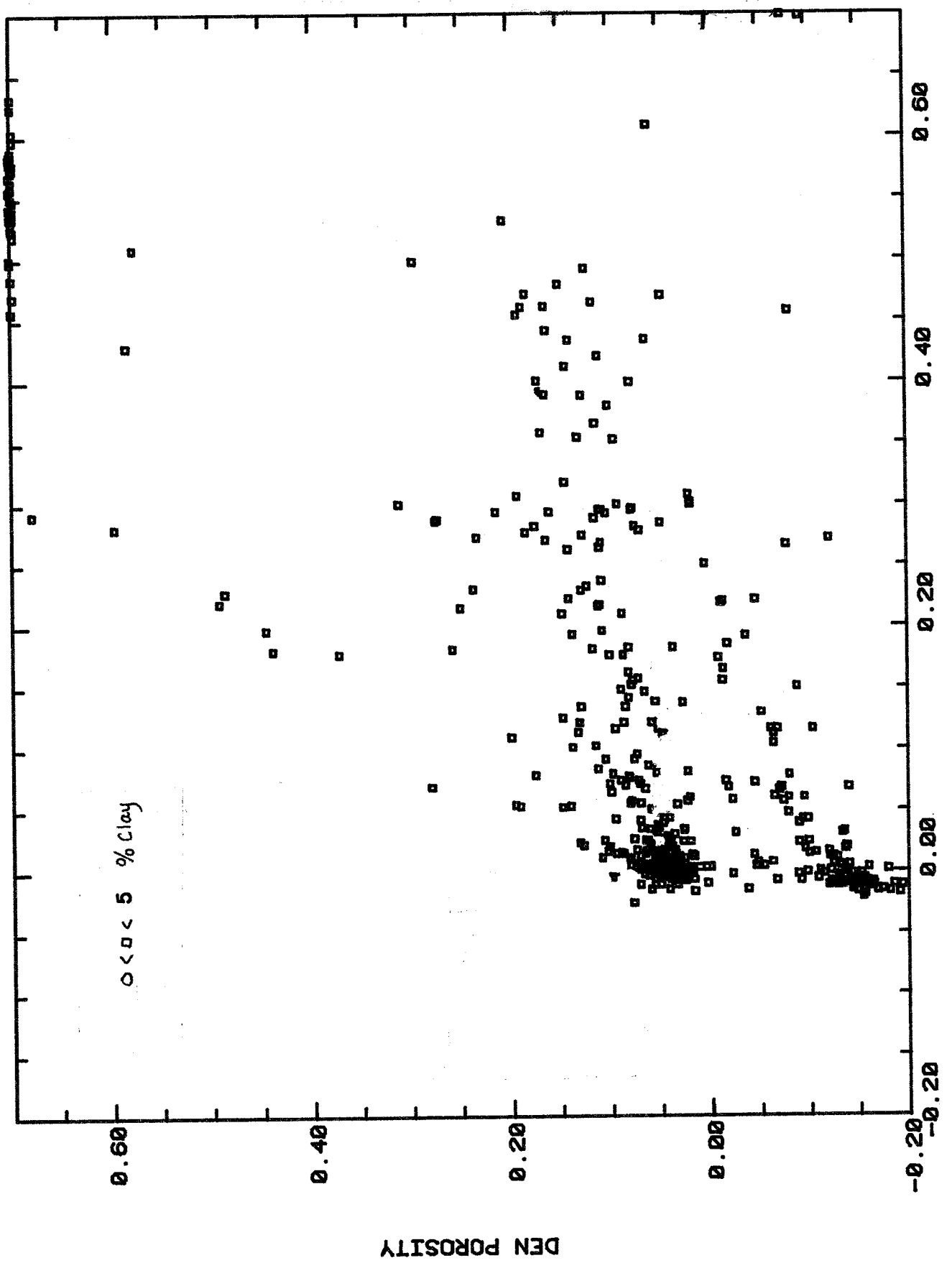

App 1n. Z-plot for well no 11

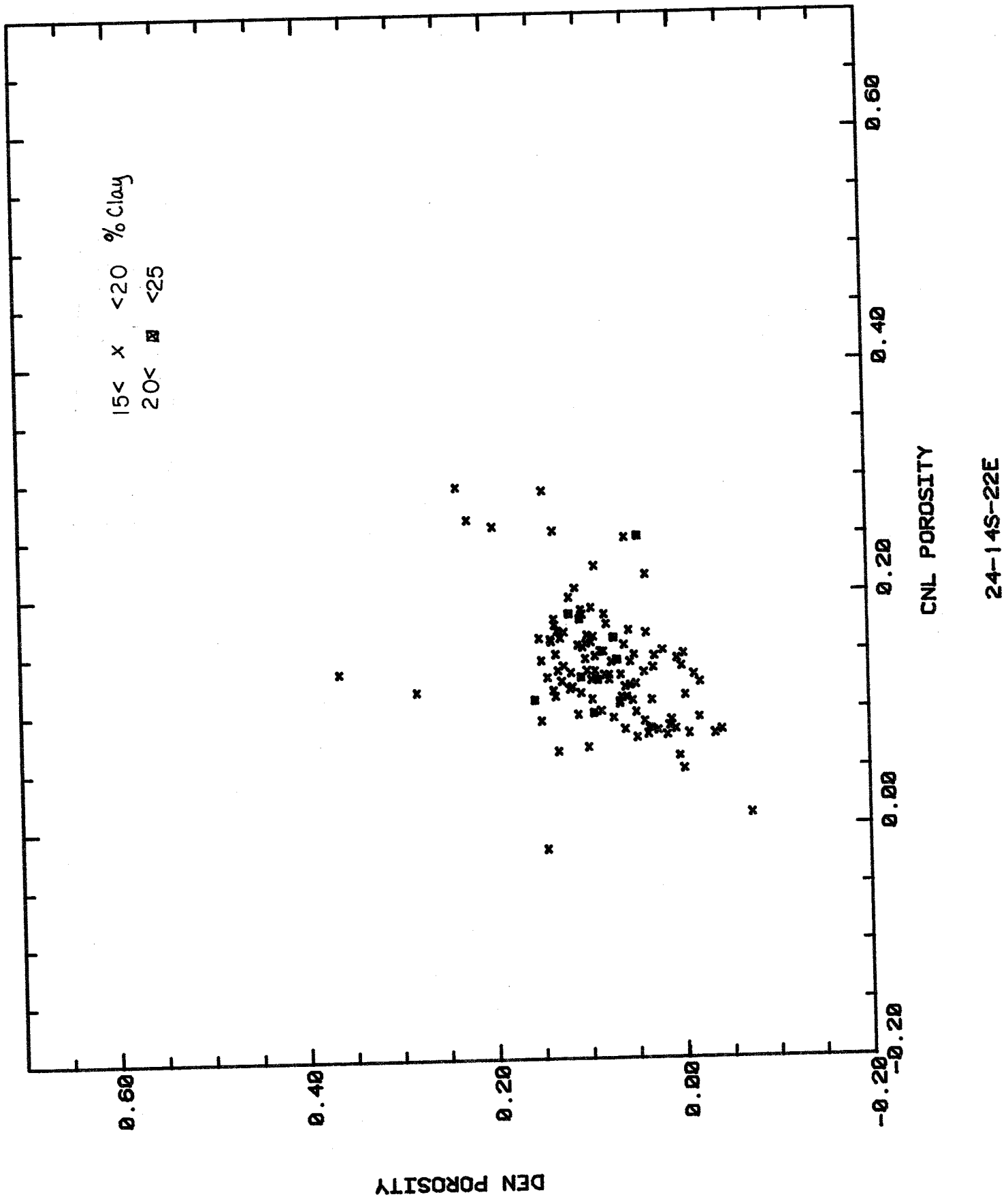

App lo. Z-plot for well no 11

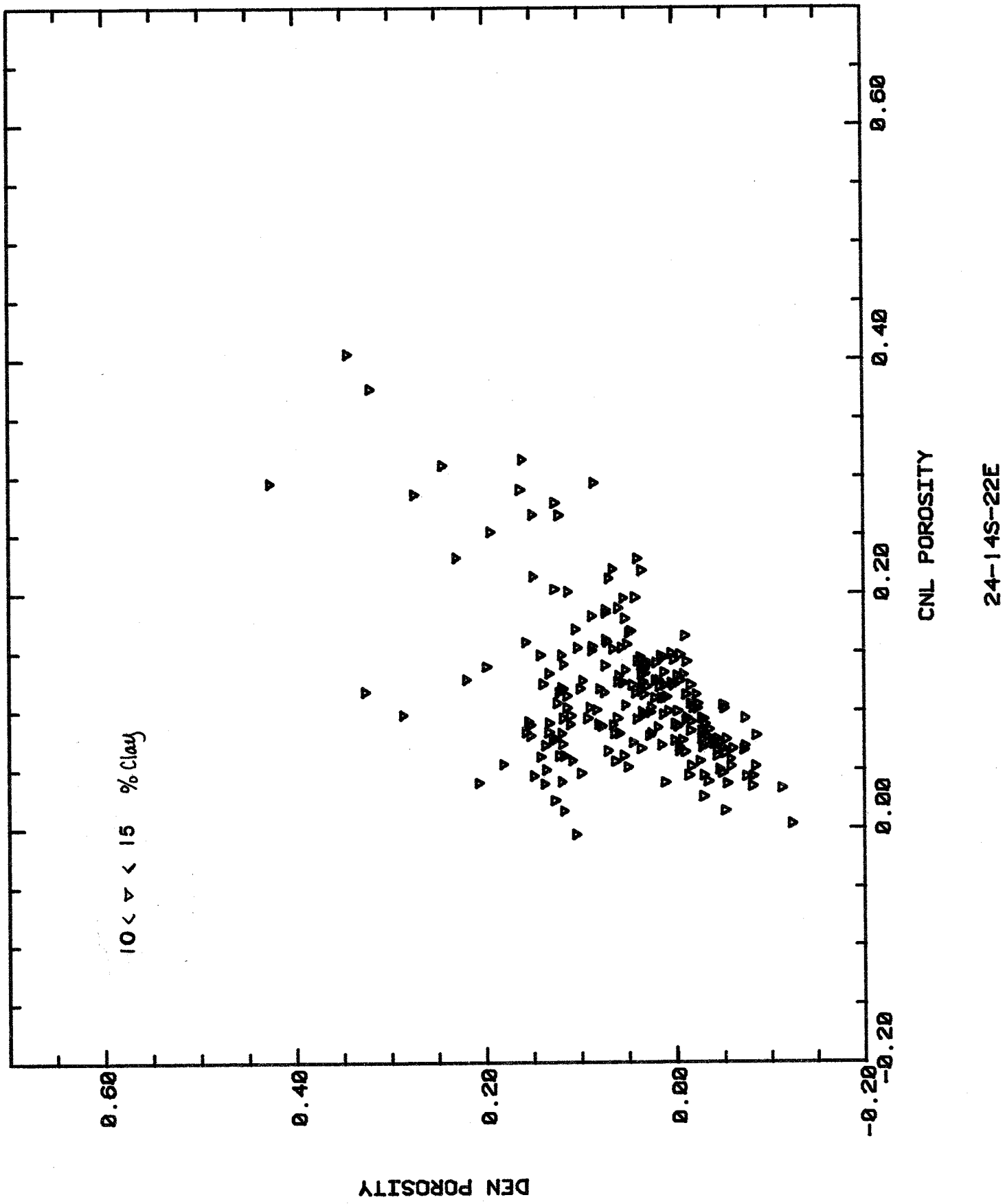

App 1p. Z-plot for well no 11

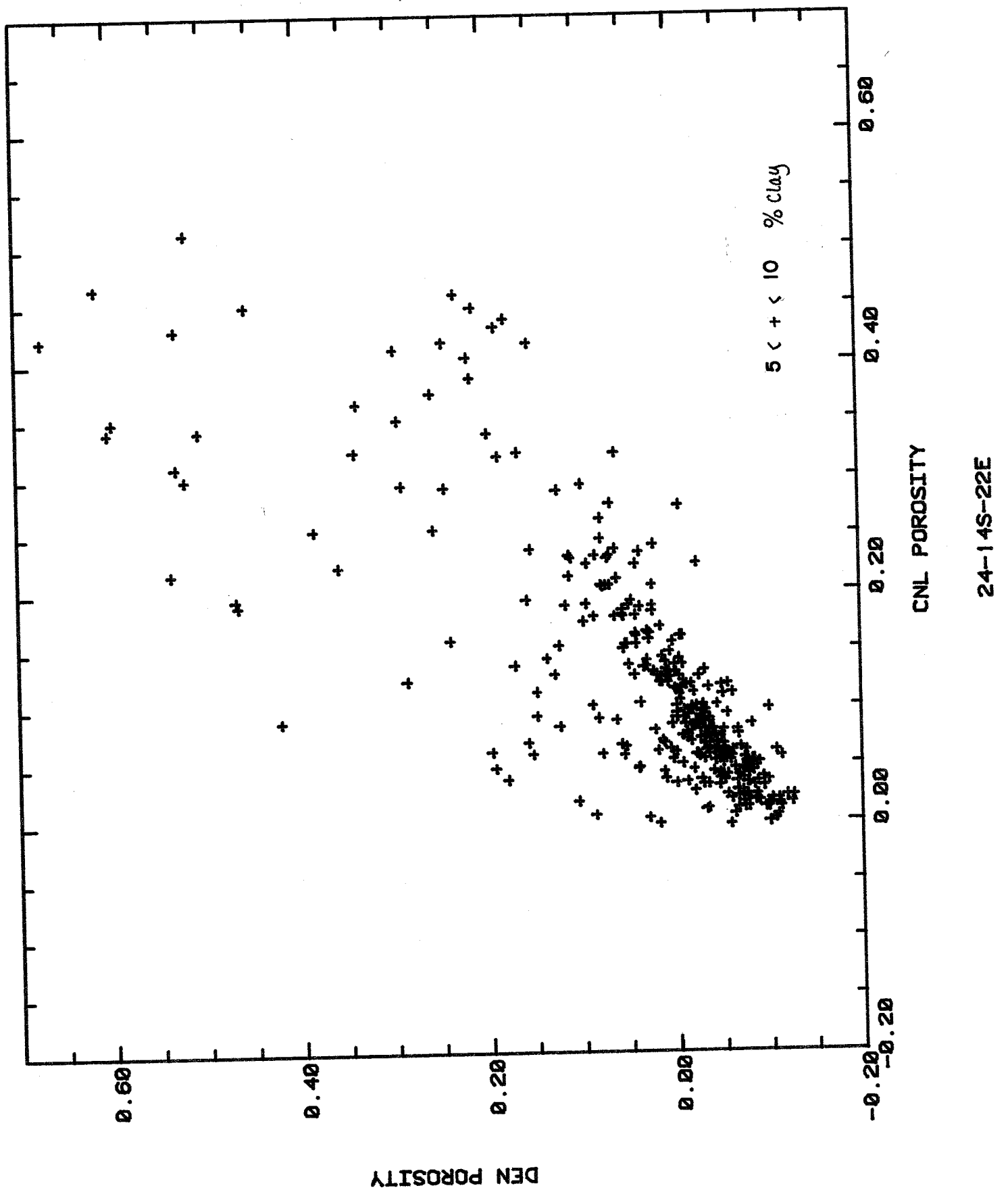

App 1q. Z-plot for well no 11

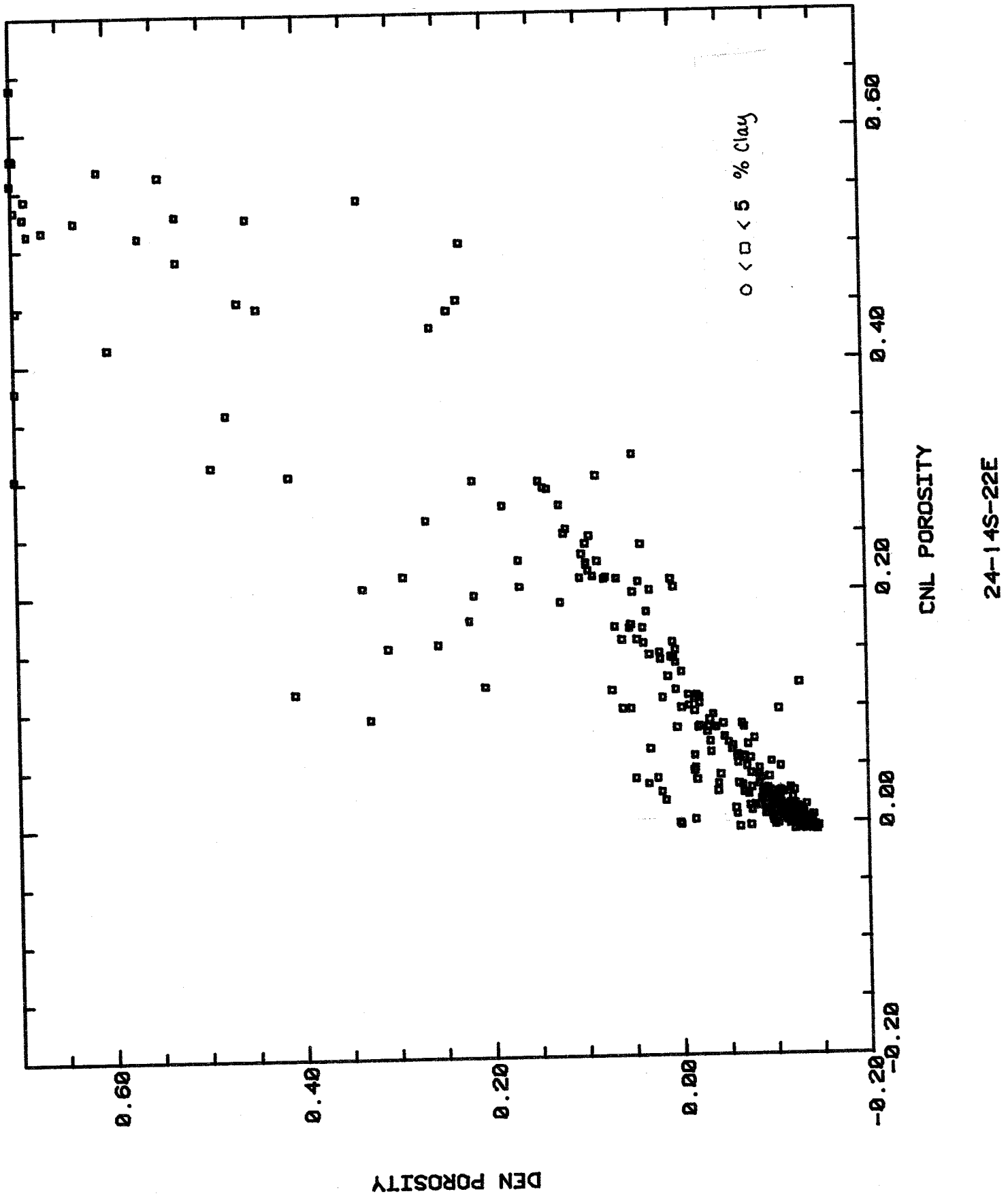

App 2a. Resistivity versus Porosity Crossplot for well no 1

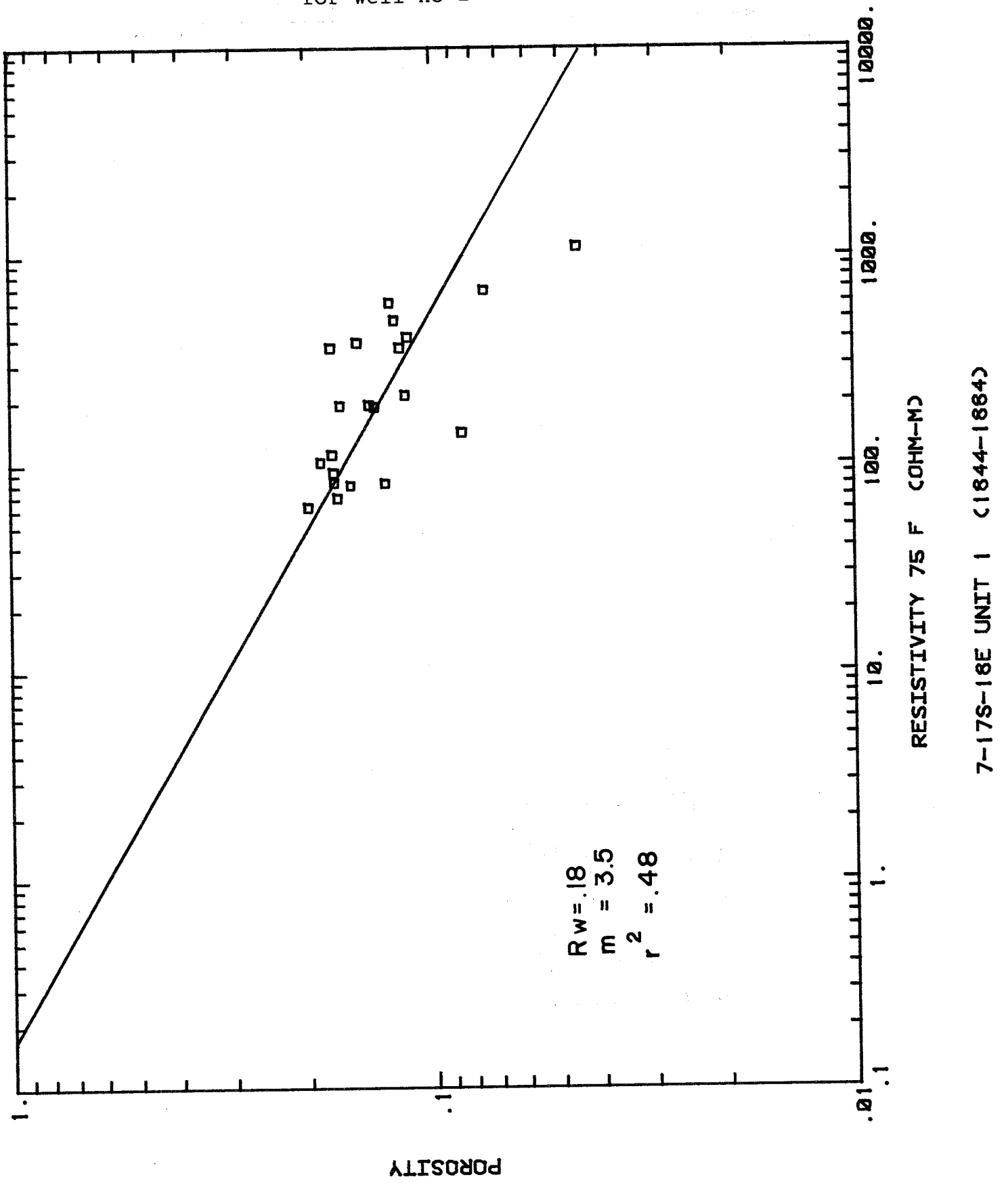

App 2b. Resistivity versus Porosity Crossplot for well no 1

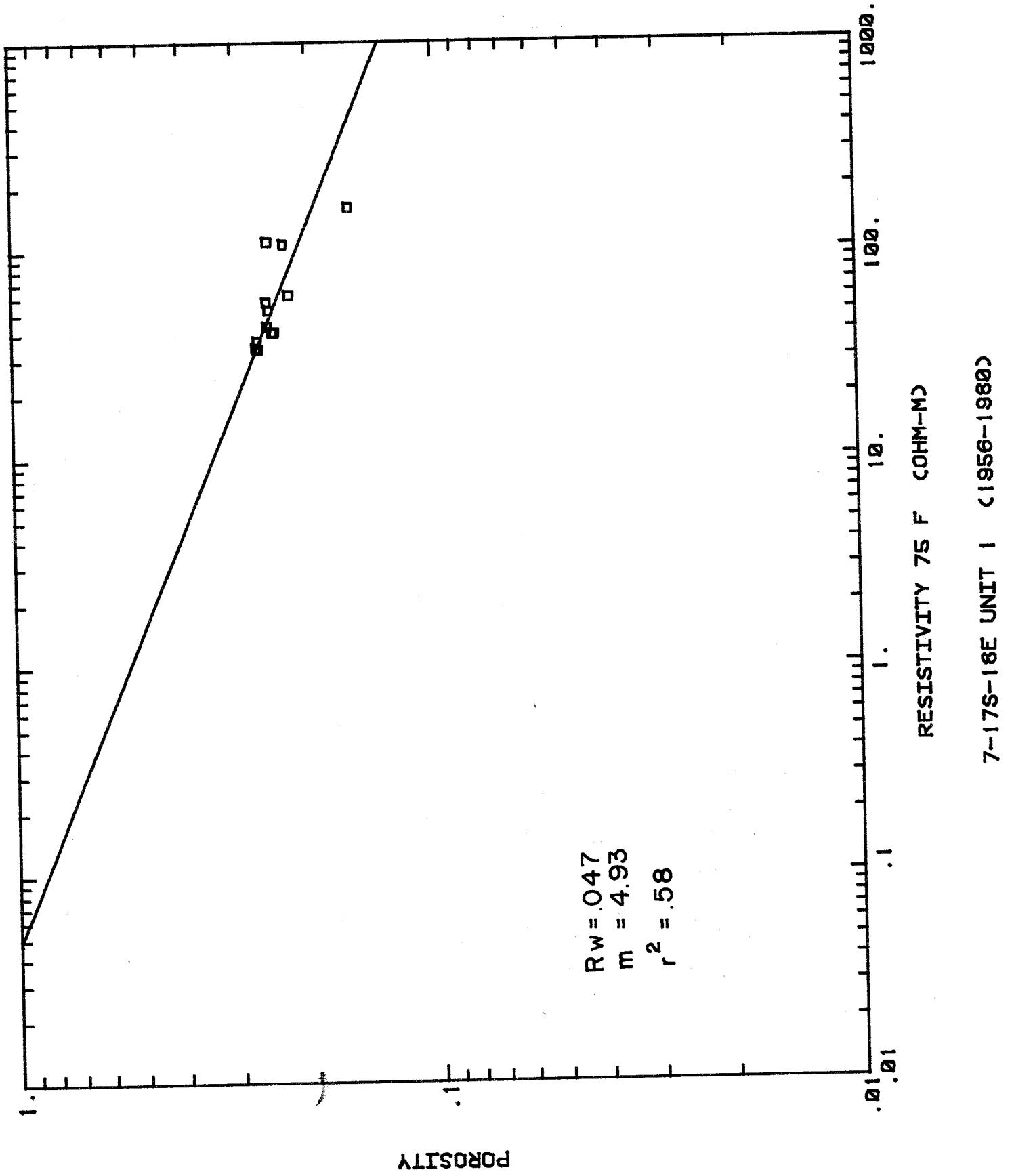

App 2c. Resistivity versus Porosity Crossplot for well no 3

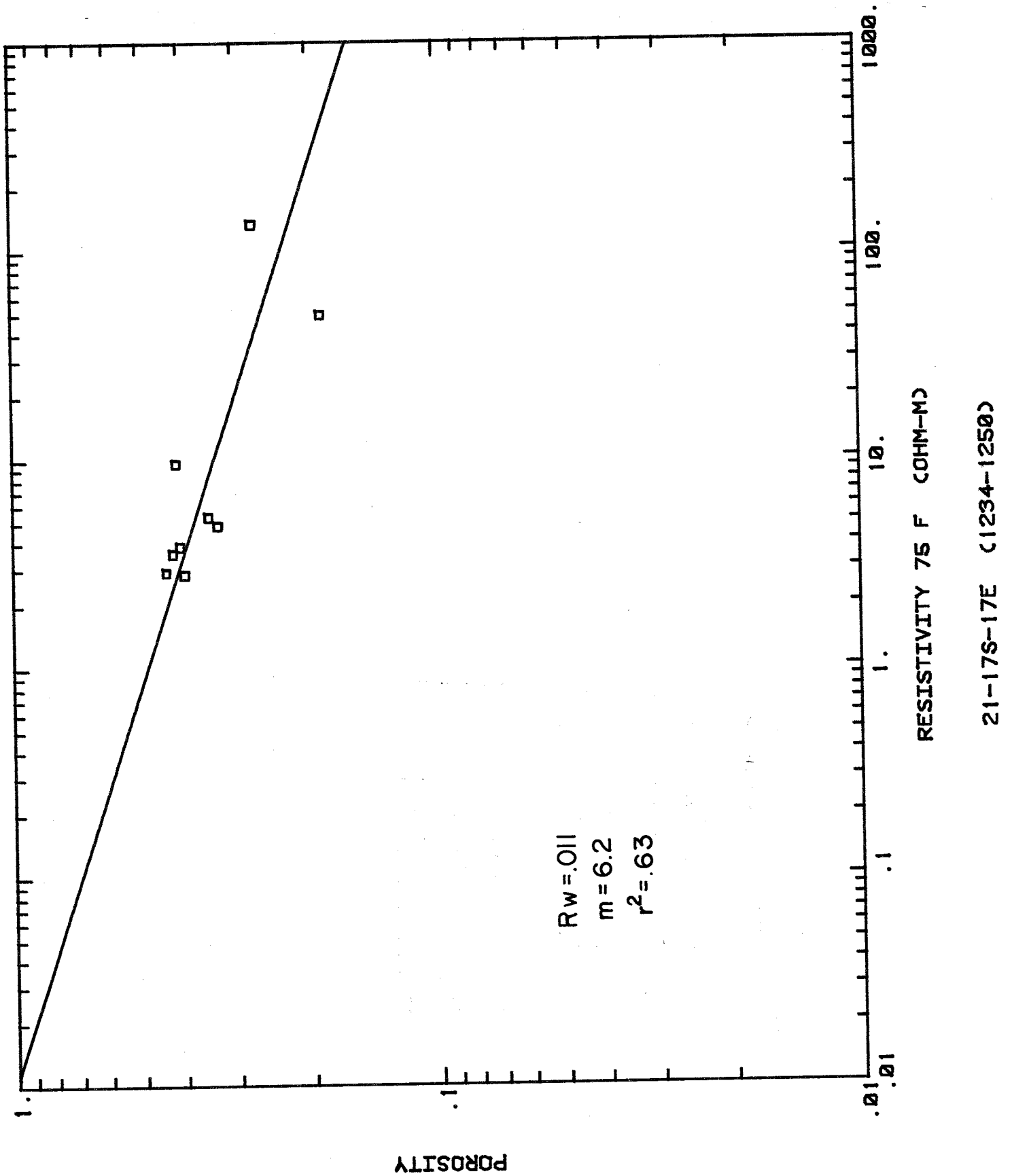

App 2d. Resistivity versus Porosity Crossplot for well no 4

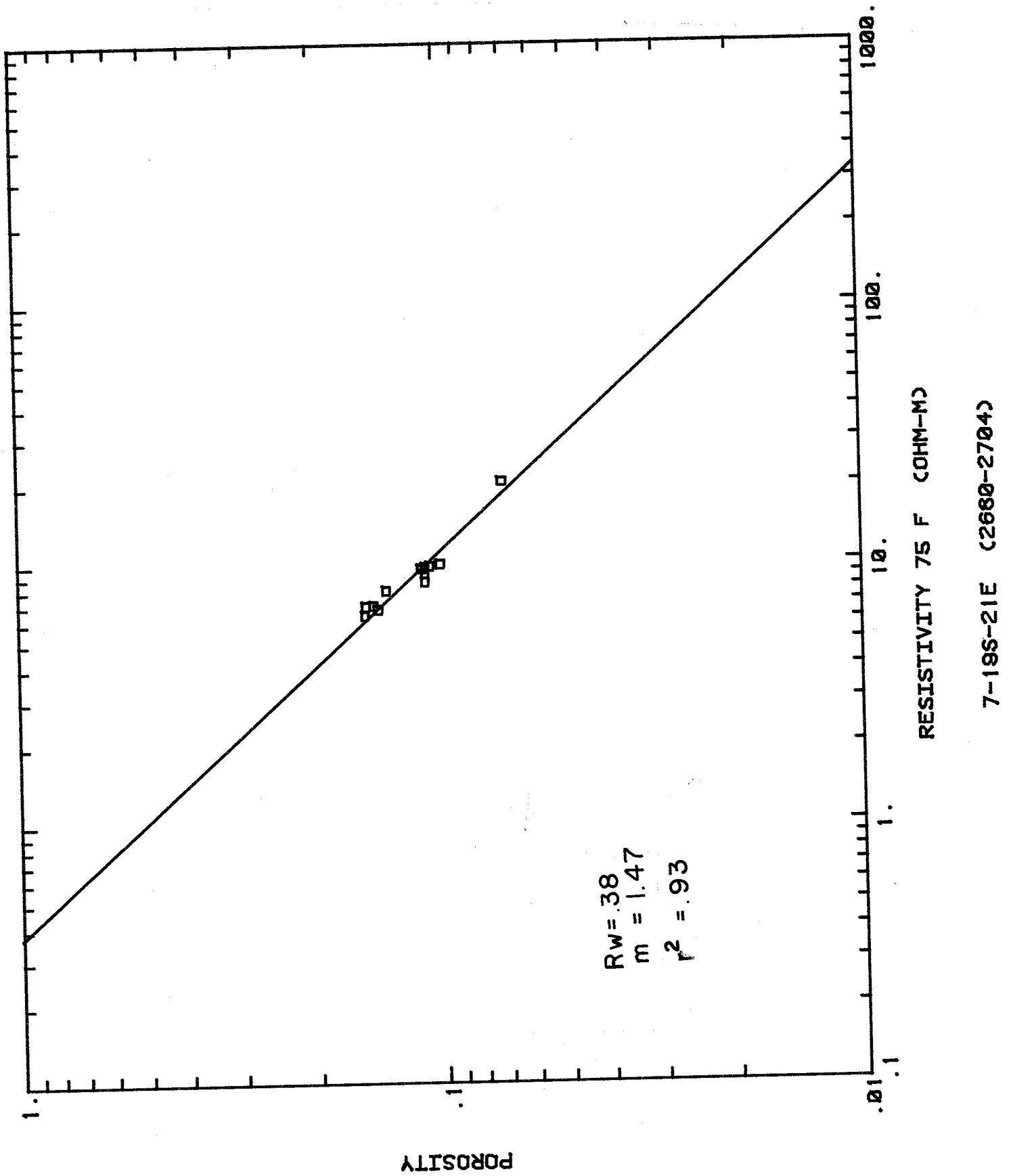

App 2e. Resistivity versus Porosity Crossplot for well no 10

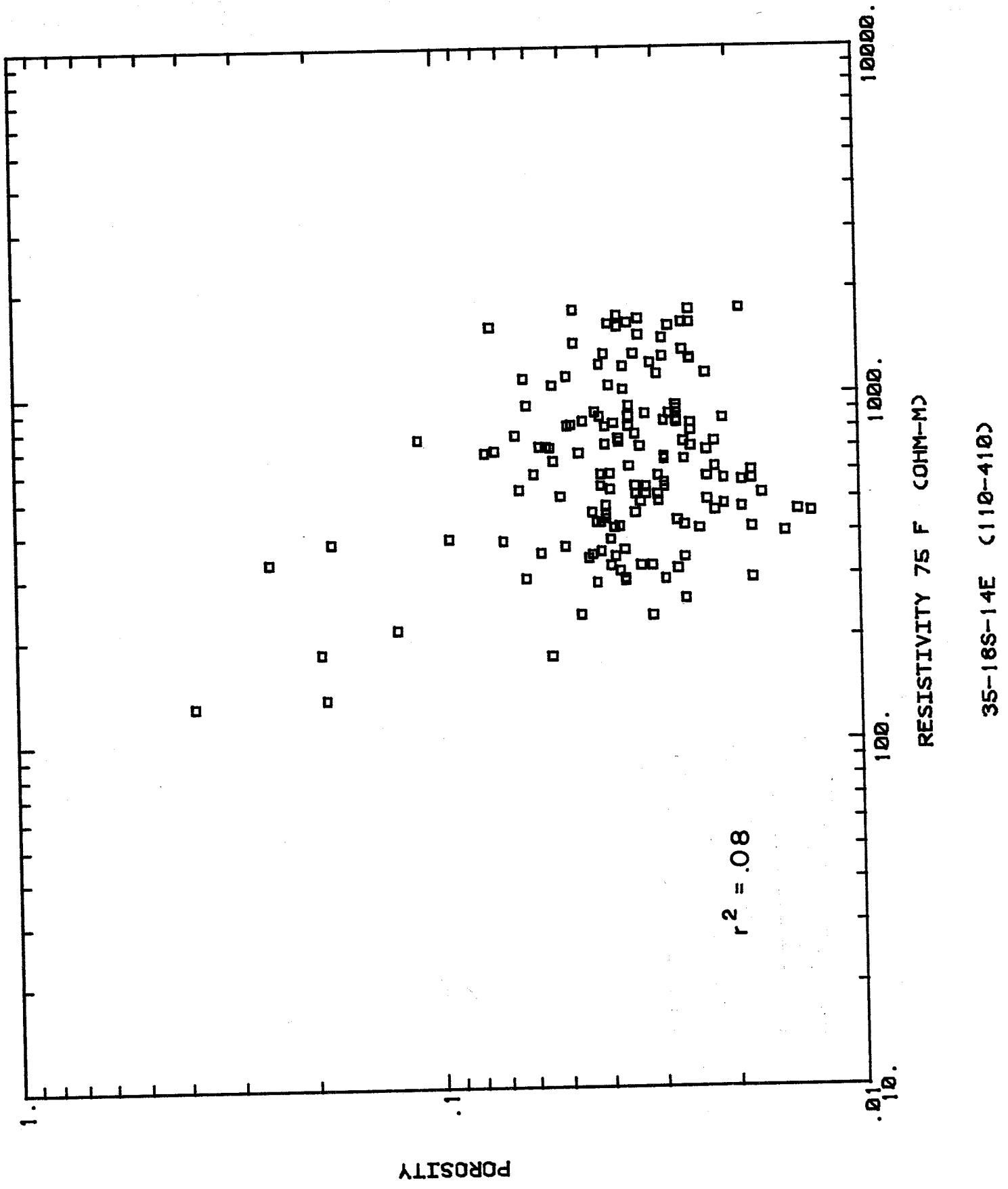

App 2f. Resistivity versus Porosity Crossplot for well no 10

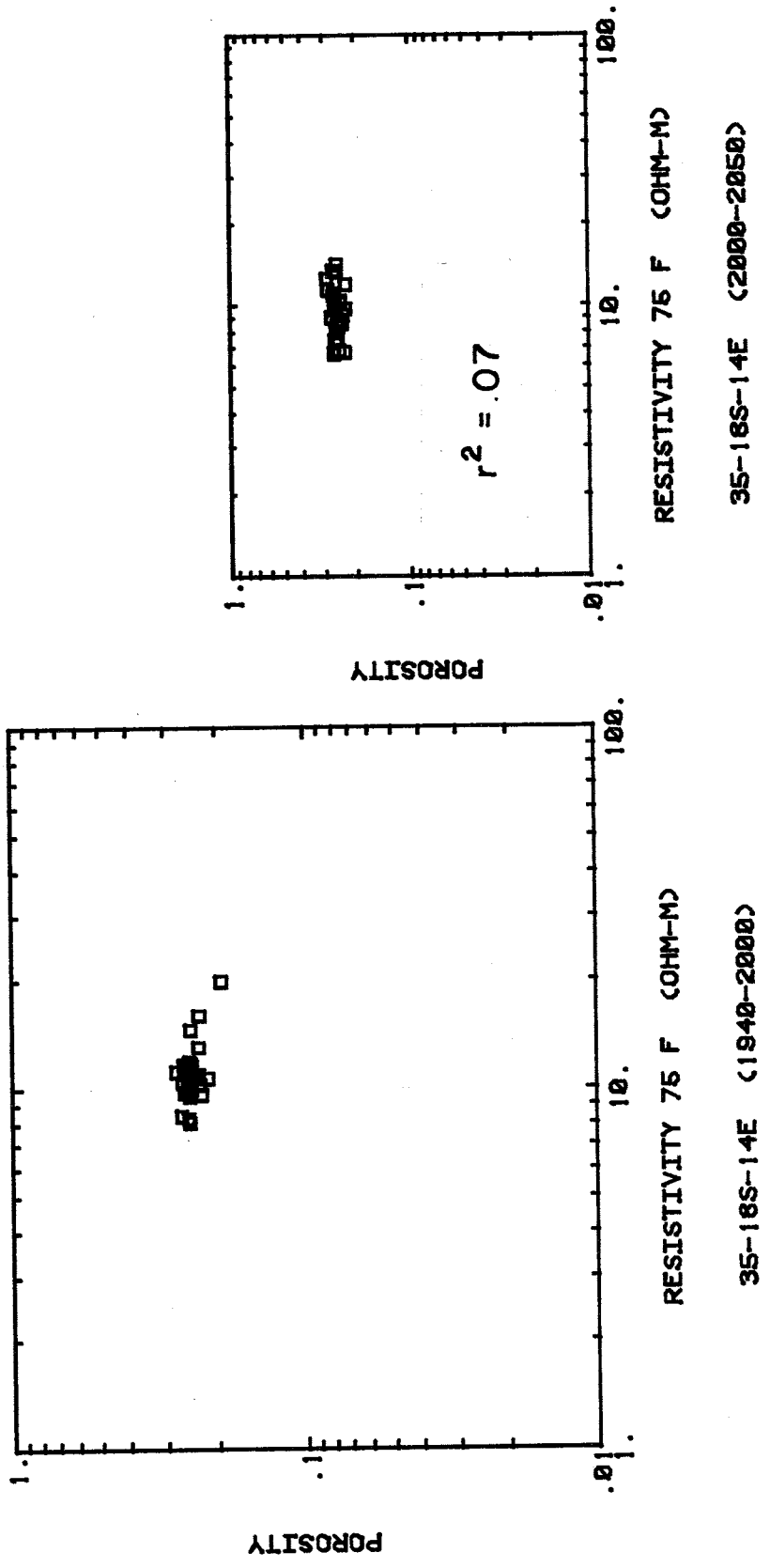

App 2g. Resistivity versus Porosity Crossplot for well no 10

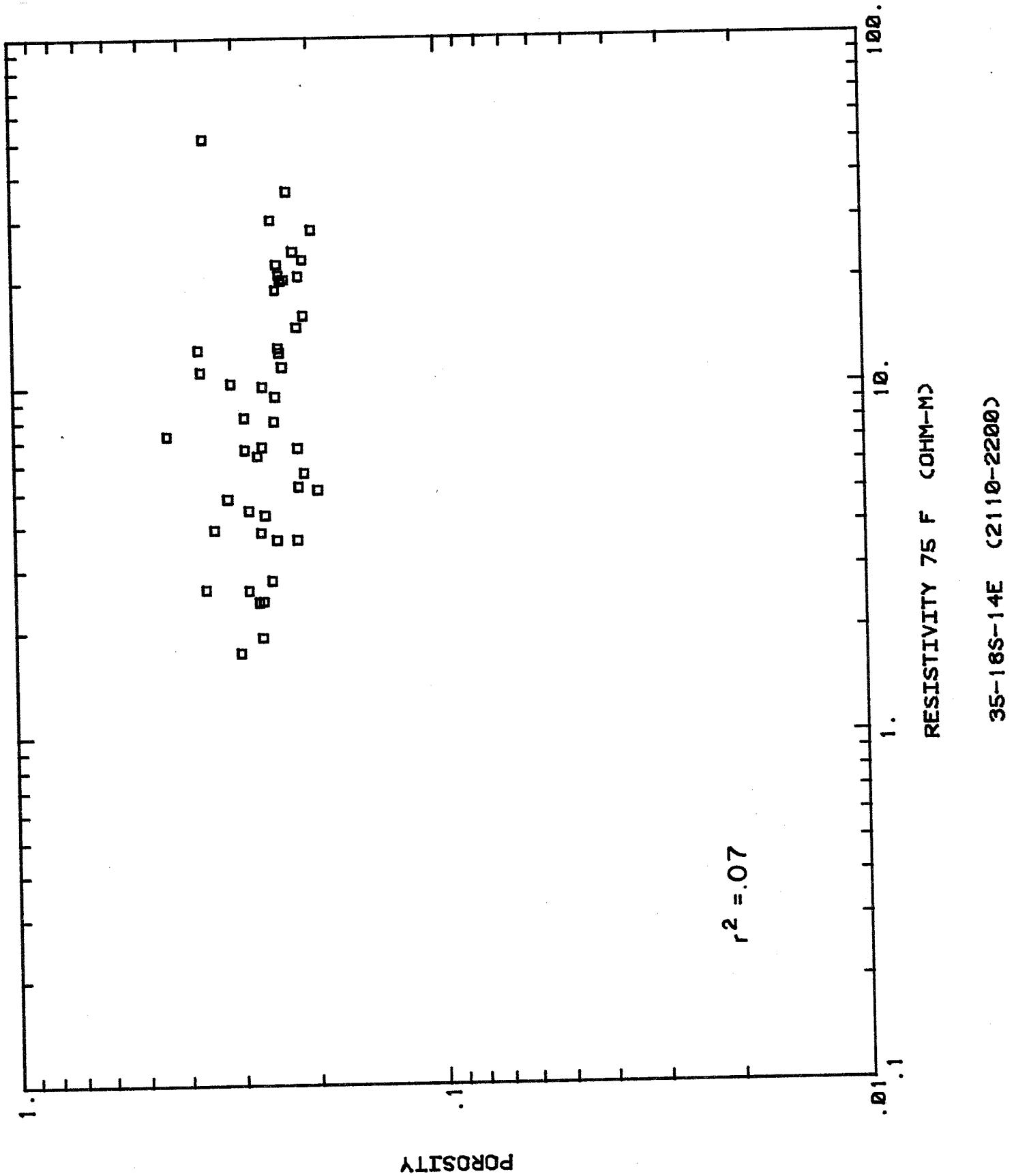

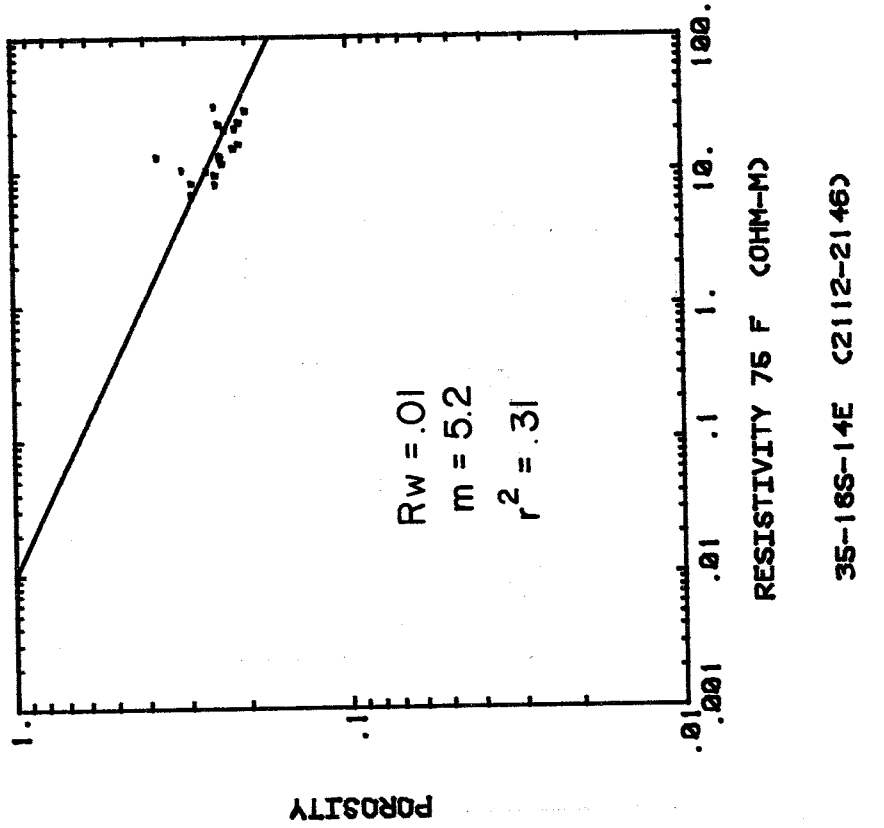

App 2h. Resistivity versus Porosity Crossplot

for well no 10

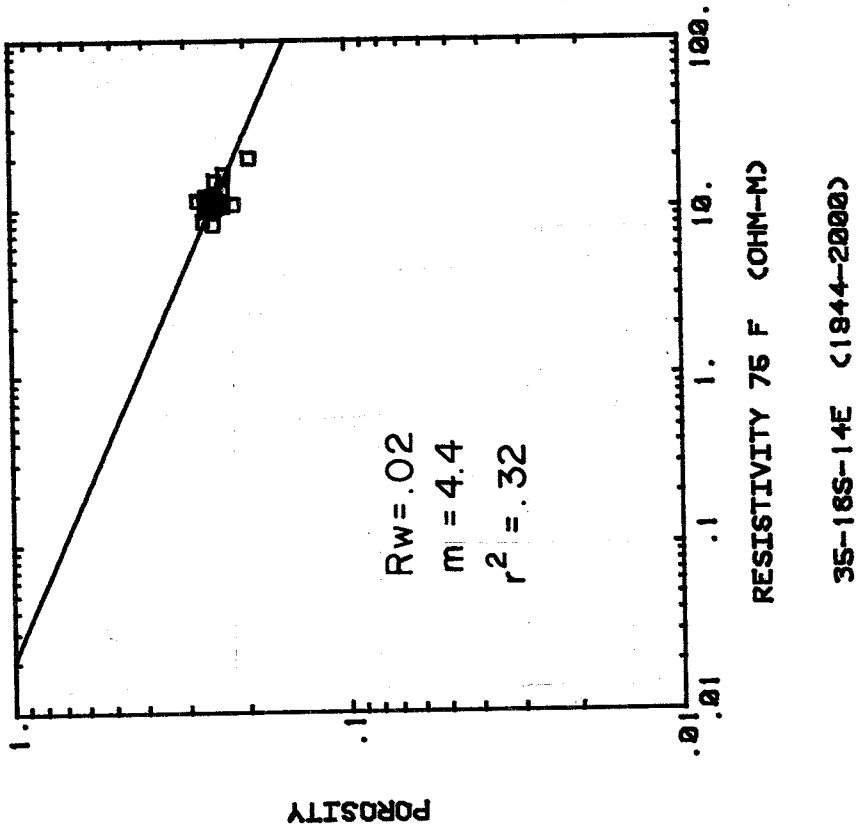

App 2i. Resistivity versus Porosity Crossplot for well no 11

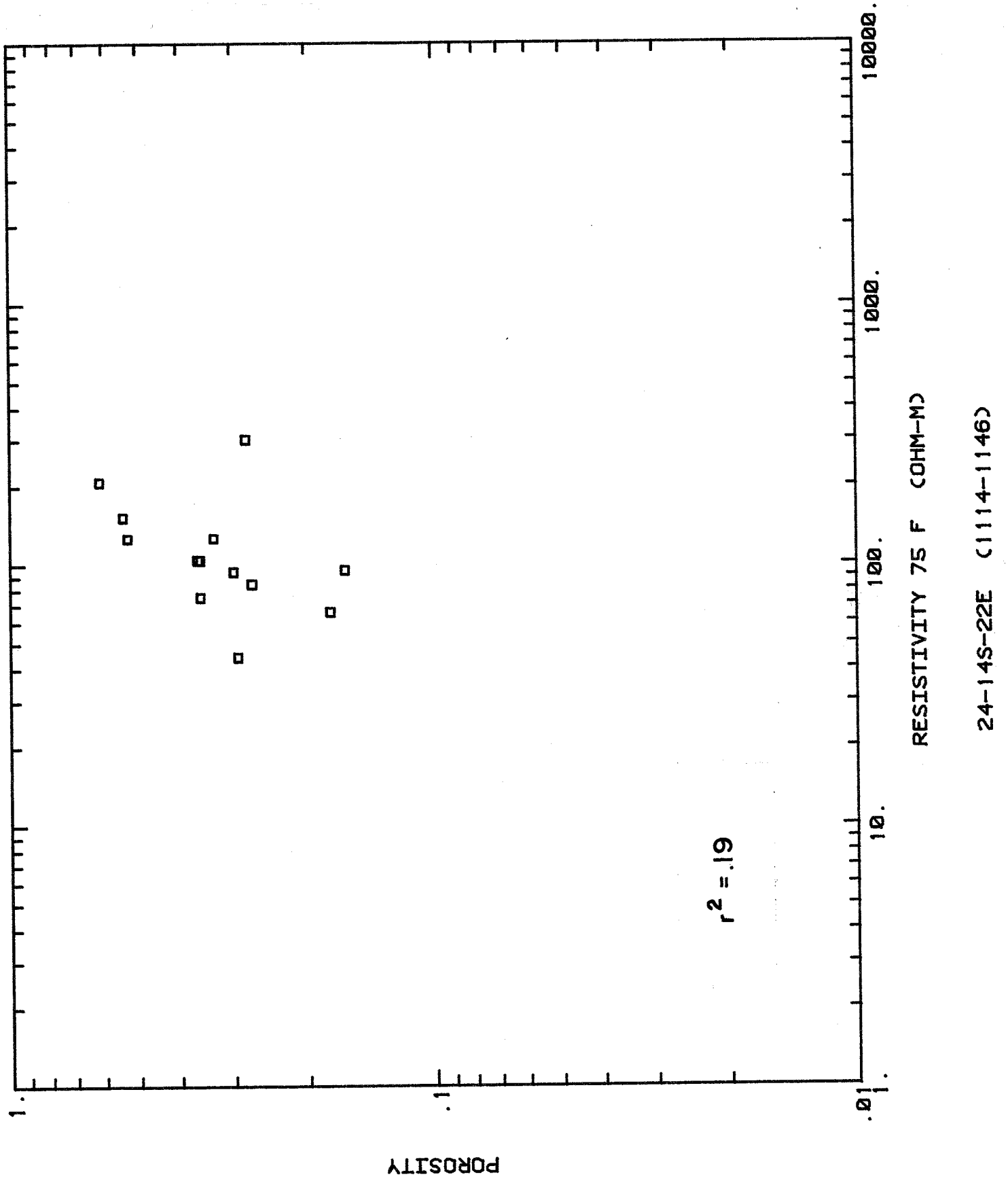

App 2j. Resistivity versus Porosity Crossplot for well no 11

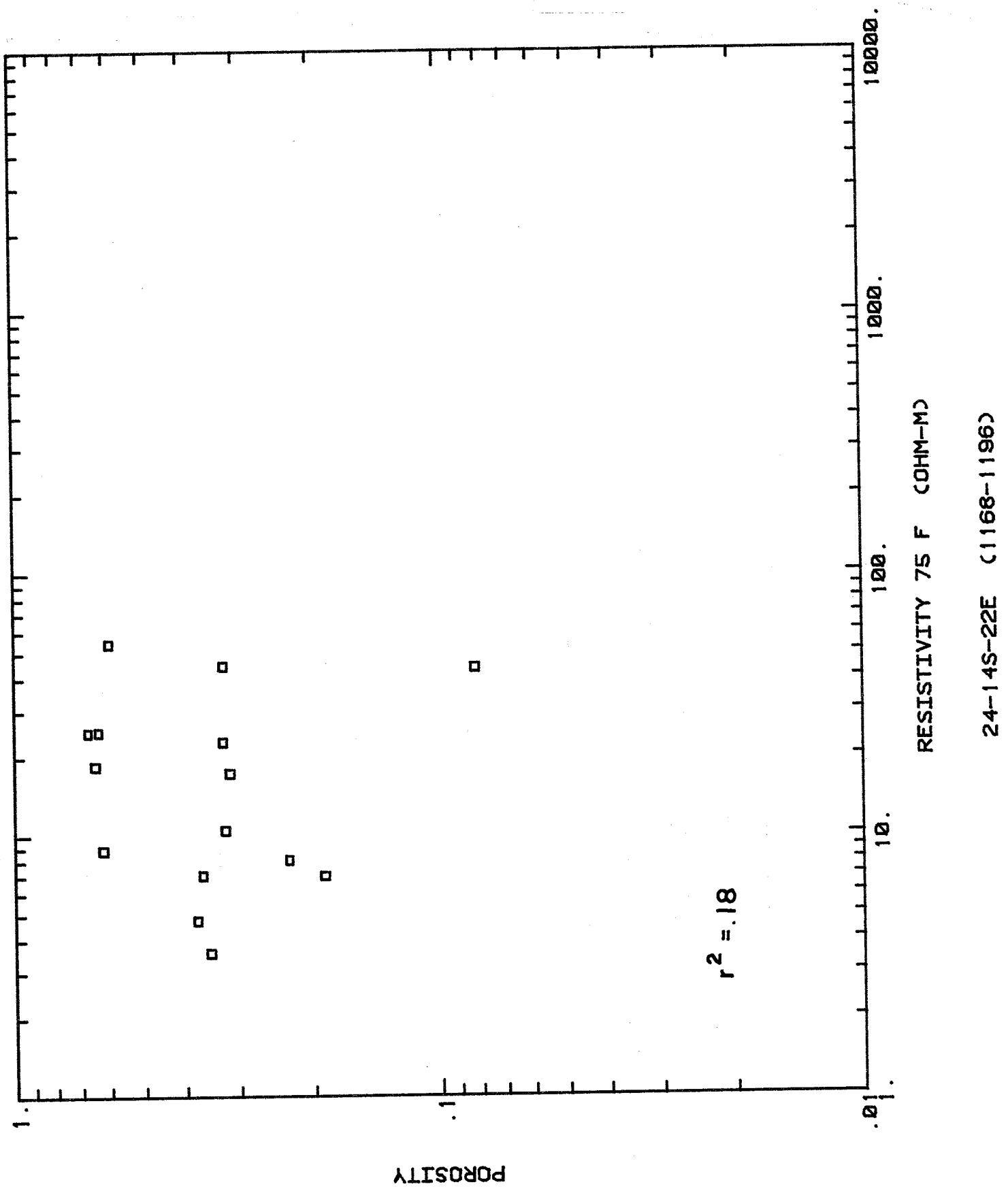

App 2k. Resistivity versus Porosity Crossplot for well no 11

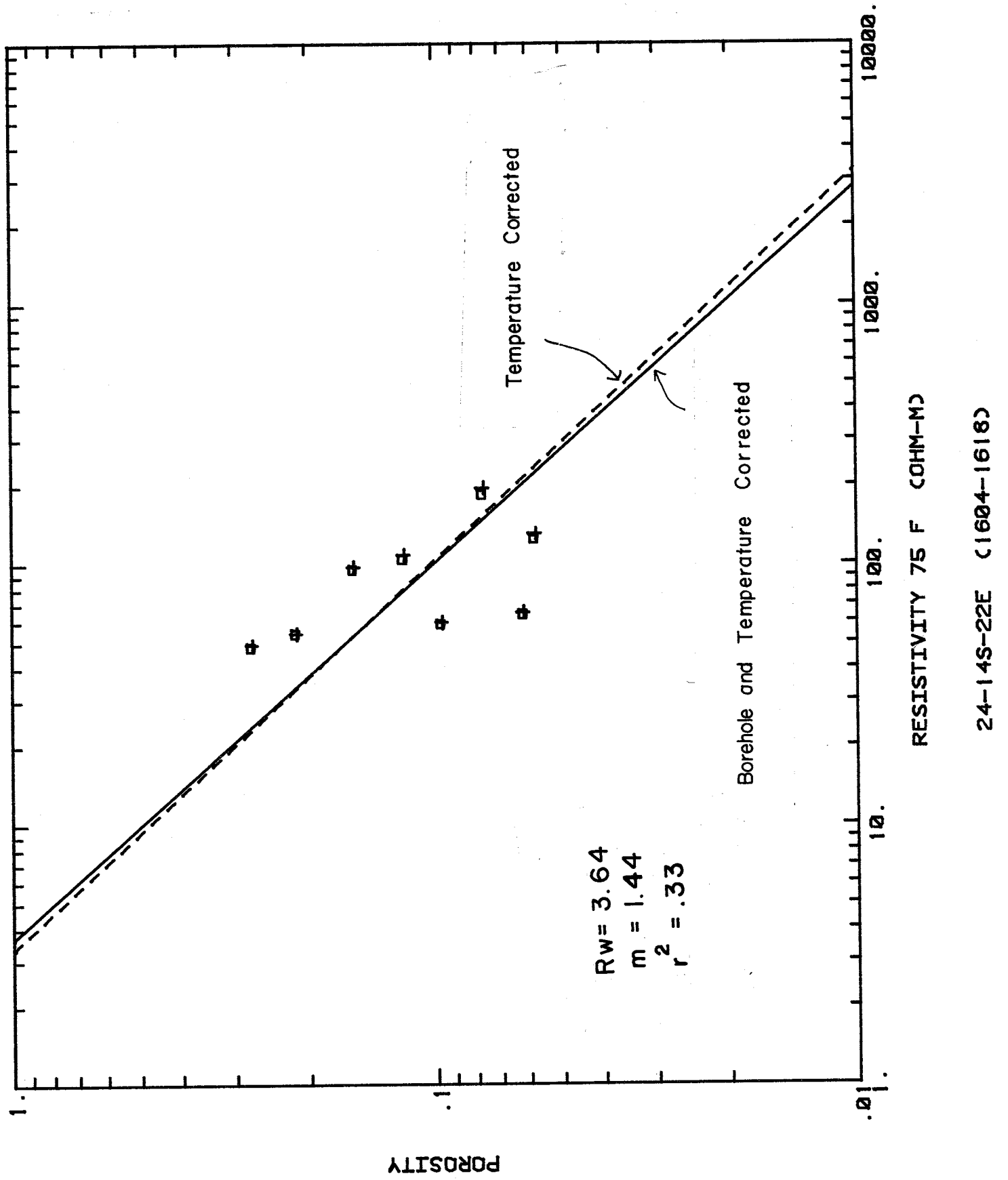

App 21. Resistivity versus Porosity Crossplot for well no 11

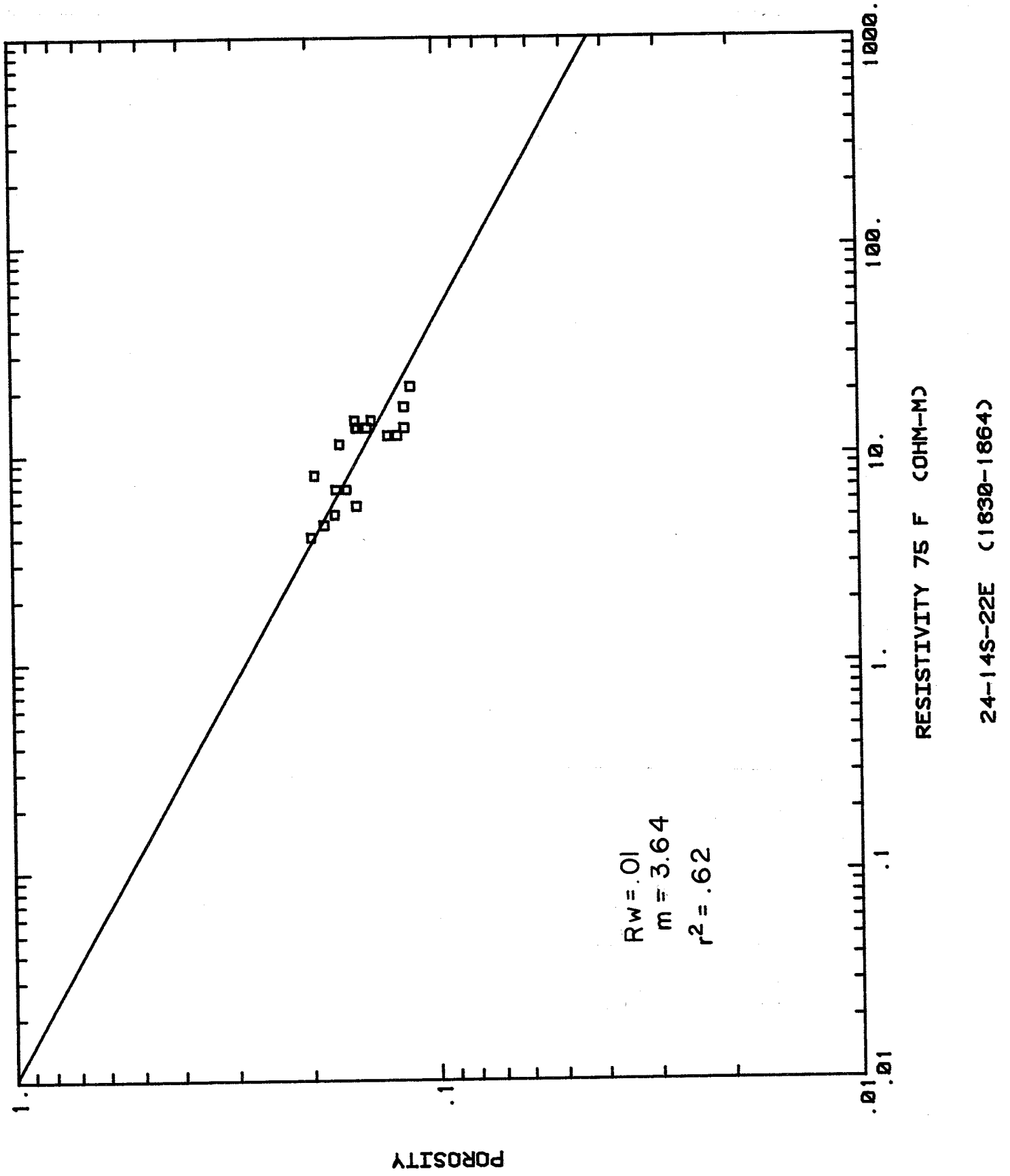

App 2m. Resistivity versus Porosity Crossplot for well no 11

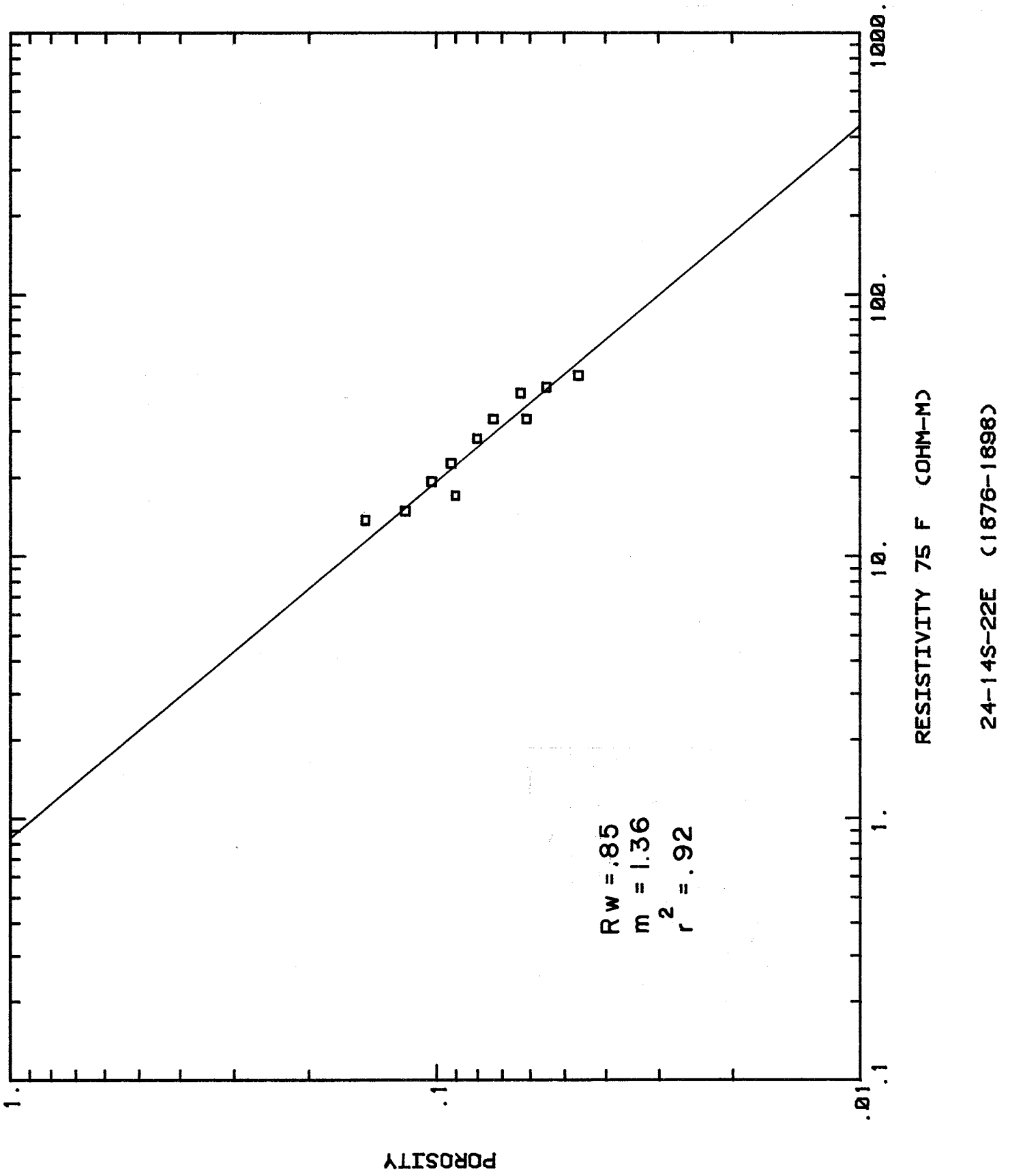

App 2n. Resistivity versus Porosity Crossplot for well no 11

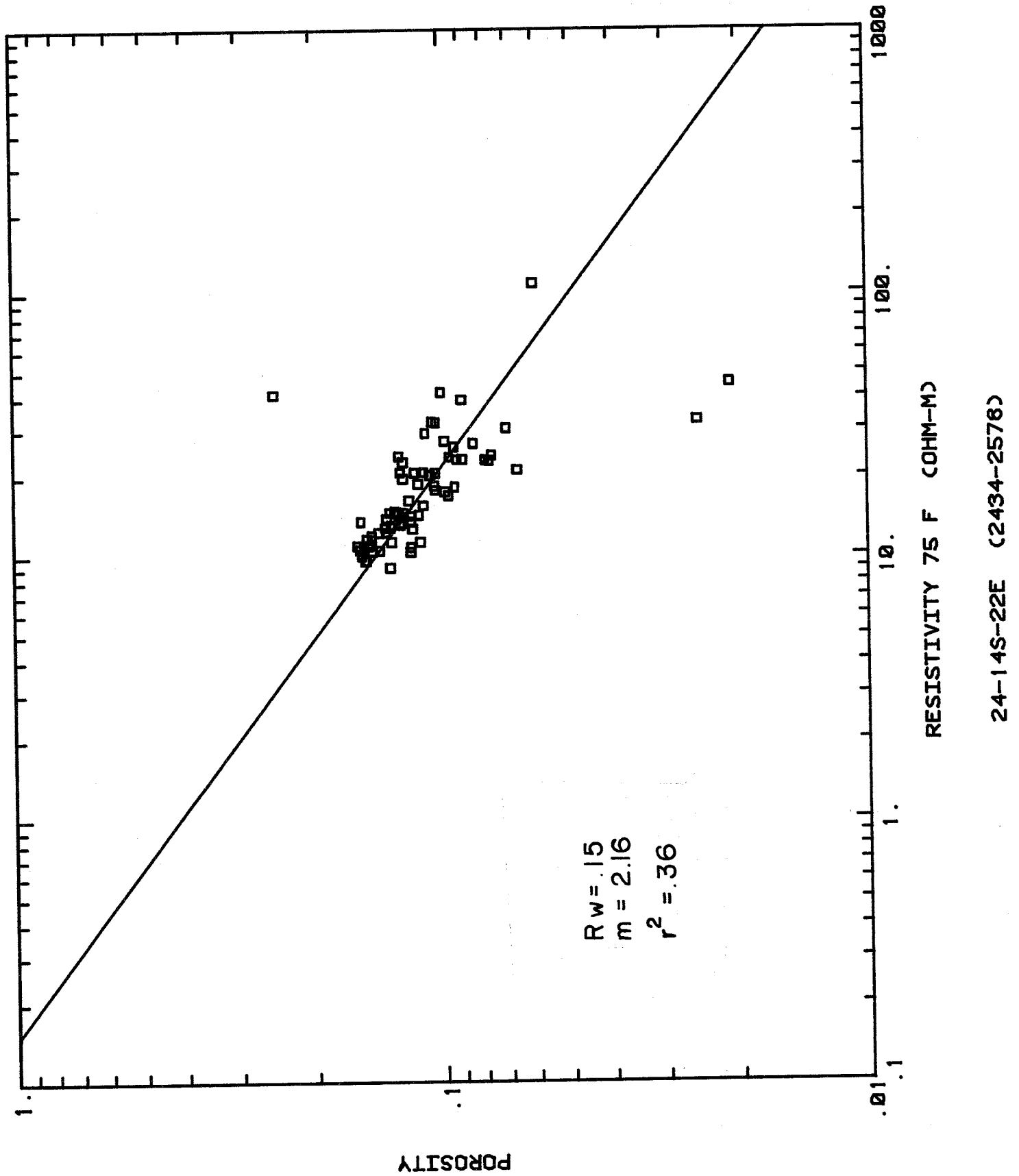

App 2o. Resistivity versus Porosity Crossplot for well no 11

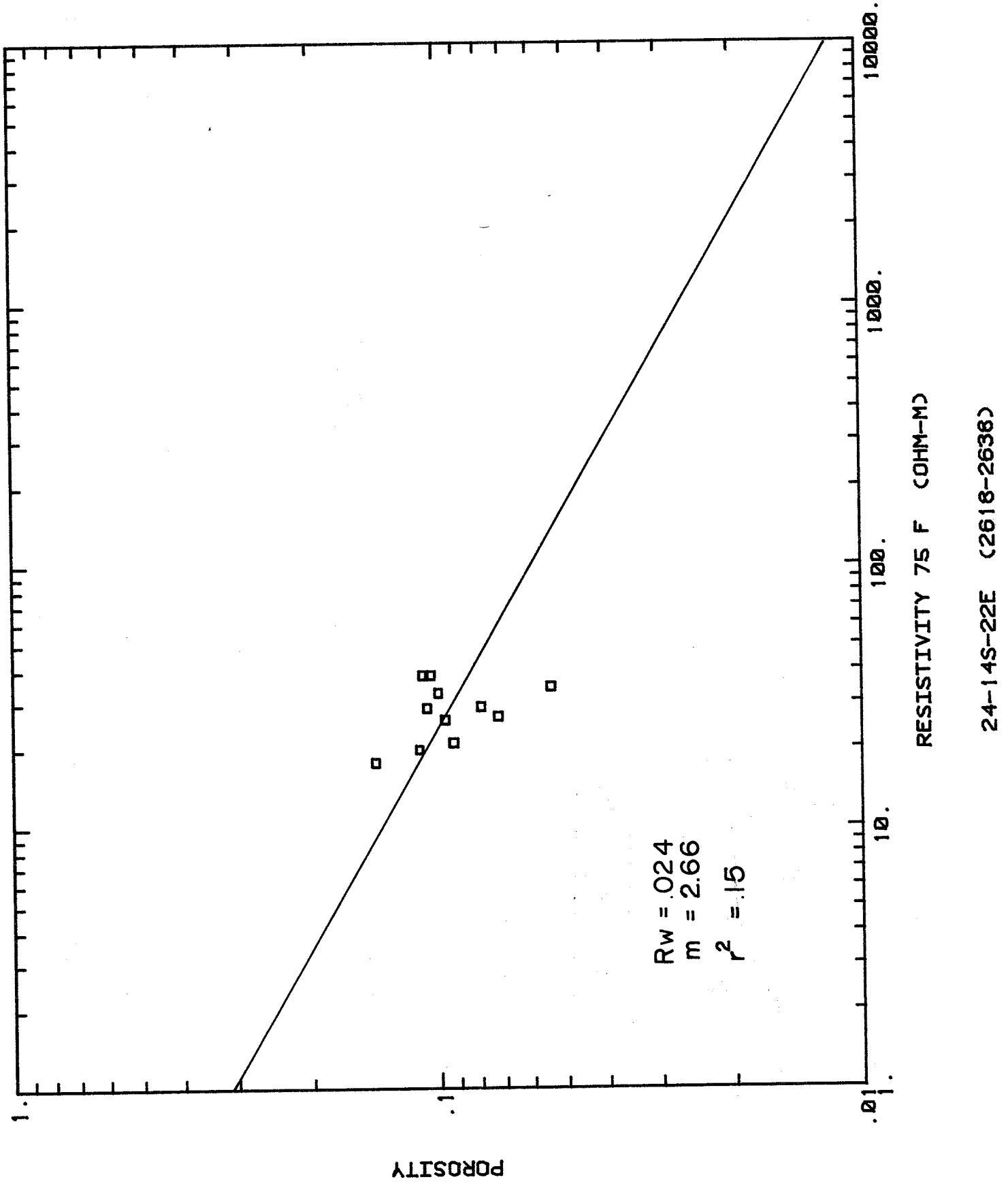

App 2p. Resistivity versus Porosity Crossplot for well no 12

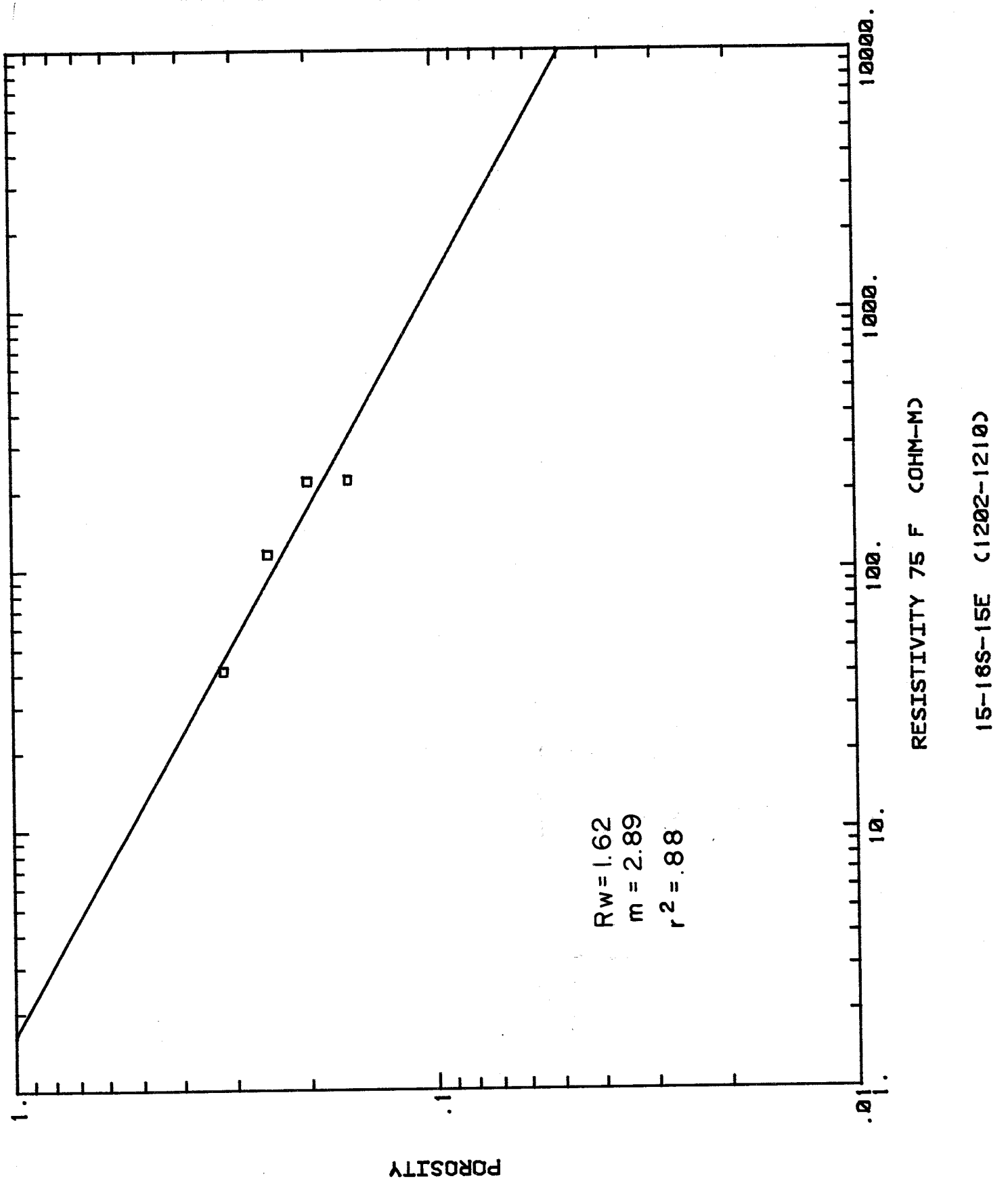

App 2q. Resistivity versus Porosity Crossplot
for well no 11 (corrected for invasion)

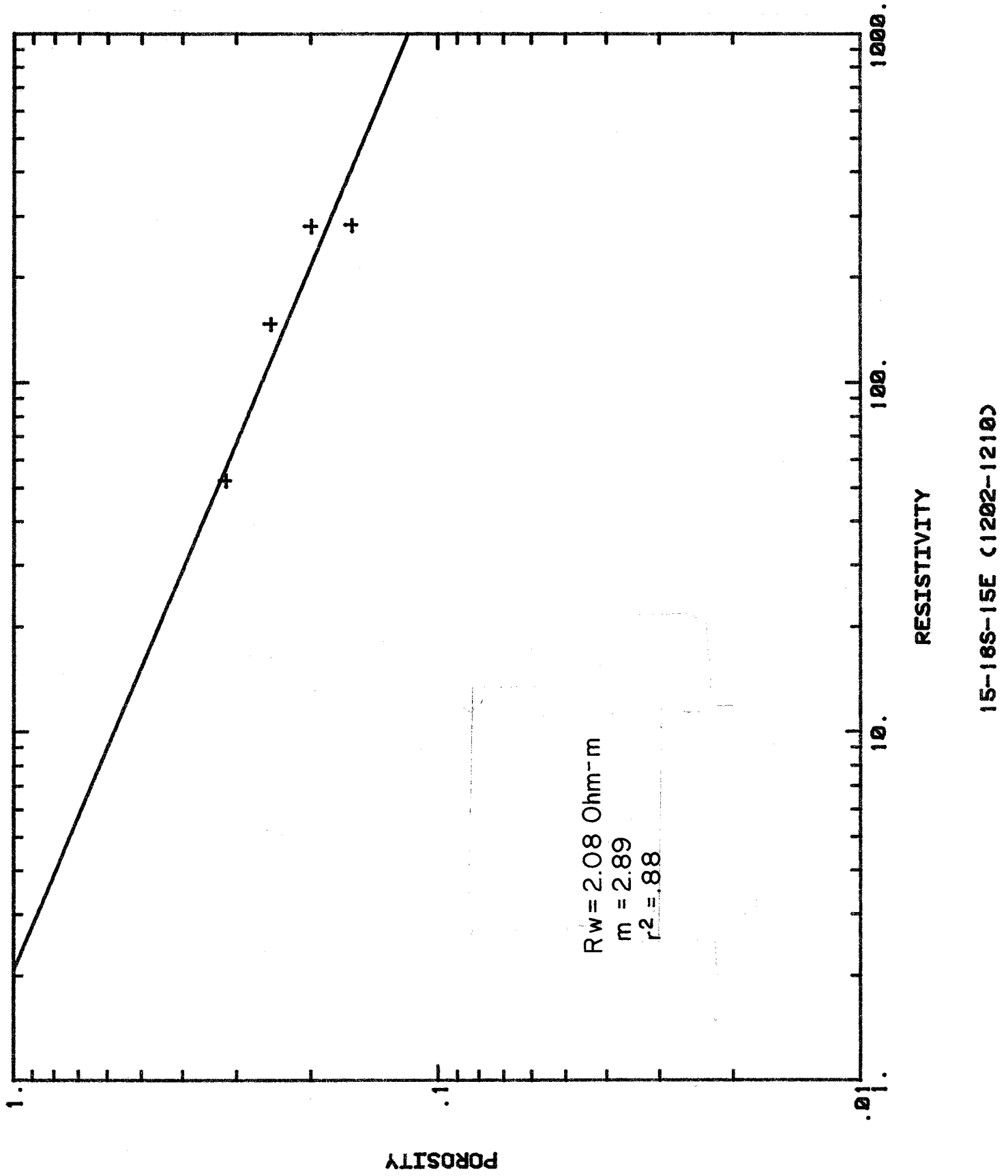

App 2r. Resistivity versus Porosity Crossplot for well no 11

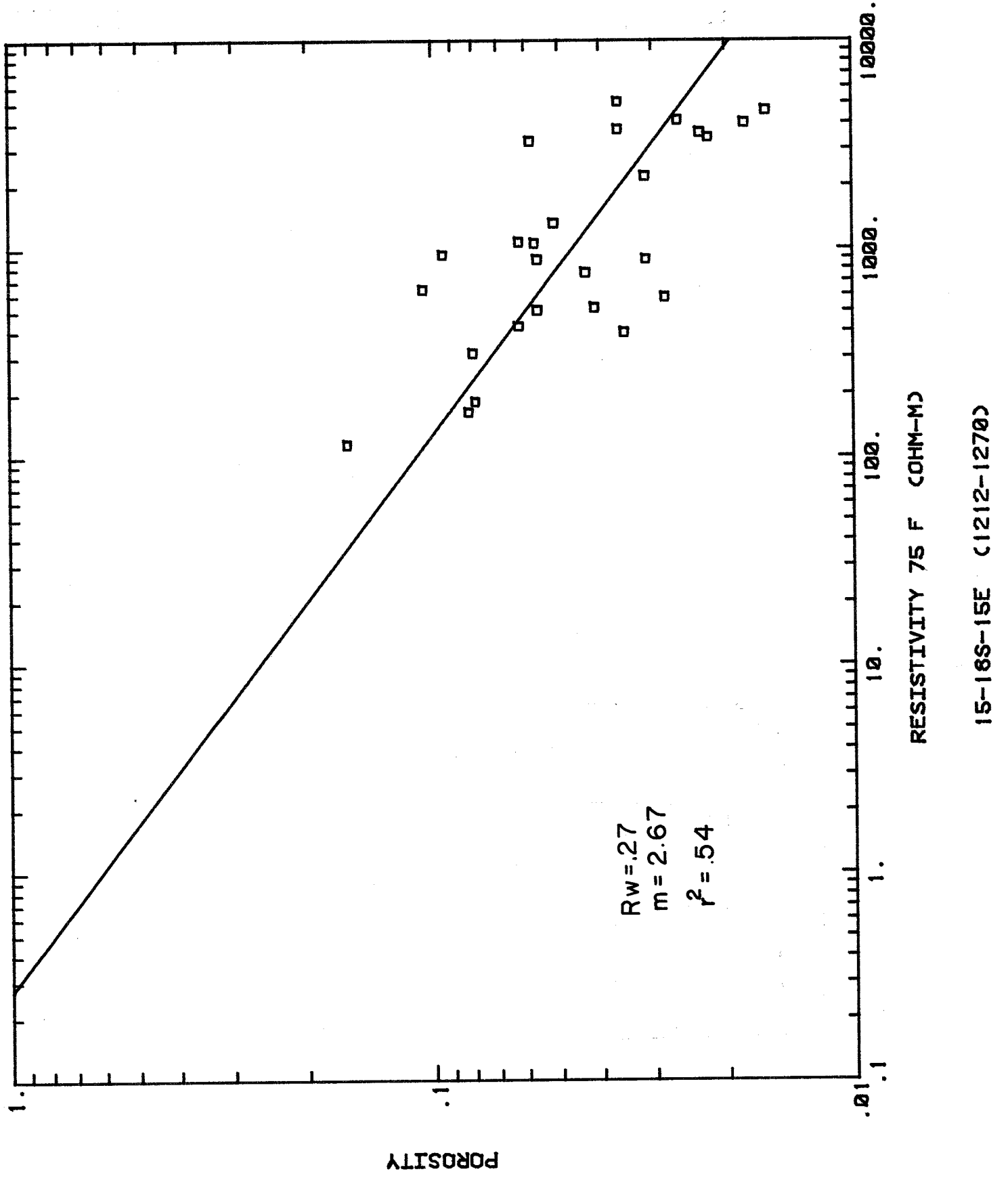

App 2s. Resistivity versus Porosity Crossplot
for well no 11 (corrected for invasion)

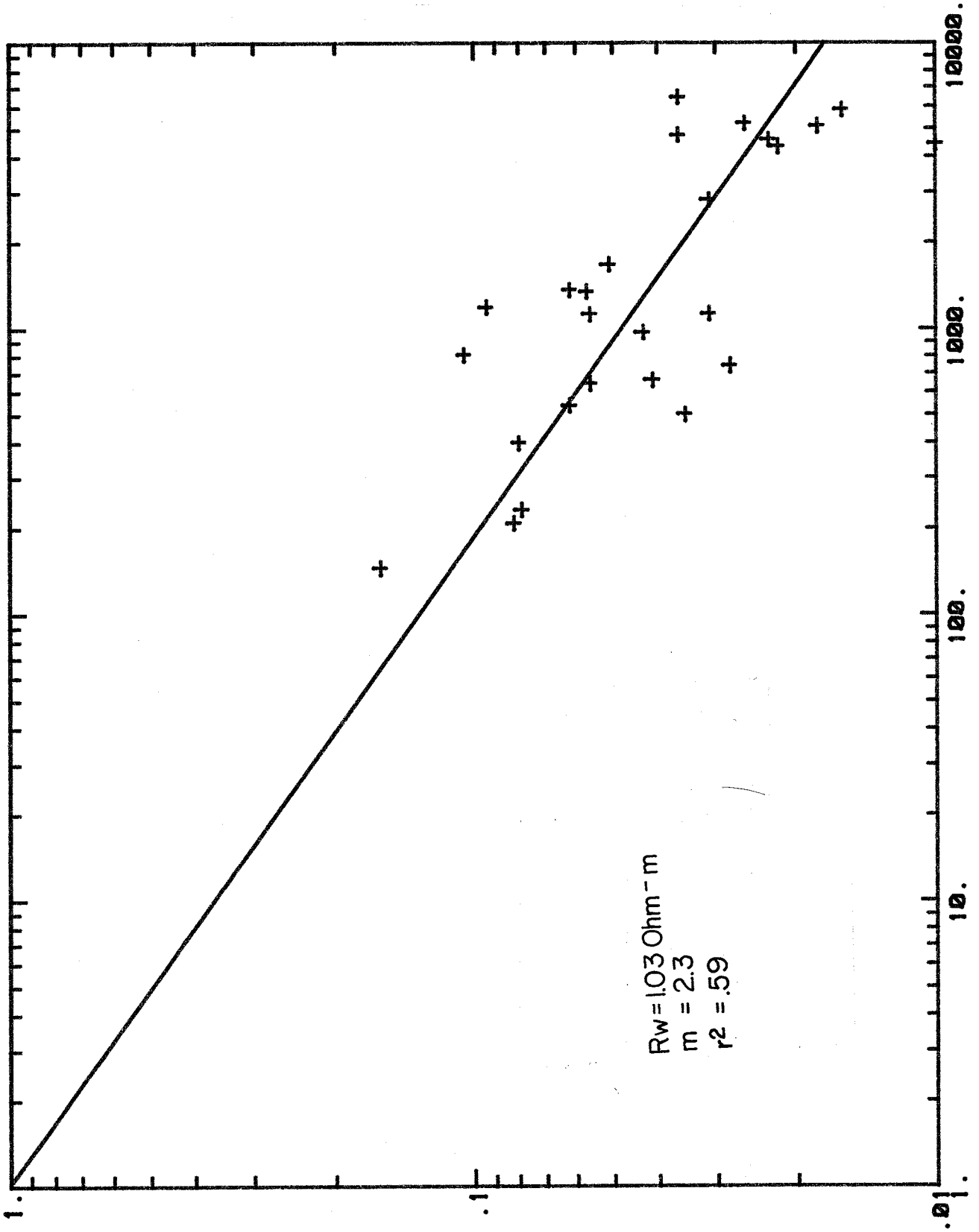

App 2t. Resistivity versus Porosity Crossplot for well no 11

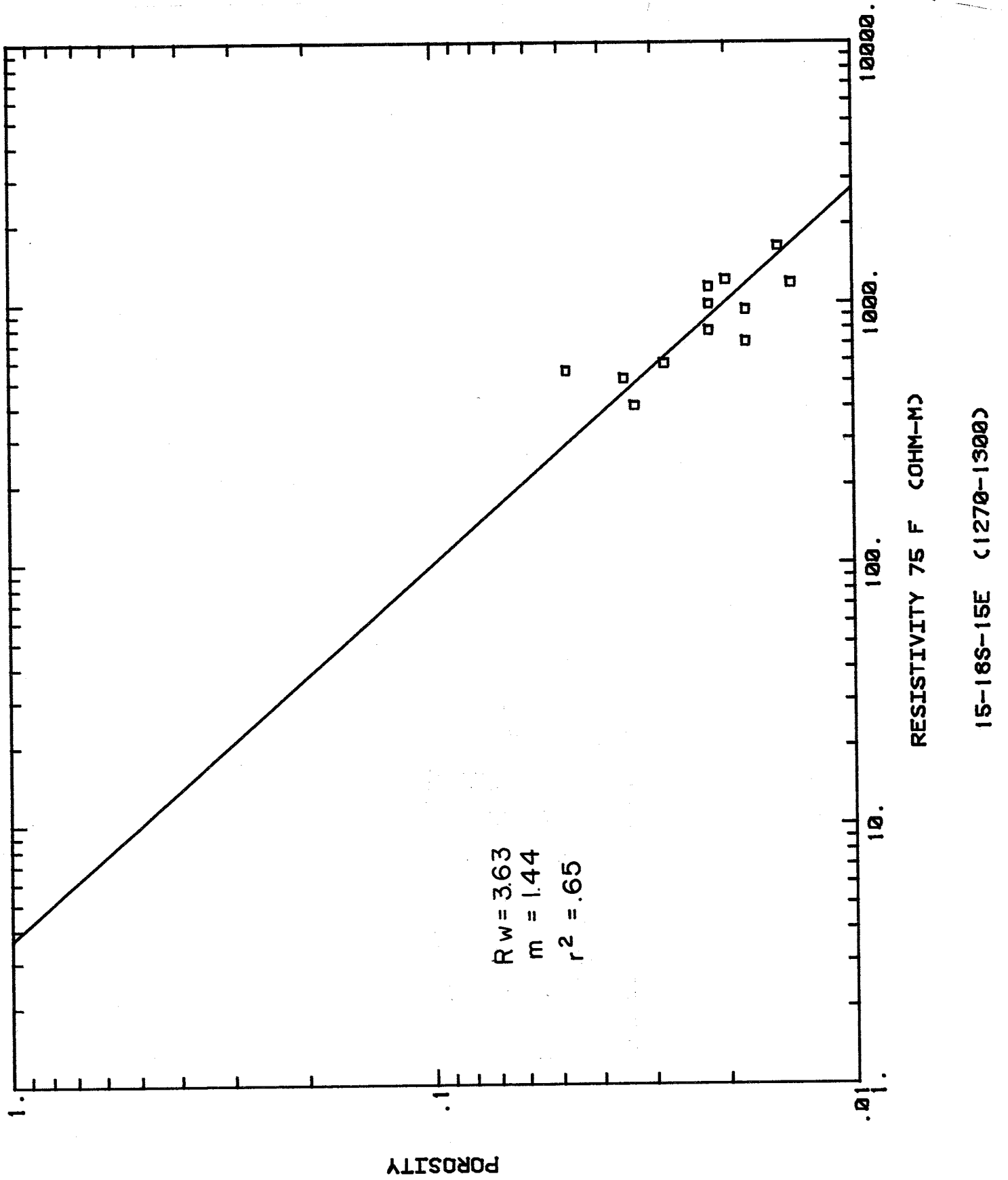

App 2u. Resistivity versus Porosity Crossplot for well no 12

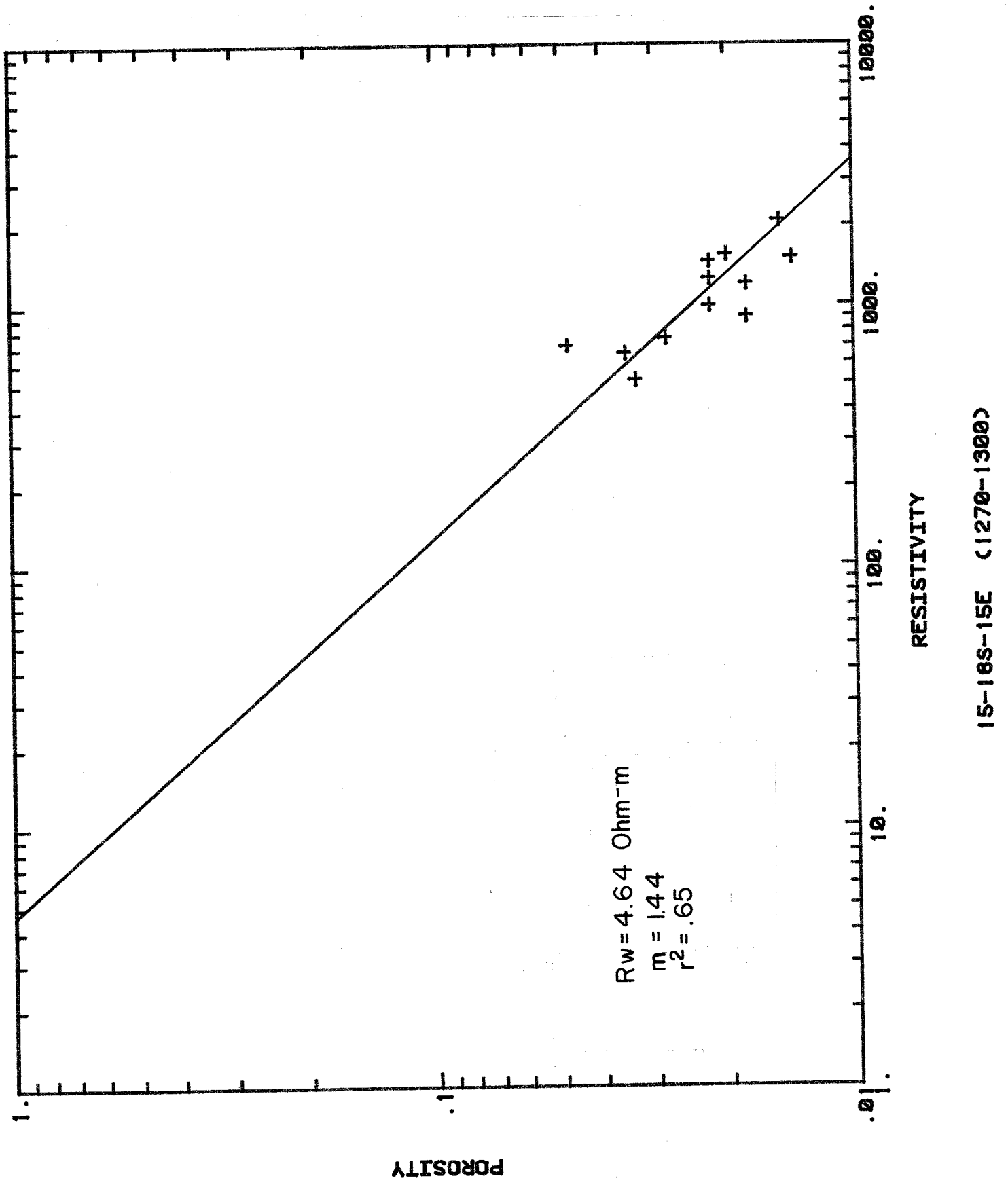

App 2v. Resistivity versus Porosity Crossplot for well no 11

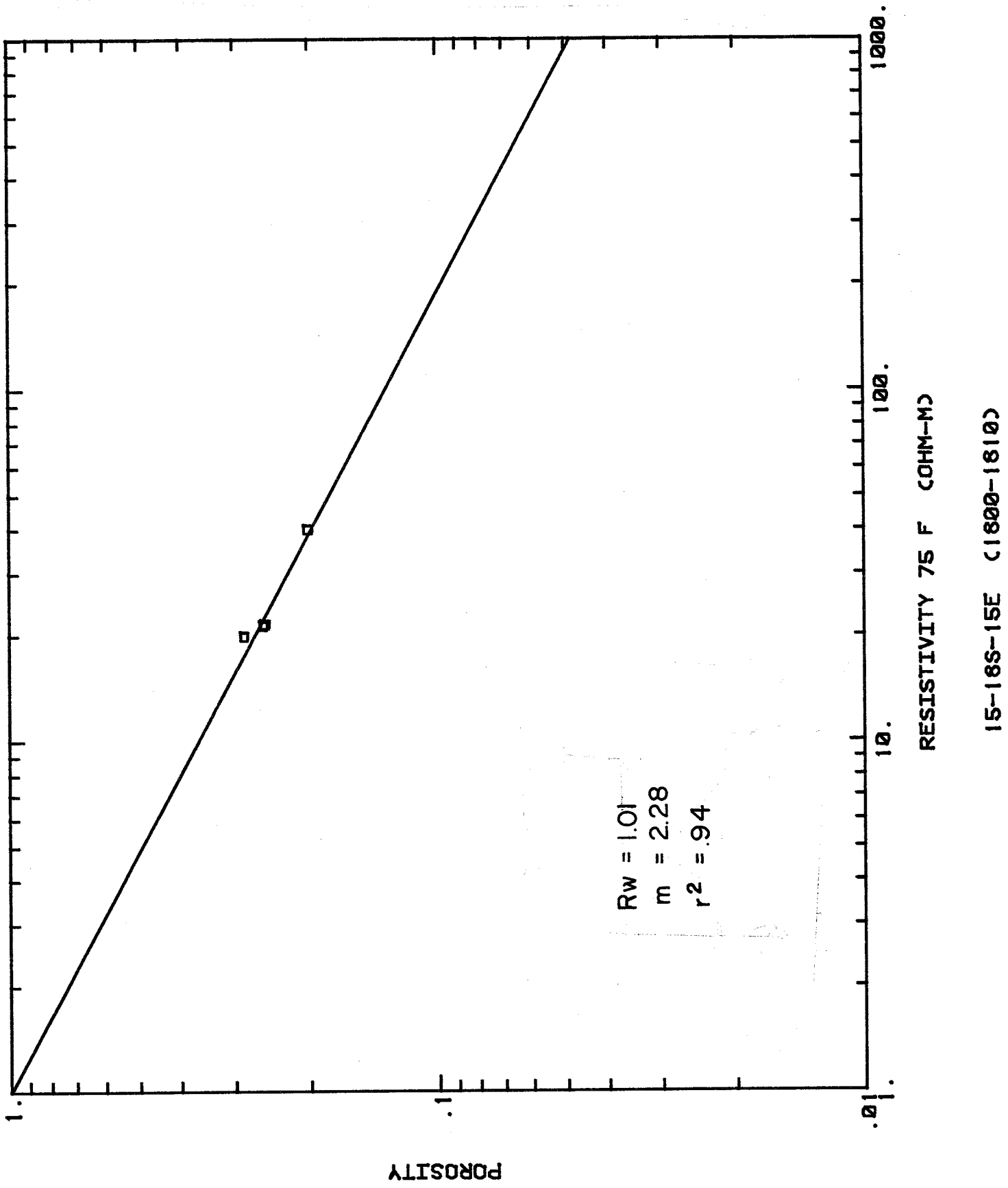

App 2w. Resistivity versus Porosity Crossplot
for well no 11 (corrected for invasion)

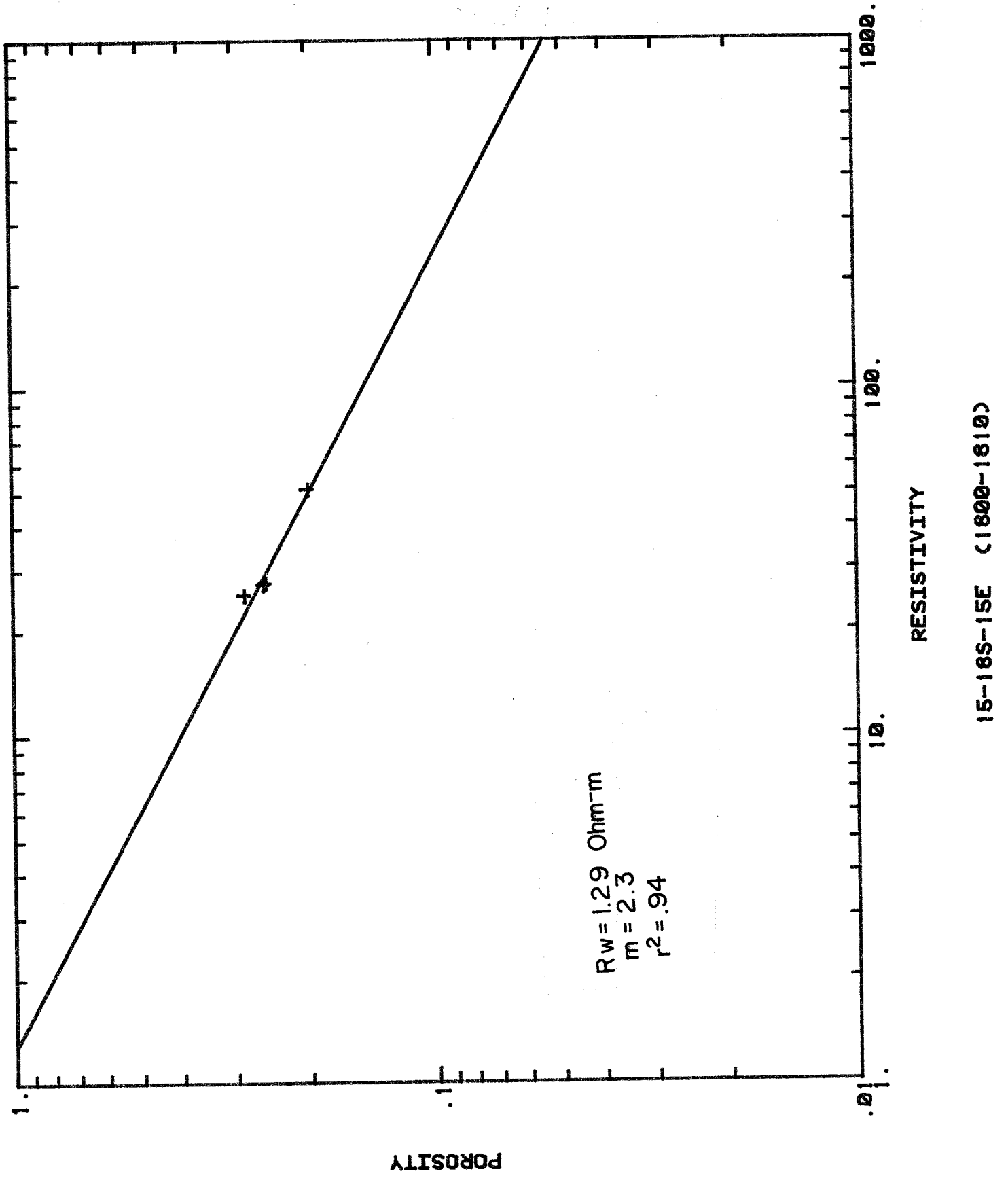

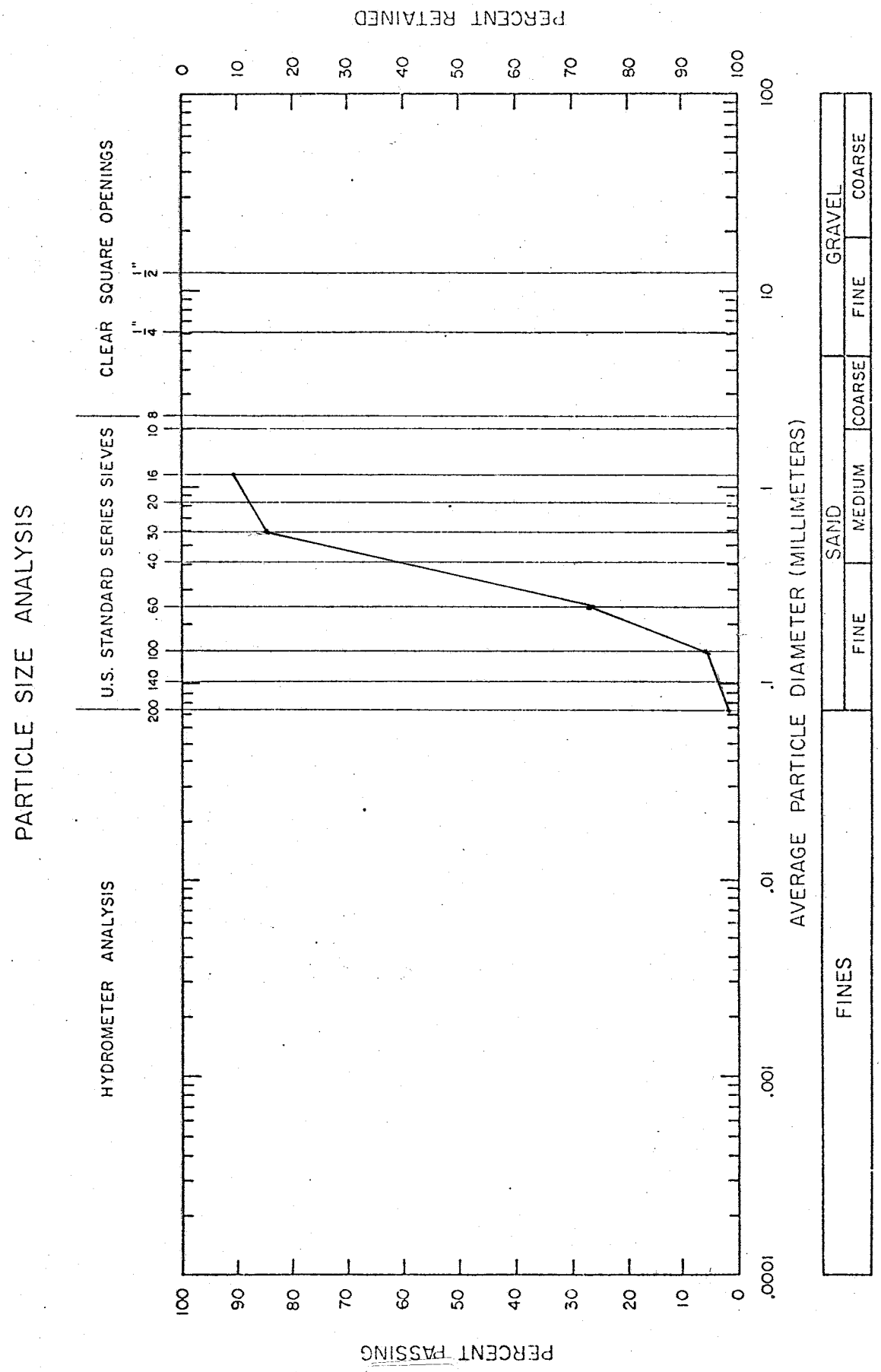
PARTICLE SIZE ANALYSIS
PERCENT RETAINED
PERCENT PASSING
CLEAR SQUARE OPENINGS
U.S. STANDARD SERIES SIEVES
HYDROMETER ANALYSIS
AVERAGE PARTICLE DIAMETER (MILLIMETERS)
FINES
SAND
GRAVEL
FINE
MEDIUM
COARSE
FINE
COARSE
dm = .39 mm
22-17S-18E
Depth 22204

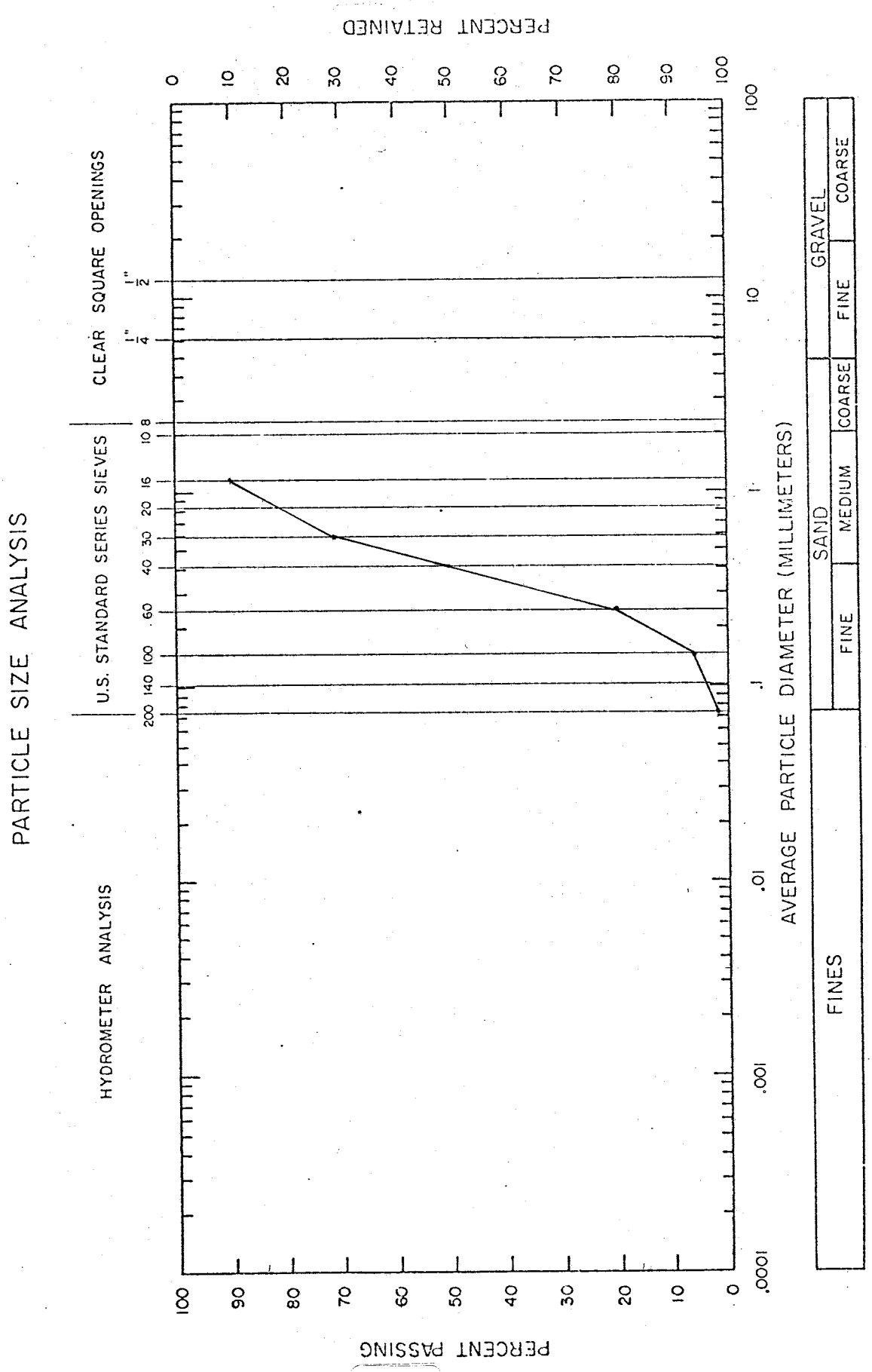
PARTICLE SIZE ANALYSIS
PERCENT RETAINED
PERCENT PASSING
CLEAR SQUARE OPENINGS
1"
1/2
1/4
U.S. STANDARD SERIES SIEVES
HYDROMETER ANALYSIS
AVERAGE PARTICLE DIAMETER (MILLIMETERS)
GRAVEL
SAND
FINES
FINE
MEDIUM
COARSE
FINE
COARSE
dm = .503 mm
22-17S-18E
Depth 2230ft

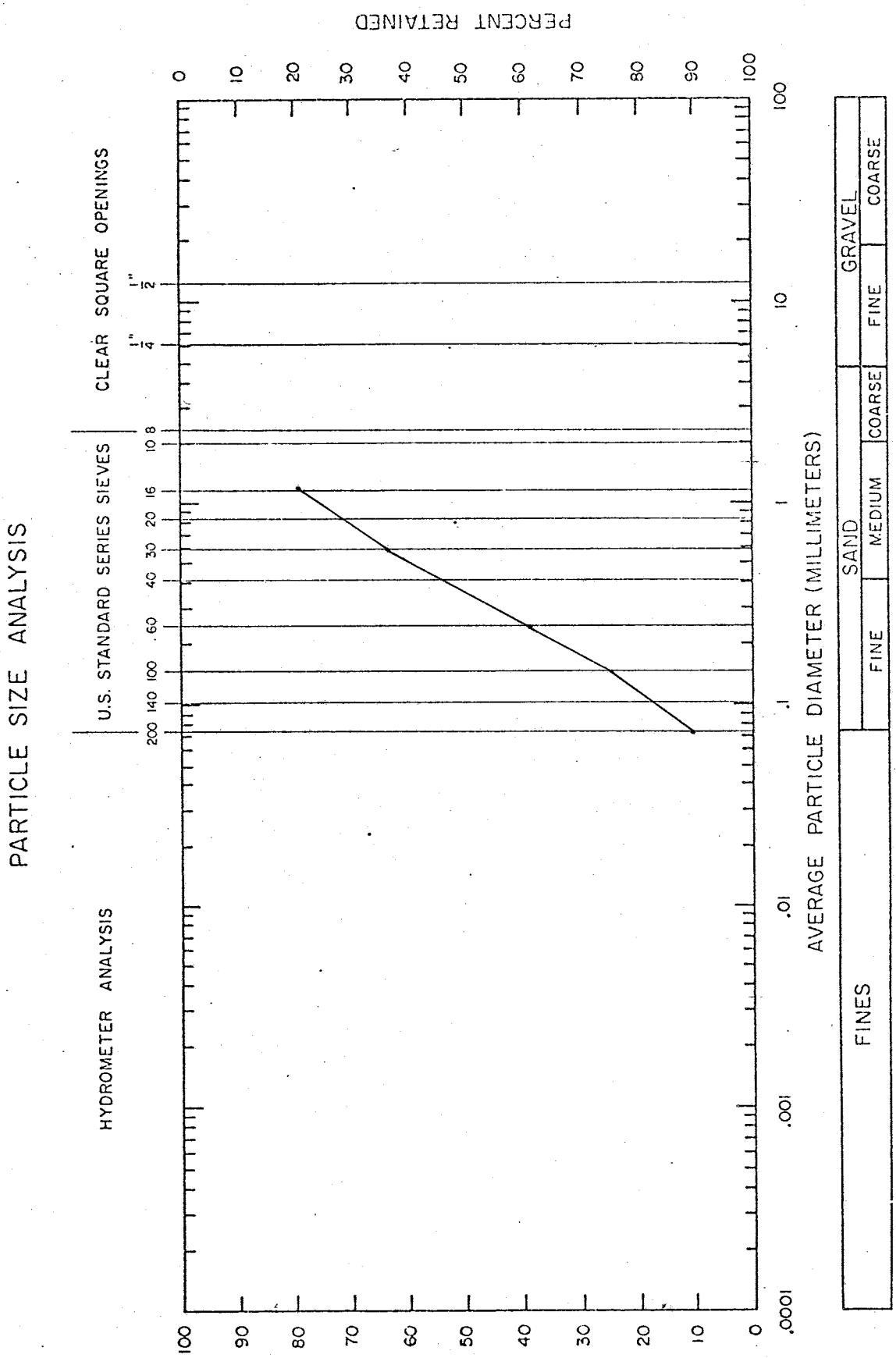
PARTICLE SIZE ANALYSIS
HYDROMETER ANALYSIS
U.S. STANDARD SERIES SIEVES
CLEAR SQUARE OPENINGS
1"
1/2
1/4
8
10
16
20
30
40
60
100
140
200
PERCENT RETAINED
PERCENT PASSING
0
10
20
30
40
50
60
70
80
90
100
.0001
.001
.01
.1
1
10
AVERAGE PARTICLE DIAMETER (MILLIMETERS)
FINES
SAND
FINE
MEDIUM
COARSE
GRAVEL
FINE
COARSE
22-175-18E
2250 ft
dm = .725 mm

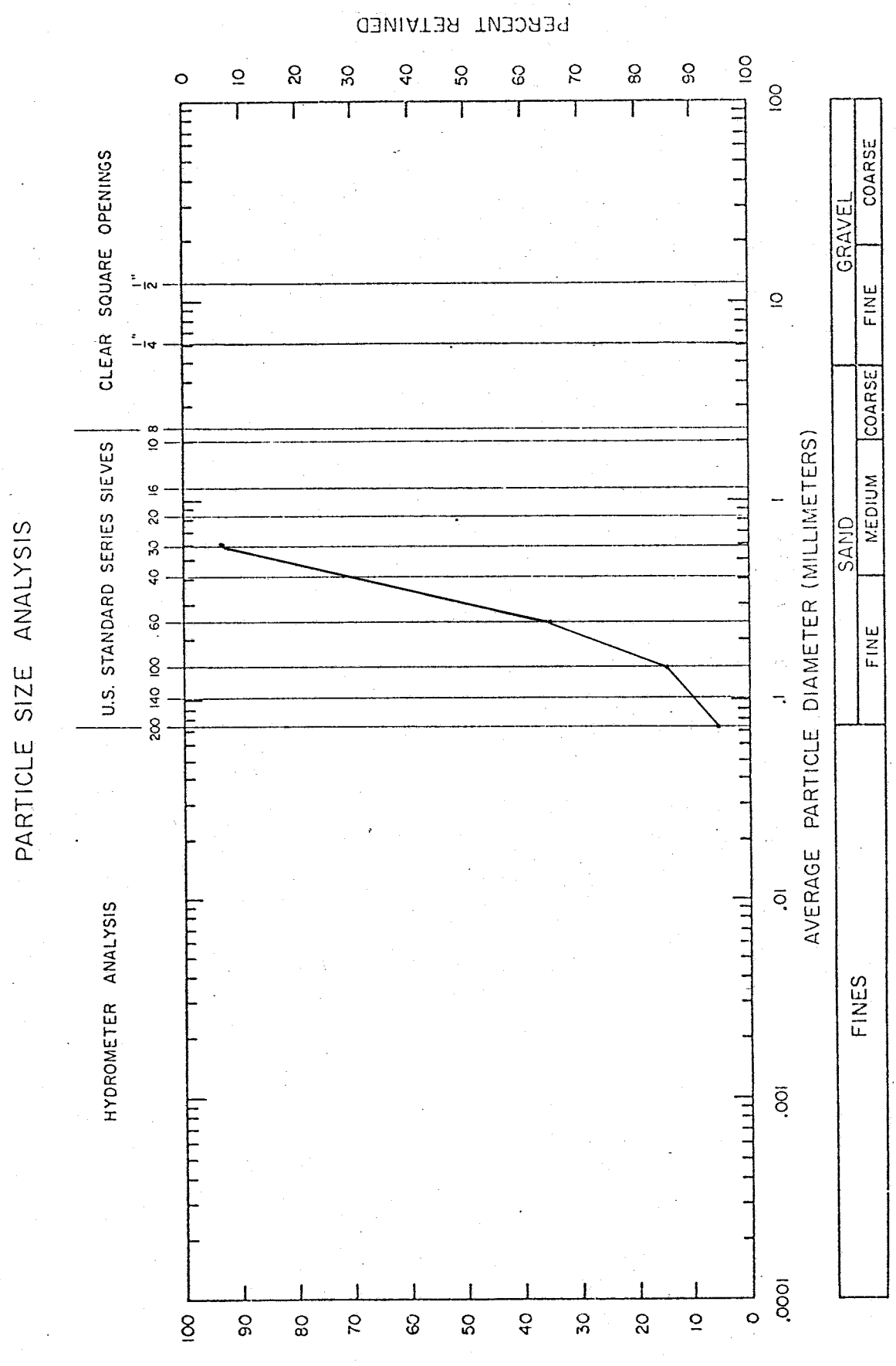
PARTICLE SIZE ANALYSIS
PERCENT RETAINED
PERCENT PASSING
CLEAR SQUARE OPENINGS
1" 1/2
1" 1/4
U.S. STANDARD SERIES SIEVES
10 8 16 20 30 40 60 100 140 200
HYDROMETER ANALYSIS
AVERAGE PARTICLE DIAMETER (MILLIMETERS)
FINES
SAND
FINE
MEDIUM
COARSE
GRAVEL
FINE
COARSE
dm = .32 mm
8-165-18E
Depth 2050 ft

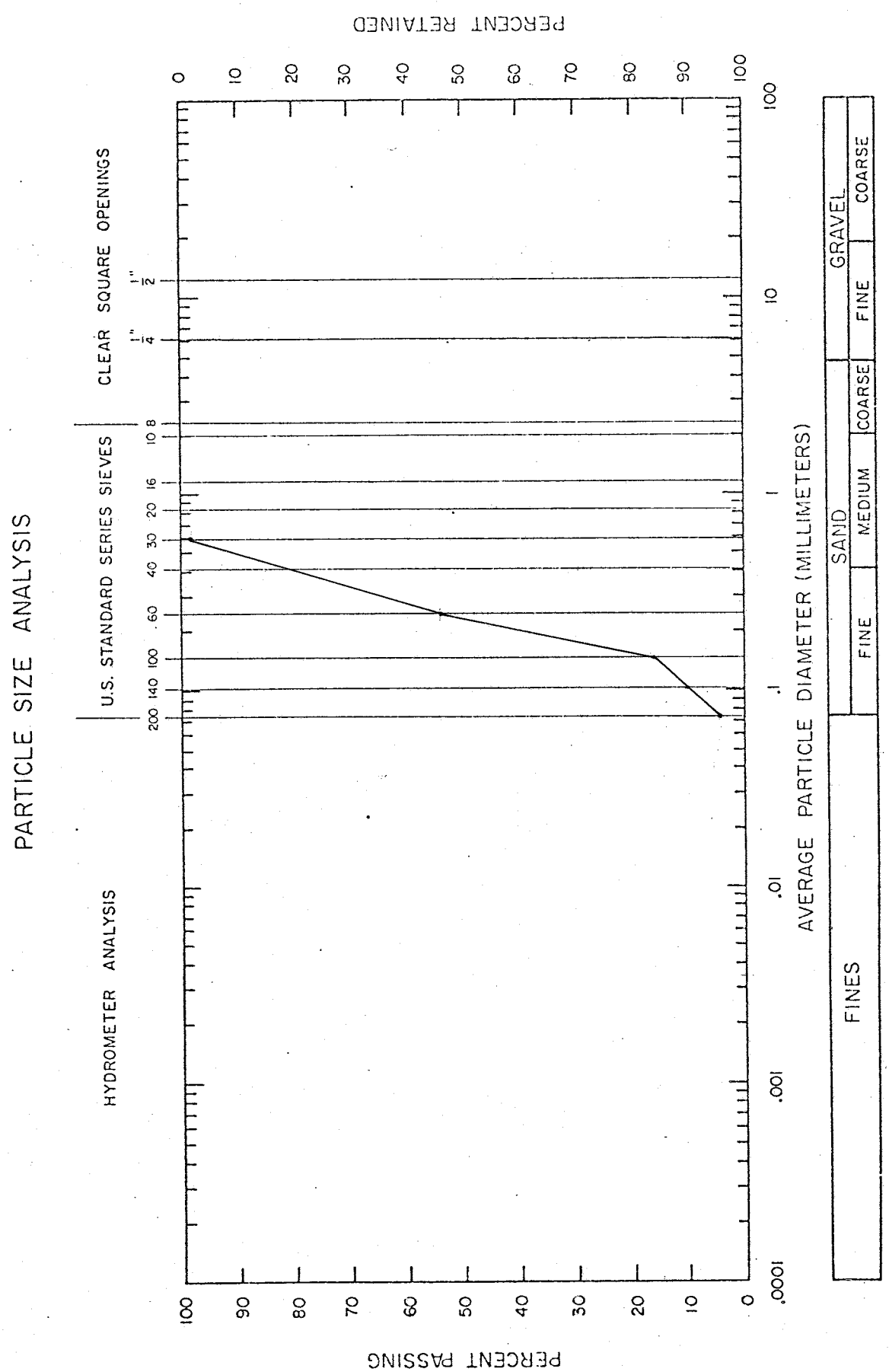
PARTICLE SIZE ANALYSIS
PERCENT RETAINED
PERCENT PASSING
CLEAR SQUARE OPENINGS
1"
2
1"
4
U.S. STANDARD SERIES SIEVES
HYDROMETER ANALYSIS
AVERAGE PARTICLE DIAMETER (MILLIMETERS)
GRAVEL
SAND
FINES
FINE
MEDIUM
COARSE
FINE
COARSE
8-165-18E
Depth 2080 ft
dm = .28 mm

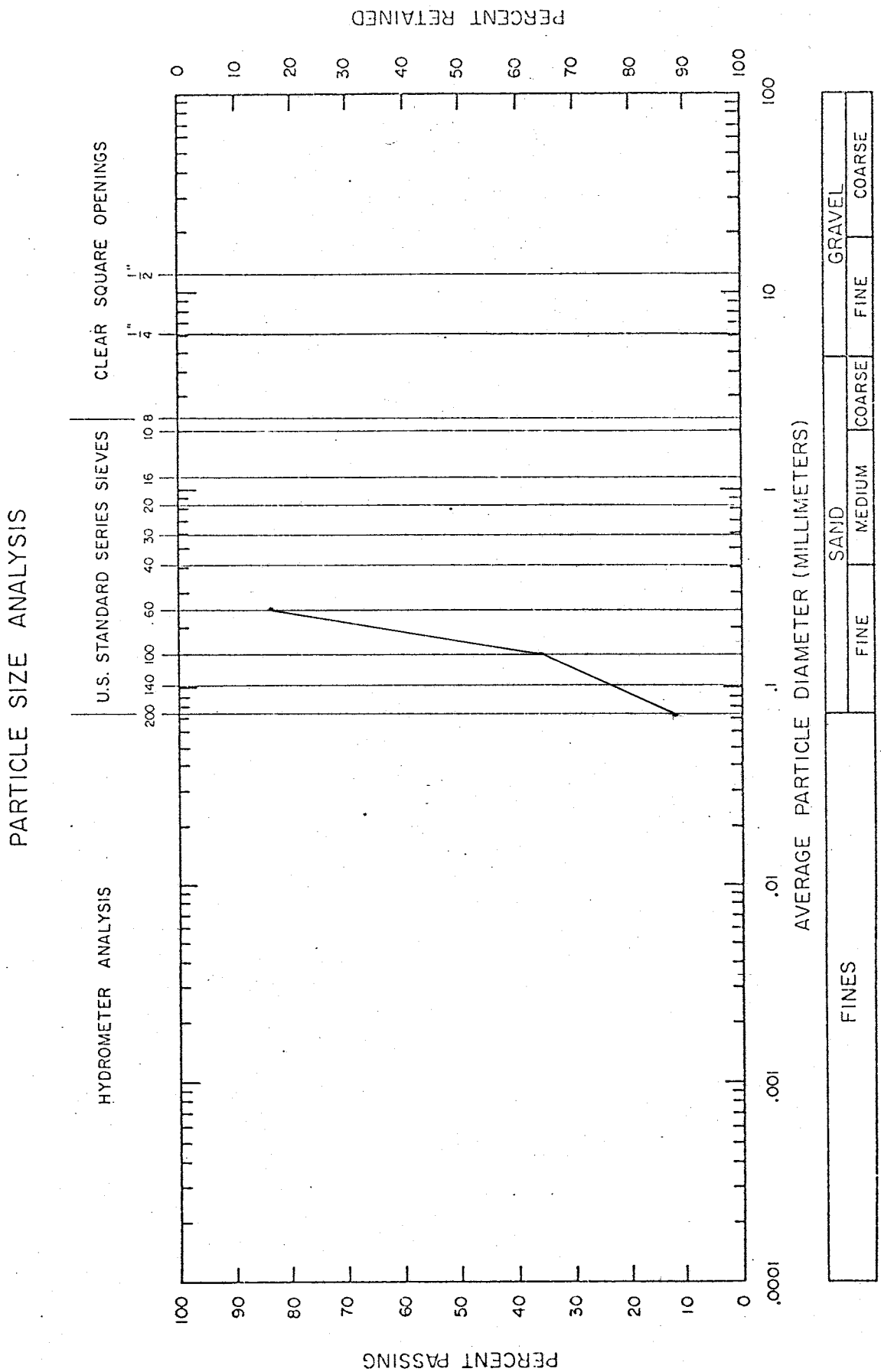
PARTICLE SIZE ANALYSIS
PERCENT RETAINED
PERCENT PASSING
CLEAR SQUARE OPENINGS
1"
1/2
1/4
U.S. STANDARD SERIES SIEVES
8
10
16
20
30
40
60
100
140
200
HYDROMETER ANALYSIS
AVERAGE PARTICLE DIAMETER (MILLIMETERS)
FINES
SAND
FINE
MEDIUM
COARSE
GRAVEL
FINE
COARSE
dm = .17 mm
8-165-18E
Depth 2100ft

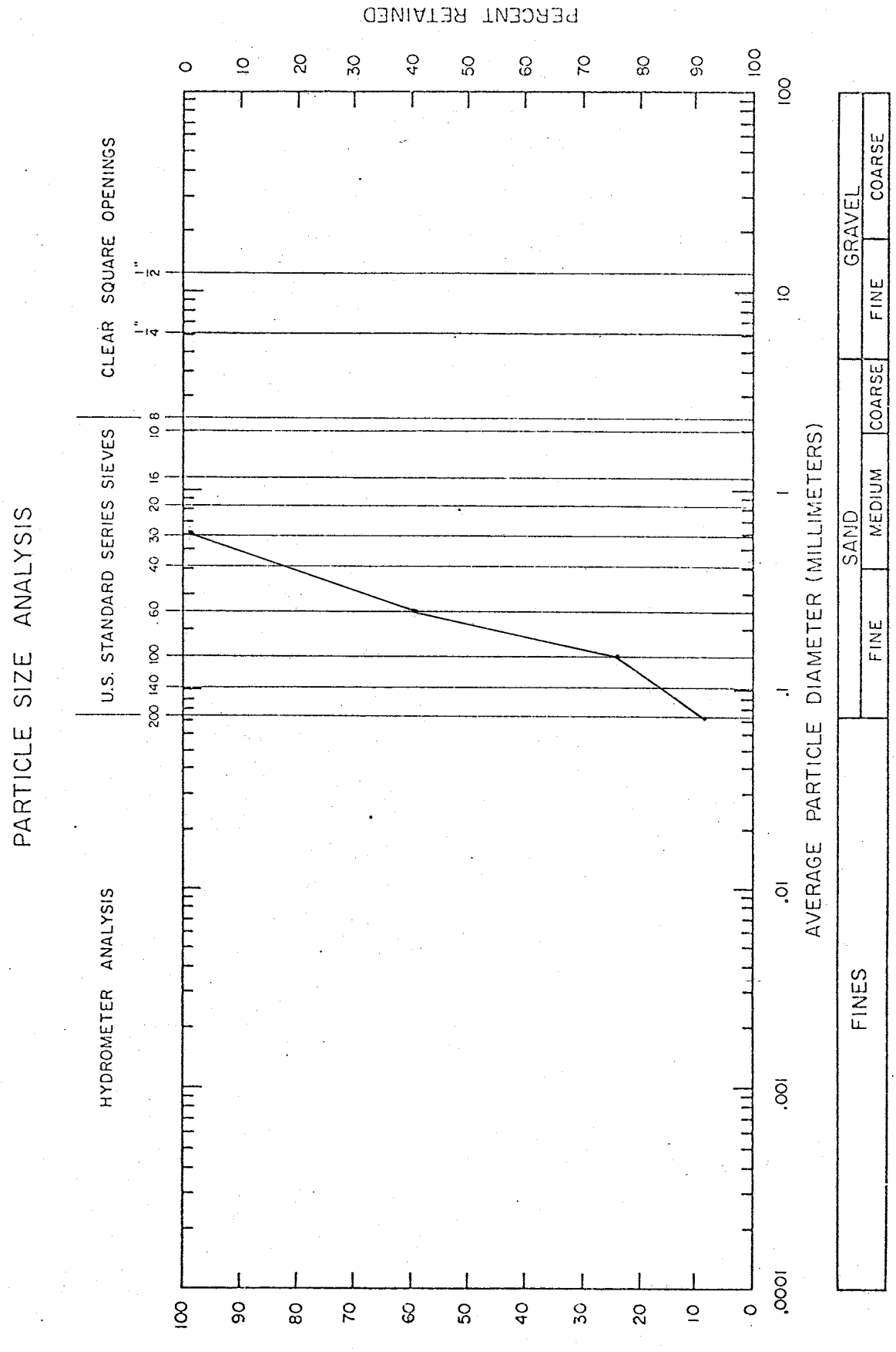
PARTICLE SIZE ANALYSIS
HYDROMETER ANALYSIS
U.S. STANDARD SERIES SIEVES
CLEAR SQUARE OPENINGS
1" 1/2
1" 1/4
10 8
16
20
30
40
60
100
140
200
PERCENT RETAINED
0 10 20 30 40 50 60 70 80 90 100
PERCENT PASSING
100 90 80 70 60 50 40 30 20 10 0
AVERAGE PARTICLE DIAMETER (MILLIMETERS)
.0001 .001 .01 .1 1 10 100
FINES
SAND
FINE
MEDIUM
COARSE
GRAVEL
FINE
COARSE
Dm = .24
8-16S-18E
Depth 2140 ft

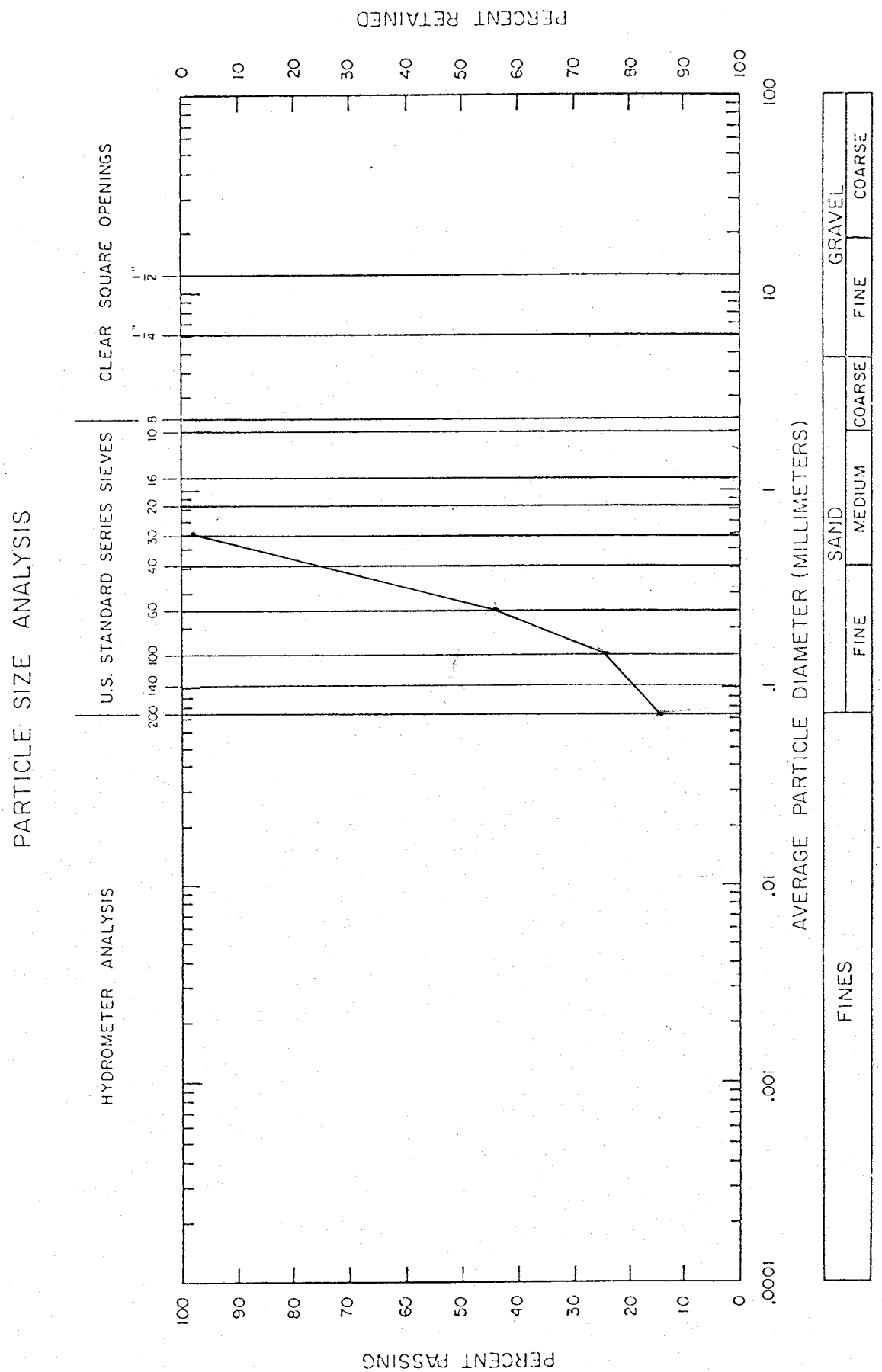
PARTICLE SIZE ANALYSIS
PERCENT RETAINED
PERCENT PASSING
CLEAR SQUARE OPENINGS
1"
1/2
1/4
U.S. STANDARD SERIES SIEVES
HYDROMETER ANALYSIS
AVERAGE PARTICLE DIAMETER (MILLIMETERS)
FINES
SAND
FINE
MEDIUM
COARSE
GRAVEL
FINE
COARSE
8-165-18E
Depth 2160 ft
dm = .523

App 3*i*. Grain size analysis of well cuttings.

Depth (feet)	Total Weight	Weight for Seive Size (grams) no. 16	no. 30	no.60	no.100	no.200	finer
22-17S-19E							
2220	7.6	.78	1.18	3.59	1.58	.35	.12
Cum % finer		90%	84%	27%	6%	2%	0%
2230	12.13	1.21	2.32	6.14	1.7	.44	.32
Cum % finer		90%	71%	20%	6%	3%	0
2250	11.05	2.34	1.77	2.67	1.61	1.56	1.1
Cum % finer		79%	63%	38.6%	24%	10%	0
8-16S-18E							
2050	8.37	---	.57	4.76	1.89	.675	.47
Cum % finer			93%	36%	14%	6%	0
2080	13.76	---	.25	6.24	4.91	1.81	.55
Cum % finer			98%	53%	17%	4%	0
2100	12.69	---	---	2.12	5.88	3.28	1.41
Cum % finer				83.3%	37%	11.1%	0
2140	14.67	---	.16	5.86	5.34	2.05	1.26
Cum % finer			99%	59%	23%	8.6%	0
2160	15.6	---	.35	8.55	3.08	1.47	2.15
Cum % finer			98%	43%	23%	13.8%	0

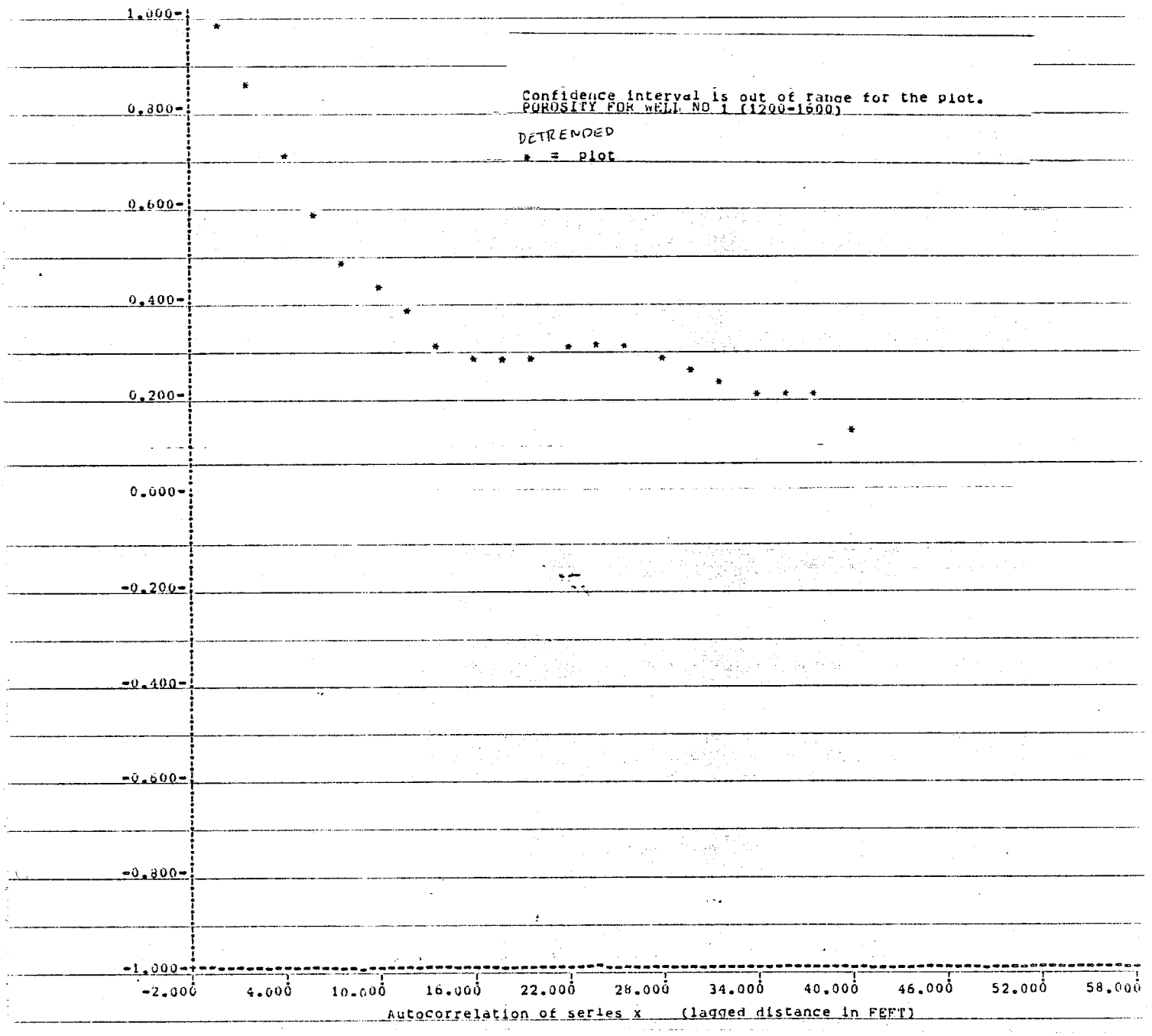

App 4a. Correlogram for porosity of upper Yeso in well no 1

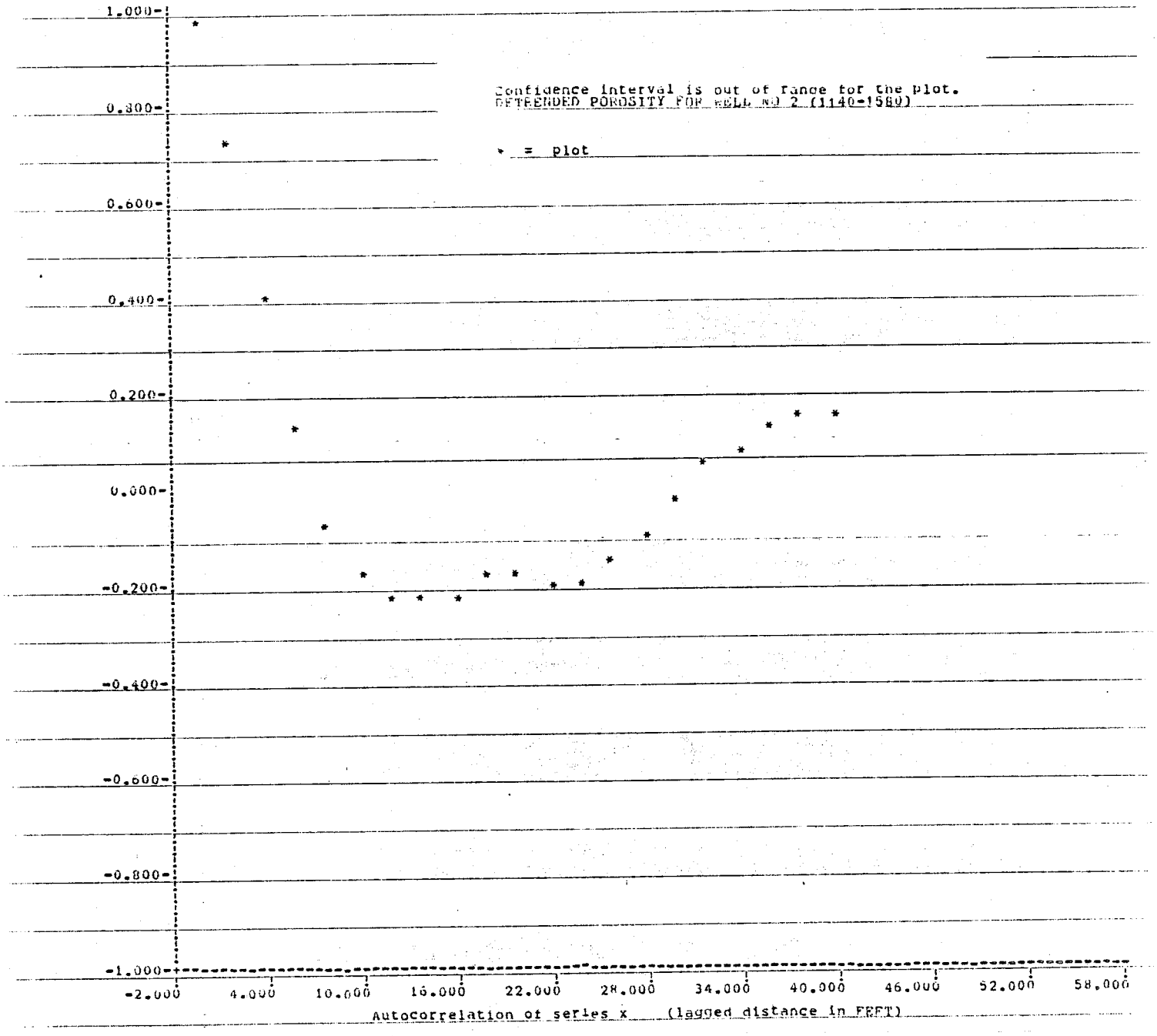

App 4b. Correlogram for porosity of upper Yeso in well no 2

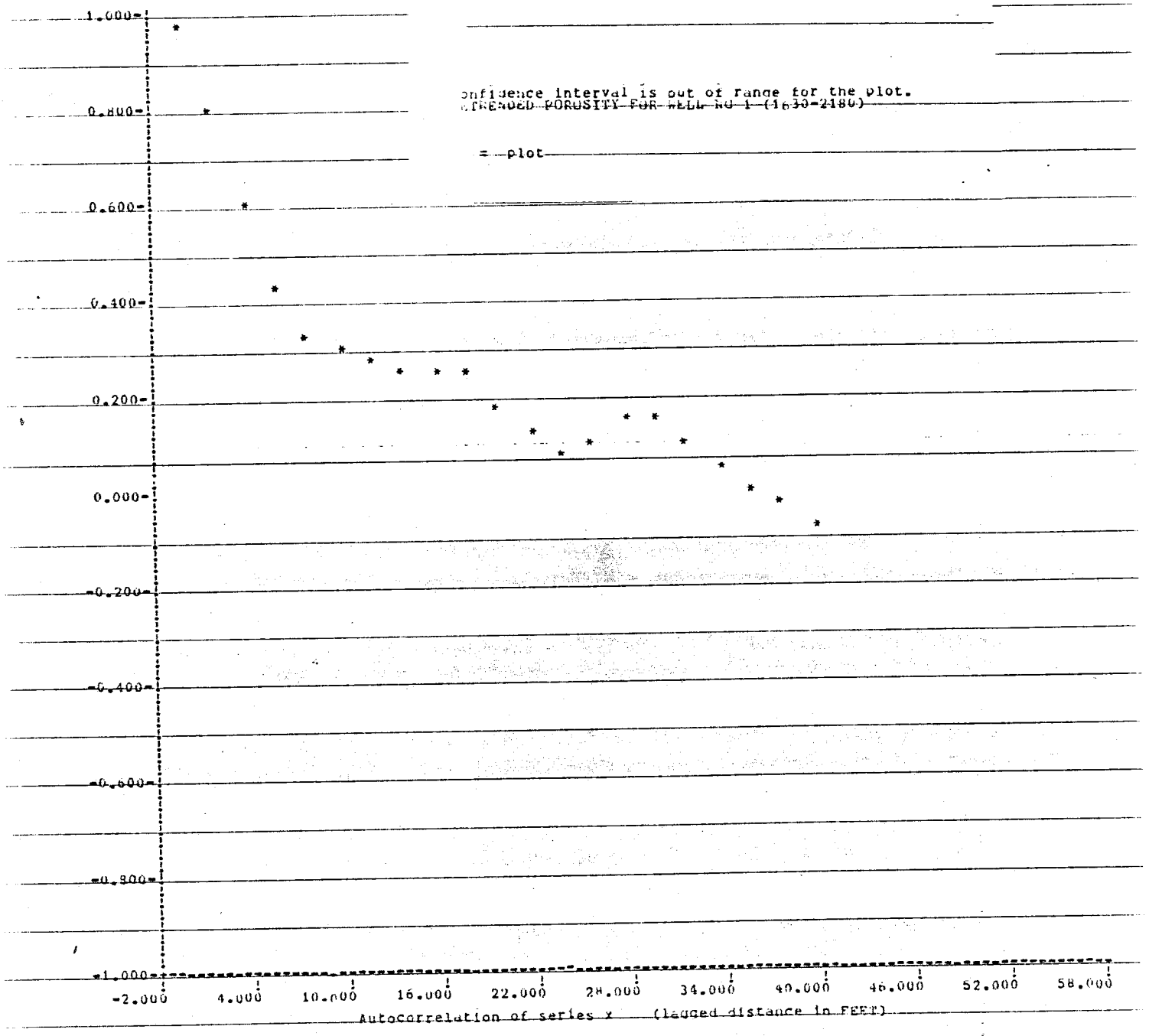

App 4c. Correlogram for porosity of upper middle Yeso in well no 1

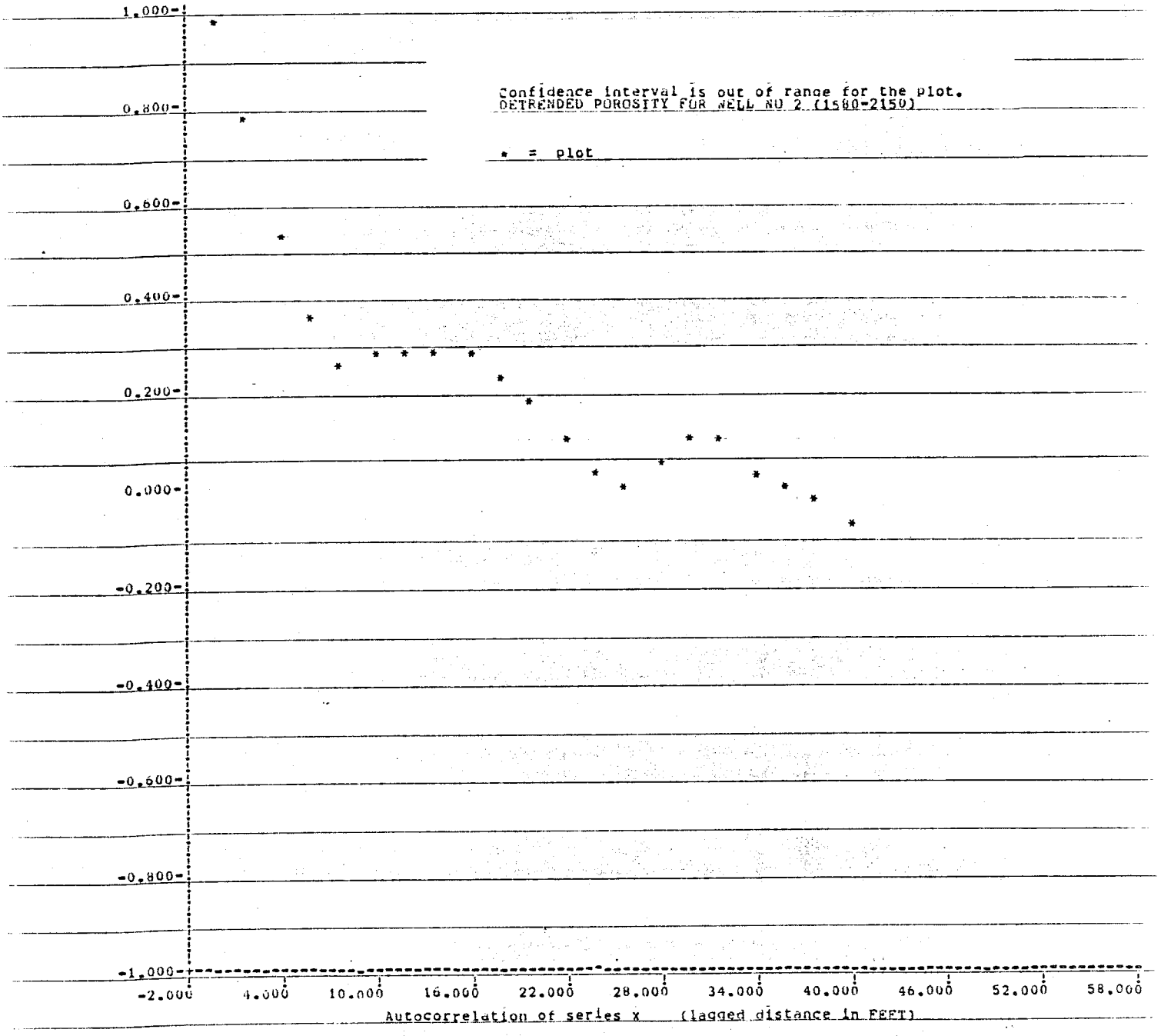

App 4d. Correlogram for porosity of upper middle Yeso in well no 2

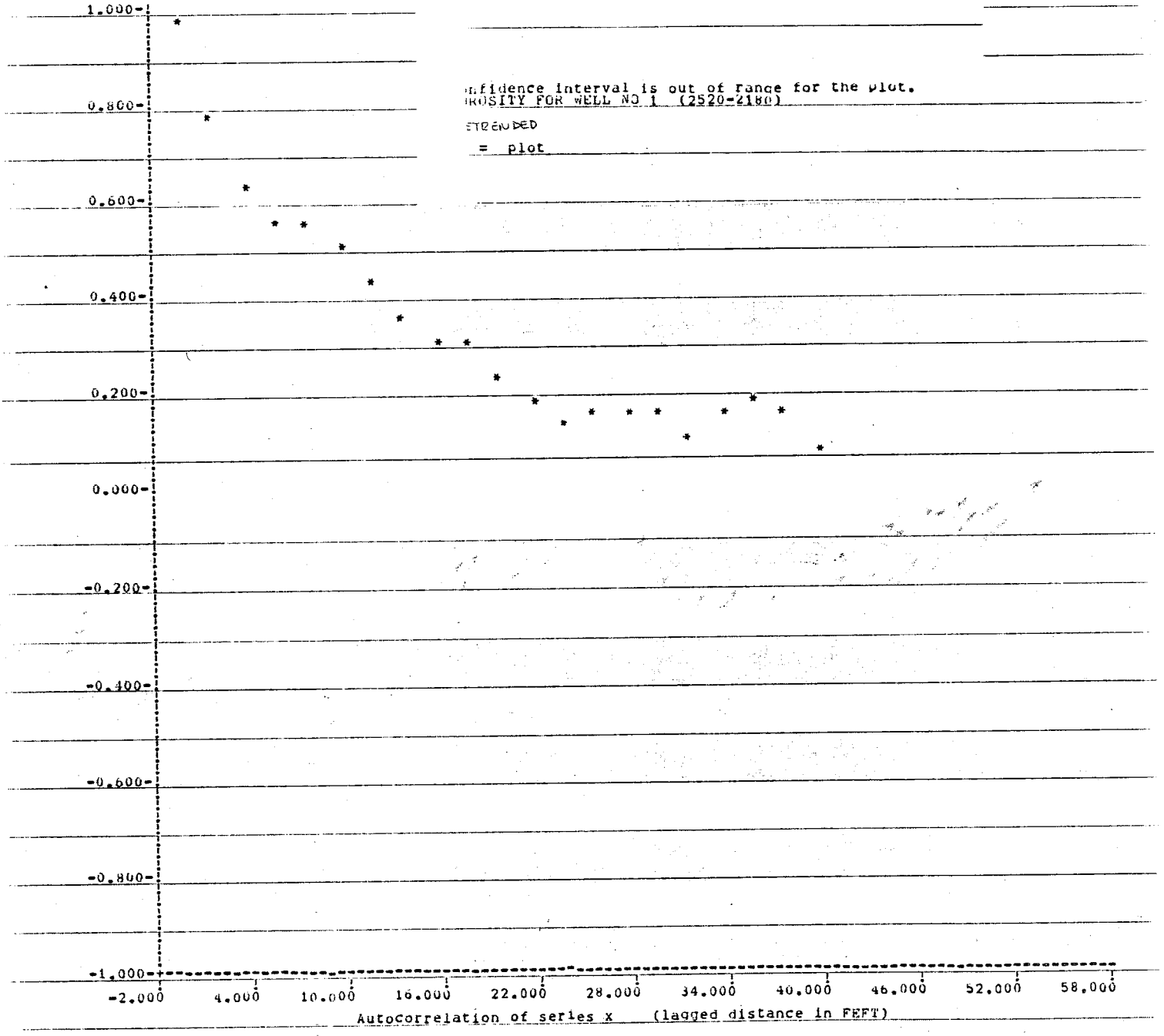

App 4e. Correlogram for porosity of lower middle Yeso in well no 1

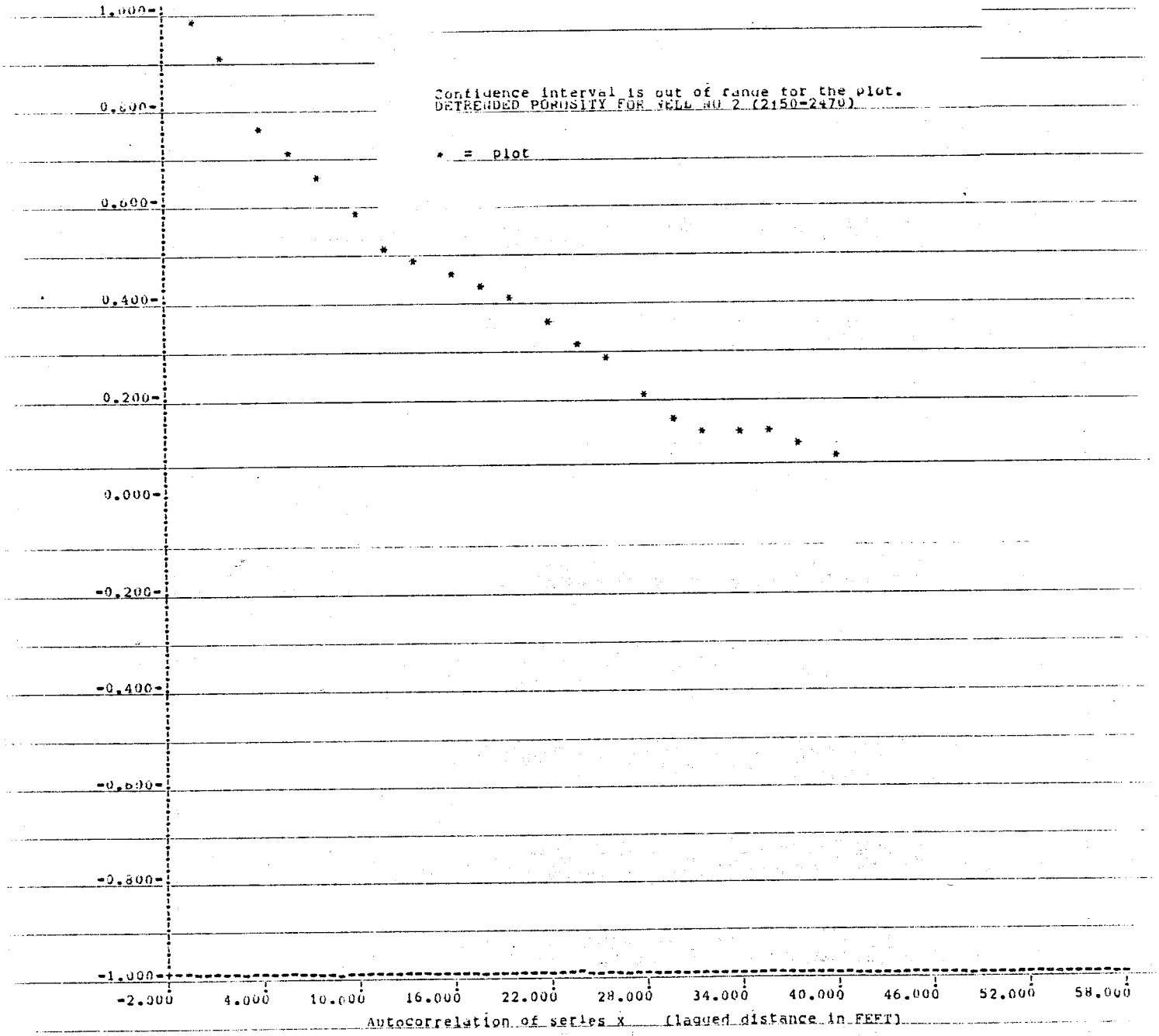

App 4f. Correlogram for porosity of lower middle Yeso in well no 2

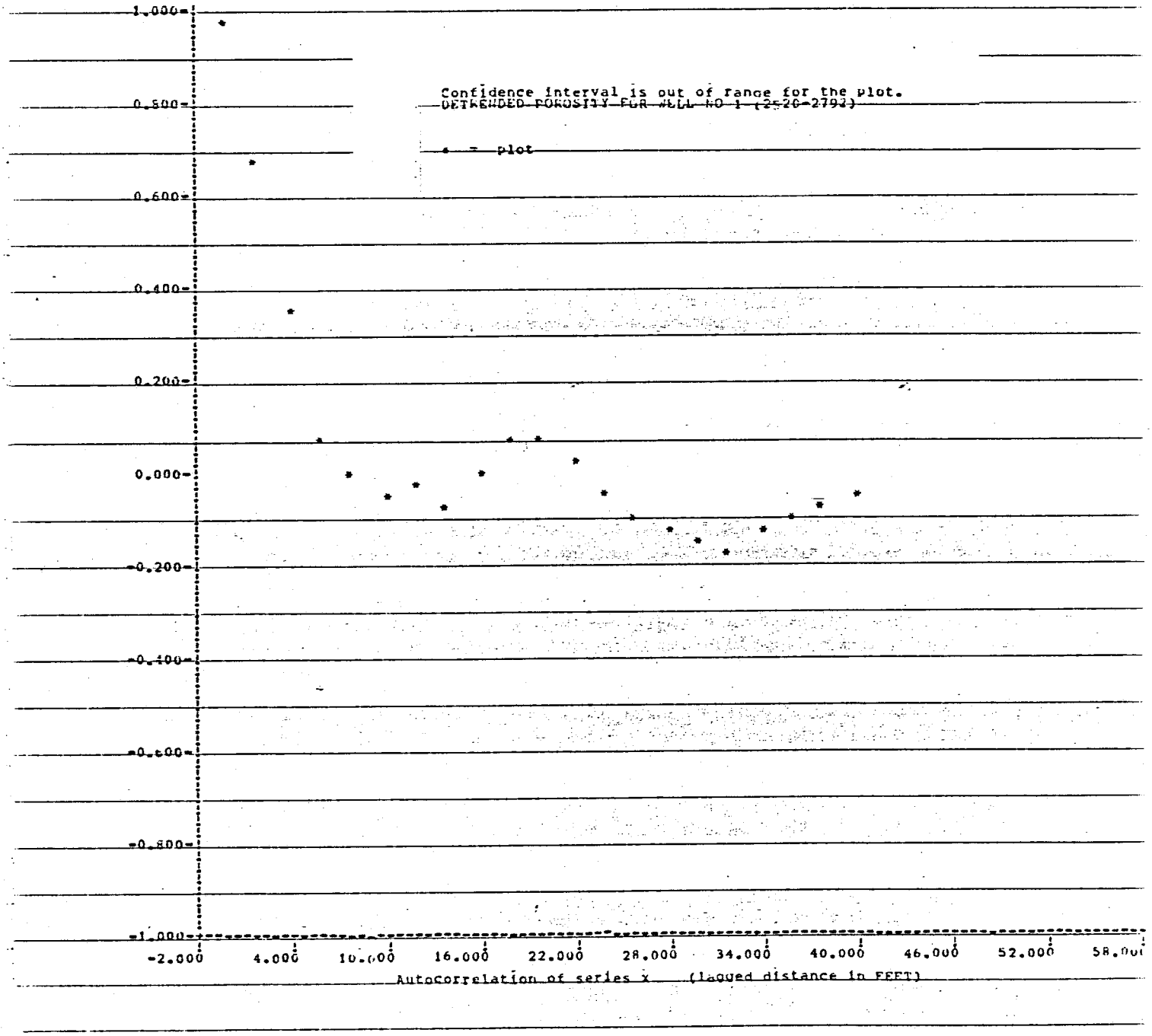

App 4g. Correlogram for porosity of lower Yeso in well no 1

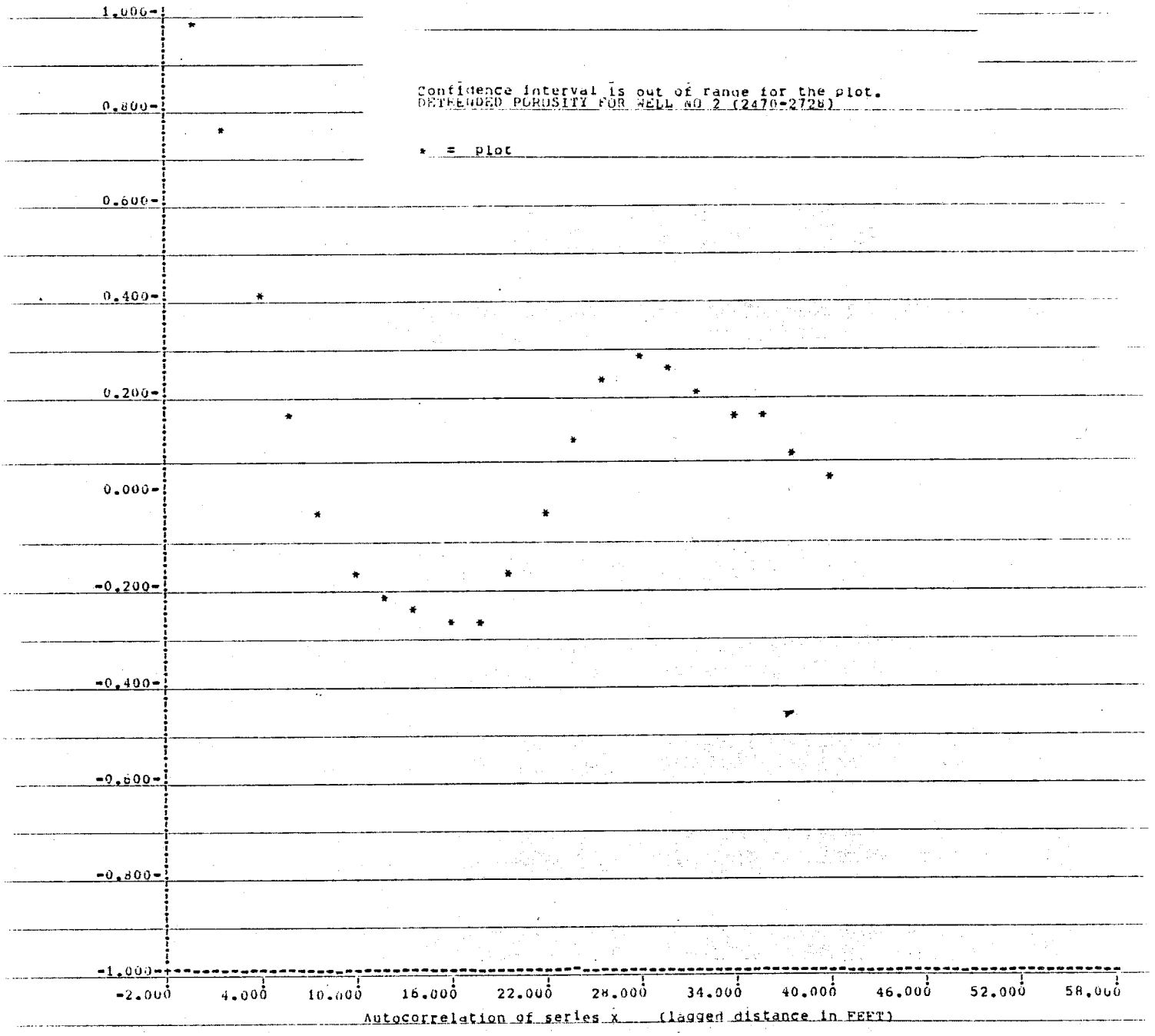

App 4h. Correlogram for porosity of lower Yeso in well no 2

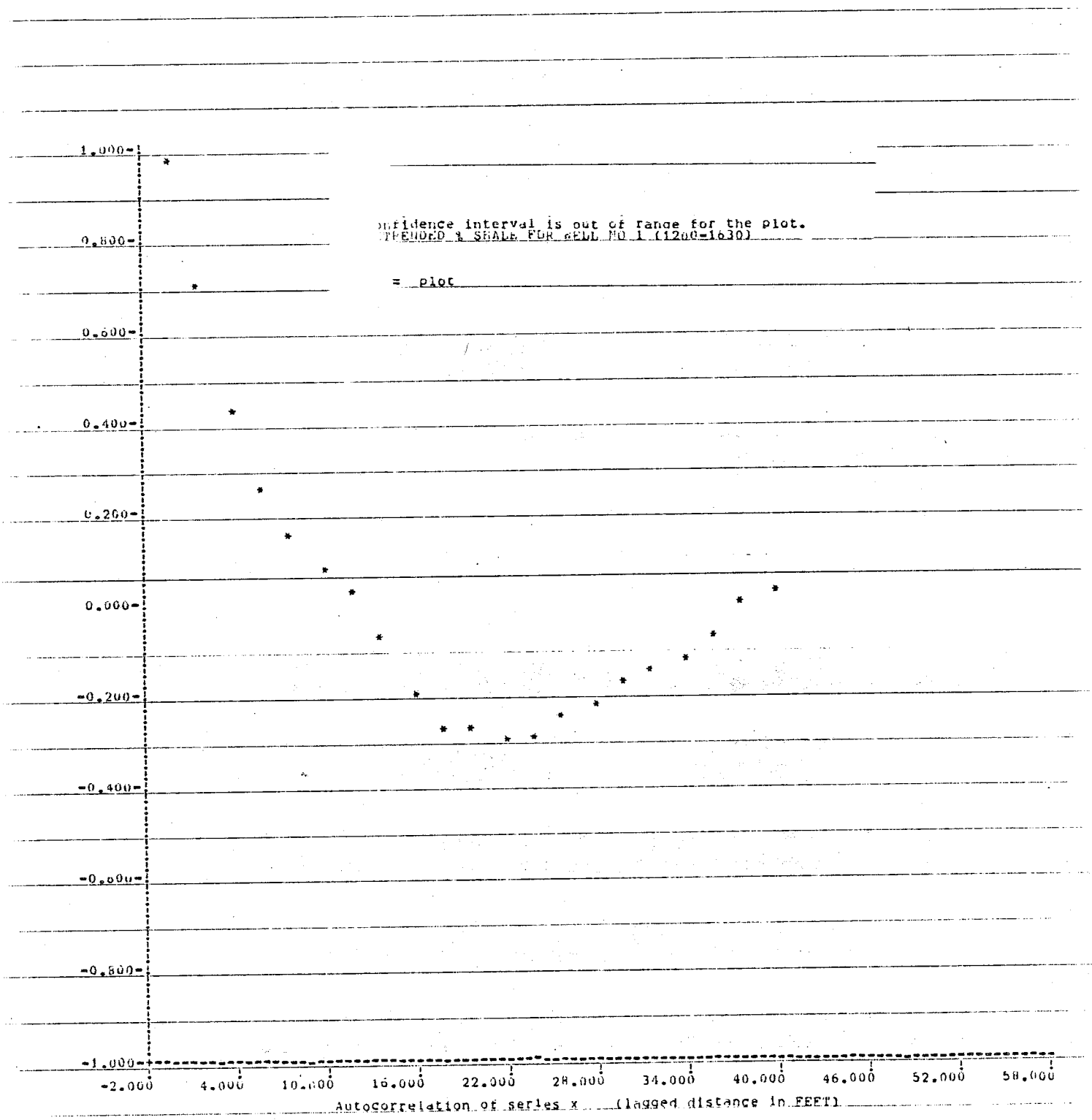

App 5a. Correlogram for % shale of upper Yeso in well no 1

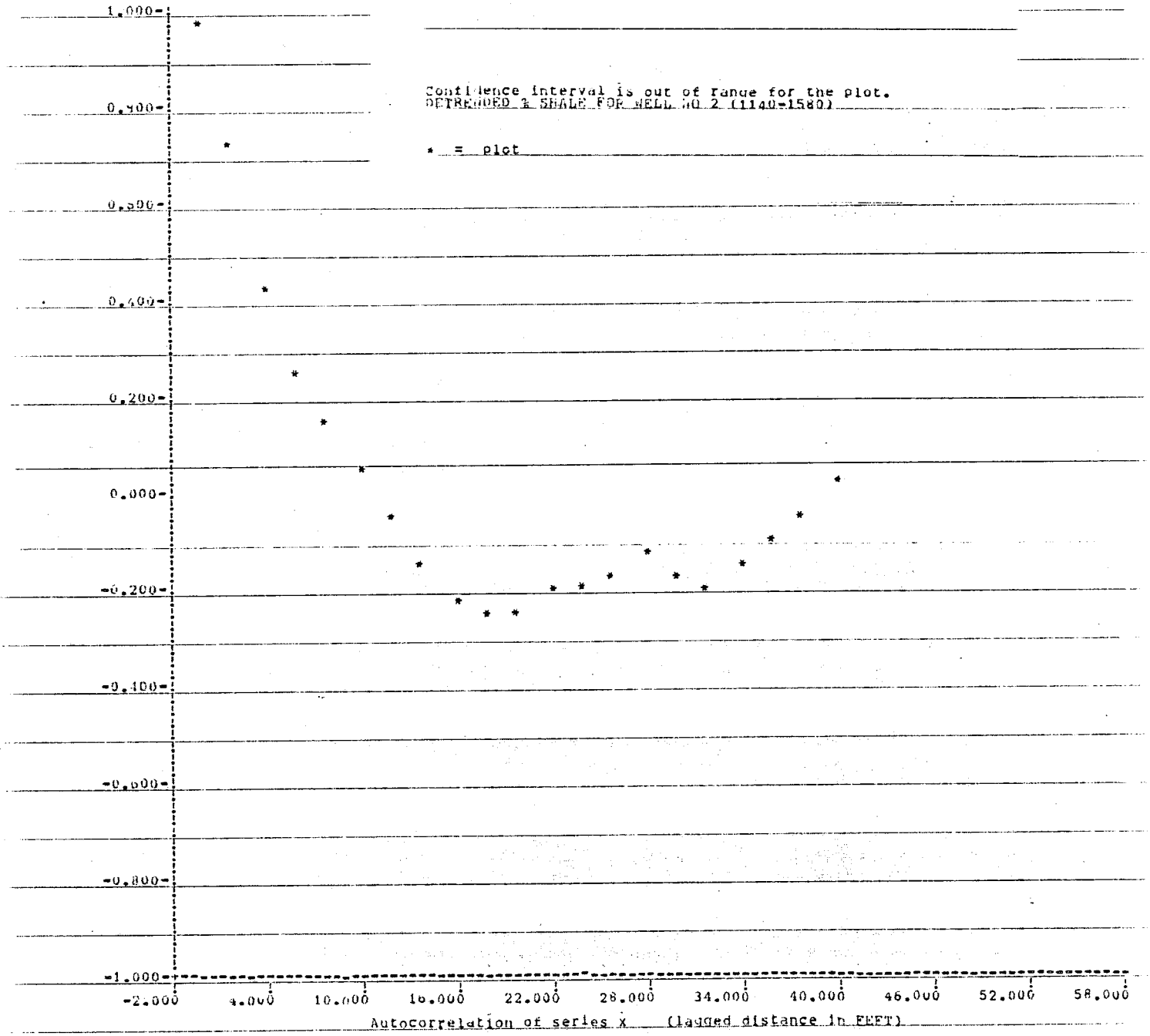

App 5b. Correlogram for % shale of upper Yeso in well no 2

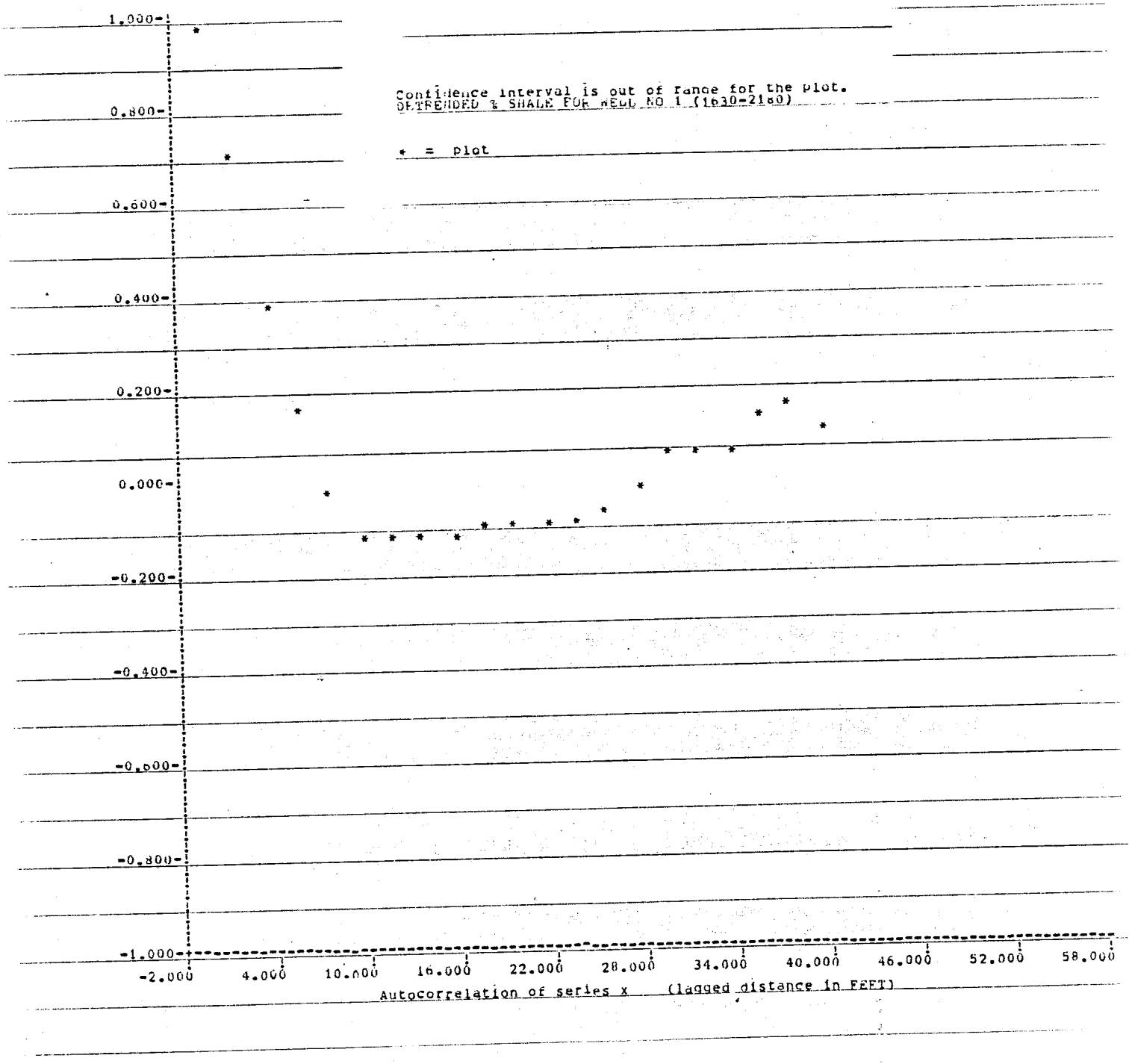

App 5c. Correlogram for % shale of upper middle Yeso in well no 1

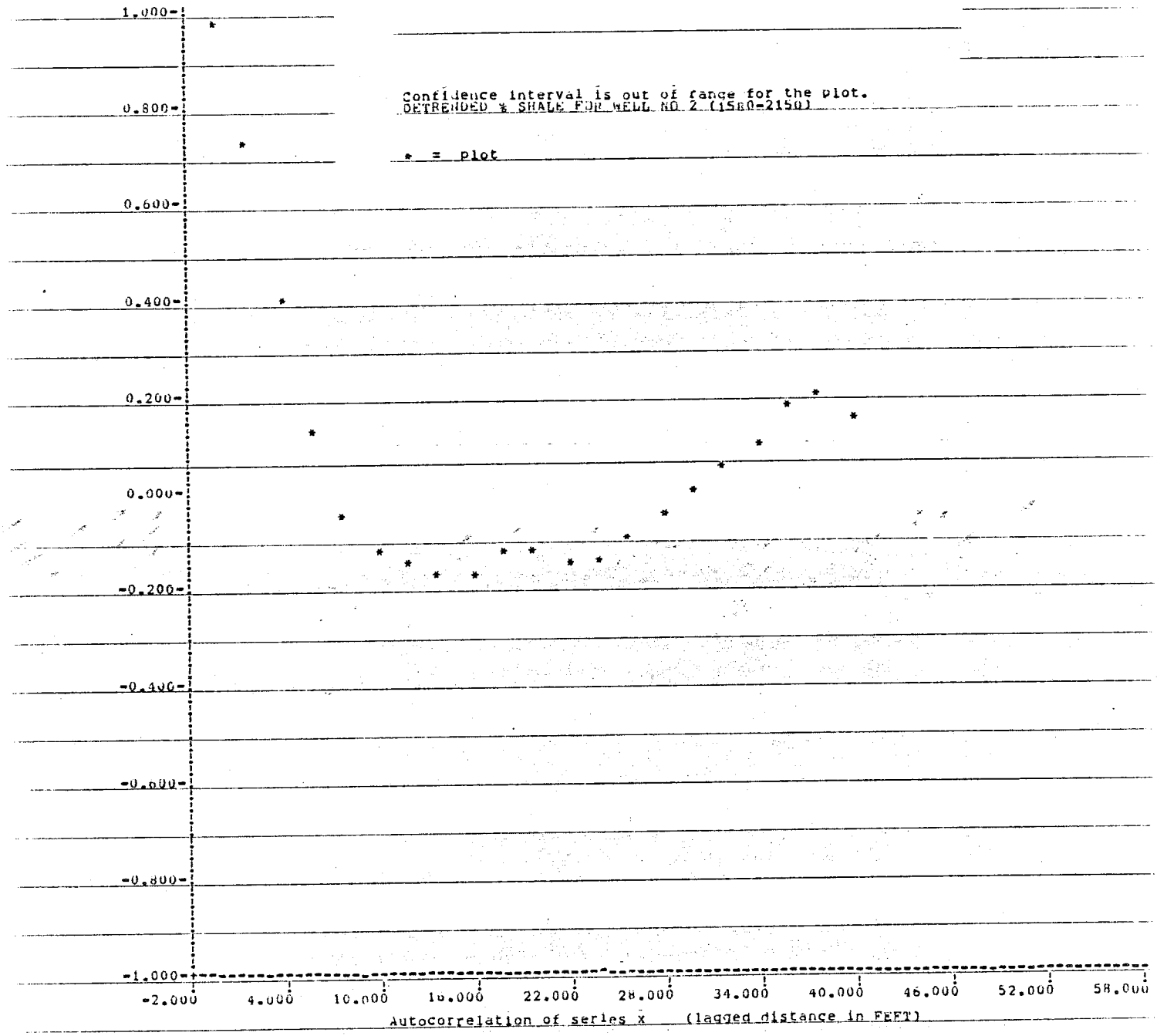

App 5d. Correlogram for % shale of upper middle Yeso in well no 2

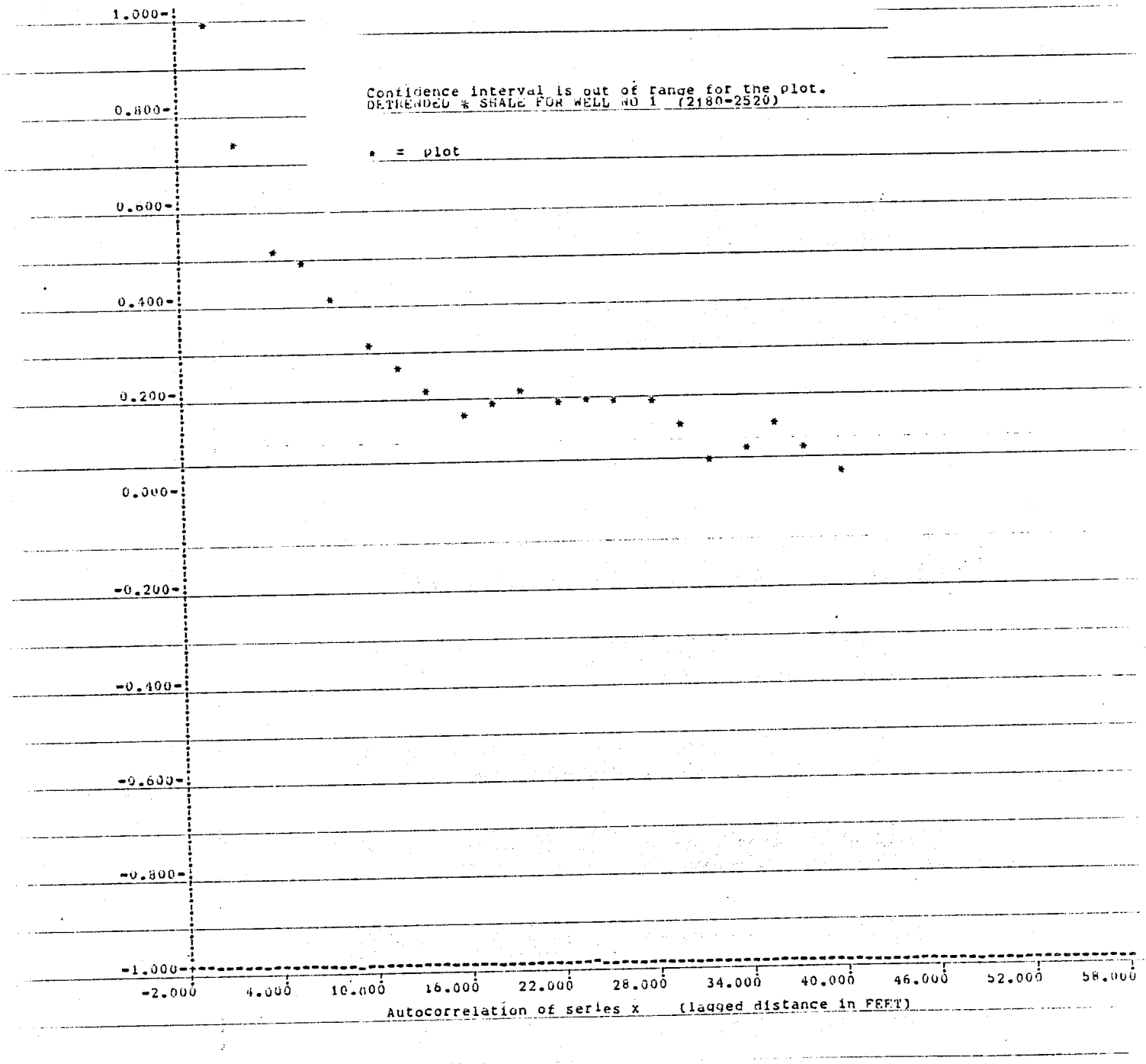

App 5e. Correlogram for % shale of lower middle Yeso in well no 1

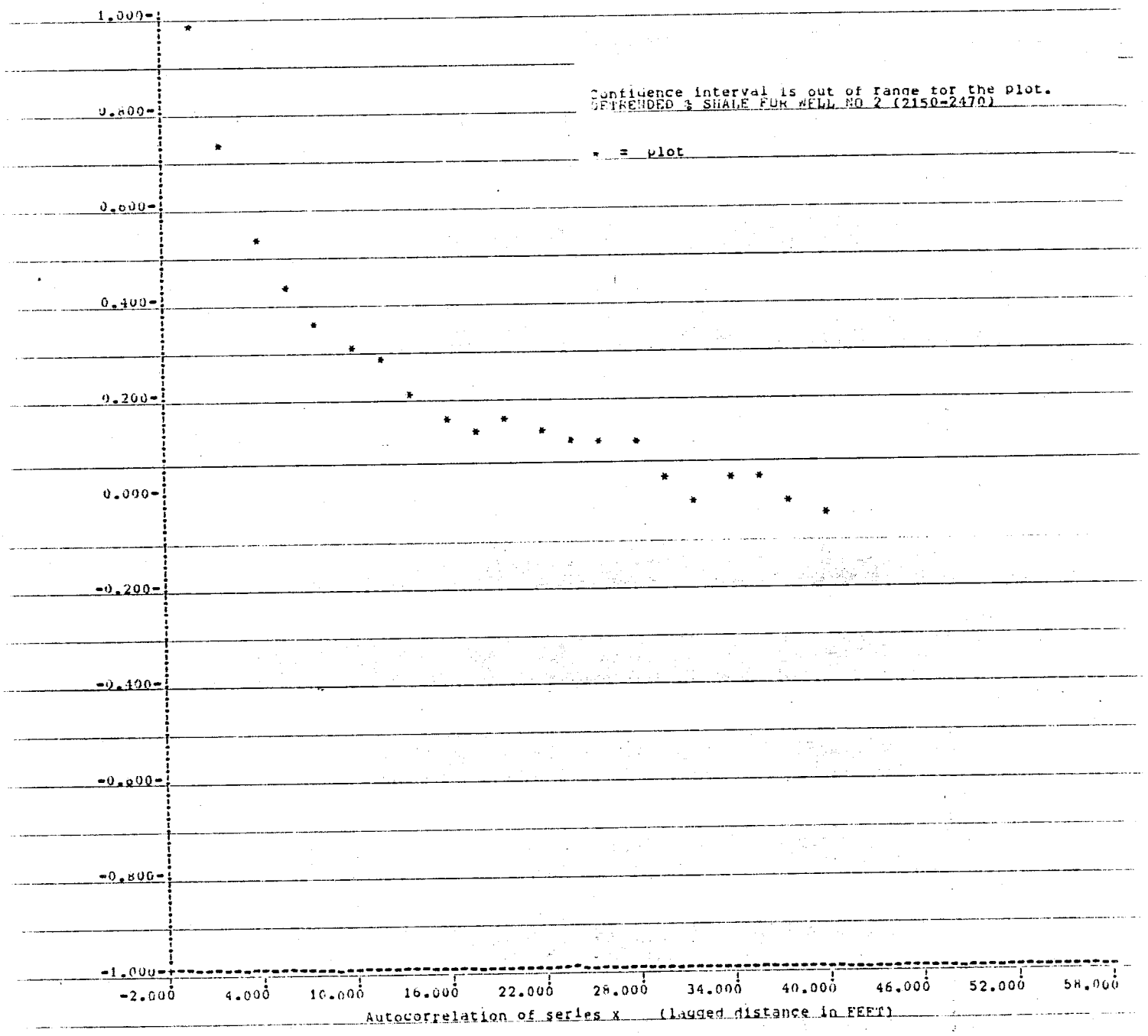

App 5f. Correlogram for % shale of lower middle Yeso in well 2

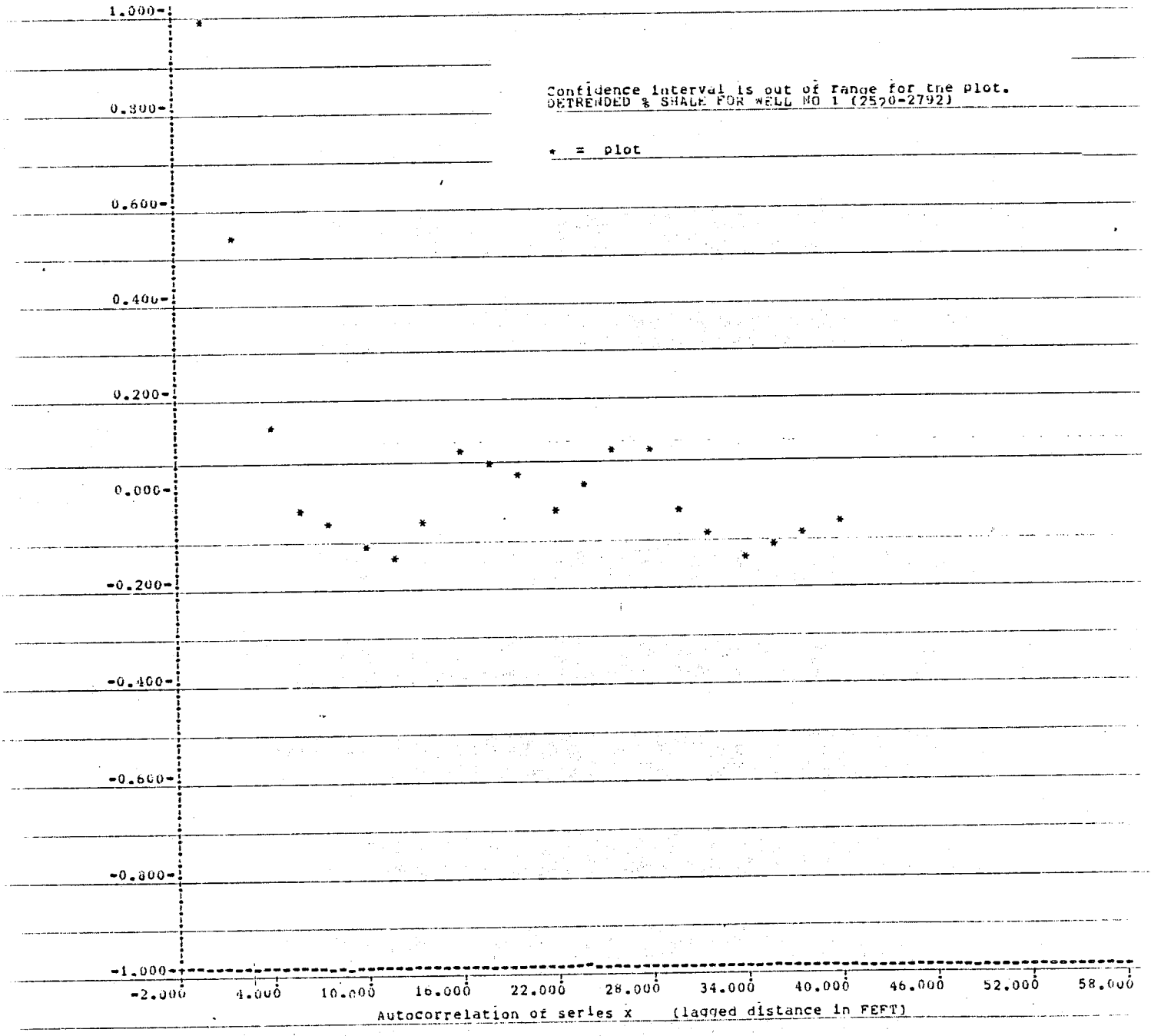

App 5g. Correlogram for % shale of lower Yeso in well 1

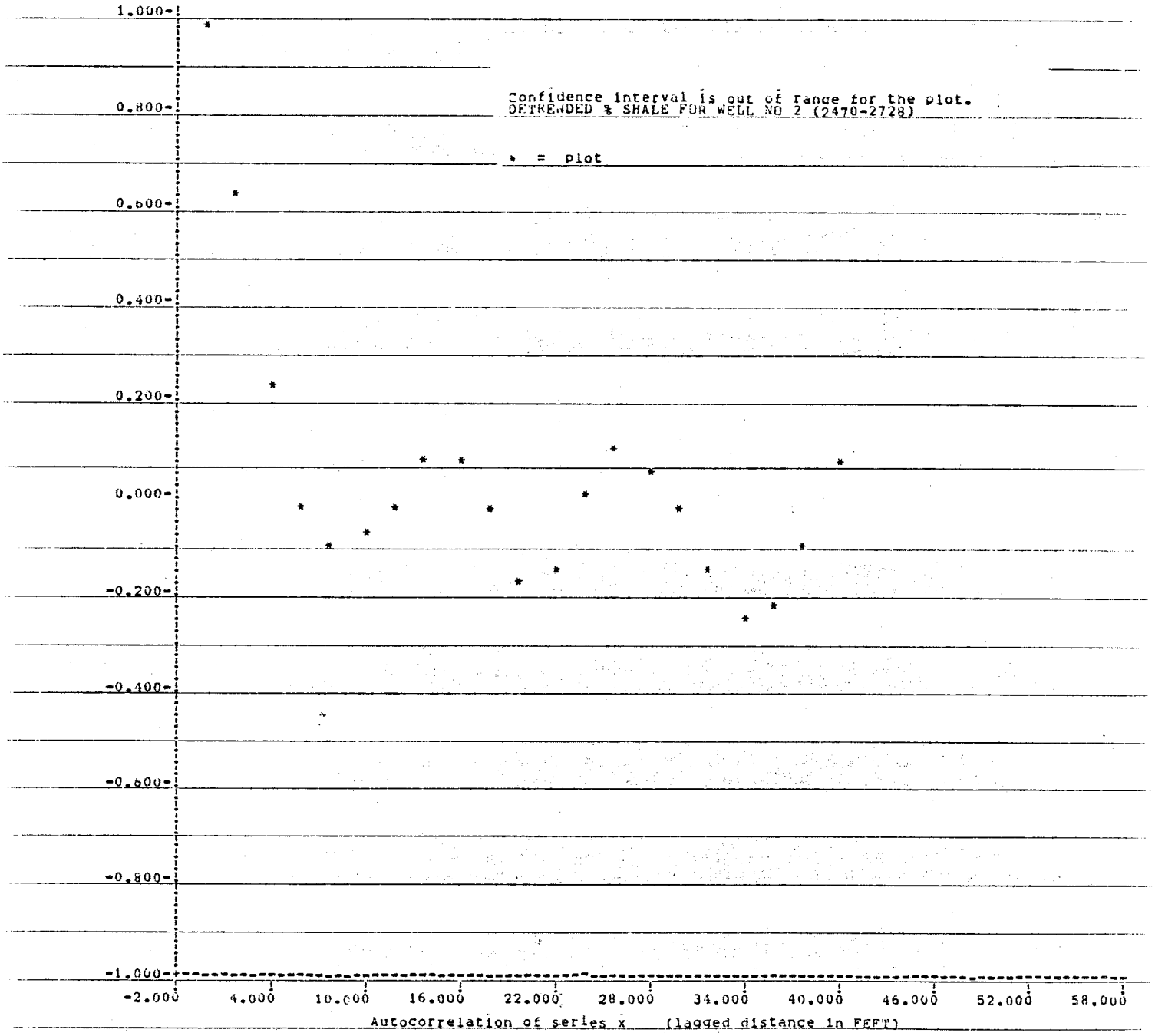

App 5h. Correlogram for % shale of lower Yeso in well 2

10

35-18S-14E

12

15-18S-15E

3

21-17S-17E

2

7-17S-18E unit 2

1

7-17S-18E unit 1

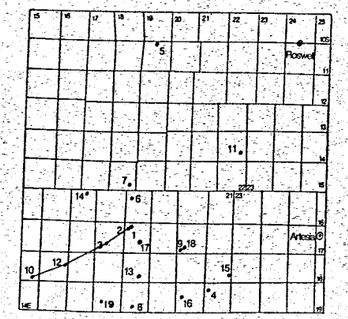

Location of wells in cross section

% CLAY POROSITY

land surface

Glorieta Ss.

Yeso fm.

top Abo fm.

Drinkard Ss.

Explanation

Permeable Pertrable Zone

Line connecting Geologic units

no horizontal scale

Elevation above sea level (feet)

7900. 7800. 7700. 7600. 7500. 7400. 7300. 7200. 7100. 7000. 6900. 6800. 6700. 6600. 6500. 6400. 6300. 6200. 6100. 6000. 5900. 5800. 5700. 5600. 5500. 5400. 5300. 5200. 5100. 5000. 4900. 4800. 4700. 4600. 4500. 4400. 4300. 4200. 4100. 4000. 3900. 3800. 3700. 3600. 3500. 3400. 3300. 3200. 3100. 3000. 2900. 2800. 2700. 2600. 2500. 2400. 2300. 2200.

3

21-17S-17E

17

20-17S-18E

6

31-17S-20E

18

28-17S-20E

25-18S-21E

15

land surface

5600.
5500.
5400.
5300.
5200.
5100.
5000.
4900.
4800.
4700.
4600.
4500.
4400.
4300.
4200.
4100.
4000.
3900.
3800.
3700.
3600.
3500.
3400.
3300.
3200.
3100.
3000.
2900.
2800.
2700.
2600.
2500.
2400.
2300.
2200.
2100.
2000.
1900.
1800.
1700.
1600.
1500.
1400.
1300.
1200.
1100.
1000.
900.

% CLAY POROSITY

Glorieta Ss.

top Yeso fm.

Oshkosh 96

top Abo fm.

% CLAY

Abo

% CLAY POROSITY

Explanation

Permeable Zone

Line connecting Geologic units

no horizontal scale

Roswell

Artesia

Location of wells in cross section

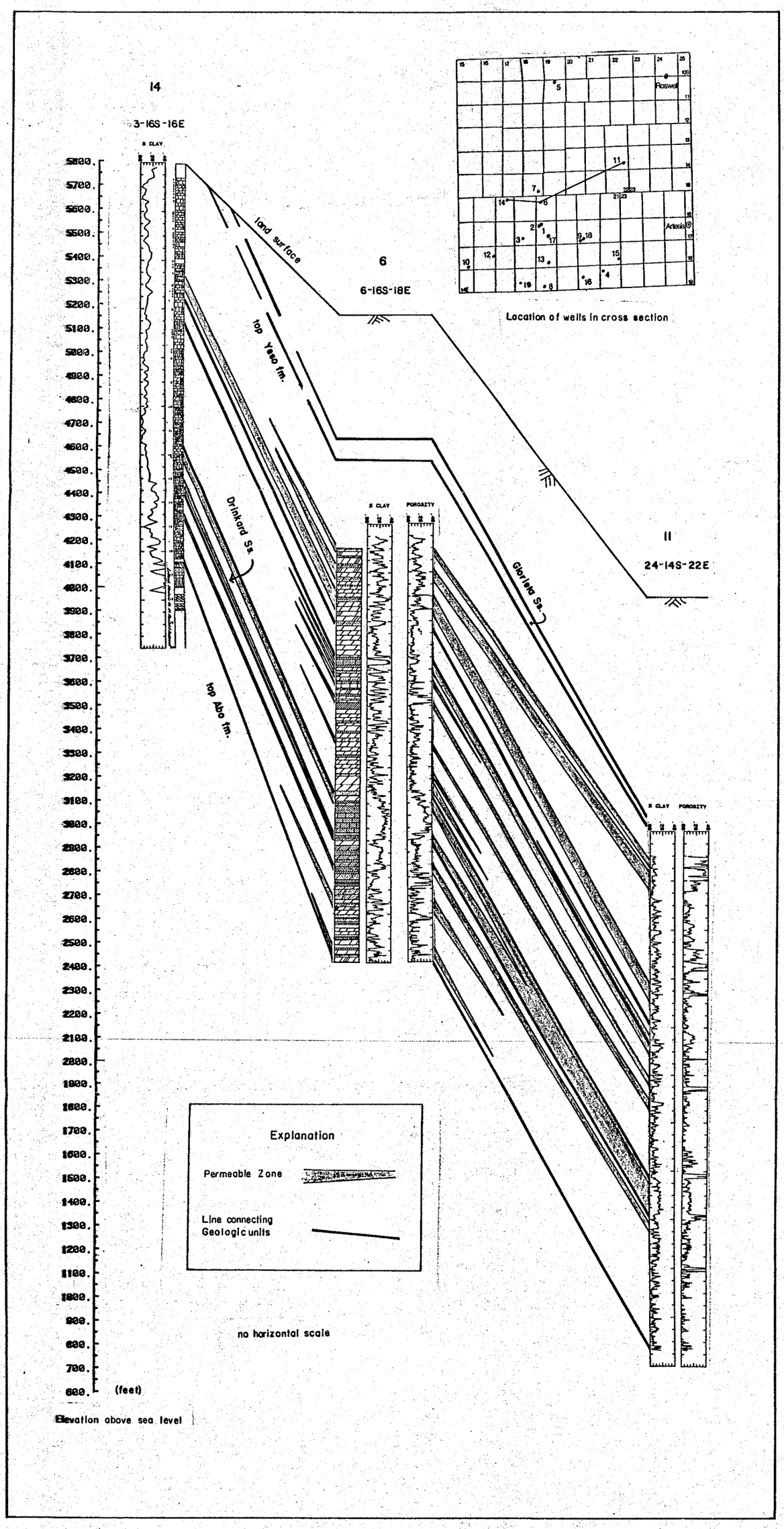
14
3-16S-16E
% CLAY
6
6-16S-18E
11
24-14S-22E
land surface
top Yeso fm.
Drinkard Ss.
top Abo fm.
Glorieta Ss.
% CLAY
POROSITY
% CLAY
POROSITY
Roswell
Artesia
Location of wells in cross section
Explanation
Permeable Zone
Line connecting Geologic units
no horizontal scale
5800.
5700.
5600.
5500.
5400.
5300.
5200.
5100.
5000.
4900.
4800.
4700.
4600.
4500.
4400.
4300.
4200.
4100.
4000.
3900.
3800.
3700.
3600.
3500.
3400.
3300.
3200.
3100.
3000.
2900.
2800.
2700.
2600.
2500.
2400.
2300.
2200.
2100.
2000.
1900.
1800.
1700.
1600.
1500.
1400.
1300.
1200.
1100.
1000.
900.
800.
700.
600.
(feet)
Elevation above sea level

10
35-18S-14E
19
19-19S-17E
8
28-19S-18E
16
17-19S-20E
4
7-19S-21E

Top Abo fm.
Drinkard Ss
Top Yeso fm.
land surface

Explanation

Permeable Zone

Line connecting Geologic units

no horizontal scale

Elevation above sea level (feet)

7000.
6900.
6800.
6700.
6600.
6500.
6400.
6300.
6200.
6100.
6000.
5900.
5800.
5700.
5600.
5500.
5400.
5300.
5200.
5100.
5000.
4900.
4800.
4700.
4600.
4500.
4400.
4300.
4200.
4100.
4000.
3900.
3800.
3700.
3600.
3500.
3400.
3300.
3200.
3100.
3000.
2900.
2800.
2700.
2600.
2500.
2400.
2300.
2200.
2100.
2000.
1900.
1800.
1700.
1600.
1500.
1400.
1300.
1200.
1100.
1000.

Location of wells in cross section